Nicotinic modulation of excitatory amino acid release in the rat frontal cortex

Rousseau, Stephen John

Award date:
2004

Awarding institution:
University of Bath

NICOTINIC MODULATION OF EXCITATORY AMINO ACID RELEASE IN THE RAT FRONTAL CORTEX

Submitted by STEPHEN JOHN ROUSSEAU for the degree of PhD of the

University of Bath 2004

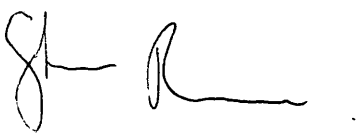

Stephen J. Rousseau **December 2003**

ProQuest LLC
789 East Eisenhower Parkway
P.O. Box 1346
Ann Arbor, MI 48106-1346

Summary

The frontal cortex serves as a crucial structure in the vertebrate CNS for the execution of certain forms of attention and memory. Of the various neurotransmitter pathways that innervate this area, it is the specific loss of cholinergic innervation that is detrimental to frontal cortex function, as demonstrated by the cognitive deficits observed in neurological disorders such as Alzheimers and schizophrenia.

Nicotinic acetylcholine receptors are activated by the endogenous ligand acetylcholine (ACh) and the major psychoactive component of tobacco, nicotine, and accordingly, the loss of cholinergic innervation to the frontal cortex and other regions of the CNS are the basis to which 'nicotinic' therapy may be beneficial to those neurological disorders where cholinergic function is compromised.

In order to examine nAChR function in the frontal cortex, pharmacological studies in Chapter 3 demonstrated that superfused frontal cortex synaptosomes (presynaptic terminals) could release [^{3}H]D-aspartate (used as a surrogate for glutamate; see Chapter 3 section 1) when evoked by application of nAChR agonists. The nAChR-evoked release of [^{3}H]D-aspartate described in Chapter 3 (section 3) was calcium-dependent, consistent with an exocytotic mechanism of release and could be blocked by both α7 and β2* nAChR specific antagonists, implying that the release of excitatory amino acids (EAA) is modulated by more than one subtype of nAChR. This work supersedes previous demonstrations of nAChR modulation of EAA release, which could only be observed when synaptosomes were stimulated with a combined depolarising and nicotinic stimulus (emulated in Chapter 3 section 2).

To corroborate the functional data described in Chapter 3, an immunocytochemical investigation (see Chapter 4) ascertained nAChR association with glutamatergic terminals and cell bodies of the frontal cortex. This investigation successfully described the co-association of α7 and β2* nAChRs with glutamatergic terminals as well as cell

bodies and provided a preliminary insight into the distribution of α7 nAChR within specific regions of the rat frontal cortex.

These studies provide a novel assessment of nAChR function and location with excitatory neurotransmitter systems in the frontal cortex by utilising direct methods of analysis.

Acknowledgements

Without a shadow of a doubt this PhD has tested every virtue of my being and therefore it is with great appreciation and thanks to the following people for the times in which their support helped me maintain my tenacious nature (currently re-fuelling!) and my sanity (presently questionable!).

Sincere thanks goes to the 'Boss', Professor Susan Wonnacott, of which her guidance and support have been the essence to the success of my work from either picking me up when I was down or redirecting the slightest hint of hyperactivity (a natural tendency of mine) by guiding the energy into more meaningful tasks. Thanks also to Dr Ian Pullar at Eli Lilly, I apologise if those three months seemed longer for him and the rest of his team, thank you for your patience!

In making my time in and out of the lab that much more enjoyable than the joys of staring at a superfusion machine, the warmest of thanks goes to the 'Wonnacott crew' past and present: Amy Bradly (who even put up with living with me for a year), Federico Dajas-Bailador (Fred) whose wisdom and calmness have also been beneficial to my own work practice, Nimish Sidpura 'the Bombay bad boy' who, despite his shameful musical tastes, has provided many comical moments to my time at Bath, Ghazelah Pashmi and Katherine Hanrott for the 'girly point of view' (and paracetomol), Monsieur Barik pour le 'Je ne sais quoi' and Dr Steve for his northern influence, a true conversational killer. A big thank you should also go to Ewan, Leslie and Louise for putting up with my singing and general idiocy at 8 in the morning. In particular my thanks goes to Dr Ian Jones and Dr Adrian Mogg whose expertise in immunocytochemistry and superfusion respectively have been greatly appreciated and I am forever indebted to these people for teaching me the elements of my imminent career.

Outside of work my thanks goes both to my family and friends for providing me glimpses of the real world and its fruits and not its statistical significance or n number requirements. In no particular order or preference these people include: my brother and sister, the loveliest Aunties and Uncles of the North, Great Auntie Violet, the Foul-Mouthed-Five (and honouree members of), Richard Judd, Seth Hawker, Daniel Squires, Anu Tayal, Mark Fenner, Graham Sanger (and all the boys of Graham's Tuckshop) and Matthew Reeves.

In particular I would like to thank the Mallet family, Dennis, Janet, Richard and lifelong best-pal David. As a family they have provided me with the support, encouragement, confidence and faith for me to endure the most difficult of times and it is this friendship that I am eternally grateful for and would be lost without.

For my Father, I am ever grateful for his patience, his help and his understanding through many testing times, and I only hope I can reward his faith in me by my future success, thanks dad!

And finally, my most endearing thank-you goes to my friend, my soul mate and my love, Laura Corria. She has recently begun her PhD in neuroscience and I pray that I provide her with the same support, understanding, patience, and encouragement that she has provided for me, for without her things would not have been as much fun, thanks for making me smile!

Dedicated to my grandfather, the late Edwin Rousseau.

"You can't start a fire, you can't start a fire without a spark"

'Dancing in the dark'. Bruce Springsteen, 1984.

Publications and Communications

In refereed Journals

Rousseau S, Jones I W, Pullar I and Wonnacott S. (2003) **Presynaptic α7 and non-α7 nicotinic acetylcholine receptors modulate the release of [^{3}H]D-aspartate from rat frontal cortex synaptosomes.** (In preparation).

Rousseau S, Wonnacott S and Pullar I. (2002) **Activation of the presynaptic nicotinic acetylcholine receptor modulates the depolarisation dependant release of [^{3}H]D-aspartate from rat frontal cortex synaptosomes.** British Journal of Pharmacology, Proceedings supplement 55P

Communications

Rousseau S, Jones I.W, I A Pullar I A and S Wonnacott (2003). **α7 nicotinic receptors are associated with glutamatergic terminals in the rat frontal cortex: Neurochemical and anatomical evidence.** British Neuroscience Association, Harrogate, April 2003.

Rousseau S and Wonnacott S. (2002) **Nicotine modulates the release of [^{3}H]D-aspartate from rat frontal cortex synaptosomes.** 3rd forum of European Neuroscience, 143.17

Rousseau S & Wonnacott S. (2001) **Activation of the presynaptic nicotinic acetylcholine receptor modulates the depolarisation dependant release of [^{3}H]D-aspartate from rat frontal cortex synaptosomes.** British Pharmacological Association. Hatfield, April 2001.

.

Oral Presentations

Rousseau S. **α7 nicotinic receptors are associated with glutamatergic terminals in the rat frontal cortex: Neurochemical and anatomical evidence.** 1st United Kingdom symposium on Neuronal nicotinic receptors at Eli Lilly and Company. July, 2003.

Table of Contents

Abbreviations

α-Bgt	α-bungarotoxin
α-CTx ImI	α-conotoxin ImI
ACh	acetylcholine
AChBP	acetycholine binding protein
AD	Alzheimer's disease
ADHD	attention deficit hyperactivity disorder
AMPA	α-amino-3-hydroxy-5-methyl-4-isoxazole propionic acid
ANOVA	analysis of variance
BSA	bovine serum albumin
°C	degrees Celsius
CNS	central nervous system
DA	dopamine
DHβE	dihydro-β-erythroidine
EC_{50}	agonist concentration which evokes a half-maximal response
EGTA	ethyleneglycol-bis-(β-aminoethylether)-N,N,N',N'-tetraacetic acid
EPSC	excitatory postsynaptic current
g	gram
GABA	γ–aminobutyric acid
Glu	glutamate
5-HT	5-hydroxytryptamine, serotonin
HEPES	N-[2-hydroxyethyl]piperazine-N'-[2-ethane sulfonic acid]
5-I-A-85380	5-Iodo-A-85380 dihydrochloride
IC_{50}	ligand concentration which reduces radioligand binding or functional response to half-maximal

IGluR	ionotropic glutamate receptor
IPN	interpeduncular nucleus
K^+	potassium ion
KB	Krebs-bicarbonate buffer
K_D	equilibrium dissociation constant
KDa	kilodaltons
K_i	inhibition constant
LGIC	ligand gated ion channel
m	metre
Mec	mecamylamine
min	minute
MLA	methyllycaconitine
MW	molecular weight
NA	noradrenaline
nAChR	nicotinic acetylcholine receptor
n-Bgt	neuronal bungarotoxin
NMDA	N-methyl-D-aspartate
NMDA-R	N-methyl-D-aspartate receptor
PBS	phosphate buffered saline
PD	Parkinson's disease
PDC	L-trans-pyrrolidine-2,4-dicarboxylic acid
PNS	peripheral nervous system
rpm	revolutions per minute
s	second
SH	sucrose-HEPES
TBOA	DL-threo-β-benzyloxyaspartic acid

TTX	tetrodotoxin
v/v	volume/volume
VGluT	vesicular glutamate transporter
VOCC	voltage operated calcium channel
VTA	ventral tegmental area
w/v	weight/volume

The nomenclature for all nicotinic acetylcholine receptor subunits described in this thesis is based on the NC-IUPHAR subcommittee recommended definitions published in 1999 (Lukas *et al.*, 1999)

Chapter 1

Introduction

1.1. General introduction: Nicotinic receptors and memory

The major compound in tobacco that causes addiction to cigarette smoking is nicotine. With approximately 560 deaths recorded per hour worldwide, attributed to smoking related diseases, constant public awareness drives such as the recent increase in size of health warnings on tobacco product packaging (see Fig. 1.1), are intended to curb the general public from smoking.

Figure 1.1 Representative health warnings displayed on tobacco product packaging. Implemented early in 2002, the UK government ruled that tobacco companies must conform to increasing the size of health warnings on tobacco products in a drive to increase social awareness of the high health risks associated with smoking.

However, the behavioural response to these public awareness initiatives are actually mediated by our ability to learn and memorise this information, a physiological mechanism that can actually be augmented by the very receptor that nicotine targets, the neuronal nicotinic acetycholine receptor (nAChR).

An overwhelming body of evidence supports the cognitive enhancing effects of nicotine in both acute and chronic treatment paradigms, displayed in both rat and human models (for review see Levin & Simon, 1998; Perry *et al.*, 2001; Levin, 2002). In the clinical environment, inhibitors of acetylcholinesterase (e.g. donezepil, galantamine) that prevent the breakdown of the endogenous ligand for the nAChR, acetylcholine (ACh), are currently the only approved drugs for the treatment of cognitive dysfunction in patients diagnosed with Alzheimer's disease (AD).

The development of a better understanding of the molecular interaction of nicotine or ACh with the nAChR and the observed behavioural responses requires an

integration of studies that examine nAChR function at the gross anatomical level as well as at the cellular level. For instance, on the anatomical level it is a well-known assumption that the formation and storage of memory does not rely on a single entity within the brain, and instead relies on complex circuits that collect, distribute and retain information between certain regions of the brain. The distribution of nAChRs that have been implicated in memory are also subject to variation in location across the brain, yet further complicated by the ability to assemble into multiple subtypes and locate on various positions along a neuron.

In light of these challenging problems, investigations of the nAChR in the hippocampus, long known for its role in attention and memory (serving cognitive functions such as spatial memory and long term memory; For review see Jarrard, 1995) have revealed evidence for nAChR receptor location, subtype specificity, cell type specificity and functional consequences of its activation, such as the induction of LTP; a cellular model of 'memory' where synapses are modified (synaptic plasticity) in either a strengthened (long term potentiation; LTP) or weakened (long term depression; LTD) manner, dependant upon the level of external stimulation, thereby increasing or decreasing the likelihood of conveying information through neuronal circuits respectively.

Few studies have examined the role of nAChR in the frontal cortex to the same degree as that of the hippocampus, perhaps hindered by the complex synaptic circuitry in this region compared to the well defined anatomical structure of the hippocampus. However, the frontal cortex is a critically important brain structure associated with attention and a crucial form of memory, working memory. This is a form of short-term memory that integrates moment-to-moment perceptions across time with that of archival information about past experiences, actions or knowledge.

Therefore, the study of nAChRs in the frontal cortex, incorporating both anatomical and functional assessments, will contribute to the understanding of nAChR in certain aspects of cognition, extending to possible treatment strategies for complex cognitive deficits that accompany disorders such as AD, schizophrenia and Parkinson's disease (PD).

1.1.2 nAChR and memory: Behavioural and Clinical observations

Behavioural and clinical studies that examine the effects of nAChR agonists in humans and experimental animals have clearly demonstrated improvements in particular cognitive tasks (for reviews see Newhouse *et al*., 1997; Levin & Simon, 1998; Rusted *et al*., 2000; Levin, 2002).

1.1.3 Behavioural observations implicating nAChR function

One of the major challenges in assessing the function of nAChR with particular cognitive tasks using experimental animals is the discrimination between different forms of memory. As a general overview there are two types of memory, explicit and implicit memory, which are classified on the basis of how information is stored and recalled; explicit memory is a memory of facts or events that require a conscious effort for recollection whereas implicit memory is a memory that is recalled unconsciously, typically utilised in training reflexive motor or perceptual skills (Kandel, 2000). Of these two main forms of long-term memory (which can be divided into further classifications), explicit memory is exploited in cognitive tasks using experimental animals to differentiate between reference memory and working memory. Reference memory is utilised in tasks that present the same information (spatial or external cues) from previous tasks in order to carry out a repeated

performance, whereas working memory is utilised on a short-term basis within a task. In a radial arm maze, nAChR agonists applied either acutely or chronically to rodents have been shown to effectively improve working memory and not reference memory, for example, in a 16-arm radial maze with 12 arms baited and 4 not, nAChR agonist treated rodents correctly entered baited arms only once (because arms were only baited once) throughout repeated tasks (working memory), whereas they failed to recall the same positioned unbaited arms between tasks (reference memory) (Levin *et al.*, 1996 & 1997). Application of nAChR antagonists was shown to inhibit this nAChR agonist induced improvement (Levin *et al.*, 1997).

Studies have revealed that nAChR induced improvements to working memory involve the hippocampal formation; small ibotenic lesions of the hippocampus blocked nAChR improvements in working memory (Levin *et al.*, 1999). As well as this, nAChR antagonists injected into the prelimbic regions of the frontal cortex also reduced working memory tasks in rodents (Granon *et al.*, 1995; For review see Levin & Simon, 1998). Indeed, prefrontal and frontal cortex association areas appear critical for the execution of working memory (For review see Fuster, 2001) and the ability for it to be processed through to higher modalities for long-term storage (Buckner *et al.*, 1999). Three component systems are crucial to the execution and functioning of working memory in humans: an attentional system that collects and regulates the information flow in the environment to the other two component systems that contain memory on a temporary basis; the articulatory loop for language and auditory events and the visuospatial sketch pad for vision and action.

Attempts have been made to ascertain the nAChR subtypes that mediate nicotinic effects on memory in rodents. However, these assessments are limited in both the

availability of sub-type specific ligands for the array of nAChR subtypes, as well as consideration of spatial concentration gradients generated from general or local injection of nAChR ligands; depending on the concentration of ligand applied, determination of specific or non-specific effects may be compromised. Nonetheless, such studies have inferred that α7 and α4β2* nAChR are involved with working memory function (for review see Levin, 2002), particularly when examined in the hippocampus. In the frontal cortex however, behavioural pharmacological evidence for subtype specific nAChR involvement with working memory is less clear, with to date only one behavioural study that implicated α4β2* nAChR (Granon *et al.*, 1995). Instead, much of the information for the determination of nAChR subtypes in the frontal cortex has been obtained from other investigative approaches, such as nAChR ligand binding studies or electrophysiological assessment of nAChR function. These studies have aimed to relate the integration of nAChR function in frontal cortex synaptic circuitry to the gross behavioural functions of nAChR, such as working memory.

1.1.4 Clinical observations implicating nAChR function

With respect to clinical observations, nAChR have been implicated in the altered state of cognitive function in neurological disorders such as AD, Parkinson's disease (PD) and schizophrenia. As well as this, evidence also exists for their possible involvement in neurological diseases such as attention deficit hyperactivity disorder (ADHD) and Tourette's syndrome.

1.1.4.1 Alzheimers disease and nAChRs

Of persons over 65 years of age, AD is the cause for almost 60% of different forms of mental deterioration in elderly people, affecting 15 million people worldwide (Francis *et al.*, 1999). A number of neurochemical deficits have been described in AD, in particular, the decreased function of the cholinergic system in AD patients, contributing to the 'Cholinergic hypothesis' of AD. It was proposed that degeneration of cholinergic neurons in the basal forebrain and the associated loss of cholinergic neurotransmission in the cerebral cortex and other areas of the brain, contributed significantly to the deterioration of cognitive function seen in patients with AD (Bartus *et al.,* 1982).

The majority of evidence associating nAChR with AD involves the loss of cortical nAChR binding in AD subjects compared to age-matched controls (Nordberg & Windblad, 1986; Nordberg *et al.*, 1988; Whitehouse *et al.*, 1986 & 1988; Warpman *et al.*, 1995; For review see Perry *et al.*, 2001). The hippocampus, entorhinal cortex and frontal cortex are particularly vulnerable to loss of nAChR, particularly α7 and α4 subunit containing nAChR. Interestingly, reduced nAChR ligand binding patterns but not mRNA levels for α7 and α4 subunit containing nAChR in AD brain indicate a presynaptic locus for loss of nAChR in the frontal cortex, hippocampus and other regions of the temporal cortex (for review see Nordberg, 2001). Presynaptic loss of nAChRs is likely to be a direct consequence from the loss of cholinergic terminals in the forebrain areas in AD as well as the loss of non-cholinergic cholinoceptive terminals such as glutamatergic terminals of pyramidal cells, cells that are primarily affected in the neuropathology of AD. nAChRs located at presynaptic terminals of pyramidal cells can modulate the release of EAA (see section 1.7 below) and therefore it is possible that cholinomimetic drugs may provide an additional

therapeutic advantage, in addition to increasing ACh levels, (i.e. improvement of glutamatergic transmission, compromised in AD subjects, via nAChR mediated release of EAA from glutamatergic terminals).

Improvements in attentional and cognitive tasks have been demonstrated in patients clinically diagnosed with AD who have received nicotine by specific injection regimes (Newhouse *et al.*, 1988, 1996) or transdermal nicotine-infused patches (Wilson *et al.*, 1995; Levin & Rezvani, 2002; For review see Newhouse & Kelton, 2000). However, it is of concern whether the cognitive improvements are a manifestation of improved attentional aspects to specific tasks (see Lawrence & Sahakian, 1995). Other nAChR ligands have been assessed (e.g. ABT-418; Potter *et al.*, 1999) for their effects on cognitive function but to date no selective nAChR subtype ligands or indeed nAChR ligands alone have been used in the treatment of AD.

1.1.4.2 Schizophrenia and nAChRs

The most prominent clinical observation supportive of nAChR association with schizophrenia is that of the prevalence of smoking in schizophrenic patients; epidemiological studies have shown that approximately 90% of the schizophrenic population smoke compared to the 30% of the 'general' population (Picciotto *et al.*, 2000). The major hypothesis for such a high prevalence of smoking in schizophrenics is believed to be a form of 'self medication', which may ameliorate attentional and psychological affects of the condition or arising from anti-psychotic drug therapy. Indeed, smoking in schizophrenics improves abnormal smooth pursuit eye movements (Olincy *et al.*, 1998) as well as normalise P50 auditory evoked responses; a measure of brain wave responses when patients are exposed to auditory stimuli, which lack inhibitory control in schizophrenics but not normal

patients (Waldo *et al.*, 1991). In this latter behavioural observation, α7 nAChR located on hippocampal interneurons are believed to be implicated: (1) These neurones are believed to provide the inhibitory control to the response by mediating incoming information from basal forebrain cholinergic neurons (Freedman *et al.*, 1993) (2) Improvement with nicotine in the above response can be blocked by α-bungarotoxin (α-Bgt; an α7 selective antagonist) (Luntz-Leybman *et al.*, 1992). (3) Linkage between a dinucleotide polymorphism on chromosome 15q13-14 which contains the α7 nAChR gene CHRNA7 and deficient auditory gating (Freedman *et al.*, 1997 & 2001). (4) Binding studies also show a marked decrease of [^{125}I]bungarotoxin (α7 nAChR) labelling in the hippocampal formation of schizophrenic post mortem brain as well as in the cingulate cortex (Freedman *et al.*, 1995; Marutle *et al.*, 2001). However, an up-regulation of [^{3}H]epibatidine (possibly α4β2* nAChR) binding in temporal cortex of schizophrenics has been described, suggesting involvement of two different nicotinic receptor mechanisms (Marutle *et al.*, 2001).

As well as attentional improvements, Levin *et al.* (1996) demonstrated improvement in a variety of cognitive tasks in schizophrenics subjected to nicotine administration, that corroborates other reports of impaired cognition in schizophrenics (Hyde *et al.*, 1994; Goldstein *et al.*, 1998).

Schizophrenia is characterised symptomatically into positive and negative symptoms (Positive; psychosis, delusions and hallucinations. Negative; cognitive impairment, and impaired sensory processing). Some of these symptoms are exacerbated with respect to existing treatment strategies for schizophrenia such as haloperidol, but interestingly, haloperidol increases smoking behaviour (McEvoy *et al.*, 1995). The majority of beneficial effects of nicotine specifically improve negative symptoms and

it is believed that nAChR modulation of dopaminergic and glutamatergic neurotransmission, particularly in the frontal cortex provide the means to which nicotine exerts its affect on these negative symptoms (Dalack *et al.*, 1998). Again, presynaptic nAChR could be pivotal in the modulation of these neurotransmitter systems, as well as others (ACh, GABA; for review see Wonnacott, 1997), and therefore the involvement of high and low affinity nAChR in schizophrenia may influence the hypofunctionality of dopaminergic and glutamatergic systems as well as improve the aberrant inhibitory modulation as described in schizophrenia (Freedman *et al.*, 2000).

1.1.4.3 Parkinson's disease and nAChRs

In addition to AD and schizophrenia, changes in CNS cholinergic systems have also been identified in PD, where a loss of cholinergic basal forebrain nuclei has been described in PD post mortem brain tissue (for review see Perry *et al.*, 1995). Indeed the degree of dementia is believed to be directly proportional to the loss of cortical cholinergic markers in PD patients (Perry *et al.*, 1995). Reduced fronto-temporal regional activity in PD patients (measured using cerebral blood flow markers) undertaking cognitive tasks again highlights the importance of basal forebrain cholinergic innervation to this area in aspects of attentional and memory processing (Reid *et al.*, 1990). Similar to the improvement of cognitive tasks in AD and schizophrenia, nicotine treatment to PD patients also improves cognition (Kelton *et al.*, 2000) and therefore although PD, schizophrenia and AD have different underlying cellular and macropathology, it is likely that the loss of cholinergic innervation and lack of nAChR function are a shared feature in mechanisms

contributing to altered attentional and cognitive performance in these diseases (Newhouse & Kelton, 2000).

It is therefore apparent that cholinergic innervation through to hippocampal and cortical areas of the brain are crucial for memory formation as well as certain attentional aspects of cognitive tasks. Supported by lesion experiments and consequent decrements in nAChR binding as well as the use of nAChR antagonists, the nAChR appears heavily implicated in the flow of cholinergic information arriving in these areas of the brain (for review see Sarter *et al.*, 2003). However, these gross anatomical studies convey little information of nAChR subtype specificity mediating these physiologies or of the intricate synaptic circuitry in which the nAChR may be located. In order to address these issues, a more detailed investigative approach is required at the cellular level of anatomy, to which this thesis in part, aims to elucidate.

1.2 nAChR subtypes and expression

1.2.1 nAChR heterogeneity in the vertebrate nervous system

From its historical experimental beginnings as a 'receptive substance' identified at the neuromuscular junction (Langley, 1905) the continued investigation of this substance in various regions of the vertebrate nervous system, eventually classified as a receptor (for review of nAChR history see Lukas *et al.*, 1999), lead to the identification of multiple subtypes of nAChR, composed of a pentameric assembly of different subunits in a region specific manner. The earliest studies of nAChR subunit composition at the site of the neuromuscular junction were aided by the identification of an analogous nAChR found in the Torpedo Electroplax; this species provided an

abundant and accessible source of nAChR for biochemical studies. These studies revealed a difference in composition between those nAChRs at the neuromuscular junction and those found within the central nervous system, the major difference being the inclusion of δ and ε/γ subunits in the neuromuscular junction nAChR compared to the nAChR found in the vertebrate brain that is composed solely of α and β subunits (heteromeric), or α subunits alone (homomeric). Also, the neuromuscular nAChR β subunit shares little homology to the vertebrate brain nAChR β subunit and is sometimes referred to as non-α subunit (See McGehee & Role, 1995).

1.2.2 Different neuronal populations of nAChR within the brain

Further heterogeneity of nAChR within the CNS was suggested from autoradiographical studies of neuronal nAChR distribution. A number of nAChR ligands, examined in the neuromuscular junction and shown to have an affect on neurotransmission, also showed binding properties to rodent brain membranes (Nordberg & Larsson, 1980; Schmidt & Freeman, 1980). However on comparison of radiolabelled nAChR ligands in rat brain sections by autoradiography, a distribution difference was noted between specific ligands; α-bungarotoxin (α-Bgt; a snake toxin from the species Bungarus Multicinctus), originally an important tool for the identification of the ligand-binding domain and structure of the neuromuscular nAChR (Changeux *et al.*, 1970; Raftery *et al.*, 1980), displayed aberrant properties of binding to rat and mouse brain preparations in its iodinated form ([^{125}I]α-Bgt) compared to that of tritiated nicotine or ACh ([^{3}H]Nicotine, [^{3}H]ACh) (Clarke *et al.*, 1985). Radiolabelled nicotine and ACh show very similar distribution patterns (as well as binding affinities to membrane preparations) in the rat brain when examined

by autoradiography and are believed to label the same nAChR (Schwartz *et al.*, 1982; Clarke *et al.*, 1985). However, at the time, controversy surrounded the significance of α-Bgt binding in the CNS: the large size of this toxin (and consequent concerns over it's ability to access synaptic receptors) and its slow onset of binding and inhibition added to the debate. Further, this toxin displayed no antagonistic affects to the central actions of the cholinergic system or nicotine, nor displacing bound [^{3}H]Nicotine (unless at very high concentrations) (Romano & Goldstein, 1980; Schmidt & Freeman, 1980; Clarke *et al.*, 1985). In fact, it appears that if not for one experiment where α-Bgt inhibited the ACh activation of a pineal enzyme in the suprachiasmatic nucleus (mimicking the light induced effects on this enzyme) then CNS α-Bgt sensitive nAChRs may have been forever obscured (Zatz & Brownstein, 1981; See McGehee & Role, 1995). Yet consistent reports of this toxin's ability to bind to rodent brain sections, producing a labelling pattern different to radiolabelled nicotine or ACh (Marks & Collins, 1982; Schwartz *et al.*, 1982; Costa & Murphy, 1984) supported the notion of more than one nAChR subtype in the CNS. By the mid-1980's it was generally agreed that [^{3}H]Nicotine and [^{125}I]α-Bgt bind to two different populations of nAChR, coining the term High and Low affinity nAChRs (Wonnacott, 1986), the latter representing receptors that bind α-Bgt with high affinity.

1.2.3 Further nAChR heterogeneity in the vertebrate CNS

With the advent of molecular cloning techniques, evidence of nAChR subunit heterogeneity amassed, where screening of various brain and PC12 cDNA libraries revealed a number of different subunits (for review see Deneris *et al.*, 1991), that are categorised into two subfamilies, the α-type and β-type; the difference based on the presence of conserved cysteine residues (Cys 192 and 193) on α-type but not β-

type subunits (Karlin, 1993; Karlin and Akabas, 1995). To date, there are thought to be at least 9 subtypes of α-type subunits (α2-α10) and 3 β-type subunits (β2-β4) (Boulter *et al*., 1986; Goldman *et al*., 1987; Deneris *et al.,* 1988 & 1989; Wada *et al*., 1988; Boulter *et al*., 1990; Couturier *et al*., 1990; Elgohoyen *et al.,* 1994 & 2001).

With this development, came the next hurdle of identifying functional nAChRs from the assembly of these identified subunits - what could be thousands of possible permutations. However, co-expression of specific subunits into oocytes of Xenopus laevis, (a common vector for the expression and assessment of function of ligand gated ion channels) coupled with electrophysiological recordings, revealed that only a small number of nAChR subtypes were functional in terms of activation of ionic currents on application of nAChR agonists. It was these experiments that finally highlighted the differences between the α-Bgt binding nAChRs to that of mainstream nicotine-binding nAChRs; nAChRs that bind α-Bgt consist of a homologous pentameric assembly of α7 subunits only (however see Anand *et al*., 1993; Palma *et al.,* 1999; Khiroug *et al*., 2002), are rapidly desensitising, display a high permeability to Ca^{2+} than other nAChRs and are highly sensitive to blockade by α-Bgt (Couturier *et al*., 1990; Bertrand *et al.,* 1992; Seguela *et al.,* 1993; Gopalokrishnan *et al*., 1995; Chen & Patrick, 1997). Similar to α7 nAChR, homomeric nAChRs have also been described for α8 and α9 subunit expression in Xenopus oocytes, however to date the homomeric/heteromeric α8 nAChR is confined to the chick brain (Keyser *et al*., 1993) whereas the α9 nAChR has only been identified in the rat and human cochlear hair cells and rat dorsal root ganglion cells and also displays unusual pharmacology in the form of responses to both muscuranic and nicotinic agonists (Elgohoyen *et al*., 1994). α10 nAChR subunit shares a high homology with α9 (Sgard *et al*., 2002) but does not form a functional nAChR when expressed alone in

Xenopus oocytes. Recent work has demonstrated a possible α9 and α10 heteromer in the rat dorsal root ganglion (Lips *et al.*, 2002).

Receptor Subtype	Subunits	Subunit combinations
Muscle-type	α1, β1, δ, ε, γ	α1,β1, γ, δ (embryonic muscle) α1,β1, ε, δ (Adult muscle)
Neuronal (α-Bgt insensitive)	α2-α6, β2-β4	α2 β2 (Xenopus oocyte) α2 β4 (Xenopus oocyte) α3 β2 (Xenopus oocyte) α3 β4 (Xenopus oocyte) α4 β2 (Xenopus oocyte) α4 β4 (Xenopus oocyte) α6 β2 (HEK cells) α6 β4 (Xenopus oocyte, Chick Retina) α 2α5 β2 (Chick optic lobe) α3 α5 β2 (Xenopus oocyte) α3 α5 β4 (Xenopus oocyte) α3α 6β2 (Xenopus oocyte) α6 β3 β4 (Xenopus oocyte) α3α5β2β4 (Xenopus oocyte) α3α5 β2β4 (Chick ciliary ganglion α3α6β3β4 (Xenopus oocyte, Chick ciliary ganglion) α4α5α6β2 (rat VTA and substantia nigra neurons) α4β2β3β4 (COS cells)
Neuronal (α-Bgt sensitive)	α7, α8	α7 (Xenopus oocyte) α8 (Xenopus oocyte, Chick optic lobe) α7β2 (Xenopus oocyte) α7β3 (Xenopus oocyte)) α7α8 (Chick retina, Xenopus oocyte)
Other (sensory epethelia)	α9,α10	α9 (rat cochlear hair cells, Xenopus oocyte) α9α10 (rat cochlear hair cells, Xenopus oocyte)

Table 1.1. Summary of nAChR subunit combinations. To date nAChRs have been categorised into two main groups, muscle type and neuronal type nAChRs. Vertebrate nAChRs in the hair cells of sensory epithelia do not fall into this classification. Subunit composition of nAChRs have been identified from heterologous expression studies of defined subunit combination and assessed for function in electrophysiological studies or defined from immunoprecipitation studies of native nAChR. Adapted from Millar. (2003)

Functional nAChR have been described for the heterologous pairwise combinations of α2, 3 and 4 subunits with β2 or β4 subunits (for review see McGehee & Role, 1995). In the brain, heterologous nAChRs are believed to arrange in the general

stoichiometry (2α, 3β) (for review see Galzi & Changeux, 1995), with, in many cases, more than one α-type subunit per pentamer (Conroy *et al.,* 1992; Vernalis *et al*., 1993; Wang *et al*., 1996).

Most recently, a study investigating the most prevalent nAChR subtype in the mammalian brain, the α4β2 subtype, described that different stoichiometries of α4 and β2 subunits co-expressed in Xenopus oocytes ($\alpha4_{(2)}\beta2_{(3)}$ or $\alpha4_{(3)}\beta2_{(2)}$ enabled by covalent linking of subunits) display marked differences in both ACh induced currents and sensitivity (Zhou *et al.,* 2003). A summary of heterologous combinations of α and β nAChR subunits is given in Table 1.1 (for review see Millar, 2003), where evidence is derived from heterologous expression studies of nAChR with defined subunit combinations or derived from studies of native nAChR to support nAChR subunit composition.

Developments made in revealing nAChR assembly and function in expression systems underlie our present understanding of native nAChR, however, many of the proposed combinations fail to match the physiological and pharmacological properties of native nAChR measured in neurons. For example, native α7 nAChRs have been described to desensitise more slowly and have a decreased channel conductance compared to recombinant homomeric α7 nAChRs, despite showing remarkably similar pharmacology (Shao & Yakel, 2000; Sudweeks & Yakel, 2000).

1.3 Distribution and localisation of nAChR with respect to cognition

The lack of subtype selective pharmacological tools for the nAChR has hampered the precise pharmacological definition of nAChR subtypes involved with cognition (Lloyd & Williams, 2000). However, the nAChR antagonist sensitivities of particular

cognitive function tests as well as those of electrophysiological assessment of nAChRs in regions of the brain highly associated with cognitive function suggest that both the α7* and β2* containing nAChR are implicated in cognitive functions (For review of cognitive tests see Levin & Simon, 1998) (α7* represents native α7 nAChRs that are possibly heteromeric in nAChR subunit composition).

The distribution of these specific subunits in the brain have been assessed using a variety of techniques that either detect the presence of individual subunits in their encoded form such as in-situ hybridisation or their native form such as immunohistochemistry. These two techniques show only distribution of subunits and inform little about the whole nAChR construct, in the former technique, only the encoded information for the nAChR subunits is detected and therefore does not reveal the amount of nAChR protein expressed.

Detection of whole nAChR subtypes in brain homogenates or tissue sections is characterised using autoradiographical analysis of tritiated nAChR ligands, however, only [^{3}H]Nicotine and [^{125}I]bungarotoxin reveal nAChR subtype specific information in the form of their relative selectivity for α4β2* and α7* containing nAChRs.

Nonetheless, nAChR distribution from ligand binding studies has been demonstrated across a wide range of brain regions in chick, mouse, rat, primate and human brain (Clarke *et al.*, 1985; Pauly *et al.*, 1991;Court & Clementi, 1995; Han *et al.*, 2003). With respect to α7 distribution in the rat brain (the animal model used in this thesis) investigations using the α7 selective ligands [^{125}I]α-Bgt and [^{3}H]methyllycaconitine ([^{3}H]MLA; however see Mogg *et al.*, 2002 for its questioned specificity to α7 nAChR; Segal *et al.*, 1978; Clarke *et al.*, 1985; Fuchs, 1989; Davies *et al.*, 1999; Whiteaker *et al.*, 1999) and α7 transcript riboprobes (Seguela *et al.*, 1993; Dominguez del Toro *et al.*, 1994) have all described similar distribution of the α7 nAChR. Radioligand

binding of these ligands is highest in the cerebral cortex, hypothalamus, inferior colliculus and in certain brain stem nuclei. In particular, layers I and VI of the cerebral cortex (extending to the frontal cortex) and the CA3 region of the hippocampus are particularly dense with labelling. Other regions displaying moderate labelling of tritiated α7 selective ligands include certain areas of the pons and medulla, medial septal nucleus and amygdala (basolateral and medial nuclei). The thalamus and striatum are relatively devoid of labelling, although weak in-situ hybridisation signals were demonstrated (Seguela *et al.*, 1993) reflecting the differences in these two methods of nAChR transcription and ultimate protein expression. This corroborates the work of Fuchs (1989) who reported transitory expression of α-Bgt binding sites in primary sensory areas (i.e. frontal cortex) of thalamic input zones suggesting a particular role of these receptors in cortical connectivity.

With respect to β2 nAChR distribution, nAChRs containing this subunit are very widespread; perhaps a reflection of the number of different types of heterologous nAChR subtypes containing this subunit. The similar labelling patterns of tritiated ligands nicotine and acetylcholine, i.e. high-affinity nAChR agonist binding sites, are believed to encompass those nAChRs containing this subunit due to vast similarities observed with the immunocytochemistry and in-situ hybridisation studies using antibodies to this subunit (Whiting & Lindstrom, 1986; Wada *et al.*, 1989; Hill *et al.*, 1993). These regions include the interpeduncular nucleus, all thalamic nuclei except posterior and intralaminar, superior colliculus and medial (but not lateral) habenula, substantia nigra pars compacta, ventral tegmental area, molecular dentate gyrus, presubiculum and cerebral cortex (in this instance, particularly layers III and IV,

extending to the frontal cortex). Moderate labelling was demonstrated in the neostriatum, ventral striatum, dorsal tegmental nucleus and cerebellum.

There is little indication of vast differences between radioligand binding and in-situ or immunohistochemistry techniques, suggesting the predominantly somato-dendritic nature of β2 containing nAChR location, however, slight discrepancies in immunohistochemistry studies have revealed fine and diffuse staining in particular regions of the brain (e.g. hippocampal molecular layer and striatum; Hill *et al.*, 1993, Jones *et al.*, 2001) that may represent terminal field staining. Indeed electron microscope analysis of β2 nAChR in rat nigrostriatal dopaminergic neurones reveal the presynaptic location of the β2 subunit, lending support to the dendritic and axonal transport of β2 containing nAChR (Swanson *et al.*, 1987; Jones *et al.*, 2001).

It is therefore apparent that common place to the distribution of α7* and β2* subunits, implicated in cognition, are those brain loci common to cognition, namely the hippocampal region and frontal cortex regions of the cerebral cortex, in the latter an apparent dissociation between the two sets of layers exists; I and VI for α7 and III-V for β2 nAChR (Wada *et al.*, 1989, Clarke *et al.*, 1985; Hill *et al.*, 1993; Seguela *et al.*, 1993).

1.4 nAChRs and Acetycholine

1.4.1 A brief history

Acetylcholine (ACh) is arguably one of the founding substances of modern day pharmacology. In the earliest of case studies and unbeknown to the investigator, ACh served as one of the first 'pharmacological tools' used in the understanding of blood pressure control (Hunt, 1895), cardiac function (Loewi, 1926) and

neuromuscular transmission. It was not until 1936 from work by Dale and colleagues that ACh was identified as a neurotransmitter at the skeletal neuromuscular junction. Dale himself dismissed the term 'receptors' as sophistry rather than science, yet the physiological effects of ACh implored the need for defining a 'receptive substance' that could turn a chemical signal into a physiological consequence. With definitive evidence of ACh acting on neuronal nAChRs (for review see Changeux & Edelstein., 1998), the path was then set to then integrate native nAChR function with its endogenous neurotransmitter.

1.4.2 ACh synthesis and cholinergic pathways in the rat CNS

Acetylcholine is synthesised in cholinergic neurons from choline and acetyl-coenzyme A by choline acetylcholine transferase and is packaged into synaptic vesicles by vesicular acetylcholine transporters (VAChT) (Eiden, 1998; for review see Parsons *et al.*, 1993). Therefore on exocytosis of these packed vesicles (ACh concentration approximately 100 mM), ACh synthesis is maintained by active transport of choline (from its subsequent breakdown in the synapse by acetylcholinesterase) by a high affinity choline transporter (CHT). Blockade of this transporter ultimately abolishes ACh production and release suggesting a presynaptic location of this transporter (Haga & Noda, 1973; Simon & Kuhar, 1976; Maire & Wurtman, 1985; Ferguson *et al.*, 2003).

The utilisation of antibodies and riboprobes to the transporter proteins and mRNA of CHT or VAChT have revealed the distribution of cholinergic neurons and their afferent pathways (Woolf, 1991; Descarries *et al.*, 1997; Schafer *et al.*, 1998). The broad distribution of these cholinergic pathways in the rat brain is summarised in Fig. 1.2. Mesulam and colleagues (1983), devised nomenclature that grouped the major

cholinergic cell groups providing long projection systems of the rat brain, termed 'Ch' 1-8.

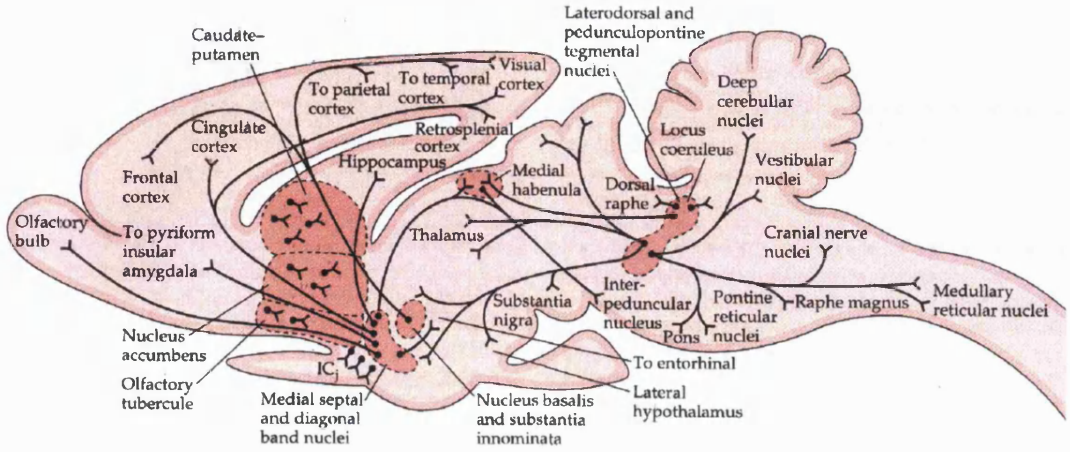

Figure 1.2. Sagital section through rat depicting the major cholinergic pathways. Of particular importance are the forebrain projection pathways originating from the Nucleus basalis and the medial septal and diagonal band nuclei supplying the cortex, hippocampal areas, amygdala and olfactory bulb with cholinergic innervation. (Adapted from Feldman, Meyer & Quenzer. 1997. Principles of Neuropsychopharmacology. Chapter 7.)

The medial septum (Ch1 group), the nuclei of the vertical and horizontal limbs of the diagonal band (Ch2 and Ch3 groups) and the nucleus basalis of Meynert (Ch4 group), make up the basal forebrain cholinergic groups, supplying afferent cholinergic connections to the olfactory regions, entire cerebral cortex (incorporating frontal, parietal, temporal and visual cortices), hippocampal and amygdala regions. One other cholinergic projection from the medial septum to the second major area of cholinergic cell bodies in the diencephalon, the medial habenula, makes up the Ch7 group which together, project to the interpeduncular nucleus. A major cholinergic set of interconnections between the telencephalon and the diencephalon are the lateral dorsal tegmental nuclei and pedunculopontine cholinergic projections (Ch5 and Ch6

groups). These pathways essentially divide into two, that terminate in the thalamus and basal forebrain areas and are believed to be associated with arousal, attention and memory, linking the responsiveness of cortical and thalamic neurons to the sensory stimuli collated from the periphery, collectively known as the ascending arousal system. Other projections from the Ch6 group link this area with the brain stem reticular formation (Mesulam *et al.*, 1983; Woolf *et al.,* 1991; Schafer *et al.*, 1998).

The main projection fields of cholinergic cell groups from the basal forebrain areas are very widespread and encompasses an extrinsic innervation to practically all layers of the cortex and hippocampus and amygdala (Woolf, 1991; Schafer *et al.*, 1998), however an intrinsic level of innervation also exists, revealed by riboprobe hybridisation in cell bodies of these regions, suggesting the possible existence of cholinergic interneurons. Cholinergic interneurons have been well characterised in the striatum (for review see Calabresi *et al.,* 2000) and are predominantly innervated by glutamatergic projections from the cortex and thalamus. Frontal cortex areas also display the presence of these giant neurones (Kawaguchi & Kondo, 2002), although the functional integration of these neurons into synaptic circuitry presently lacks detail.

1.4.2.1 ACh and diffuse neurotransmission

Despite this large degree of cholinergic innervation in the CNS an extremely important observation made from an array of electron microscope studies in various regions of the rat brain revealed that at the very most, less than 10% of all ACh nerve terminals (encompassing axon terminals, boutons or variscosities) made junctional membrane specialisations i.e. hallmarks of synapses (Umbriaco *et al.,* 1994, 1995; For review see Descarries *et al.*, 1997). In fact the majority of ACh

terminals are 'non-synaptic' and thus support a prevailing view that the majority of ACh release might diffuse into the extracellular space over a large spatial and temporal domain to exert its influence.

It is therefore the current opinion that, at least in densely innervated areas of the CNS, an ambient level of ACh is maintained that contributes to the physiological and physiopathological aspects of cholinergic transmission, supported by the inference that AChesterase does not serve the same level of ACh breakdown in neuro-neuronal synaptic transmission as it does at the neuromuscular junction (Constant *et al.*, 1996; Descarries *et al.*, 1997; Sarter & Bruno, 1999). For instance, microdialysis studies have revealed that ACh efflux is uniform across cortical areas rather than cortical area specific, modality specific or task specific (Sarter & Bruno, 1997). However at the cellular level, inferred from electrophysiological studies, the ACh mediated enhancement of selective synaptic effects appears to be with the integration of other converging afferent inputs from other neurotransmitter systems.

In summary, the presence of ACh and cholinergic cell groups appears crucial in the processing of incoming sensory information from the reticular formation, through to the basal forebrain areas, where its detection, selection and discrimination are processed into forms of higher cognitive functions such as memory and retrieval. In fact, aberrations of this cortical cholinergic neuron input contribute to some of the symptoms of cognitive and behavioural symptoms of neuropsychiatric and neuropathological disease as outlined above (section 1.1.4; for review see Perry *et al.*, 1999; Sarter *et al.*, 2003).

The diffuse nature of the cholinergic system and indeed the diffuse release of ACh itself create an inherent problem with respect to the receptors that mediate its

actions, particularly fast actions exerted by ACh in the CNS. In fact one of the leading and unanswered questions in nAChR research is the effect of diffuse volume transmission of ACh on nAChR function, where to date, only the effects of direct synaptic contact and the application of exogenous nAChR agonists (including ACh) have been examined (See McGehee, 2002). What could be the role of such a diffuse transmission? One particularly interesting example is the induction of fast (so-called gamma) oscillations (mainly 30-40 Hz) in both the thalamus and the cortex that are characteristic of brain-activated states in particular attention-requiring tasks (the beginning aspects of information processing). This phenomenon was attributed to a generalised responsiveness of neuronal collectivities from various sources that depend on a diffuse rather than synaptic specific focused transmission (Steriade *et al*., 1991). Therefore a plausible physiological role for the nAChR is that in these heightened states of cholinergic activity, nAChR transduces this information into an increased excitability of the receiving neuronal populations, nAChR could serve to modulate the processing of the incoming information by way of increasing the synaptic strength of the connections that contribute to these gamma oscillations, at either a presynaptic or postsynaptic locus.

1.5 Structural determinants of the nAChR and nAChR ligand binding

To bind and transduce the chemical signal of ACh into a functional application, the nAChR relies on certain elements of its structure.

In gross anatomy, the nAChR is a large glycoprotein complex (approximately 290 kDa) formed from five membrane spanning subunits. Each of the subunits exhibit

significantly high amino acid sequence homology (Le Novere & Changeux, 1995), reflected in their primary structure.

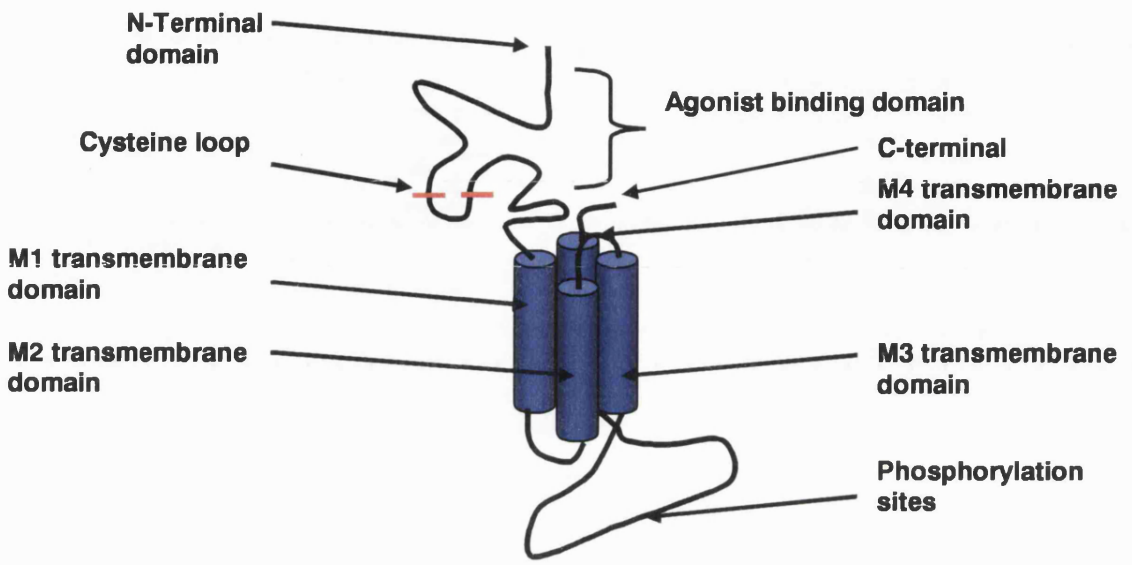

Figure 1.3. nAChR subunit structure. Membrane topology of the individual nAChR subunit, revealing the extracellular N and C-terminus, membrane spanning domains M1-4, the agonist binding domain and cysteine loop (characteristic of the ligand gated ion channel superfamily and the large variable sequence loop linking M3 and M4 that contains a number of phosphorylation sites.

Each subunit, shares the generalised features of: (1) A signal peptide removed from the polypeptide chain during translocation, (2) a large, conserved hydrophilic N-terminal domain containing one or more glycoslylation sites, a 15 residue cysteine loop and a portion of the ACh binding site, (3) A compact hydrophobic domain split into three segments of 19-27 amino acids termed M1, M3 and M4, (4) An ampipathic α-helical M2 domain that lines the channel of the receptor, (5) A large and variable hydrophilic intracellular loop (between 100-200 amino acids in length), found between M3 and M4 containing consensus serine/threonine and tyrosine phosphorylation sites and lastly (6) a small hydrophilic C-terminal segment of around 10-20 amino acids (see Fig. 1.3; Galzi & Changeux, 1995; For review see Corringer *et al*., 2000).

The secondary and tertiary elements of nAChR structure (defined from the Torpedo electrolax nAChR) are still disputed (Hucho *et al.*, 1996; Corringer *et al.*, 2000); structural analysis using Fourier Transform infrared (FTIR) and circular dichroism (CD) suggest different percentages of α-helices and β-sheet conformations of the nAChR, although these methods agree that the majority of the receptor is composed of these structures (Gorne-Tschelnokow *et al.*, 1994; Corbin *et al.*, 1998).

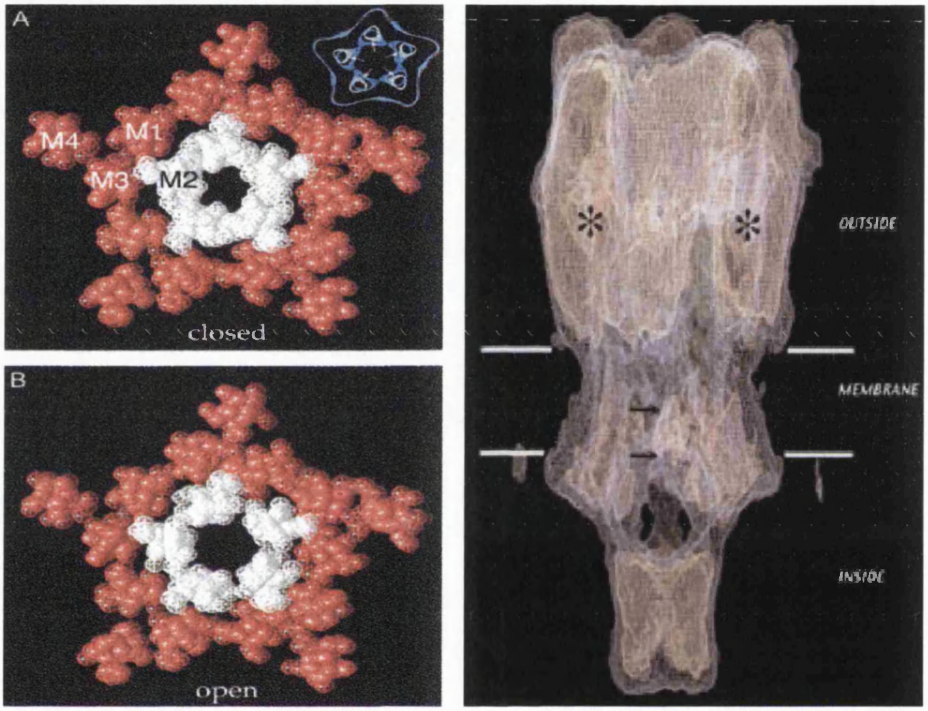

Figure 1.4. Tertiary and quaternary structures of the nAChR from the Torpedo electrolax. (A) and (B), cross sections of the nAChR in the middle of the membrane revealing the closed and open states of the nAChR gate, lined by the M2 membrane spanning segments of each subunit around a fivefold axis of pseudosymmetry (Unwin, 2003). (C) Three dimensional reconstruction of the nAChR based on the electron micrograph analysis of the Torpedo electrolax nAChR at 9 Å resolution; Approximately 170 Å long, of which 65 Å protrudes into the extracellular domain and 20 Å into the cytoplasmic domain (Unwin, 1993)

Photoaffinity labelling experiments have helped elucidate the disposition of the membrane spanning segments in relation to the lipid bilayer for each of the subunits; M4 displays an α–helical like structure based on its label binding properties, which reveals that in all subunits, M4 faces the lipid bilayer (Blanton & Cohen, 1994). M2

faces the ion channel lumen of the nAChR (Hucho *et al*, 1986) and M1 and M3 also bind labels that approach the receptor through the lipid phase (Hucho *et al*., 1996). The first electron microscope studies of the nAChR revealed more elements to the tertiary and quaternary structure, at first suggesting a 5 or 6 subunit structure, shaped like a 'donut' all arranged around a central pore (Nickel & Potter, 1973; Cartaud *et al*., 1973). Since this first observation, much the same has been inferred; the present consensus is that the nAChR is a pentameric structure, made of five subunits arranged in a fivefold axis of pseudosymmetry (Brisson & Unwin, 1985), also confirmed in the neuronal nAChR using quantified radiochemistry (Anand *et al*., 1991). Resolution has been increased to 4.6 Å for the Torpedo electrolax nAChR (Unwin, 1993 & 2003; Miyazawa *et al*., 1999; see Fig. 1.4).

1.5.1 nAChR ligand binding

The ligand binding site for the nAChR has been the subject of renewed attention in light of a recent set of publications revealing the cloning and atomic structural determination of a soluble acetylcholine binding protein (AChBP), derived from and released by the glial cells of the snail *Lymnaea stagnalis* (Smit *et al*., 2001; Brejc *et al*., 2001). This protein shares remarkable homologies to the extracellular domains of both the neuromuscular and neuronal nAChR (it lacks the intracellular ion channel pore domain); a pentameric structure, the presence of binding loops A-F (see below Fig. 5), a disulphide loop between Cys 128 and Cys 142, key conserved aromatic residues, vicinal cysteine residues and the MIR at the top of α-subunits. Smit *et al*, (2001) describe how AChBP is associated with the modulation of cholinergic transmission in response to presynaptically released ACh, essentially suppressing

the postsynaptic action of ACh, as well as demonstrating that this protein can bind several other nAChR ligands with high affinity, including nicotine and ACh.

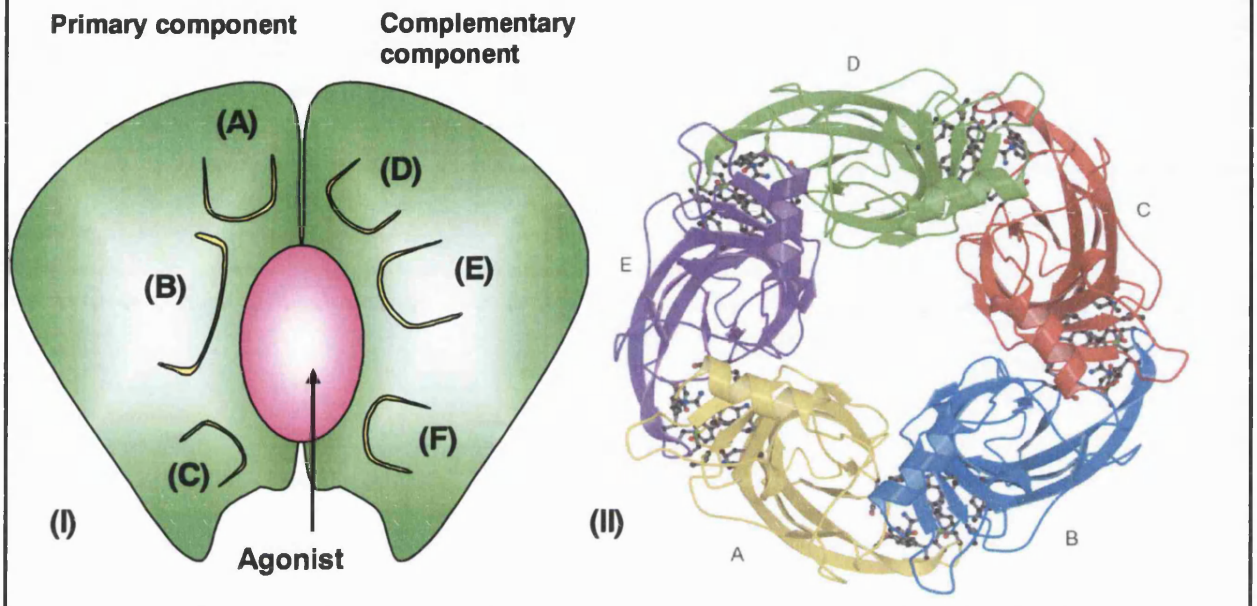

Figure 1.5. Representation of nAChR ligand binding site determined from Torpedo electroplax nAChR (I) and the pentameric structure of AChBP (II). Left diagram. Specific residues involved with nAChR agonist binding are found on loops A-F. Loops A, B and C reside on the primary component (α1 subunit of Torpedo nAChR) and loops D, E and F reside on the complementary component of the ligand binding site (δ/γsubunit of Torpedo nAChR) Residues were identified by affinity labelling and site directed mutagenesis experiments (for review see Corringer *et al.*, 2000). Right picture. Conservation of these loops is preserved in AChBP, where ligand binding (represented as ball-and-stick) exists between the interfaces of each subunit (represented in different colours; adapted from Brejc *et al.*, 2001)

The work by Brejc *et al.* (2001) demonstrated that ACh binding occurs between the interfaces of two subunits, similar to that previously demonstrated using Torpedo electroplax or expression of pairwise combinations of nAChR subunits in cell lines (for review see Corringer *et al.*, 2000). Further to this, Brejc *et al.* (2001) revealed identical binding 'loops', principal (loops A-C; found on the α subunit of the Torpedo electroplax) and complementary (loops D-F found on the δ/γ subunits of the Torpedo electroplax) components of the binding pocket for ACh (See Fig. 1.5). Because the AChBP is a homopentamer, at least 5 ligand binding sites exist for ACh, a predicted

value of binding sites for the neuronal homomeric nAChRs e.g. α7 nAChR (Palma *et al.*, 1996), compared to the two ACh binding sites of the neuromuscular nAChR. One disparity that was presented by Brejc *et al.* (2001) in contrast to the findings of Miyazawa *et al.* (1999), was that ACh appeared to gain access to the binding site from the periphery of the pentamer rather than through the central vestibule.

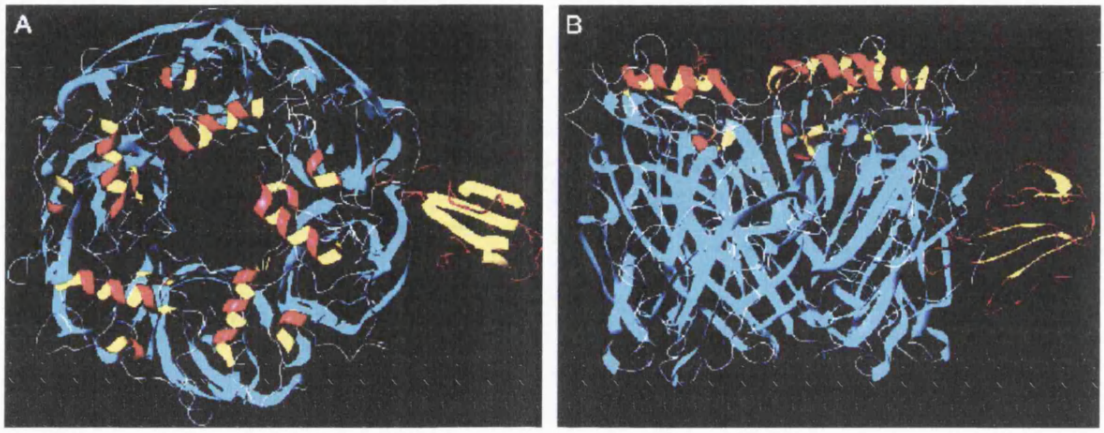

Figure 1.6 3D Structural model of the α7 receptor-αCbtx (cobratoxin) complex. The five subunits of the receptor are depicted with their β-sheets colored blue and the apical helices colored red and yellow. One toxin molecule is shown at an arbitrary subunit interface with its β-sheet in yellow and its backbone in red. (*A*) Top view of the model (*B*) The receptor is seen perpendicularly to the 5-fold axis with the toxin in an equatorial position. Adapted from Fruchart-Gaillard *et al.* (2002)

In a complex assessment of complementary loop F of the wild type and mutated α7 nAChR subunit, expressed in HEK 293 cells, both binding assays and 3D-modelling predictions (based on the AChBP) identified specific residues involved with the binding of snake-neurotoxins and proposed a model for the spatial orientation to which the nAChR-toxin complex binds to the extracellular region of the nAChR (Fruchart-Gaillard *et al.*, 2002; see Fig. 1.6).

1.5.2 nAChR ion gate

The nAChR is an allosteric protein and therefore another main objective in the research of the nAChR ligand binding domain, is its second function; coupling of ligand binding into structural changes of the ion channel pore.

The nAChR channel has three main functions; it moderates the energy barrier for ionic conductance, selects among ions and it opens and closes (Karlin, 2003). Data collected from photoaffinity labelling experiments and mutational analysis have identified that certain amino acids that line the pore of the nAChR contribute to these functions, and that that these amino acids are conserved to each α-helical membrane spanning segment, likely to be the M2 segment of each subunit (Unwin, 1995; Le Novere *et al.*, 1999).

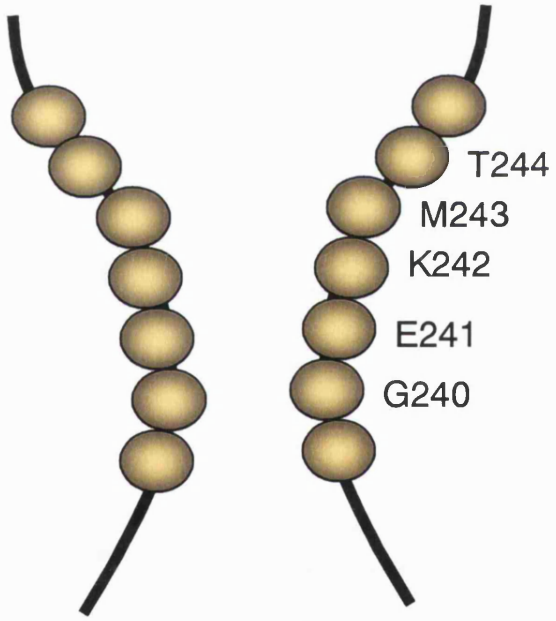

Figure 1.7. Representation of specific amino acid determinants of nAChR ion channel gate defined from mouse muscle type nAChR. SCAM analysis of specific residues within the M2 domain of the nAChR ion channel gate revealed specific hydrophobic interactions of these residues in the closed state. On binding ACh, these hydrophobic interactions are broken and allow for the passage of ions

Use of non-competitive blockers, of which their site of action is believed to be the ion channel pore, helped postulate that these aligned amino acids formed rings of mostly negatively charged residues; an outer, extracellular ring, a cytoplasmic ring and an intermediate ring (inner ring). SCAM (substituted-cysteine accessibility

method) was utilised to assess the mutational effects of M1 and M2 domain amino acids to cysteine, ultimately revealing those amino acids that are exposed to water (Akabas *et al.,* 1994 & 1996; Zhang & Karlin, 1997 & 1998). This data supported evidence from electron microscope studies, in that mutated residues of M2 were exposed to water over its entire length, however in the M1 only one third of the amino-terminal domain was exposed, suggesting that M2 domains form a funnel like structure into the cytoplasm, creating gaps at the pore entrance that exposes residues of the M1 α-helix to water (see also the electron microscopy findings of Unwin, 1993).

Further structural assessment of this 'funnel like structure' using cryo-electron microscopy revealed that a 'kink' existed in the M2 pore lining segments, and that these kinks were inferred to block the channel of the nAChR in the absence of ACh, but then move out of the way on binding ACh (Unwin, 1995). This supported previous mutational data and electrophysiological data (Dani, 1989; Imoto *et al.*, 1991; Konno *et al.*, 1991; Cohen *et al.*, 1992), that a 'gate' existed for the passage of ions depending on the 'open' or 'closed' state of the receptor. However, it required SCAM analysis again to define the currently accepted residues forming this gate, where initial experiments described mutated residues (that would react with water) of the nAChR in the closed state only up until (and including) T244, which lines the beginning of the gate at the intracellular region of the pore. Specific mutations of residues within the proposed gate (M243, K242, E241 and G240) were not exposed to water in the closed state (ACh bound receptor) but on application of ACh, the hydrophobic interactions of these residues between subunits were broken and allowed for the passage of ions (see Fig. 1.7; Pascual & Karlin, 1998; Wilson & Karlin 1998)

1.5.3 Ionic selectivity of the nAChR

Except for the anion selective invertebrate nAChR (Takahama & Klee, 1990), all known nAChRs are cation selective, for both monovalent and divalent ions where in neuronal nAChRs, compared to neuromuscular nAChRs, a particular high permeability to Ca^{2+} is displayed, particularly that of $\alpha 7$ nAChR where its p_{Ca}/p_{Na} ratio (the ratio of Ca^{2+} permeability relative to Na^{+}) is 20 (For comparison of p_{Ca}/p_{Na} ratios of neuronal nAChR see McGehee & Role, 1995). The selectivity to ions seems again to be from inherent residues located on the M2 domain of the nAChR, where mutations particularly in the intermediate rings of negative charge or polar residues in this region reduce or abolish cation conductance and even in some cases cation selectivity (Imoto *et al*., 1988; Leonard *et al*, 1988; Cohen *et al*., 1992). Mutations of two adjacent rings of leucines (Leu-254 and Leu-255) at the synaptic end of the M2 domain selectively reduces calcium permeability without affecting other properties of the nAChR (such as inactivation or desensitisation) suggesting that these particular amino acids are pertinent to calcium conductance through the nAChR (Bertrand *et al*., 1993). One notable example for their meticulous efforts and surprising findings is the work of Corringer *et al*, (1999), where by, implicating three changes to the M1-M2 loop and M2 of the $\alpha 7$ nAChR (removal of the negative residues of the intermediate ring, lengthening the M1-M2 loop and substitution of Val13 in the wider part of the channel to threonine) had the effect of changing the receptor cation selectivity to anion selectivity.

All together, these data highlight the contribution of the M2 domain to ion selectivity and transport, however as highlighted above, the conformational changes that convert ligand binding into ion conductance are still today of much attention in nAChR research. A recent publication by Unwin. (2003), explicitly details the

conformational changes induced by β-sheets on binding ACh (structures that compose the majority of the ligand binding domain of the nAChR) that are communicated through to the α-helices of the M2 that break apart the hydrophobic interactions of the gate, allowing for ion passage.

1.6 nAChR and desensitisation

Mutational analysis of the nAChR in a variety of residues within and outside of the M2 domain and their consequent effects on ionic conductance support the notion that the nAChR is subject to a series of structural changes on binding ACh or other nAChR ligands, thus supporting the notion first suggested by Monod and colleagues (1965) that the nAChR isomerises between a number of structural conformations in the absence, presence and persistence of binding ligand.

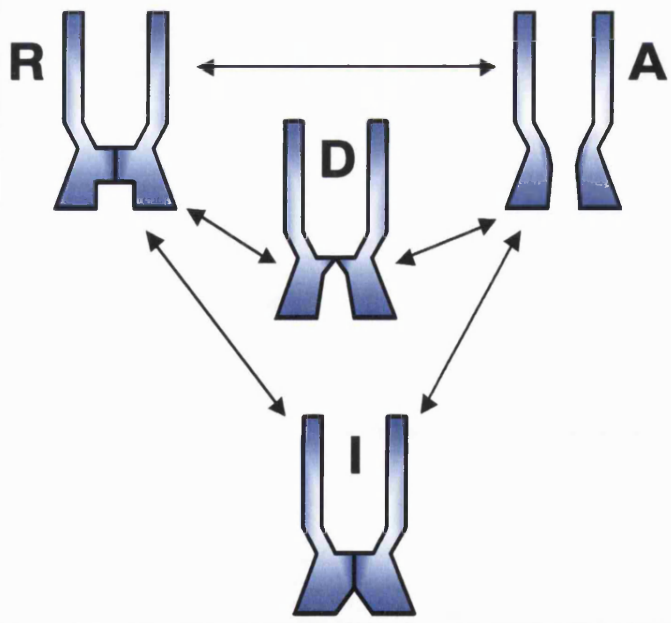

Figure 1.8. Diagram representing the minimal four state model of allosteric transitions of the nAChR (adapted from Galzi & Changeux, 1995). From rapid mixing experiments performed on Torpedo membranes rich in nAChR, a model with a minimum of four transition states was proposed. R is the low affinity resting state that occurs in the absence of agonist, A represents the active receptor state and D and I are the desensitised states.

These different theoretical conformations were generalised into a minimum of four allosteric interconvertible transitions of the receptor (see Fig. 1.8), termed the

'concerted model'; an active state A, where the channel opens and possesses a low affinity for ACh (60-100 μM), two desensitised states I and D, which are refractory to activation, exhibit a high affinity for agonists (I;10 μM. D; 10 nM), that represent the quickly and more slowly desensitised states of the receptor respectively and lastly, the R state, the resting state of the receptor of low affinity to agonists occurring in the absence of agonist and where competitive antagonists are supposed to selectively bind (Galzi & Changeux, 1995).

Because these transformations are dependant on the local concentration of ligand this model therefore implies that in certain physiological conditions, release of ACh at the synaptic cleft will first stabilise the A state (due to high concentrations of ACh) prior to slowly stabilising the I and D desensitised states. These latter two states would then ultimately regulate the amount of nAChR in the R state depending on the level of ACh in the synaptic environment.

In terms of channel opening times, the rate of desensitisation onset is therefore a crucial property in the regulation of ion flow through the receptor, necessary for the prevention of repetitive stimulation of the receptor and ionic exocytotoxicity of the neuron.

The rate of desensitisation can vary dependent upon the subunit composition of the nAChR (for review see Quick & Lester, 2002). Homomeric α7 nAChR undergo rapid desensitisation upon high concentrations of agonist. In fact, of all the nAChRs, this receptor displays the fastest desensitisation time constant, where single cells from hippocampal neurons (Alkondon & Albuquerque, 1991), ciliary ganglion cells (Zhang *et al.*, 1994) and cortical neurons (Kawai & Berg, 2001) report a single exponential component in α-Bgt sensitive currents of around 20 ms. Interesting observations by

Papke *et al*, (2000), from recordings of α-Bgt sensitive currents of hypothalamic neurons, propose that this nAChR receptor desensitisation properties depends on fractional agonist occupation (of the five sites available; Palma *et al*., 1996), where complete receptor binding site occupation, enabled in high agonist concentrations, permit rapid and complete desensitisation whereas in low agonist concentrations (low receptor binding site occupancy) a prolonged channel opening state exists (100 ms). However, heteromeric assemblies of α7 incorporating the β2 subunit, such as the α7β2 nAChR expression study in Xenopus oocytes, report almost a two-fold slower desensitisation time constant than homomeric α7 nAChR assembly in these cells (Khiroug *et al*., 2002).

Of the heteromeric assemblies of nAChR, much of the data revealing desensitisation properties has been obtained from a combination of binding assays and electrophysiology studies, where these two approaches, particularly with respect to the desensitised affinity states of the nAChR, should produce equivalent results. Indeed, nicotine displacement by the high affinity broad spectrum nAChR agonist [^{3}H]epibatidine in rat CNS tissue is biphasic, revealing two sites of high affinity (K_d approx 3-5 nM) and moderate affinity (K_d approx 90-250nM) (Perry & Kellar, 1995; Whiteaker *et al*., 2000). The high affinity component likely reflects α4β2* nAChR binding whereas the more moderate affinity nAChRs putatively contain α3* subunits. Moreover, IC50 values for desensitisation of functional channels of α4 and α3* nAChRs are in the same range as their binding K_d's (0.1-10 nM for α4* and 150-400 nM for α3*; Hsu *et al*., 1996; Fenster *et al*., 1997; for review see Quick & Lester, 2002).

In heteromeric assemblies of non-α7 nAChR, α-subunits and β-subunits display slower desensitisation time constants than the homomeric α7 nAChR. Summarised

by Fenster *et al.* (1999) desensitisation kinetics of the heteromeric nAChRs was ordered (from fastest to slowest) $\alpha3\beta2 > \alpha4\beta2 > \alpha3\beta4 > \alpha4\beta4$, thus reflecting the structural importance of both heteromeric assembly and the inherent properties of the α and β subunits themselves. Presently, β-subunits ($\beta2/\beta4$) have been shown to dramatically influence the rate of onset of desensitisation, where $\beta2^*$ containing nAChR desensitise faster than $\beta4^*$ containing nAChR (Fenster *et al.*, 1997; Wang *et al.*, 1998; Boulter *et al.*, 2001).

1.6.1 Physiological significance of desensitisation

At this point, attention needs to be drawn to two aspects presented above in the introduction: (A) receptors heavily implicated in working memory and the frontal cortex, (the $\alpha7^*$nAChR and the high affinity nAChR $\alpha4\beta2^*$ nAChRs) and (B) the concept of diffuse transmission of ACh (see section 1.4.2.1) with respect to the desensitising properties of these receptors. Because these receptors are either rapidly desensitising ($\alpha7$ nAChR) or have a high affinity for ACh ($\alpha4\beta2^*$ nAChR) then in an environment of diffuse ACh, these receptors are likely to be, in the majority, desensitised. Desensitised nAChRs have been reported to potentiate certain forms of synaptic plasticity, exampled in the rat hippocampus where MLA (an $\alpha7$ nAChR antagonist) mimicked the nicotine-induced potentiation of LTP, inferring that desensitised nAChRs are implicated in this process (Fuji *et al.*, 2000). As well as this, desensitisation of nAChRs, in the presence of chronic nicotine, is purported to lead to the up-regulation of nAChR (Fenster *et al.*, 1999).

The physiological significance of persistent desensitised states of nAChR in the frontal cortex remains unanswered. In this configuration, nAChRs are unlikely to augment an increase in either neurotransmitter release from the presynaptic terminal

or an increase in cell excitability via activation at the postsynaptic membrane, therefore their normal physiological role may be to prevent over-excitation in response to increased cholinergic activity from the basal forebrain areas, selectively filtering certain aspects of information processing to specific higher modalities of the CNS. Alternatively, with little information of the exact concentration of ACh within the synaptic environment of nAChR, these nAChRs could change their conformation from a desensitised state to an active configuration from only slight increases in ACh concentration in response to increased cholinergic activity, thereby desensitised nAChR acts as 'coincidence detectors' to increased cholinergic activity. In support of this possibility, Rogers & Sargent (2003) demonstrate that ACh released from nerve terminals of the chick ciliary ganglion can induce increases in calyceal nerve terminal calcium concentration, mediated by presynaptic $\alpha 7$ nAChR.

1.7 nAChR and neurotransmitter release

The majority of nAChR characterisation, from subunit expression to structural quantification is determined from nAChRs located on somatodendritic membranes. Because of this location, ionic currents and other intracellular events can be easily recorded in an electrophysiological or spectroscopic paradigm. Yet as highlighted in Section 1.3, above, nAChRs are also located on the presynaptic terminal, made directly evident from electron microscopy studies in the guinea pig frontal cortex, rat hippocampus, auditory cortex and basal ganglia (Hill *et al.*, 1993; Lubin *et al.*, 1998; Jones *et al.*, 2001; Fabien-Fine *et al*, 2001; Levy & Aokie, 2002). Functional studies, preceding the recent electron microscopy data, from intact synapses in-vivo, newly formed synapses in vitro and from biochemical isolates of presynaptic terminals (Wonnacott, 1997; MacDermott *et al.*, 1999), also define a presynaptic locus by

modulating neurotransmitter release in a Ca^{2+}-dependent and tetrodotoxin insensitive manner. Notably, the very first study that presented the case for presynaptic receptor modulation of neurotransmitter release was the discovery that ACh could modulate its own release from preganglionic sympathetic neurons (Koelle, 1961), nowadays termed 'autoreceptor' regulation.

Since then, presynaptic nAChRs have been described to modulate the release of other neurotransmitters other than ACh, including dopamine (DA) noradrenaline (NA), 5-hydroxy-tryptamine (5-HT), γ-aminobutyric acid (GABA) and glutamate. The release of these neurotransmitters can be detected either directly by analysis of perfusate from the tissue source (superfusion, amperometry, microdialysis) or indirectly by measurement of postsynaptic effects of neurotransmitter release (generally whole cell recordings in an electrophysiology paradigm or spectroscopic detection of increases in intracellular Ca^{2+}). In general, direct analysis of nAChR-evoked neurotransmitter release has been demonstrated for monaminergic neurotransmitters DA and 5-HT, whereas indirect analysis of neurotransmitter release has been, in the majority demonstrated for excitatory amino acid release (glutamate). The release of inhibitory neurotransmitter GABA evoked by nAChR agonist has been detected by both methods.

1.7.1 Direct detection of nAChR-evoked neurotransmitter release: Measuring glutamate release

Superfusion has served as one of the most utilised methodologies for the direct detection of nAChR-evoked neurotransmitter release (for review see Raiteri & Raiteri, 2000). Brain preparations, either synaptosomes or slices, are commonly loaded with exogenous radiolabelled neurotransmitter and then placed within a

chamber on top of a filter bed (see Chapter 2, Methods section 2.7). Physiological buffer medium is then perfused over the tissue and the perfusate is collected in timed aliquots. After establishing a basal release of radiolabel, the buffer medium is switched to agonist containing medium (in this thesis either depolarising agents or nAChR agonists or both) and then back to the physiological buffer medium after a timed period for the remainder of the experiment. Incorporation of antagonists into the physiological buffer can also be used to assess the pharmacological identity of nAChR-evoked release in conjunction with agonist sensitivities of evoked neurotransmitter release. After the experiment has ended, each aliquot containing radiolabelled perfusate is counted on a scintillation counter and results determined appropriately. Within one experiment, up to 6 different conditions can be assessed on the standard superfusion apparatus (see Chapter 2, Methods section 2.7.1) although a recent adaptation to a 96 well plate has enabled a high throughput assay for the detection of nAChR-evoked release of dopamine and noradrenaline (Anderson *et al*., 2000; Puttfarcken *et al*., 2000).

Despite this relatively straightforward approach for the examination of neurotransmitter release, direct detection of glutamate release (or EAA release) via nAChR activation has eluded demonstration (discussed below), whereas superfusion analysis of nAChR-evoked release of other neurotransmitters has provided a good deal of information with respect to nAChR subtype association and mechanism of release. In particular, the nAChR-evoked release of dopamine from the rat striatum has been extensively studied using this method from our own laboratory, and has provided pharmacological evidence for nAChR heterogeneity at the presynaptic terminals, inferring the presence of $\alpha3(\alpha6)\beta2^*$ containing nAChR on dopaminergic striatal terminals as well as a Conotoxin MII insensitive,

mecamylamine sensitive component, presumably α4β2* containing. (Kaiser *et al.*, 1998; Sharples *et al.*, 2000; Mogg *et al.*, 2002). Superfusion techniques have also revealed that nAChR evoked dopamine release is both Ca^{2+} and Na^{+} dependent (by incorporation of Ca^{2+} and Na^{+} channel blockers into the perfusion medium), specifically revealing an association with P/Q and N-type Ca^{2+} channels (Soliakov *et al.*, 1995; Soliakov & Wonnacott, 1996). More recently, nAChRs (α3β2* containing) have been shown to possibly couple to these channels (Kulak *et al.*, 2001).

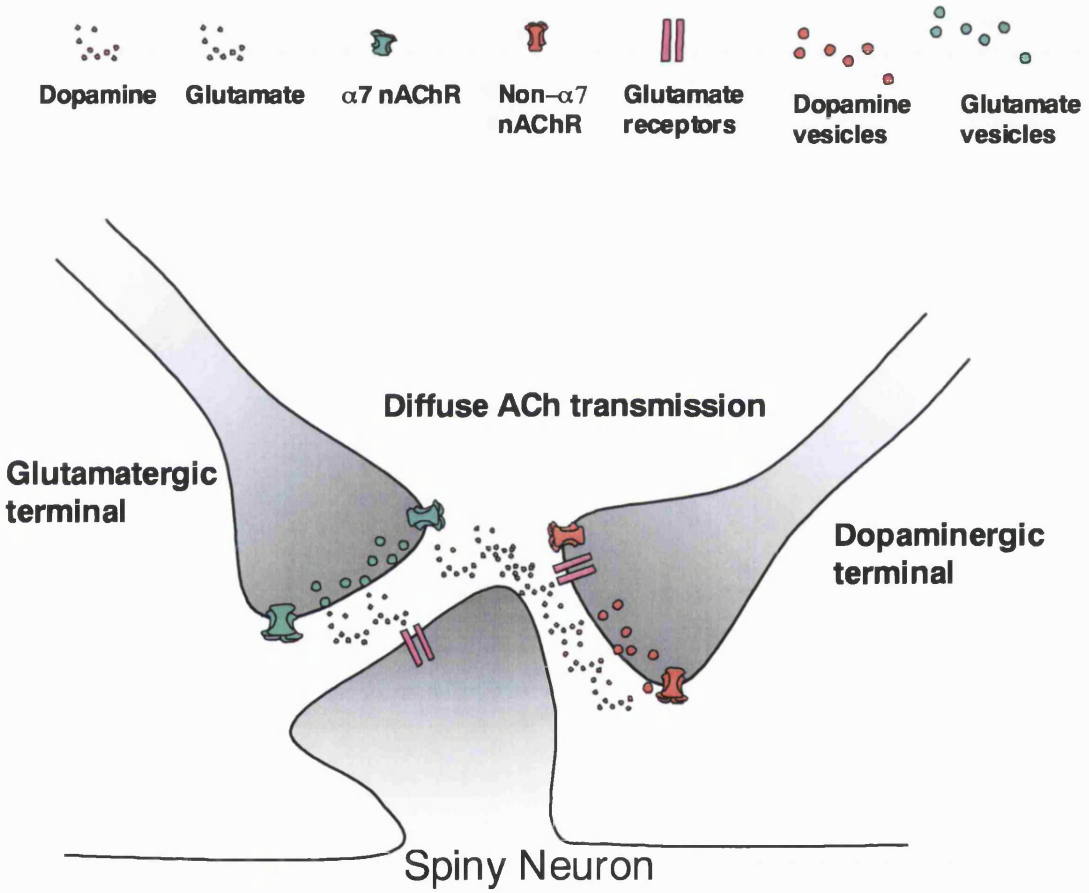

Figure 1.9. Model of the indirect nAChR-evoked release of DA from dopaminergic terminals of the striatum. Diffuse transmission of ACh within the rat striatum activates α7 nAChR on glutamatergic terminals making synaptic contact with spiny neurons. In turn, α7 nAChR activation elicits glutamate release, which activates glutamate receptors located on dopaminergic terminals, evoking dopamine release. Dopamine release can be evoked directly by non-α7 (α6β2*) containing nAChR on these terminals. Adapted from Kaiser & Wonnacott, 2000

However, one interesting feature to the pharmacological analysis of nAChR-evoked dopamine release, and of relevance to this thesis, was the revelation of a α7 nAChR component, demonstrated in rat striatal slices but not in synaptosomes (see Fig. 1.9; Kaiser & Wonnacott, 2000). In consideration of the complexity of examining slices over synaptosomes, these authors inferred that this component of nAChR-evoked dopamine release was the result of activating α7 nAChRs located on glutamatergic terminals in the striatum (the facilitation of dopamine release could be blocked by α7 nAChR antagonists and iGluR antagonists). In turn, this would release glutamate that acted upon ionotropic glutamate receptors of dopamine terminals to elicit dopamine release.

This study provided the first indirect evidence for nAChR evoked release of glutamate using a superfusion paradigm, which, until now has eluded direct demonstration using superfusion on the notion that this method lacks the fast application and high temporal resolution required for the detection of EAA release.

In spite of this, Marchi *et al*, (2002) reported the direct detection of nAChR evoked glutamate release using superfusion (modelled by using [^{3}H]D-aspartate as a surrogate for glutamate) in the rat striatum. These authors report a α7 nAChR-mediated, Ca^{2+}-dependent release of [^{3}H]D-aspartate when nAChR agonists were combined with a depolarising agent (KCl 12 mM), however, nAChR agonists applied alone did not facilitate release (See Chapter 3 Section 2). Perfusion rates in this study were increased to almost twice the rate used to detect nAChR evoked dopamine release in attempt to override the efficient uptake systems utilised for glutamate as well as prevent nAChR desensitisation by increasing the time resolution of agonist application. However the success of this investigation was based on the assumption that nAChR activation enhanced the release evoked by

KCl by increasing the preterminal Ca^{2+} concentration, thereby increasing the probability of vesicular exocytosis, analogous to the inferences made from nicotine enhancement of glutamate release in the hippocampus (Gray *et al.*, 1996; Sharma & Vijaraghavan, 2003).

Microdialysis provides another means of direct detection of neurotransmitter release revealing a more in-depth analysis of the possible inter-circuitry connections that might influence endogenous nAChR-evoked neurotransmitter release. However, in contrast to superfusion techniques, expediency is hampered by low throughput and lengthy procedures of neurotransmitter analysis (such as HPLC analysis of dialysate), has poor temporal resolution and is impractical for detailed dose-response relationships. Nonetheless, this technique has revealed nAChR-mediated release of ACh, NA, DA, 5-HT and glutamate in a number of brain regions and implicating a variety of nAChR subtypes. The majority of microdialysis studies have examined the nAChR modulation of DA release in the basal ganglia and associated structures (Marshall *et al.*, 1997), corroborating superfusion data inferences, and with the use of nAChR gene knockout animals, have recently provided new information on the contribution of β2 and α4 subunits to the nAChR subtype(s) contributing to DA release (Picciotto, 1998; Marubio *et al.*, 2003).

Microdialysis analysis of nAChR evoked glutamate release has implicated α7* nAChR subtype in the ventral tegmental area (VTA), nucleus accumbens and striatum (Toth *et al.*, 1992; Reid *et al.*, 1997; Reid *et al.*, 2000; Schilstrom *et al.*, 1998 & 2000). These latter studies report increased glutamate levels evoked by nicotine, which is blocked by nAChR antagonists mecamylamine, α-Bgt and MLA and is Ca^{2+}-dependent. However, in contrast to this, in the nucleus accumbens, which receives prominent glutamatergic innervation from limbic structures, it was

reported by Reid *et al.* (2000), that the nicotine-evoked release of glutamate appeared to be Ca^{2+}-independant, where the glutamate transport inhibitors (L-trans-pyrrolidine-2,4-dicarboxylic acid; PDC) inhibited the nicotine-induced release, indicating a novel mechanism of nAChR modulation of release. Microdialysis studies of nAChR-mediated glutamate release in the frontal cortex are few in number, however, Gioanni *et al.* (1999) demonstrated nicotine-evoked release of glutamate in the prelimbic (Prl) area rat of the frontal cortex, which was Ca^{2+}-dependent and sensitive to the β2* preferring antagonist dihydro-β-erythroidine (DHβE). Although no α7 nAChR specific antagonists were applied in the microdialysis paradigm, MLA at high concentrations (100 nM) applied to slices of the Prl prevented the facilitation of glutamate release examined by electrophysiology.

Other direct evidence for the implication of α7 nAChR in the modulation of glutamate release comes from cell culture studies. Cortical cultures and cerebellar cultures released glutamate (and aspartate; assessed by either HPLC or scintillation counting of exogenously loaded [^{3}H]D-aspartate) when exposed to nicotine or ACh, in a Ca^{2+} -dependant manner (Beani *et al.*, 2000; Lim *et al*, 2000: Lopez *et al.*, 2000). Beani *et al.* (2000) reported a poor facilitation of [^{3}H]D-aspartate release by nicotine or ACh when these drugs were applied alone to cortical cultures, but when concomitantly applied with electrical stimulation a more robust and pharmacologically definable response was produced, implicating both α7 and β2* nAChR in the facilitation of EAA release. These reports examining cell cultures fail to define the mechanism of nAChR-evoked release, but again implicate the possibility that nAChRs are in someway associated with glutamate transporter function: glutamate transport activity of glial cells was reduced, NMDA responses of cerebellar granule cells were increased after exposure to nicotine and cortical cells display a large calcium

independent component of nicotine-evoked glutamate release (Lim *et al.*, 2000; Lopez *et al.*, 2000).

Direct methods of detecting glutamate release reveal a presently unclear picture of the nAChR subtype-association and mechanism of release, however, the fast kinetics of α7 nAChR activation/desensitisation and glutamate release/uptake per se are more suited for detection in a system that pertains the ability to detect these types of changes, i.e. electrophysiology.

1.7.3 Indirect detection of nAChR-evoked neurotransmitter release

The majority of studies that have provided evidence for the nAChR facilitation of glutamate release have utilised an electrophysiological paradigm. These studies have demonstrated the presynaptic release of glutamate by examining the post-synaptic responses of glutamate acting upon ionotropic receptors, such as miniature excitatory postsynaptic potentials (mEPSPs) or evoked excitatory postsynaptic currents (eEPSCs). These events are mediated by the activation of ionotropic glutamate receptors and can be pharmacologically defined by blockade of these responses in the presence of glutamate receptor antagonists such as DL-2-amino-5-phosphonopentanoic acid (DL-AP5) and 6-cyano-7-nitoquinoxaline-2,3-dione (CNQX).

mEPSPs are small depolarisations in the post synaptic neuron that are the result of quanta of transmitter release by spontaneous fusion of vesicles at nerve terminals, independent of action potentials arriving at the presynaptic terminal (Katz & Miledi, 1967). The physiological significance of mEPSPs, originally thought of as 'synaptic noise' has gained renewed attention in a series of experiments by Sharma & Vijaraghavan (2003), where presynaptic nAChR activation can increase both the

frequency and amplitude of nicotine-evoked mEPSPs. These events are shown to drive the postsynaptic neuron above its firing threshold, ultimately resulting in efficient impulse propagation. mEPSPs have frequently been observed in both rodent CA1 and CA3 regions of hippocampal slices and from hippocampal neurons in culture (Gray *et al.*, 1996; Radcliffe & Dani, 1998; Ji *et al.*, 2001; Alkondon & Alburquerque, 2002; Maggi *et al.*, 2002) as well as at the synapse of the medial habenula and interpeduncular neurons and the synapse of olfactory bulb and amygdala neurons (McGehee *et al.*, 1995; Alkondon *et al.*, 1996; Girod *et al.*, 2000; Girod & Role, 2001; Covernton & Lester, 2002).

All of these experiments report the nAChR facilitation of glutamate release to be Ca^{2+} dependant, TTX insensitive and sensitive to α7 nAChR specific antagonists (α-Bgt and MLA), inferring predominantly that α7 nAChR governs the presynaptic release of glutamate. However, in the frontal cortex, virtually no pharmacological evidence exists for α7 nAChR and their involvement with glutamate release (Vidal & Changeux, 1989; Vidal & Changeux 1993; Vidal, 1996; Gioanni *et al.*, 1999; Lambe et al., 2003) Gioanni *et al.* (1999) are the only group to report MLA inhibition of nAChR mediated facilitation of glutamate release on to prelimbic frontal cortex neurons, although the concentration used (100 nM) is unlikely to be selective for α7 nAChR. One of the first investigations postulating the involvement of presynaptic nicotinic receptors in the rodent brain was carried out in the rat prefrontal cortex (Vidal & Changeux, 1993). These authors reported an increase in amplitude of eEPSC in pyramidal cells located in layers II and III of the rat PFC when nicotine or ACh was applied iontophoretically, which could only be inhibited by the non-α7

nAChR antagonists DHβE and neuronal bungarotoxin, thereby implying that β2* containing nAChRs modulate this type of presynaptic release of glutamate.

eEPSCs are the result of 'stepping' the postsynaptic membrane potential via depolarising voltage increments or by stimulation of afferents serving the postsynaptic neuron (e.g. Schaffer collateral afferents serving a postsynaptic pyramidal cell in CA1 of the hippocampus). Essentially this serves to increase the membrane potential above firing threshold where increases in amplitude or duration of postsynaptic responses are easily recorded and defined into NMDA or non-NMDA components. Both the amplitude and duration can be modified dependant upon the level of presynaptic input to that neuron. Similar to the study of Vidal & Changeux, (1993), the enhancement, in terms of amplitude, of eEPSCs was demonstrated in cultured hippocampal neurones making autaptic connections (Fisher & Dani, 2000). However, these authors went on to further demonstrate that this increase in amplitude, evoked by presynaptic release of glutamate, was only in the non-NMDA component of the eEPSC. By inhibiting the action of calmodulin postsynaptic nAChR activation reduced the responsiveness of the NMDA component of the eEPSC via a calmodulin-dependent mechanism. This gave rise to the possibility that nAChRs, particularly α7 nAChRs, could modulate glutamate transmission in the hippocampus at both the pre and postsynaptic membrane respectively. Indeed, postsynaptic nAChRs on hippocampal neurons and interneurons have been identified for some time and have been categorised into four groups based on their current kinetics and pharmacology (See Chapter 3 section 3). Of these groups type IA serves as the most frequently identified nAChR current in both sets of neurones and is likely to include α7 subunits (Alkondon & Alburquerque, 1993; Alburquerque *et al.*, 1996; Alkondon *et al.*, 1998; Frazier *et al.*, 1998).

It is therefore a common theme from these studies that the nAChR exerts an influence on glutamatergic transmission, so much so that LTP, the cellular model of memory, can be induced by ACh or nicotine, dependent on the timing and location of nicotinic activity (Mansvelder & McGehee, 2000; Ji *et al.*, 2001; For review see McGehee, 2002). Indeed the most noteworthy observation from the studies of presynaptic α7 nAChR mediated release of glutamate, is that the effect of nicotine or ACh is long-lasting (up to 40 minutes in the absence of nicotine or ACh), particularly that of eEPSCs recorded in pyramidal cells of the hippocampus (Radcliffe & Dani, 1998; Dani & Fischer, 2000; Fuji *et al.*, 2000; Ji *et al.*, 2001) and in the VTA (Mansvelder & McGehee, 2000), suggesting that activation of presynaptic nAChR can substitute for presynaptic stimulation usually required for LTP induction. As well as the evidence for glutamate release in mature developed hippocampal circuits and in cultures, brief application of nicotine or ACh to immature glutamatergic synapses of hippocampus from newborn rats can convert 'silent' synapses, that exhibit no mEPSPs, into functional ones (Maggi *et al.*, 2002). This study went on to infer that activation of presynaptic α7 nAChRs that release glutamate contribute to the maturation of the functional synaptic contacts of the developing hippocampus.

In summary, electrophysiology has provided substantial evidence for the nAChR-evoked release of glutamate from presynaptic terminals, mainly via the activation of α7 subunit containing nAChR, although in the frontal cortex evidence is only provided for non-α7, possibly β2*-containing nAChR. Therefore it is plausible that different subtypes of nAChR are distributed in a region specific manner, or indeed cell specific manner.

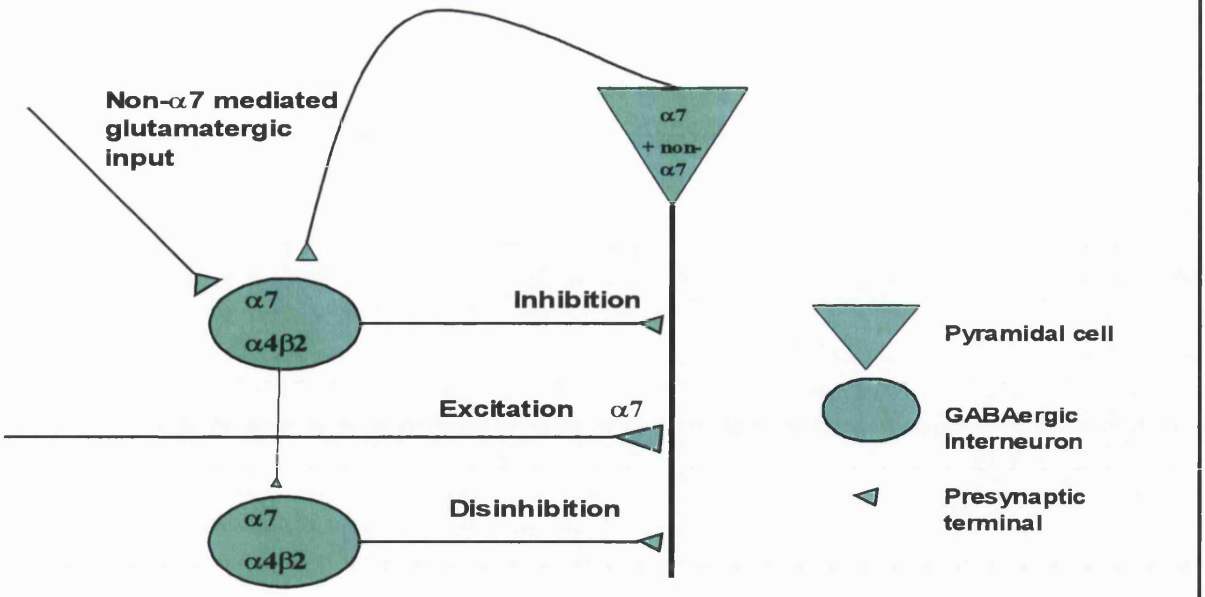

Figure 1.10. Representative circuit diagram of nAChR modulation of hippocampal activity. α7 nAChRs modulate the release of glutamate from presynaptic terminals and the excitation of postsynaptic membranes. α7 and α4β2 nAChRs also modulate the excitability of pyramidal cells, but also regulate inhibitory neuron activity. Evidence also exists for a non-α7 modulation of glutamate release onto inhibitory neurons (Adapted from Alkondon & Albuquerque, 2002)

In support of the latter, it has been recently made evident that certain hippocampal interneurons (in the CA1 region) receive non-α7 mediated glutamatergic input (Alkondon & Alburqeurque, 2001) and therefore the different properties of subtypes of nAChR (α7 or non-α7) as well as their location (on inhibitory terminals or excitatory terminals) may exert an influence on the overall activity (excitation or inhibition) of the output neurons (see Fig. 1.10). It is therefore the goal of current nAChR research to determine the precise definition of nAChR subtype and location within synaptic circuitry in different regions of the brain in order to understand how the cholinergic system and/or nicotine may exert its influence in learning, memory and addiction.

1.8 Thesis aims and objectives

A substantial body of evidence supports the α7 nAChR-mediated release of glutamate from presynaptic terminals from various regions of the brain. However this has not been reported in the frontal cortex, despite one small and overlooked observation of MLA inhibition of glutamate release in this area (Gioanni *et al.*, 1999). Electron microscopy analysis has only confirmed the presence of α7* nAChR on presynaptic terminals of the guinea pig frontal cortex but not β2* nAChR, although the presence of β2* nAChR on presynaptic terminals has been confirmed elsewhere. nAChR subtype distribution studies support the presence of both α7* and β2* nAChR in the frontal cortex, and interestingly, their distribution appears separated across the layers of the frontal cortex. It is therefore likely that the failure to observe 'α7 nAChR-like' modulation of glutamate release, an arduous task in the very least, may be the result of the position in which recording probes and/or stimulating probes are placed, indeed electrophysiological recordings have only positioned these probes in layers II-V where β2* nAChR has been identified in autoradiographical analysis.

To address this disparity this study aimed to investigate α7 nAChR function and location in the rat frontal cortex, as well as to corroborate the existing evidence for non-α7 nAChR function and location in this region, using direct methods of analysis: superfusion and immunocytochemistry.

In the first part of this thesis, superfusion experiments were undertaken to validate the use of [^{3}H]D-aspartate as a suitable marker for glutamate release from presynaptic terminals (see Chapter 3 section 1). Secondly, recently reported attempts that reveal nAChR modulation of EAA release found this to only occur

when nAChR agonists are combined with depolarising stimuli. We aimed to emulate this data using a variety of depolarising agents and nAChR agonists combined (see Chapter 3 section 2). In the third part we investigated direct nAChR–evoked release of EAA, without the need of concomitant depolarising stimulation. Having established that this could be reproducibly demonstrated we subsequently characterised the nAChR response with the presently available nicotinic pharmacopia (see Chapter 3 section 3).

Lastly, we endeavoured to provide support for the nAChR functional data described in Chapter 3 (section 2 and 3) with immunocytochemical data, using probes specific for α7 nAChR and β2* nAChR (either fluorescent labelled ligands or antibodies) that can be detected using confocal microscopy (Chapter 4).

Chapter Two

2.1 Materials And Methods

2.2. Materials & Equipment

[^{3}H]D-aspartate (14-21 Ci/mmol) was purchased from Amersham International, Amersham, Bucks, UK. Percoll™ was obtained from Amersham Pharmacia Biotech, Uppsala, Sweden. Conotoxin ImI was obtained from Calbiochem. 5-Iodo-A-85380 dihydrochloride (5-I-A-85380), L-trans-pyrrolidine-2,4-dicarboxylic acid (PDC), DL-*threo*-β-benzyloxyaspartic acid (TBOA), (±)anatoxin-a fumarate, and MLA were obtained from Tocris Cookson, Bristol, UK. α-Bgt and α-Bgt Alexa Fluor® 488 and 546 conjugate were obtained from Molecular Probes Europe BV, PoortGebaow, The Netherlands. Anti-β2-nAChR subunit rat polyclonal (mAb 270) was generously provided by Professor Jon Lindstrom, University of Pennsylvania. Anti-synaptophysin mouse monoclonal, VGluT1 and VGluT2 rabbit and guinea pig polyclonal antibodies were obtained from Synaptic Systems GmbH, Göttingen, Germany. Vectorshield™ mountant was obtained from Vector laboratories Inc Burlingame, Canada. All other chemicals were of analytical grade and obtained from Sigma Aldrich Company Ltd, Poole, Dorset, UK.

Equipment

Homogenisor: Cilenco® rotor with attached Teflon™ homogenisor.

Superfusion systems: 12 parallel open chamber modified Brandel® superfusion apparatus (Model SF-12; Brandel, Gaithersburg, MD; (Soliakov *et al.,* 1995), containing Whatman GF/B filter discs. 20 parallel closed chamber automated Brandel® superfusion apparatus with combined Electrical Stimulation Unit.

Scintillation Counter: Packard Tri Carb 1600® TR Liquid scintillation analyser.

Vibratome: Model Vibratome™ 1000 (General Scientific, Redhill, Surrey).

Confocal imaging system: Zeiss Axiovert 100 M microscope combined with LSM 510 confocal system.

Floor standing centrifuge: Beckman Coulter Avanti™ J-25.

2.3 Buffers

Krebs-Bicarbonate (KB): in mM; NaCl 118, KCl 2.4, $CaCl_2.H_2O$ 2.4, $MgSO_4$ 1.2, KH_2PO_4 1.2, Na_2HCO_3 25, glucose 10; oxygenated with 95% O_2/5% CO_2 for 1 hour (and adjusted to pH7.4).

Sucrose-Hepes (SH): 0.32 M sucrose, 5 mM Hepes pH 7.4 (and adjusted to pH7.4).

Phosphate Buffer Saline (PBS): 10 mM phosphate buffer containing NaCl 150 mM and KCl 2 mM, (pH 7.4).

2.4 Rat brain dissection

Male Sprague-Dawley rats of approximate weight (250-300 g) were killed by cervical dislocation and the brains rapidly removed. Frontal cortex tissue (approximately 350 mg) was dissected by cutting anterior to the corpus callosum, after removing the olfactory lobes and striatum. Tissue was immediately placed in ice cold SH buffer and then subject to synaptosome preparation, section preparation (for electrical stimulation) or vibratome sectioning (for immunocytochemistry experiments).

2.5 Frontal cortex tissue preparation

2.5.1 P2 synaptosome preparation

Synaptosomes were isolated by differential centrifugation using a method previously employed by Soliakov *et al.* (1995). For each superfusion experiment frontal cortex from two male Sprague-Dawley rats was homogenised 10% (w/v) in ice-cold SH buffer at pH 7.4 by 12 strokes of the glass/Teflon homegenisor attached to the Cilenco® rotor, set at a rotation speed of 2000 rpm.

This homogenate was then transferred to a polycarbonate centrifuge tube (16 ml) and made up to 10-11 ml with the SH buffer. This sample was centrifuged for 10 min at 1000g (using the Sorvall® SM-24 rotor and Beckman Coulter Avanti™ J-25 centrifuge). The resulting supernatant (S_1) was then transferred to a clean polycarbonate centrifuge tube and made up to 10-11 ml with SH Buffer. This sample was then centrifuged using the same rotor for 20 min at 12000g. The supernatant from this spin (S_2) was discarded and the resulting pellet (P_1) was then initially resuspended in 4 ml of ice-cold KB buffer and triturated gently using a 1 ml pipette for 20 s. The sample was further resuspended to a total volume of 10 ml in KB buffer and centrifuged for a final 10 min at 1000g. The supernatant from this final spin was removed and the remaining pellet (P_2) was re-suspended in 2.5 ml of KB buffer (to a final concentration of 4-5 mg/ml), triturated for 30 s and then left on ice to await further experimentation.

2.5.2 Percoll™ purified synaptosomes

Subjecting the initial S_1 supernatant to centrifugation on discontinuous Percoll™ gradients, allows for a suspension that is enriched with synaptosomes and has a reduced content of other intracellular debris (e.g. mitochondria, myelin and plasma membranes) from the homogenised frontal cortex tissue (Dunkley *et al.*, 1988; Thorne *et al.*, 1991; Thomas *et al.,* 1993) (See Fig. 2.1 for summary of the procedure). The enrichment of synaptosomes is particularly advantageous for immunocytochemical examination, as this preparation minimises intracellular debris and other membrane components that might otherwise be labelled for receptors and transporters that are not associated with an intact nerve terminal.

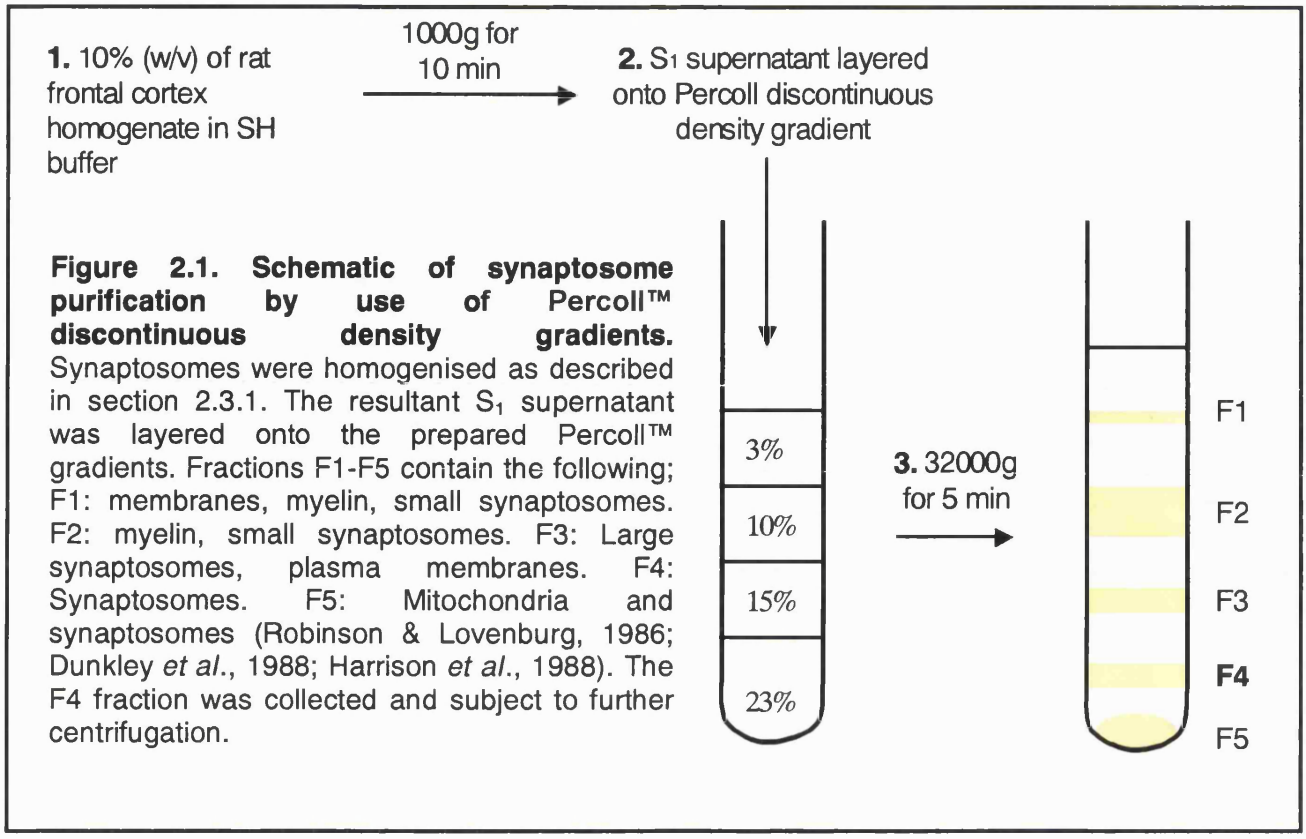

Figure 2.1. Schematic of synaptosome purification by use of Percoll™ discontinuous density gradients. Synaptosomes were homogenised as described in section 2.3.1. The resultant S_1 supernatant was layered onto the prepared Percoll™ gradients. Fractions F1-F5 contain the following; F1: membranes, myelin, small synaptosomes. F2: myelin, small synaptosomes. F3: Large synaptosomes, plasma membranes. F4: Synaptosomes. F5: Mitochondria and synaptosomes (Robinson & Lovenburg, 1986; Dunkley *et al.*, 1988; Harrison *et al.*, 1988). The F4 fraction was collected and subject to further centrifugation.

2.5.3 Percoll™ Gradients

Percoll™ was filtered using 5μM Millipore SM filters to remove coagulates. Four solutions of SH buffer were made up consisting of 23,15,10 and 3% (v/v) Percoll™ respectively. Starting with the highest percentage Percoll™/SH solution, 2 ml of each of the solutions were layered upon one another using a peristaltic pump (via tubing fitted with 12g needle ends) set at a rate of 0.5 ml per min in polycarbonate centrifuge tubes. Four centrifuge tubes were prepared in this manner and then left in the fridge at <4°C until required.

Frontal cortex supernatant (S_1 fraction; described above) was layered onto the gradients (using 20g needles attached to the tubing). The gradients were then centrifuged for 5 min (not including acceleration/deceleration times) at 33,000g (using a Sorvall SM-24 rotor and Beckman Coulter Avanti™ J-25 centrifuge)

This produced five visible fractions above, below and between the gradients, numbered sequentially from the top with fraction 1 being the first visible fraction from the top of the centrifuge tube. (See Fig. 2.1.). Fraction 4 was carefully removed using a Pasteur pipette

and pooled equally into two clean centrifuge tubes. The pooled F4 fractions were then re-suspended to 10 ml of cold sucrose-Hepes buffer and centrifuged at 20,000g for 15 minutes. The resulting pellet was extracted, re-suspending with cold KB buffer centrifugation at 20,000g was repeated leaving a small pellet of synaptosomes that could then be transferred for immunocytochemical investigation.

2.5.4. Frontal cortex mince preparation

Frontal cortex minces were prepared using a McIlwain tissue chopper; 250uM slices cut at 3x 60º angles (minces). Minces were then placed in 5 ml of ice cold KB and subject to washing (three times in 6 ml KB buffer, spinning down between washes using a bench centrifuge; 2000 rpm for 5 seconds). The final pellet was gently resuspended in 4 ml of KB buffer and left to incubate for 10 min in a 10 ml universal sterile tube placed in a thermostatically controlled water bath set at 37°C, prior to subsequent steps detailed below (section 2.7.2).

2.6 [^{3}H]D-aspartate uptake.

2.6.1 Standard [^{3}H]D-aspartate uptake for release experiments

The final P2 suspension in KB buffer (described at end of section 2.5.1) was incubated for 15 min at 37°C containing a final concentration of 0.2 μM [^{3}H]D-aspartate (14-21 Ci/mmol) in a closed polycarbonate centrifuge tube. These 'loaded' synaptosomes were then subject to [^{3}H]D-aspartate release experiments (see below; section 2.7.1).

2.6.2 Temperature dependency of [^{3}H]D-aspartate uptake

The uptake of [^{3}H]D-aspartate was assessed at two different temperatures, <4°C and 37°C. For the <4°C experiments, an 800 μl aliquot taken from the final 2.5 ml P2 suspension in KB buffer was placed in a 1.5 ml Eppendorf and left on ice for 15 min. [^{3}H]D-

aspartate was then added to the Eppendorf to give a final concentration of 0.2 μM and left to incubate on ice for a further 15 min. For the 37°C experiments, the investigation was carried out in parallel to the <4°C experiment. All subsequent steps were exactly as described for the <4°C experiment except that of the incubation temperature, maintained at 37°C using a thermostatically controlled water bath. All subsequent steps for both conditions are described below in section 2.6.5 (see below).

2.6.3 Concentration dependence of [^{3}H]D-aspartate uptake

[^{3}H]D-aspartate was added to 800 μl aliquots of the final P2 suspension described above (section 2.5.1) to give final concentrations of 0.03, 0.1, 0.2 and 0.3 μM. Each suspension was then incubated for 15 minutes at 37°C in a temperature controlled water bath. All subsequent steps are described in section 2.6.5 (see below).

2.6.4 Substrate specificity of [^{3}H]D-aspartate uptake: Glutamate transporter blockers and endogenous glutamate transporter ligands

To determine if the uptake of [^{3}H]D-aspartate was via a transporter mediated process, natural ligands and transporter blockers were added to the synaptosome suspension medium, prior to and during the incubation with [^{3}H]D-aspartate (Final concentration 0.2 μM).

Similar to the temperature and concentration dependence experiments, 800 μl aliquots of the final P2 synaptosome suspension were initially placed in a 1.5 ml Eppendorf and incubated at 37°C for 15 min. The aliquots of synaptosomes were then subject to the following: For glutamate transporter blocker experiments, the compound DL-TBOA (10-100μM) or L-trans-2,4-PDC (1-100 μM) was added to an 800 μl aliquot suspension of synaptosomes and incubated for a further 15 minutes prior to the addition of [^{3}H]D-

aspartate (Final concentration 0.2 μM). For natural transporter ligand experiments L-glutamate and D-aspartate were added as a 1000 fold excess concentration (200 μM) to the synaptosome suspension at the same time as the addition of [^{3}H]D-aspartate (Final concentration 0.2 μM). Aliquots were incubated for 15 min at 37°C in a temperature controlled water bath. All subsequent steps are described in section 2.6.5 (see below).

2.6.5 Filtration and scintillation counting

At the end of these procedures (sections 2.6.2-2.6.4), 3 x 150 μl of each suspension was extracted from the Eppendorf tubes and dispensed onto a GF/C Millipore filter within a chamber of the Millipore® Manifold filtration system. Each filter was then washed twice with KB buffer and the filters carefully removed and placed into scintillation vials. Optisafe liquid scintillant (4 ml) was added to each of the vials and then counted for radioactivity using a Packard Scintillation counter (Packard Tri Carb 1600 TR Liquid scintillation analyser). 2 x 150 μl of each unfiltered suspension from the Eppendorf tubes was added directly to the scintillation vials containing 4 ml of Optisafe liquid scintillant and also counted for radioactivity (Counting efficiency = 46 %).

2.7 [^{3}H]D-aspartate release: Superfusion

2.7.1 Superfusion of frontal cortex synaptosomes loaded with [^{3}H]D-aspartate

From the 2.5 ml final suspension of synaptosomes in KB buffer, (pre-loaded with a final concentration of 0.2 μM [^{3}H]D-aspartate; Section 2.5.1) 120 μl aliquots were added (approximately 0.2 mg of protein per aliquot) to each of the 12 parallel open chambers of a modified Brandel® superfusion apparatus (Model SF-12; Brandel, Gaithersburg, MD; Soliakov *et al.,* 1995. See Fig. 2.2.), containing Whatman GF/B filter discs. Synaptosomes were superfused at a rate of 0.75 ml/min with KB buffer. After a 24 min washout period,

two-min fractions of perfusate were collected. After a further 6 min, nAChR agonist and/or depolarising agent in KB buffer or buffer as a control, were delivered to the chambers as a 90 s pulse, separated from the bulk buffer flow by 2 s air gaps. Synaptosomes were superfused for a further 22 min with Krebs-bicarbonate buffer. The radioactivity of each fraction was measured in a Packard Tri Carb 1600 TR Liquid scintillation analyser. When present, nAChR antagonists or glutamate transporter inhibitors were included in the perfusing buffer for 10 min prior to agonist stimulation (except for α-Bgt which was applied for 20 min and PDC or TBOA applied throughout). Antagonist was present during the stimulation and remained throughout the rest of the experiment. To determine the Ca^{2+}-dependency of KCl and nAChR evoked release, synaptosomes were perfused with Ca^{2+}-free Krebs-bicarbonate buffer, replacing $CaCl_2$ with 2.4 mM $MgCl_2$ throughout the experiment.

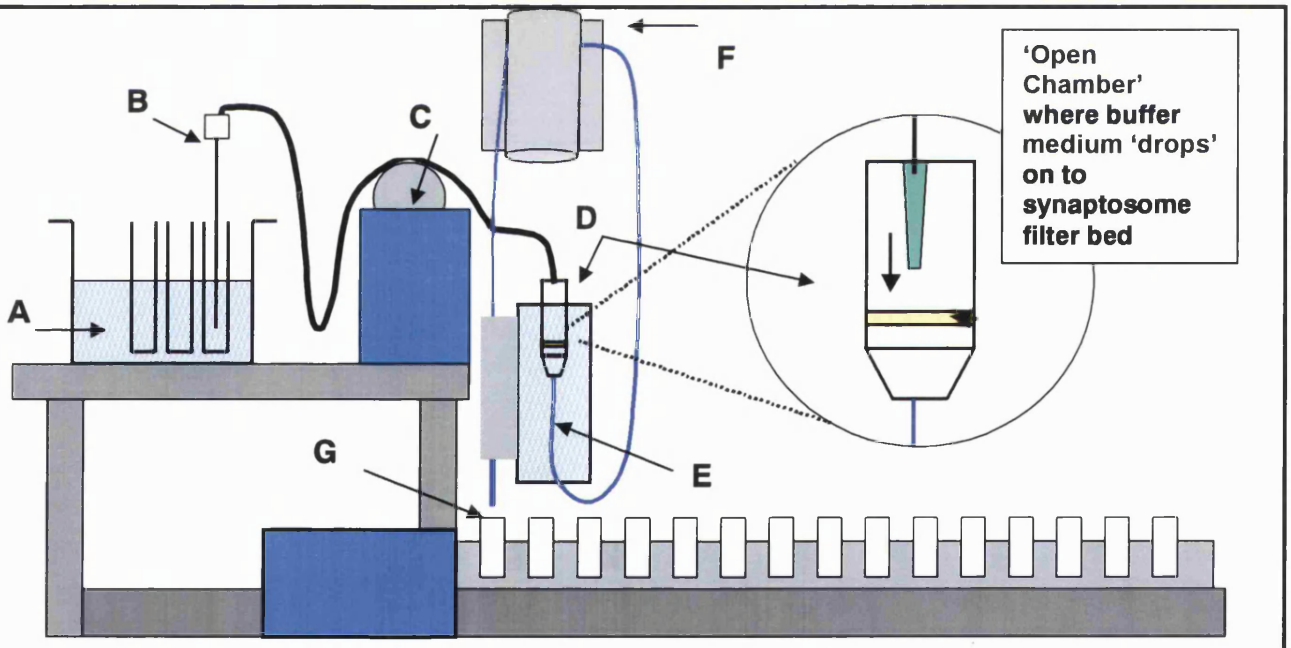

Figure 2.2. Diagram of the 12 channel manual Brandel® superfusion system. P2 synaptosomes (120 μl) loaded with [^{3}H]D-aspartate were placed directly on each of the twelve chambers containing 2x Whatman GFB filters (**D**). Collecting probes (**B**), are placed in test tubes containing KB perfusing buffer, agonists or antagonists, kept at 37°C in the attached water bath reservoir (**A**). Attached peristaltic pump; (**C**), pumps buffer over the filter bed containing the synaptosomes and perfusate is collected via tubing (**E**, blue) attached to a second peristaltic pump (**F**), that pumps perfusate through to scintillation vials set in an automated fraction collection tray; (**G**).

Each set of conditions described above (depolarising agent, agonist, antagonist and glutamate transport blocker) was carried out in a triplicate set of chambers within each experiment. Radioactivity remaining in the synaptosomes at the end of the experiment was determined by counting the filters from the superfusion chambers. Total radioactivity present in synaptosomes at the time of agonist stimulation was calculated as the sum of subsequently released [^{3}H]D-aspartate plus radioactivity remaining on the filters.

2.7.2 Superfusion of frontal cortex sections loaded with [^{3}H]D-aspartate

Frontal cortex slices ('minces', prepared from section 2.5.4) were spun down using a bench centrifuge (2000 rpm for 5 seconds) to form a loose pellet and re-suspended again in 4 ml of KB (pre-warmed to 37°C). [^{3}H]D-aspartate (13 Ci/mmol -final concentration 0.2μM) was added to the suspension of minces and left to incubate for 30 min at 37°C. After priming the superfusion system with KB buffer, aliquots of the mince suspension (100 μl; 30 mg tissue) were loaded onto each of the 20 chambers of the superfusion apparatus. A Nylon mesh and GF/B filter were placed at each end of the chamber to prevent slices from flowing out of the apparatus (See Fig. 2.3). Minces were then superfused at a rate of 0.75 ml/min with KB buffer. After a 30 min washout period, 90 s fractions of perfusate were collected. After a further 6 min, nAChR agonist in KB buffer or buffer as a control, were delivered to the chambers as a 90 s pulse. Minces were superfused for a further 22 min with KB. The radioactivity of each fraction was measured in a Packard Tri Carb 1600 TR Liquid scintillation analyser. When present, nAChR antagonists or glutamate transporter inhibitors were included in the perfusing buffer for 10 min prior to agonist stimulation (except for α-Bgt which was applied for 20 min and TBOA which was applied throughout). Antagonist was present during the stimulation and remained throughout the rest of the experiment.

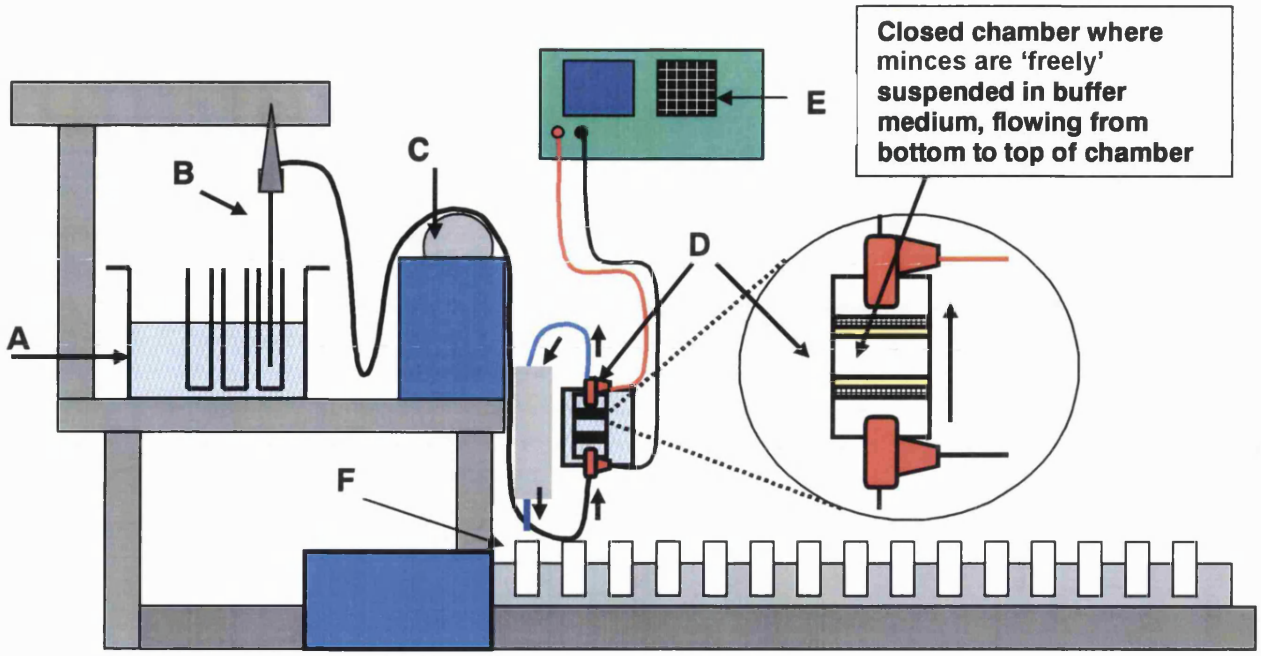

Figure 2.3. Diagram of the automated 20 channel Brandel® superfusion system combined with electrical stimulation generator. Frontal cortex mince suspension (100 μl) loaded with [^{3}H]D-aspartate were placed directly on each of the twenty chambers. Chambers were sealed at each end with a nylon mesh and GF/B filter to contain the minces. Electrical stimulation pegs were attached to either end of the chambers (See insert **D**). Collecting probes attached to robotic arm for automated changing (**B**), are placed in test tubes containing KB perfusing buffer, agonists or antagonists, kept at 37°C in the attached water bath reservoir (**A**). Attached peristaltic pump (**C**), pumps buffer into the closed chambers containing the minces from bottom to top of the chamber. Electrical stimulating pegs (red) attached to electrical stimulation generator (**E**). Perfusate collected in scintillation vials set in an automated fraction collection tray (**F**).

Electrical stimulation was applied as a 90 s 5Hz, 50mA bi-directional pulse, 12 min after the start of perfusate collection, this allows for an approximate 90 s washout of nAChR agonist from the closed chamber prior to electrical stimulation. Each set of conditions described above (electrical stimulation, agonist, antagonist) was carried out in a triplicate set of chambers within each experiment. Control conditions within the experiment consisted of disconnecting three individual chambers from the electrical stimulation generator.

Radioactivity remaining in the minces at the end of the experiment was determined by solubilising the filters containing the minces from the chambers in Solvable™ and then

adding scintillant to count the filters from the superfusion chambers. Total radioactivity present in minces at the time of agonist stimulation was calculated as the sum of subsequently released [^{3}H]D-aspartate plus radioactivity remaining on the filters.

2.8. Immunocytochemistry

2.8.1 Immunolabelling of synaptosomes

Percoll™ purified synaptosomes (Fraction 4 and some of 3, resuspended in 1.5 ml Krebs-bicarbonate buffer) were layered onto poly-L-lysine coated slides (0.75 ml of synaptosome suspension per slide) in a humidified chamber, and incubated for 45 min at room temperature to allow the synaptosomes to adhere. Slides were rinsed in Krebs bicarbonate buffer to remove non-adherent synaptosomes and incubated with 100 nM Alexa-Fluor® 488 α-Bgt for 20 min. The specificity of labelling with Alexa-Fluor® 488 α-Bgt was assessed by pre-incubating the slides with a 100 fold excess of MLA or α-Bgt for 20 min, prior to the addition of the fluorochrome. Further controls were incubated with Krebs buffer alone. Slides were rinsed in Krebs and fixed in PBS (10 mM phosphate buffer containing NaCl 150 mM and KCl 2 mM), containing 4% paraformaldehyde (PFA) for 10 min. Slides were washed in PBS to remove fixative and incubated in PBS containing 10% normal goat serum, 0.5% BSA and 0.1% saponin for 30 min at room temperature. Primary antibodies (mouse anti-synaptophysin (1/500 dilution), rabbit anti-VGluT 1(1/1000 dilution) and anti-VGluT2 (1/500 dilution) were added in PBS containing 1% normal goat serum, 0.5% BSA and 0.1% saponin. For those experiments where β2 nAChR identification was necessary, the primary rat antibody specific for the β2 nAChR subunit (mAb 270; generously donated by Professor J Lindstrom, University of Pennsylvania) was also incubated, with the omission of the mouse anti-synaptophysin antibody from the incubation. Slides were incubated overnight at 4°C in a humidified chamber. After three 5 min washes with PBS

containing 0.1% saponin, slides were incubated with secondary antibody solution (anti-rabbit IgG 633 and anti-mouse IgG 546, (and/or anti-rat IgG 546 for β2 subunit labelling experiments) both 1:750 in 1% normal goat serum, 0.5% BSA and 0.1% saponin in PBS) for 1 h at room temperature in the dark. Slides were washed in PBS containing 0.1% saponin for 5 min followed by PBS alone, to remove excess secondary antibodies before mounting with Vectorshield™ and viewing under the Zeiss Axiovert 100 M microscope combined with an LSM 510 confocal system.

2.8.2 Immunolabelling of rat frontal cortex sections

For rat frontal cortex sections, male Sprague Dawley rats (250 g) were anaesthetised with sodium pentobarbitone (Sagatal™, 60mg/kg, i.p) and trans-cardially perfused with 150 ml 4% PFA in PBS. Coronal and sagital sections of the frontal cortex (50 μM thick) were cut using a Vibratome™ 1000 (General Scientific, Redhill, Surrey) and incubated in PBS containing 1% sodium borohydride for 10 min to block free aldehyde groups. After washing in PBS, sections were blocked in PBS containing 10% normal goat serum, 0.5% BSA and 0.5% Triton-X100 for 30 min at room temperature. Primary antibodies (mouse anti-NeuN (1/500 dilution), rabbit anti-VGluT1 (1/1000 dilution), anti-VGluT2 (1/500 dilution) and 100 nM Alexa-Fluor® 488 α-Bgt were added in PBS containing 1% normal goat serum, 0.5% BSA and 0.5% Triton-X100 and the sections incubated overnight at 4°C on a shaker. For those experiments where β2 nAChR identification was necessary, the primary rat antibody specific for the β2 nAChR subunit (mAb 270; generously supplied by Professor Jon Lindstrom) was also incubated, with the omission of the mouse anti-NeuN antibody from the incubation. All subsequent steps followed the same procedures as for synaptosomes, with the replacement of 0.1% saponin with 0.5% Triton-X100 in all washing and antibody solutions. After the final washing step, sections were mounted on slides with

Vectorshield™ and viewed under the Zeiss Axiovert 100 M microscope combined with LSM 510 confocal system. Controls were performed in the same manner as for the synaptosomes experiments, by preincubating with a 100-fold excess of MLA or α-Bgt and by the omission of the primary antibodies.

2.8.3 Confocal microscopy

Immunolabelled synaptosomes and tissue sections were analysed using the Zeiss multi-tracking protocol, which eliminates the possibility of fluorochrome 'cross-talk' through the use of sequential fluorochrome excitation. Fluorochromes were excited using an argon laser at 488nm (505-530nm emission filter), a helium-neon laser at 543nm (560-615nm filter) and a helium-neon laser at 633nm (650nm emission filter). To ensure that the respective fluorescence emissions were recorded at the same level, the emission pinhole for each track was set at 1 airy unit.

α-Bgt labelling was recorded from ten random fields in each test group at the same magnification (x63 objective lens). The density of the α-Bgt binding in control and antagonist competition groups was compared using the Student's paired t-test. To assist the interpretation of the spatial localisation of α-Bgt labelled sites with respect to other neurochemical markers, such as VGluT, the Zeiss profiling software was utilised. This tool enables the quantification of individual fluorescence emission intensities along a user-defined axis through the sample. Colocalisation of α-Bgt with VGluT fluorescent labelling was quantitated in fifteen random fields by inspection of intensity profiles

2.9 Protein Estimation

To ensure consistent protein concentration of synaptosome preparations between experiments, protein concentration was measured using the Bradford method (Bradford,

1976). Now adapted commercially, the Biorad™ protein assay kit enables a fast determination of protein in tissue samples.

Essentially the assay reagent was diluted 1:4 using distilled water and filtered through Whatman filter paper. A standard protein curve was constructed using triplicate samples of Bovine Serum Albumin (BSA), dissolved in assay buffer (the same buffer used for incubation of synaptosomes) over a concentration range of 0.1-1 mg/ml. Rat synaptosome samples were diluted 1:2, 1:4 and 1:8 in KB buffer, in triplicate. Using LP4 tubes, the reaction mixture consisted of 1 ml diluted assay reagent plus 10 µl of either BSA standards or diluted synaptosome samples. Tubes were vortexed and left to react for 1 h. Samples were then transferred to 1 ml optical cuvettes and measured for optical density at 595 nm using a Helios Gamma spectrometer.

2.10 Data analysis

For release experiments, superfusion data were analysed by fitting a double exponential decay equation to the baseline data (Soliakov *et al*; 1995) using the Sigma plot (v.2.0) for programme for Windows 3.1 (Jandel Scientific):

$$y = ae^{-bx} + ce^{-dx}$$

where a and c are initial (at x=0) release in each phase, b and d are the decay constants in each phase, and x is the fraction number. Evoked [^{3}H]D-aspartate release was calculated as the area under the peak after subtraction of baseline and expressed as a percentage of the total radioactivity present in the synaptosomes at the point of stimulation (fractional release). This was taken to be the sum of subsequently released [^{3}H]D-aspartate plus that on the filters (synaptosomes or minces).

Data are presented as either fractional release, which has been subtracted for buffer response, or expressed as a percentage of buffer control, i.e. the release evoked by buffer (containing no drug conditions), was taken as 100%. Values in histograms and concentration response curves represent the mean ± S.E.M of the number of independent experiments carried out, with each experiment consisting of 2 or 3 replicate chambers for each condition. Statistical analysis of data was carried out using Student's unpaired t-test or ANOVA with post hoc tukeys analysis, as stated in the figure legends. Values of $P<0.01$ or $p<0.05$ were taken to be statistically significant.

Chapter 3 Section 1

3.1 Characterisation of [^{3}H]D-aspartate uptake and release in the rat frontal cortex

3.1.1 Introduction

3.1.2 A critical analysis of the use of D-aspartate

[^{3}H]D-aspartate is one of the most widely employed radiolabelled EAA used to examine the release of EAA from vertebrate CNS tissue. Added exogenously, in vivo or in vitro, to brain slices, synaptosomes or neuronal cell cultures, [^{3}H]D-aspartate (and D-aspartate) has elucidated the identification of glutamatergic terminals and pathways (Taxt & Storm-Mathisen, 1984; Jay *et al.,* 1992; Saint-Mairie 1996; Gundersen *et al.*, 1996) as well as reveal the ionic dependency for uptake and release of EAA (Erecinska *et al.*, 1983. Arqueros et al., 1985; Simonato *et al.*, 1993; Palmer & Reiter, 1994; Muzzolini *et al.*, 1996; Savage *et al.*, 2001). As well as these studies, [^{3}H]D-aspartate has proved a useful marker for EAA uptake experiments with respect to the identification of novel ligands for the EAA transporters and indeed for the characterisation, localisation and sub-cellular localisation of EAAT subtypes in brain tissue (Ferkany & Coyle, 1986; Bridges *et al.*, 1991; Kuwahara *et al.*, 1992; Dunlop *et al.*, 1993; Waagepetersen *et al.*, 2001; For review see Takahashi *et al.*, 1997 and Danbolt, 2001).

Several advantages of D-aspartate support its use as a surrogate for the examination of uptake and release of endogenous EAA. Firstly, D-aspartate is a ligand for the EAAT (the family of presently cloned glutamate transporters) and is actively taken up into brain preparations in vivo and in vitro (Davies & Johnston, 1976; Storm-Mathisen & Wold, 1981; Fischer *et al.,* 1986; Dunlop *et al.*, 1993; Dunlop, 2001; Waagepetersen *et al.*, 2001; Suchak *et al.*, 2003). EAA transporters affinity for D-aspartate is typically in the low micromolar range (30-80 μM) and a factor of two less than L-glutamate (Drejer *et al.*, 1983; Gegelashvilli *et al.*, 1998: for review see Danbolt, 2001). Secondly, D-aspartate has a limited role in cellular

metabolic activities, compared to that of endogenous EAA's such as L-glutamate, thereby increasing the 'releasable' pool of neurotransmitter available for detection of its release. However, this does not rule out that D-aspartate does not exist endogenously within the vertebrate CNS, where possible roles of this amino acid in neuroendocrine function have been demonstrated (Schell *et al.*, 1997). Possible roles in neurotransmission have yet to be demonstrated, at present this ligand fails to evoke responses in reconstituted ionotropic or metabotropic glutamate receptors (NMDA/AMPA/mGluR receptors; for review Dingledine *et al.*, 1999), yet an interesting observation by D'Aniello & colleagues (2000) demonstrate that intra-peritoneal administration of D-aspartic acid in rats increases the concentration of NMDA in the adenophysis, suggesting that D-aspartate acts as a precursor substrate to in vivo formation of NMDA catalysed by the enzyme methyltransferase. Thirdly D-aspartate displays no affinity for EAA receptors (either metabotropic or ionotropic) that can mediate excitatory neurotransmission, thereby avoiding any receptor interaction that might influence auto-regulation of release (however the release of endogenous EAA may influence this possibility) (Zhou *et al.*, 1995; Patel & Croucher, 1997; Thomas *et al.*, 2000; for review see Cartmell & Schoepp, 2000).

However the use of this analogue has not been without criticism (see Nicholls, 1989; Nicholls & Attwell, 1990) mainly based on the lack of evidence supporting the containment of D-aspartate in synaptic vesicles of glutamatergic terminals and the apparent lack of evidence for Ca^{2+}-dependant release of [^{3}H]D-aspartate.

More recently, the concern of whether [^{3}H]D-aspartate is taken up into vesicles has been addressed in an extensive study by Fleck *et al.* (2001). Using rat synaptic vesicles purified by immunoprecipitation with monoclonal anti-synaptophysin

antibodies, these authors reported that D-aspartate does accumulate into a common vesicular pool shared with L-glutamate.

With respect to release of [^{3}H]D-aspartate, a number of superfusion studies demonstrate Ca^{2+}-dependancy; [^{3}H]D-aspartate release is reduced in the absence of Ca^{2+} in the perfusing buffer and sensitive to the synaptic vesicle toxin bafilomycin, consistent with an exocytotic mechanism of vesicular release as described for endogenous glutamate release (Simonato *et al.*, 1993; Palmer & Reiter, 1994; Muzzolini *et al.*, 1997; Savage *et al.*, 2001). As well as this, the propensity for the EAAT to reverse in depolarising conditions is also observed using [^{3}H]D-aspartate (Waagepetersen *et al.*, 2001) in agreement with the calcium-independent component of depolarisation-evoked [^{3}H]D-aspartate and glutamate release being attributed to EAA transporter reversal (Nicholls & Attwell, 1990; Szatkowski *et al.*, 1990; Phillis *et al.*, 1994).

The purpose of this section is to provide supporting evidence for the use of D-aspartate as a suitable surrogate to EAA in both uptake and release experiments using rat frontal cortex synaptosomes.

[^{3}H]D-aspartate uptake experiments demonstrate the effect of temperature and substrate specificity of the transporter mechanisms that exist in rat frontal cortex synaptosome preparations. General depolarising agents (KCl, 4-AP and veratradine) were examined for their effect on release of [^{3}H]D-aspartate from rat frontal cortex synaptosomes. Release evoked by KCl displayed both Ca^{2+}-dependant and Ca^{2+}-independent components of release in agreement with reports described for glutamate release from rat synaptosomes (Reviewed by Nicholls, 1998).

3.1.3 Results

3.1.4 Characterisation of [^{3}H]D-aspartate uptake

The accumulation of [^{3}H]D-aspartate into synaptosomes was first assessed using rat frontal cortex Percoll™ purified synaptosomes (See methods; Thorne *et al.*, 1991). Aliquots of Percoll™ purified synaptosomes were incubated for 15 min at 37°C prior to the addition of [^{3}H]D-aspartate (See methods). Percoll™ purified synaptosomes incubated with [^{3}H]D-aspartate over a concentration range of 0.03-0.3 μM, displayed a relatively uniform percentage uptake of radiolabel (49.9-56.9%; see Fig. 3.1.1).

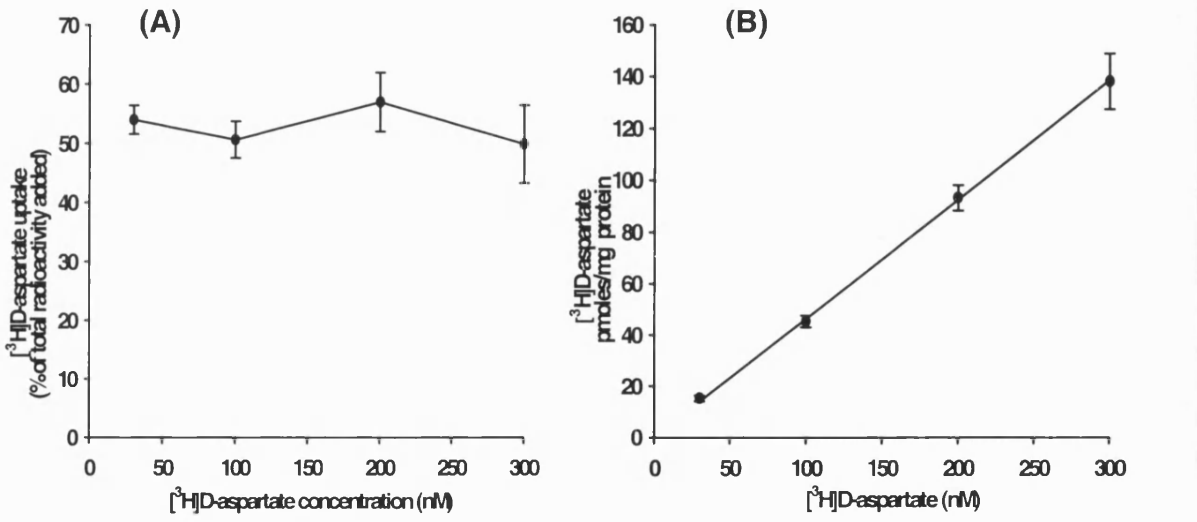

Figure 3.1.1 Uptake of [^{3}H]D-aspartate into rat frontal cortex Percoll™ purified synaptosomes. Percoll™ purified synaptosomes were incubated for 15 minutes and divided into aliquots prior to the addition of [^{3}H]D-aspartate. Each aliquot was then incubated for a further 15 min with a specific concentration of [^{3}H]D-aspartate. After this period, synaptosomes were placed on filters, washed twice with KB buffer and then counted for radioactivity (see Methods 2.6.5). **(A)** Radioactivity taken up by synaptosomes retained on the filters is expressed as a % of the total radioactivity added to the respective aliquot. **(B)** Uptake of [^{3}H]D-aspartate is expressed as pmoles per mg of synaptosome protein. Results are expressed as the mean ± S.E.M of at least three independent experiments.

Protein concentration of each aliquot was also examined using the Bradford method (see Methods section 2.9) and showed that each aliquot had a relatively constant synaptosome concentration in each condition examined (1.09 ± 0.03 mg/ml). Combining both the raw C.P.M of the uptake data and the synaptosome protein

concentration, uptake can be expressed as pmoles/mg of protein (See Fig. 3.1.1 B). Uptake showed a linear increase with concentration reflecting that uptake is not saturated in this concentration range.

Both the temperature dependency of uptake and ligand specificity were examined to confirm that the uptake of [^{3}H]D-aspartate is via a transporter-mediated process in rat frontal cortex synaptosomes.

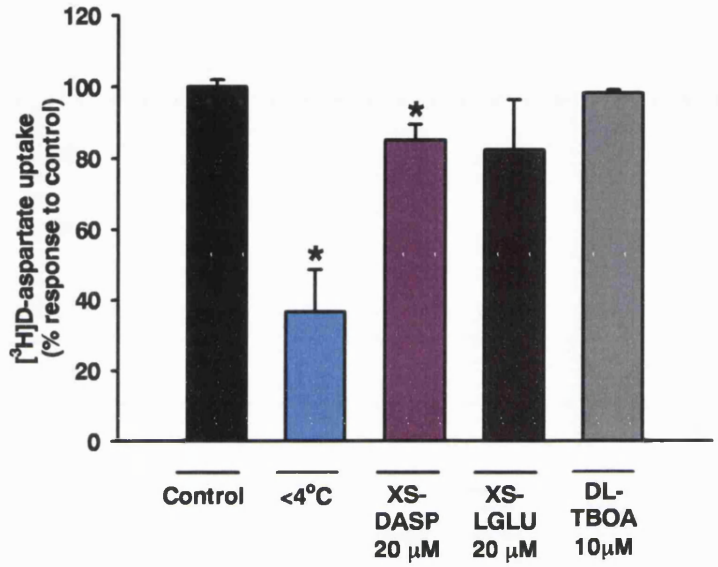

Figure 3.1.2 Temperature dependency and substrate specificity of [^{3}H]D-aspartate uptake into rat frontal cortex Percoll™ purified synaptosomes. Percoll™ purified synaptosomes (1.1 ± 0.2 mg/ml) were incubated for 15 minutes and then divided into aliquots. Each aliquot was then incubated for a further 15 min with [^{3}H]D-aspartate + specific condition (see Methods 2.6.1-2.6.4). After this period, synaptosomes were filtered, washed twice with KB buffer and counted for radioactivity (see Methods section 2.6.5). Results are expressed as the % of uptake in control conditions. Results are expressed as the mean ± S.E.M of at least three independent experiments.

To assess the effect of temperature dependency, synaptosomes were pre-incubated for 15 min in ice cold KB (<4°C) prior to the addition of [^{3}H]D-aspartate (0.2 μM) (see Methods section 2.6.2). As shown in Fig 3.1.2, incubation of synaptosomes at <4°C reduces uptake by 63.3 ± 11.9% compared to control. However, the addition of synaptosomes to buffer containing [^{3}H]D-aspartate (0.2 μM) and an excess of D-aspartate or L-glutamate (20 μM), reduced uptake by only 14.2 ± 4.3% and 17.6 ±

14.0% respectively. Transporter specificity was also assessed using the transporter blocker DL-TBOA, a non-transportable blocker of EAAT1-3 (Shimamoto *et al.*, 1998; Jabaudon *et al.*, 1999; Waagpetersen *et al.,* 2000). Synaptosomes pre-incubated for 15 min at 37°C with 10 μM DL-TBOA and then further incubated with KB containing DL-TBOA and [^{3}H]D-aspartate (0.2 μM) demonstrated no blockade of [^{3}H]D-aspartate uptake (see Fig. 3.1.2).

The lack of effect of these conditions raised grave concerns over the specificity of uptake and so a repeat of these conditions was assessed in P2 synaptosomes on the grounds that the preparatory conditions required for Percoll™ purified synaptosomes made them unviable for assessment of uptake (see discussion). In support of this, it was observed from release experiments that basal release of [^{3}H]D-aspartate from Percoll™ purified synaptosomes was approximately 4 fold higher than that shown for P2 synaptosomes (See Fig. 3.1.11 below), raising the argument that the membranes of Percoll™ purified synaptosomes are 'leaky' and simply allow for the passive movement of [^{3}H]D-aspartate across the membrane independent of EAAT.

P2 synaptosomes displayed a similar level of uptake for 0.2 μM [^{3}H]D-aspartate compared to Percoll™ purified synaptosomes (47.1 ± 3.4% of total radioactivity added to synaptosome aliquot). P2 synaptosomes were slightly higher in protein concentration compared to Percoll™ purified synaptosomes (1.75 ± 0.18 mg/ml) where the final amount of [^{3}H]D-aspartate taken up into synaptosomes was 58.01 ± 3.4 pmoles/mg. When P2 synaptosomes were subjected to different incubation temperatures and substrate conditions, a clear case for transporter specificity of uptake was demonstrated. At low temperatures (<4°C), uptake of a standard concentration of [^{3}H]D-aspartate (0.2 μM) is reduced by 39.9 ± 13.1% compared to

control (control conditions 37°C; 100 ± 3.4%). With respect to the presence of excess D-aspartate and L-glutamate (20 μM), uptake is reduced to a similar extent: 35.0 ± 6.2% and 44.2 ± 5.8% respectively. In addition, the presence of TBOA in the incubating medium reduced uptake by P2 synaptosomes by 40.0 ± 3.1 % (See Fig. 3.1.3).

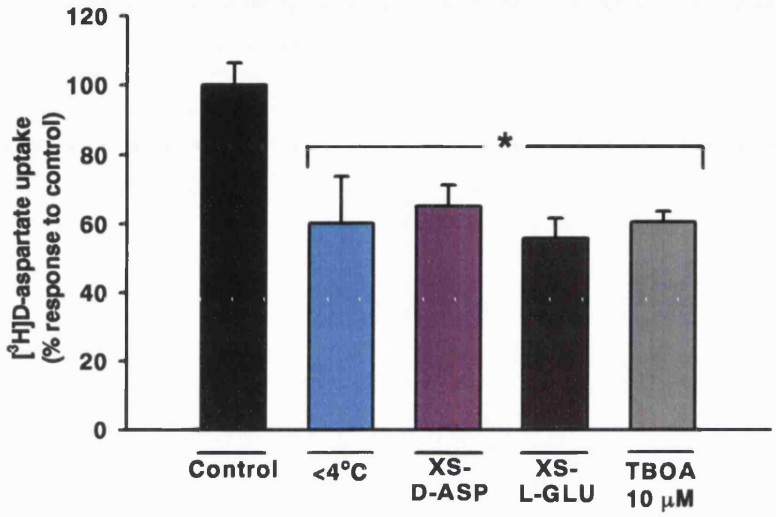

Figure 3.1.3 Temperature dependency and substrate specificity of [^{3}H]D-aspartate uptake into rat frontal cortex P2 purified synaptosomes. P2 synaptosomes (1.8 ± 0.3 mg/ml) were incubated for 15 minutes prior and then divided into separate aliquots. Each aliquot was then incubated for a further 15 min with a [^{3}H]D-aspartate + specific condition (see Methods 2.6.1-2.6.4). After this period, synaptosomes were filtered, washed twice with KB buffer and counted for radioactivity (see Methods 2.6.5). Results are expressed as the % of uptake compared to control conditions. Results are expressed as the mean ± S.E.M of at least three independent experiments. * Significantly different from control $P<0.05$, one way ANOVA with post hoc Tukeys analysis.

All these values were significantly different from control ($P<0.05$) using a one-way ANOVA with post-hoc analysis. (See Fig. 3.1.3).

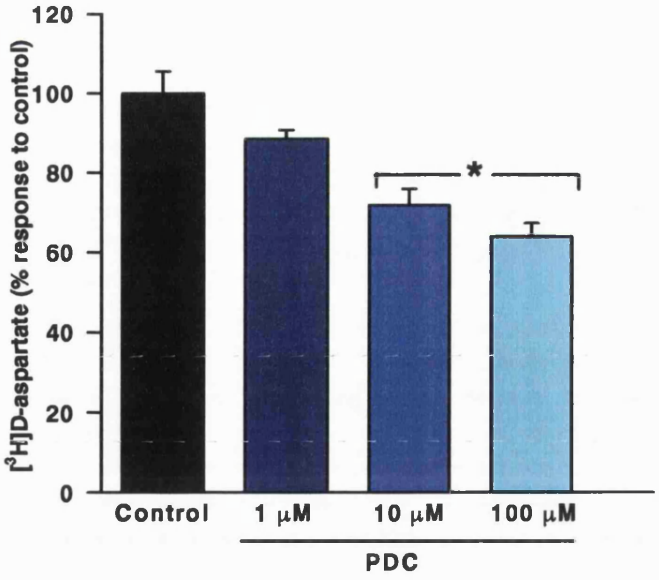

Figure 3.1.4 Concentration dependant effect of L-Trans-2,4-PDC (PDC) on [^{3}H]D-aspartate uptake into rat frontal cortex P2 purified synaptosomes. P2 synaptosomes (1.8 ± 0.3 mg/ml) were incubated for 15 minutes prior and then split into separate aliquots. Each aliquot was then incubated for a further 15 min with [^{3}H]D-aspartate (0.2 μM) + PDC (see Methods section 2.6.4). After this period, synaptosomes were filtered, washed twice with KB buffer and counted for radioactivity. Results are expressed as the % of compared to control conditions. Results are expressed as the mean ± S.E.M of at least three independent experiments. * Significantly different from control $P<0.05$, one way ANOVA with post hoc Tukeys analysis.

Another glutamate transporter inhibitor, L-trans-Pyrrolidine-2,4-dicarboxylic acid (PDC) was assessed for inhibition of [^{3}H]D-aspartate over a range of concentrations. Concentration dependant inhibition of uptake was observed at 10 and 100 μM PDC, reducing uptake by 28.3 ± 4.1% and 36.1 ± 3.4% respectively (control conditions = 100 ± 5.5%: See Fig. 3.1.4).

Another set of uptake experiments aimed to look at the effect of diluting the P2 synaptosome sample. Endogenous release of synaptosome metabolites or neurotransmitters may effect the local pH environment as well as other receptors on the synaptosome membrane, which may, in turn, effect the functioning of the EAA transporter. In diluted conditions these changes may be buffered more efficiently,

thereby decreasing any possible effects on the transporter, in terms of transporter reversal or non-specific entry of [^{3}H]D-aspartate into synaptosomes.

In control conditions total radioactivity taken up in the 1 in 5 diluted synaptosomes (48.4 ± 3.9 %) was not statistically different from undiluted synaptosomes. However the amount of [^{3}H]D-aspartate per mg of synaptosome protein was approximately 5 fold higher than undiluted synaptosomes (245 ± 12.4 pmoles/mg of synaptosome protein) reflecting efficient uptake when synaptosome protein concentration is lower. Uptake into synaptosomes diluted 1 in 5 in KB demonstrated a different profile of inhibition compared to the undiluted P2 synaptosomes when subjected to the conditions described above.

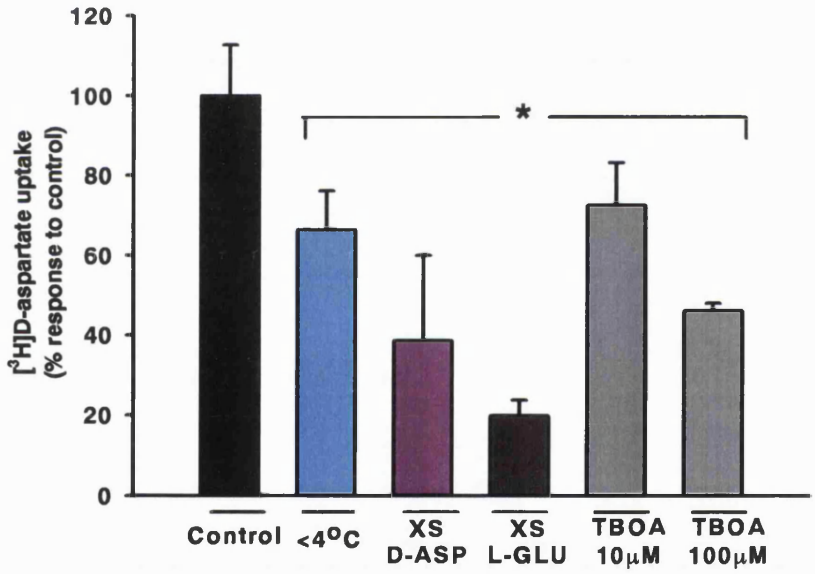

Figure 3.1.5 Temperature dependency and substrate specificity of [^{3}H]D-aspartate uptake into rat frontal cortex P2 purified synaptosomes diluted 1 in 5 in KB. P2 synaptosomes diluted 1 in 5 from their original suspension (0.41 ± 0.08 mg/ml) were incubated for 15 min at 37°C and then split into separate aliquots. Each aliquot was then incubated for a further 15 min with [^{3}H]D-aspartate (0.2 μM) + specific condition (see Methods 2.6.2-2.6.4). After this period, synaptosomes were filtered, washed twice with KB buffer and counted for radioactivity. Results are expressed as the % uptake compared to control conditions. Results are expressed as the mean ± S.E.M of at least three independent experiments. * Significantly different from control $P<0.05$, one way ANOVA with post hoc Tukeys analysis.

Both low temperature and excess D-aspartate resulted in relatively similar levels of uptake inhibition as described for undiluted synaptosomes (33.7 ±9.8% and 61.5 ± 21.3% inhibition respectively, compared to control; 100 ± 12.7%). However, the presence of excess glutamate in the incubation medium produced an 80.2 ± 4.0% inhibition of [^{3}H]D-aspartate uptake (see Fig. 3.1.5; compare 44.2 ± 5.8% inhibition in undiluted P2 synaptosomes in Fig. 3.1.3). TBOA (10 μM) also inhibited uptake at 10 μM, reducing uptake by 27.5 ± 10.8%, which is lower, although not statistically different, than that observed in undiluted P2 synaptosomes. Increasing the concentration of TBOA to 100 μM further increased inhibition of uptake to 54.0 ± 1.8%.

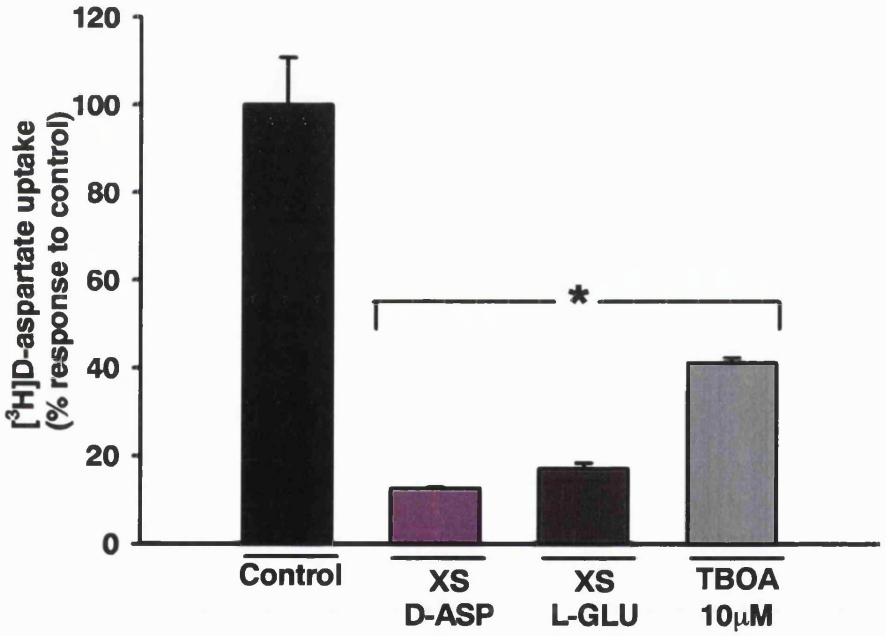

Figure 3.1.6 Substrate specificity of [^{3}H]D-aspartate uptake into rat frontal cortex P2 purified synaptosomes diluted 1 in 10 in KB. P2 synaptosomes diluted 1 in 10 from their original suspension (0.2 ± 0.04 mg/ml) were incubated for 15 min at 37°C and then split into separate aliquots. Each aliquot was then incubated for a further 15 min with [^{3}H]D-aspartate (0.2 μM) + specific condition (see Methods 2.6.2-2.6.4). After this period, synaptosomes were washed twice with KB buffer and counted for radioactivity. Results are expressed as the % uptake compared to control conditions. Results are the mean ± S.E.M of at least three independent experiments. * Significantly different from control $P<0.05$, one way ANOVA with post hoc Tukeys analysis.

A similar set of experiments looked at further diluting the original P2 synaptosome suspension to 1 in 10 in KB. In this case the total amount of radioactivity taken up in control conditions represented 20.9 ± 2.7% of the total radioactivity added however the amount of [^{3}H]D-aspartate per mg of protein was approximately similar to the 1 in 5 dilution of synaptosomes (244 ± 15.4 pmoles/mg of synaptosome protein). Only the effect of different substrates and TBOA was examined in these experiments (Fig. 3.1.6 above). In these diluted synaptosomes the presence of excess D-aspartate had a dramatic effect on the inhibition of [^{3}H]D-aspartate, reducing uptake by 82.4 ± 0.3%, whereas the inhibition incurred in the presence of excess L-glutamate was similar to that obtained in the synaptosomes diluted 1 in 5 (82.9 ± 1.3%). TBOA (10 μM) inhibited [^{3}H]D-aspartate uptake by a 58.9 ± 1.4% again similar to that obtained in synaptosomes diluted 1 in 5.

3.1.5 Characterisation of [^{3}H]D-aspartate release

The release of [^{3}H]D-aspartate from frontal cortex synaptosomes was studied by superfusion, and was first assessed using classical depolarising agents, applied as a 90 s pulse to the superfused synaptosomes. 4-Aminopyridine (4-AP), KCl and veratradine each provoked the release of [^{3}H]D-aspartate (Fig. 3.1.7).

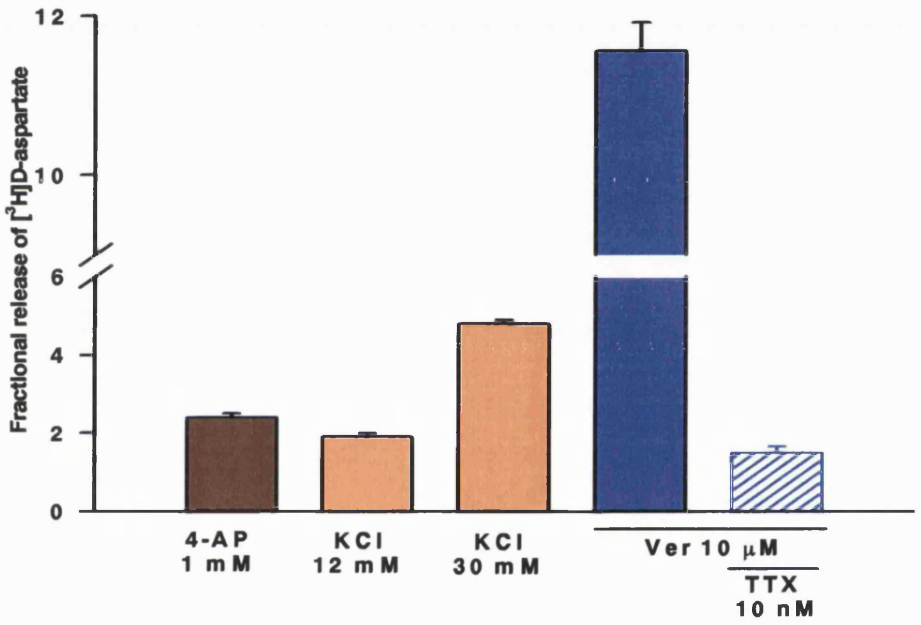

Figure 3.1.7 [^{3}H]D-aspartate release as evoked by depolarising agents applied to frontal cortex synaptosomes. Rat frontal cortex P2 synaptosomes were superfused with KB buffer and stimulated for 90 s with a range of depolarising agents using a 12 channel Brandel™ superfusion apparatus. Release evoked by veratridine was also examined in the presence of TTX, applied 10 min prior to and throughout veratradine stimulation. Release is expressed as a fraction of the total radioactivity remaining in the preparation at the point of stimulation. Results represent the mean ± S.E.M of at least three independent experiments for each depolarising agent concentration.

4-AP (1 mM) released 2.4 ± 0.1% of the total radioactivity ('fractional release'). Veratradine (10 μM) produced a bigger response, of 11.6 ± 0.9%, and this was inhibited by 87% in the presence of tetrodotoxin (TTX; 10 nM), to 1.5 ± 0.2%. The

response to KCl was concentration-dependent, with 12 mM and 30 mM KCl stimulating the release of 1.9 ± 0.1% and 4.8 ± 0.1% of [^{3}H]D-aspartate respectively. Over a concentration range of 3-100 mM, KCl-evoked release displayed an exponential increase in release whereas the concentration-dependant release of 4-AP was relatively linear, with an EC_{50} of 0.14 mM (Fig 3.1.8 A & B).

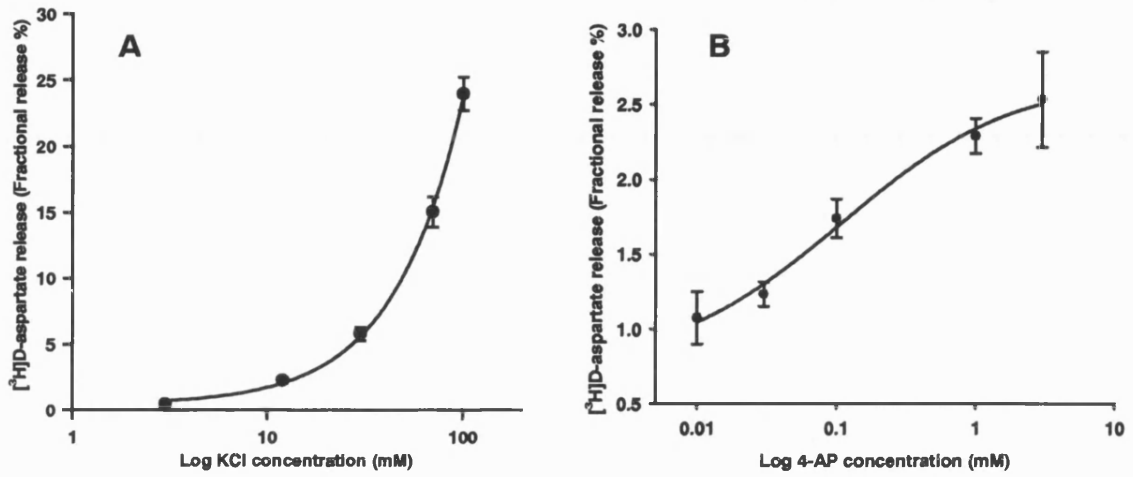

Figure 3.1.8 Concentration-dependant effect of KCl and 4-AP-evoked release of [^{3}H]D-aspartate from rat frontal cortex synaptosomes. Rat frontal cortex P2 synaptosomes were superfused with KB buffer and stimulated for 90 s with either KCl or 4-AP over a range concentrations (KCl, 3-100 mM and 4-AP, 0.01-1 mM). Release for both depolarising agents has been adjusted for buffer-evoked release and is expressed as a fraction of the total radioactivity remaining in the preparation at the point of stimulation. **(A)** Concentration dependant release of [^{3}H]D-aspartate evoked by KCl. **(B)** Concentration dependant release of [^{3}H]D-aspartate evoked by 4-AP. Results represent the mean ± S.E.M of at least three independent experiments for each depolarising agent concentration. Curves fitted using Regression Wizard from Sigma plot v8.0 for Windows XP.

In view of the propensity of the glutamate transporter to reverse, thereby releasing the amino acid in a Ca^{2+}-independent manner (Nicholls & Atwell, 1990), [^{3}H]D-aspartate release in response to the lower concentration of KCl was further evaluated. This concentration of KCl was chosen because the magnitude of the response is more akin to the responses evoked by nAChR stimulation, in studies of dopamine release (Soliakov *et al.*, 1995) and was also used in on-line fluorescence assays to determine the effect of glutamate transporter reversal of endogenous

glutamate release (McMahon & Nicholls, 1989). Synaptosomes were perfused in the absence of Ca^{2+} (Fig. 3.1.9 A and 3.1.10), and/or the presence of an inhibitor of the glutamate transporter (Fig. 3.1.9 B and 3.1.10).

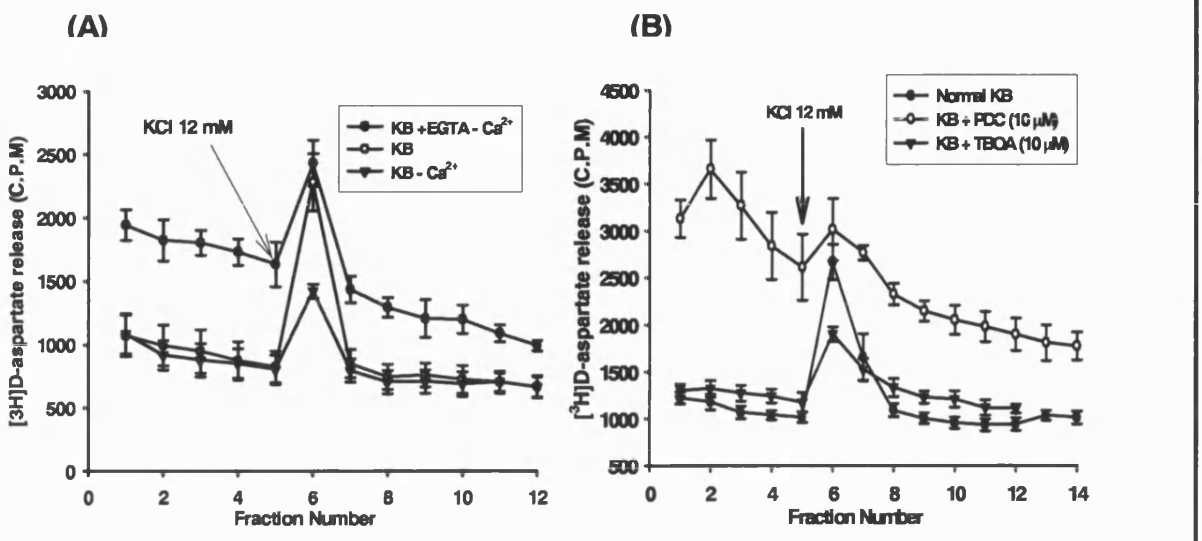

Figure 3.1.9 Representative [^{3}H]D-aspartate release profiles from rat frontal cortex synaptosomes: (A)The effect of absence of Ca^{2+} and the addition of EGTA and (B) The effect of glutamate transport inhibitors PDC and TBOA. (A) Rat frontal cortex P2 synaptosomes were superfused with KB buffer (± Ca^{2+} and or EGTA 5 mM) and stimulated for 90 s with KCl 12 mM in normal KB (open circles), KB (– Ca^{2+}; closed triangles) and KB (– Ca^{2+} + EGTA 5 mM; closed circles). **(B)** Rat frontal cortex P2 synaptosomes were superfused with KB buffer (± PDC or TBOA) and stimulated for 90 s with KCl 12 mM in Normal KB (closed circles), KB (+ PDC 10 μM; open circles) and KB (+ TBOA 10 μM; closed triangles). Release is expressed as C.P.M of [^{3}H]D-aspartate collected in 12-14 fractions using the 12 channel Brandel superfusion system. Results represent the mean ± S.E.M of at least three chambers from a representative experiment

The decision to use KB buffer devoid of any Ca^{2+} rather than standard KB devoid of Ca^{2+} and supplemented with EGTA (5 mM), was because EGTA significantly raised the baseline release of [^{3}H]D-aspartate from the frontal cortex synaptosomes and interfered with the extent of KCl-evoked release compared to control conditions (see Discussion for reasoning). The absence of Ca^{2+} (replaced with an equimolar concentration of Mg^{2+}) in the KB did not affect baseline release of [^{3}H]D-aspartate compared to control, but evoked release was decreased (See Fig. 3.1.9 A).

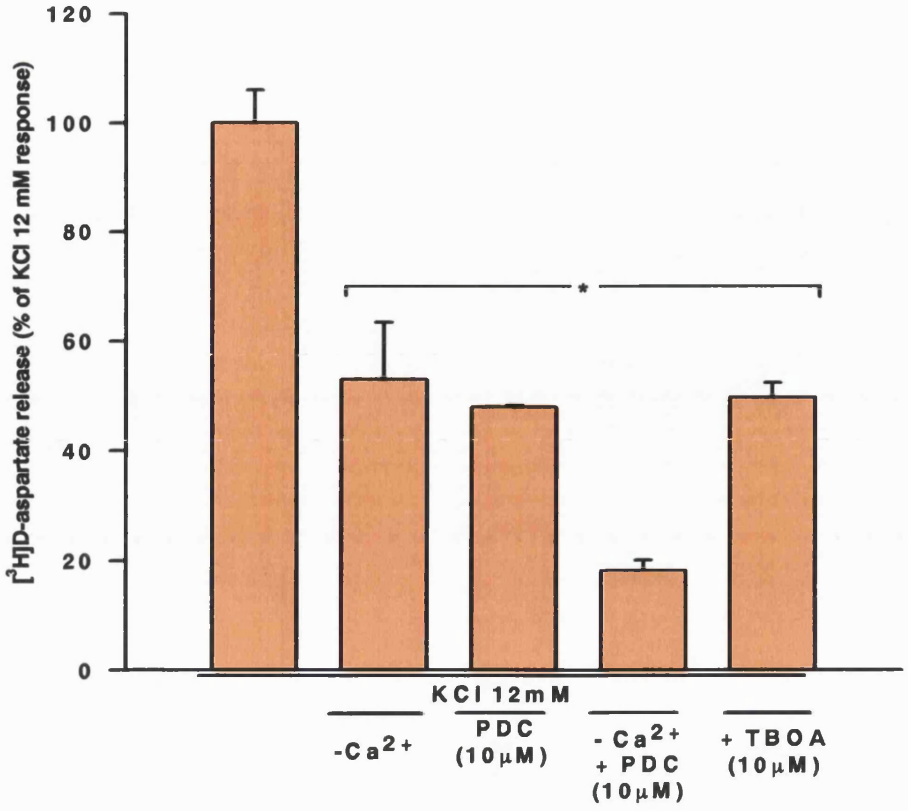

Figure 3.1.10 Release of [^{3}H]D-aspartate from rat frontal cortex synaptosomes in response to KCl 12 mM. Rat frontal cortex P2 synaptosomes were superfused with KB buffer (± Ca^{2+} and or transport blockers) and stimulated for 90 s with KCl 12 mM. The glutamate transporter was blocked by perfusing with Krebs buffer containing L-trans-2,4-PDC (PDC; 10 μM) or DL-TBOA (TBOA; 10 μM). To see if Ca^{2+}-dependence was additive with transporter blockade, PDC was also applied in Ca^{2+}-free buffer. Release of [^{3}H]D-aspartate is expressed as a % of the KCl control, determined in parallel in Krebs buffer without inhibitors. Values are the mean ± S.E.M of three independent experiments with each condition examined in triplicate. * Significantly different from KCl control conditions, $P<0.05$ students unpaired t-test, n=4

The carrier itself transports PDC, whereas TBOA is a non-transportable inhibitor (Bridges *et al*., 1991; Dunlop *et al*., 1993; Shimamoto *et al*., 1998; Waagepetersen *et al*., 2001); both compounds were compared. In the absence of Ca^{2+} there was no change in basal release, but KCl-evoked release was significantly diminished by 47.0 ± 11.0%, (Fig. 3.1.9 A and 3.1.10). PDC (10 μM) and TBOA (10 μM) reduced KCl-evoked release by 52.1 ± 0.4% and 50.3 ± 2.7% respectively (Fig. 3.1.9 B and 3.1.10). PDC (10 μM) in the absence of Ca^{2+} produced a partially additive inhibition, with KCl-evoked release reduced by 81.8 ± 1.9% (Fig. 3.1.10), suggesting that under

the conditions of our assay, exocytosis and reversal of the transporter contribute approximately equally to [^{3}H]D-aspartate release elicited by 12 mM KCl. Similar findings have been reported with respect to the release of endogenous glutamate from synaptosomes (Nicholls *et al.*, 1987).

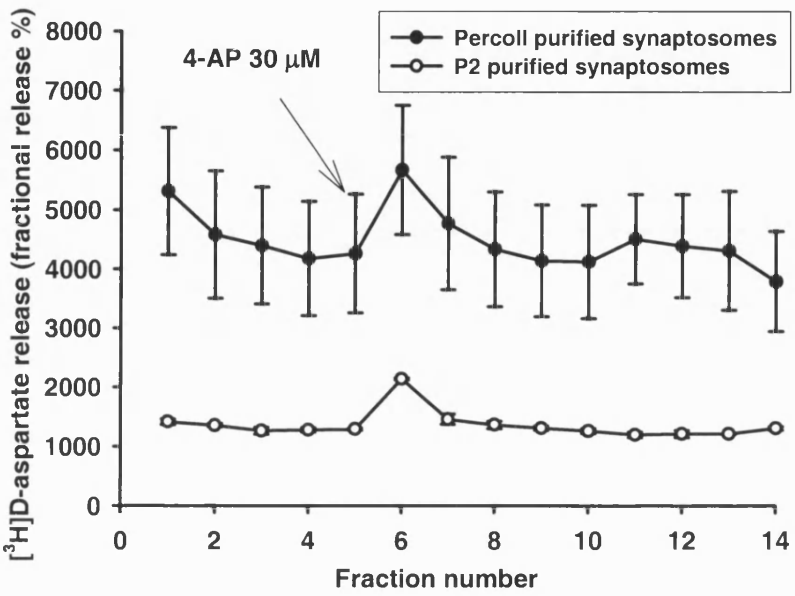

Figure 3.1.11 Representative [^{3}H]D-aspartate release profiles from rat frontal cortex Percoll™ purified and P2 purified synaptosomes: Rat frontal cortex Percoll synaptosomes (closed squares) and P2 synaptosomes (open squares) were superfused with KB buffer and stimulated for 90 s with 4-AP (30 μM). Release is expressed as raw C.P.M values of [^{3}H]D-aspartate collected in 14 fractions using the 12 channel Brandel superfusion system. Results represent the mean ± S.E.M of at least three chambers from a representative experiment.

These findings were from experiments with P2 frontal cortex synaptosomes. Initial studies used Percoll purified synaptosomes to assess the effect of depolarising agents, however it was soon observed that the baseline release of [^{3}H]D-aspartate was approximately 4 fold higher than that observed for P2 synaptosomes and also displayed a high degree of variability (See Fig. 3.1.11). This raised the possibility that the lengthy procedure required to form these synaptosomes may have led to adverse effects on the synaptosome membrane integrity. The high baseline release of [^{3}H]D-aspartate also raised doubt that with a 'high background release' we would

be unable to detect, in future experiments, the nAChR modulation of [^{3}H]D-aspartate release. The decision to use P2 synaptosomes was based on these observations and assumptions.

3.1.6 Discussion

To verify the use of [^{3}H]D-aspartate as a surrogate for glutamate, we assessed its suitability in both uptake and release studies using rat frontal cortex synaptosomes (sections 3.1.1 and 3.1.5).

3.1.7 Uptake of [^{3}H]D-aspartate

Initial experiments into uptake of [^{3}H]D-aspartate utilised the preparation of Percoll™ purified synaptosomes. Although this preparation displayed accumulation of [^{3}H]D-aspartate after filtration and counting (Fig. 3.1.1 A and B), there appeared little evidence of a transporter-mediated process of uptake (Fig. 3.1.2). Lowering the temperature of the incubation medium inhibited uptake: although this could reflect the indirect energy dependence of the EAAT's, (Danbolt, 2001), it is more likely to reflect a reduction in passive movement of [^{3}H]D-aspartate across the lipid bilayer of the synaptosomes or compromised functioning of EAAT. In terms of membrane viability, Percoll™ purification of an S_1 fraction of synaptosomes is a relatively extensive procedure (approximately 1 hour longer than a P2 preparation), where the tissue is subjected to a more severe mechanical procedure in the final resuspension and separation of the synaptosome pellet compared to P2 synaptosomes. Although synaptosomes are maintained in isotonic conditions, the harsh resuspension steps, due to the dense nature of the final pellet, could result in lower membrane integrity for Percoll™ purified synaptosomes compared to that of P2 synaptosomes. This possibility is supported further in our own experiments where it is noted that the baseline release of [^{3}H]D-aspartate in superfused synaptosomes is considerably higher (approximately 4 fold) in Percoll™ synaptosomes than in P2 synaptosomes (see Fig. 3.1.11). However, according to the reports by Dunkley *et al.* (1988), and

Harrison *et al.* (1988), fractions 3 and 4 of the Percoll™ separation of S_1 have a high content of viable synaptosomes with slight differences detailed in the size of synaptosomes between the two fractions. These authors report that synaptosomes are functional in terms of protein phosphorylation, and NAdr uptake and release. Further to this, results presented in Chapter 4 demonstrate that Percoll™ purified synaptosomes can be labelled with anti-synaptophysin and anti-VGluT 1 & 2, indicative of a glutamatergic presynaptic terminal; confocal images of these synaptosomes appear as clear rounded terminals with little evidence that membrane integrity is compromised. It therefore remains to be determined that this viability extends to the efficient functioning of EAAT; interestingly, many studies looking at [^{3}H]D-aspartate uptake or [^{3}H]L-glutamate uptake in synaptosomes do not utilise Percoll™ purified synaptosomes (Bridges *et al.*, 1991; Mitrovic & Johnston 1995; Fleck *et al.*, 2001).

One important consideration that may account for the differences of uptake described for Percoll™ versus P2 synaptosomes is the possible contamination of the synaptosome preparations with gliosomes (closed vesicle elements of glial cells). Percoll™ gradients are believed to contain gliosomes in fractions 2 and 3, whereas P2 synaptosomes should contain a higher content of these vesicles. It is believed that the major contribution to EAA transport is via glial cells, which contain the EAAT, EAAT1 and EAAT2 (Danbolt, 2001; Anderson & Swanson, 2000). These transporters, on gliosomes, could be responsible for retaining [^{3}H]D-aspartate described from the Percoll™ and P2 synaptosomes, however according to the literature, they should be sensitive to TBOA as well as excess D-aspartate or glutamate which was displayed for P2 but not for Percoll synaptosomes (see Fig. 3.1.2; Anderson & Swanson, 2000). This could support the low content of gliosomes

in the suspension of Percoll™ purified synaptosomes compared to P2 synaptosome suspension. Therefore the [^{3}H]D-aspartate uptake demonstrated in Percoll™ purified synaptosomes remains unaccounted for and is likely to represent compromised membrane integrity or transporter function.

The use of P2 synaptosomes has been extensively used in our laboratory for the examination of nAChR modulation of [^{3}H]Dopamine release (Soliakov *et al.*, 1995; Wilkie *et al.*, 1996; Kaiser & Wonnacott 2000; Mogg *et al.*, 2002). Although this preparation is essentially contaminated by non-synaptosomal elements (Nakamura *et al.*, 1993; Suchak *et al.*, 2003), the intention of use was to minimise the possible mechanical damage and time of preparation of the synaptosomes compared to Percoll™ purified synaptosomes. P2 synaptosomes showed a similar proportion of total radioactivity taken up in control conditions compared to Percoll™ purified synaptosomes, however, the amount of [^{3}H]D-aspartate contained in the synaptosomes was significantly less (approximately 50%); this is likely to be the result of P2 synaptosomes having a higher protein concentration from other membrane components.

P2 synaptosomes displayed a reduced uptake of [^{3}H]D-aspartate at <4ºC and in the presence of excess substrates, D-aspartate and L-glutamate (see Fig. 3.1.3). A complete inhibition of uptake was not described, particularly in the presence of a thousand fold excess of D-aspartate or L-glutamate. This suggests a proportion of [^{3}H]D-aspartate uptake may still be via a passive mechanism in this synaptosome preparation. Interestingly DL-TBOA inhibited uptake to the same extent as excess substrates. This non-transportable inhibitor is selective for EAAT1 and EAAT2, as well as EAAT3, and therefore should block all known EAAT's present in this preparation, although additional unidentified EAATs could exist (for review see

Danbolt, 2001). The IC_{50} for DL-TBOA varies between 1-100 μM, depending on the CNS tissue being used and the transporter being assessed (Jaubudon *et al.,* 1999; Shimamoto *et al.*, 1998; Waagpetersen *et al.*, 2001;). Therefore it is not possible to ascertain if the concentration used (10 μM) in these experiments would completely inhibit all known EAAT's and subsequently block all uptake of [^{3}H]D-aspartate.

Uptake, in most conditions, could only be inhibited by approximately 50%, a consistent observation seen especially with low temperature experiments. However it is this latter observation that lends support for a passive mechanism of [^{3}H]D-aspartate uptake when either transporter or membrane viability is compromised. Essentially, low temperatures will cease energy production that maintains the ionic gradients across the plasma membrane. In turn, the directional import of EAA into the cytoplasm, which relies on these ionic gradients, will be prevented. In these conditions no uptake of EAA should occur, more likely, the EAA transporter should reverse (Nicholls & Attwell, 1990), yet approximately 50% uptake is still observed. If disruption of ionic gradients or transport/cell membrane viability is the factor contributing to the inability to see complete inhibition of uptake by assessment of the transporter specificity, then, by improving the local environment of the synaptosomes and hence decreasing the likelihood of non-specific uptake, it was hoped that we could then detect, to a better extent, the transporter specific uptake of [^{3}H]D-aspartate. By increasing the volume to which the original synaptosomes suspension is diluted in, the hypothesised increase in buffer capacity and decreased effect of synaptosome metabolites and endogenous neurotransmitters on synaptosome viability, membrane viability and EAAT function enabled almost a complete inhibition of uptake in the presence of excess substrates. In diluted volumes, excess substrate inhibited [^{3}H]D-aspartate by as much as 80% (Both excess D-aspartate and L-

glutamate; Fig. 3.1.6). Notably, the effect of low temperature was consistent in either of the dilutions (approximate 50 % uptake inhibition), supporting the possibility that the ionic disruption leads to non-specific, passive uptake of [^{3}H]D-aspartate into the synaptosome, as seen in the original P2 preparation. The approximate 50% blockade by incubating synaptosomes with TBOA suggests that the concentration applied was sub-maximal. However, the inhibition described is in good agreement with IC_{50} values described for the compound in cerebellar granule neurons (Waagepetersen *et al.*, 2001).

It is possible that other co-transport mechanisms for glutamate/aspartate that compensate for the loss of action of the EAAT1 and 2 through DL-TBOA inhibition, may be at play at the level of the synaptosome membrane. Of the five EAATs cloned to date (EAAT1-5), the subtype specificity of EAATs at the presynaptic terminal membrane is poorly characterised, where only EAAT2 (Suchak *et al.*, 2003) and a subtype variant form of EAAT2 (GLT 1b; Chen *et al.*, 2002) have been described so far, despite a large body of evidence that EAAT's responsible for [^{3}H]D-aspartate uptake are present on nerve terminal endings (Robinson *et al.*, 1993; Palmer *et al.*, 2003; Suchak *et al.*, 2003). However, this considered, the effects of TBOA and PDC reported here are consistent with the EAAT2 subtype at the presynaptic terminal.

Other than these transporters, it is possible that other high-affinity transporters such as the glutamate-cytisine heteroexchanger or glutamate-ascorbate heteroexchanger could contribute to the uptake of D-aspartate, that cannot be blocked by TBOA or PDC, or are unaffected by low temperatures. These plausible transport mechanisms are poorly characterised and therefore the contribution of these means of transport uptake is purely speculative.

3.1.8 Release of [^{3}H]D-aspartate

The utility of [^{3}H]D-aspartate as a marker for EAA release was demonstrated using general depolarising agents. All the data presented was obtained from the use of P2 frontal cortex synaptosomes. This was on the basis that the use of the Percoll™ purified synaptosomes displayed high baseline release of [^{3}H]D-aspartate and displayed no transporter specificity for [^{3}H]D-aspartate uptake. For reasons outlined in results section 3.1.5, the decision was made to discontinue with the use of Percoll™ purified synaptosomes for the study of EAA release.

4-AP, KCl and veratridine all successfully evoked release of [^{3}H]D-aspartate from synaptosomes (Fig. 3.1.7). 4-AP blocks the rapidly inactivating voltage sensitive K^+_A channels (Tibbs *et al.*, 1989), thus raising the threshold point of the membrane potential to increase the likelihood of depolarisation. Interestingly, increasing 4-AP concentration did not evoke the release of [^{3}H]D-aspartate to the same extent as increasing concentrations of KCl (see Fig. 3.1.8 A & B), which is likely to be a consequence of its mechanism of action; 4-AP induces brief depolarising spikes (mediated by Na^+ channels) that avoids the propensity of the glutamate transporter to reverse and adds to the largely Ca^{2+}-independent release of [^{3}H]D-aspartate as exampled by KCl-evoked release (Nicholls *et al.*, 1989; Tibbs *et al.*, 1989; McMahon & Nicholls, 1991; reviewed by Nicholls, 1989 and 1993). Veratridine-evoked release was TTX sensitive, indicating a reliance on the activation of Na^+ channels for membrane depolarisation, which is in agreement with previously published reports (Arqueros *et al.*, 1984; Nicholls, 1989; Heron *et al.*, 1994).

To investigate the propensity of the EAAT to reverse, the release evoked by KCl was examined further. Initial investigations utilised the incorporation of the Ca^{2+}-chelator EGTA to ensure that no Ca^{2+} was in the perfusing buffer. This has previously been

employed in superfusion investigations of our laboratory to demonstrate the Ca^{2+}-dependency of nAChR modulation of [^{3}H] dopamine release (Soliakov *et al.*, 1995). However, as demonstrated in Fig. 3.1.9 A, baseline release of [^{3}H]D-aspartate from synaptosomes perfused with KB (+ EGTA) was almost two fold greater than normal KB buffer. Serendipitously, the use of EGTA actually reveals EAAT reversal; EGTA increases Na^+ influx – the rise in intracellular Na^+ removes the gradient necessary for EAA uptake and accordingly reverses the EAAT (Szatkowski *et al.*, 1990; Bernarth *et al.*, 1992; Simonato *et al.*, 1993). In the absence of Ca^{2+}-chelators (substituting Ca^{2+} with equimolar Mg^{2+} in the KB), baseline release of [^{3}H]D-aspartate was comparable to control conditions. However, 12 mM KCl-evoked release was reduced by approximately 50 %. This Ca^{2+}-dependent release is consistent with vesicular storage of [^{3}H]D-aspartate and exocytotic release.

Reversal of the glutamate transporter could be directly demonstrated by using EAAT inhibitors. Of the two assessed, PDC significantly raised baseline release of [^{3}H]D-aspartate, compared to TBOA which did not affect baseline release. This is consistent with the two modes of action of these transport inhibitors. PDC is a transportable, competitive inhibitor of EAAT; upon binding to the transporter it is transported across the membrane into the cytosol of the synaptosome. However, when it is transported across the membrane, it exchanges with intrasynaptosomal [^{3}H]D-aspartate, contributing to a higher basal release of [^{3}H]D-aspartate (Waagepetersen *et al.*, 2001). Therefore when depolarising the synaptosomes with KCl, and instigating a reversal of the EAAT, the transporter mediated release of [^{3}H]D-aspartate will be reduced due to the intrasynaptosomal competition of PDC with [^{3}H]D-aspartate for the transporter. TBOA is a competitive, non-transportable inhibitor of EAAT (specifically EAAT1-3). The non-transportable nature of blockade

prevents the heteroexchange of this compound with pre-loaded [^{3}H]D-aspartate, consequently this would have no effect on baseline release of [^{3}H]D-aspartate compared to control conditions (as seen in Fig. 3.1.9. B). It could be hypothesised that in control conditions (normal KB perfused P2 synaptosomes), transporter reversal could be contributing to the baseline release of [^{3}H]D-aspartate from a proportion of synaptosomes where membrane functionality is compromised. If this is true, then TBOA would be expected to decrease the baseline release of [^{3}H]D-aspartate compared to control by preventing [^{3}H]D-aspartate flux through transporter reversal. However this was not observed in our results and supports the notion that P2 synaptosomes are metabolically and functionally viable. TBOA reduces KCl-evoked [^{3}H]D-aspartate release to the same extent as that described for PDC, consistent with KCl-evoked release being partly mediated via transport reversal and consistent with previous reports of K^+-evoked release of [^{3}H]D-aspartate from rat tissue (Simonato *et al.*, 1993; Palmer & Reiter, 1994; Zhou *et al.*, 1995; Savage *et al.*, 2000; Sehmisch *et al.*, 2001; Waagepetersen *et al.*, 2001). Residual [^{3}H]D-aspartate release was displayed in those experiments where both occlusion of Ca^{2+} and addition of PDC in the KB perfusing medium was utilised. This release could be attributed to the contribution of other co-transport mechanisms acting in reverse in depolarising conditions (Takahashi *et al.,* 1997) and trace amounts of Ca^{2+} that remained in the synaptosome preparation and before being perfused with Ca^{2+} free buffer.

In summary, this section supports the use of [^{3}H]D-aspartate for examining the uptake and release of EAA in presynaptic nerve terminals. Until a decade ago, the prevailing view was against the use of D-aspartate as a suitable analogue for

glutamate (see Introduction section 3.1.2). The use of this analogue is now gaining a good deal of favour. Our results demonstrate that [^{3}H]D-aspartate displays similar mechanisms of uptake and release as cited for endogenous glutamate.

Chapter 3 Section 2

3.2 nAChR enhancement of membrane depolarisation-evoked release of [^{3}H]D-aspartate

3.2.1. Introduction

Depolarising agents and electrical stimulation of CNS tissue *in vitro* have previously been employed to reveal the effects of presynaptic adenosine A_1, AMPA, D_2, mGlu, and prostaglandin E_2 receptors on facilitating the release of EAA, on the basis that application of agonists alone, specific for these receptors, demonstrated no detectable effect, but either enhanced or depressed the depolarising stimulus-evoked release (Yamamoto & Davy, 1992; Barrie & Nicholls, 1993; Nishihara *et al.*, 1995; Zhou *et al.*, 1995; Patel & Croucher, 1997; Nicholls, 1998; Cartmell & Schoepp, 2000).

The inability of detecting changes in EAA release directly using presynaptic receptor agonists or antagonists alone may be a combination of the temporal characteristics of the measuring system itself and the inability to outweigh the EAA uptake transporter system; any released EAA evoked by presynaptic receptor activation could be immediately taken up by the tissue preparation and thus avoid detection. Attempts to outweigh these problems for the direct detection of presynaptic modulation of EAA release have included fast superfusion rates (Palmer & Reiter, 1994; Collard, 1996) or inclusion of EAAT blockers (Muzzolini *et al.*, 1996; Savage *et al.*, 2001; Sehmisch *et al.*, 2001), yet it should be noted that the incorporation of transport blockers is not always necessary for some studies (e.g. See Patel & Croucher, 1997).

As demonstrated in Section 3.1 of this chapter, EAA are found in two pools, vesicular and cytoplasmic. Vesicular release of EAA relies on the calcium dynamics within the nerve terminal whereas the reversal of the EAAT is partly responsible for the release of EAA from the cytoplasm (Nicholls, 1998). With respect to the enhancement of EAA release, presynaptic receptors could modulate the release by increasing the *probability* of vesicular release in response to a depolarising stimulus or indeed by increasing the likelihood of the EAAT to reverse. The purported presynaptic mechanisms behind this enhancement were

summarised by Sanchez-Prieto *et al.* (1996), and include; (1) changing the kinetics of K^+ and Na^+ channels involved with the depolarisation-evoked release of EAA. (2) Altering the activation or inactivation state of calcium channels coupled to release mechanisms or access of Ca^{2+} to the exocytotic trigger or (3) acting via secondary messenger cascades at specific intracellular loci to change the exocytotic mechanism of release. Such possibilities have been examined, where, for example, in mGluR presynaptic modulation of glutamate release, PKC activation from activation of a G-protein-coupled facilitatory mGluR, results in inhibition of a 'delayed rectifier' type K^+ channel. Therefore on application of 4-AP and mGluR agonist, the frequency and duration of action potentials are increased, subsequently increasing glutamate release, compared to the effect of 4-AP alone (Sanchez-Prieto *et al.*, 1996; Cartmell & Schoepp, 2000).

With respect to the nAChR, evidence from electrophysiological investigations indicates that the high Ca^{2+} permeability of the α7 nAChR (Vernino *et al.*, 1999; Seguela *et al.*, 1993, Delbono *et al.*, 1996) is the likely candidate responsible for increasing the probability of glutamate release (Gray *et al.*, 1996; Ji *et al.*, 2001; Sharma & Vijaraghavan, 2003; For review see McGehee, 2002). These authors proposed that if presynaptic nAChRs open just before the arrival of an action potential, the presynaptic concentration of Ca^{2+} is elevated so that on arrival of an action potential, the probability of neurotransmitter release is increased, in a similar manner as described for paired-pulse facilitation. The most recent report to this facilitation describes that calcium flux through presynaptic nAChR leads to mobilisation of store calcium by calcium induced calcium release (CICR) (Sharma & Vijaraghavan, 2003).

It is this hypothesis that supports the theory of nAChR enhancement of depolarisation-evoked release when combining a depolarising stimulus with nAChR agonists, reported by Marchi *et al.* (2002). In this study, application of nAChR agonists alone to human neocortical or rat striatal synaptosomes in a superfusion paradigm had no effect on [^{3}H]D-

aspartate release. When nAChR agonists were combined with a KCl (12 mM) depolarising stimulus a facilitation of [^{3}H]D-aspartate release was detected. The release evoked in these conditions was Ca^{2+}-dependent and sensitive to the α7 nAChR antagonists α-Bgt and MLA also inferred from electrophysiological studies (Couturier *et al.*, 1990; Seguela *et al.*, 1993). This study prompted our own investigation into the nAChR enhancement of KCl-evoked release of [^{3}H]D-aspartate.

Prior to the Marchi *et al.* (2002) report, electrical-evoked release of [^{3}H]D-aspartate (and KCl-evoked release) from rat primary cortical cultures was shown to be enhanced on concomitant application of nicotine (Beani *et al.*, 2000). This release was Ca^{2+} dependent and sensitive to α-Bgt and mecamylamine where the authors went on to propose that nAChR facilitation of [^{3}H]D-aspartate release may be mediated by α7 and non-α7 nAChR.

By manipulation of the experimental protocol described by Beani *et al.* (2000) a Brandel™ automated 20-channel superfusion machine with combined electrical generator was utilised to assess the effect of electrical stimulation to rat frontal cortex sections pre-exposed to nicotine. These experiments are also based on previous 'electrical stimulation' superfusion experiments (Muzzolini *et al.*, 1996; Savage *et al.*, 2001; Sehmisch *et al.*, 2001). Each of these studies have demonstrated the Adenosine A1 receptor modulation of electrical-evoked release of either [^{3}H]D-aspartate or [^{3}H]L-glutamate; by inhibiting A1 receptors, evoked release was increased suggesting that endogenous adenosine acts to inhibit EAA release. Only Sehmisch *et al.* (2001) investigated the effect of nicotinic modulation of electrical-evoked release of [^{3}H]L-glutamate but reported no effect. However, only nAChR antagonists were employed (mecamylamine) to discern the involvement of nAChR. In the study presented here, frontal cortex minces loaded with [^{3}H]D-aspartate and placed in a closed chamber superfusion system will be subjected to nicotinic agonist stimulation prior to the application of an electrical stimulus. It is hypothesised that those chambers exposed

to a nAChR agonist would give a higher electrical evoked release of [^{3}H]D-aspartate compared to control conditions, on the same basis of nAChR activation increasing the 'probability' of release (Gray *et al.*, 1996; Ji *et al.*, 2001 Sharma & Vijaraghavan, 2003).

Here we describe the effect of nAChR agonists on different means of depolarisation-evoked release of [^{3}H]D-aspartate from rat frontal cortex synaptosomes or minces.

3.2.2 Results

3.2.3 nAChR agonists and depolarising agents

The initial investigation of nAChR-evoked release of [^{3}H]D-aspartate from rat synaptosomes was carried out using a 6 channel Brandel™ superfusion system. Rat striatal synaptosomes were loaded with [^{3}H]D-aspartate and superfused in the same manner as described by Marchi *et al.* (2002). Nicotine, over the concentration range 1-100 μM, applied for a 90 s stimulation concomitantly with KCl (12 mM), failed to evoke any significant additional release of [^{3}H]D-aspartate compared with KCl alone (see Fig. 3.2.1.), which is in contrast to the observation made by Marchi *et al.* (2002). Similarly, nicotine failed to enhance 12 mM KCl-evoked release of [^{3}H]D-aspartate from frontal cortex synaptosomes, monitored using a 12 channel Brandel™ superfusion system (See Fig. 3.2. 1.B).

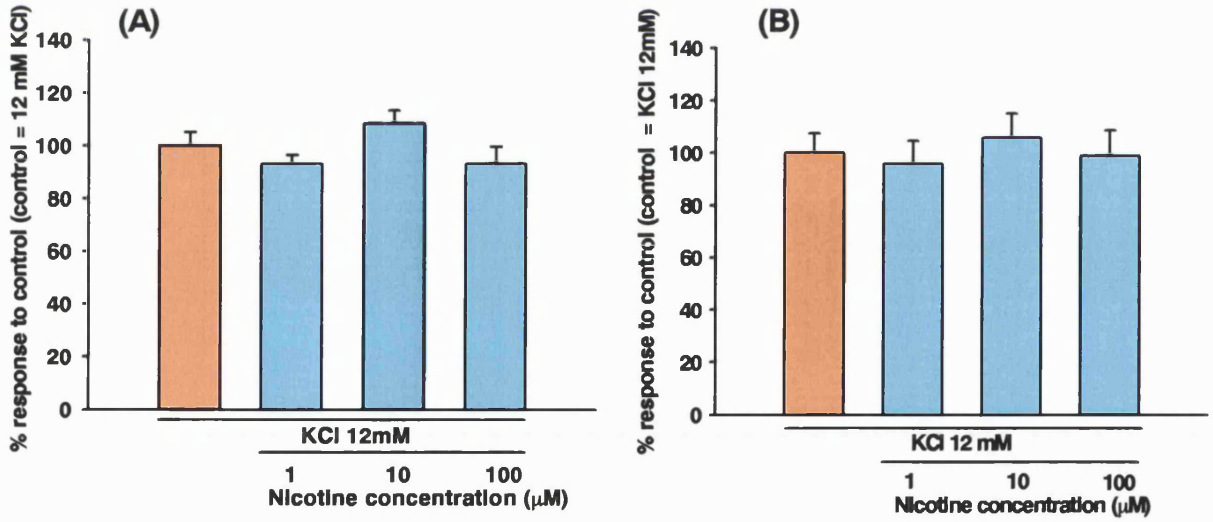

Figure 3.2.1 KCl-evoked release of [^{3}H]D-aspartate from rat frontal cortex synaptosomes: The effect of a combined nicotine stimulus. Rat synaptosomes were superfused with KB buffer and stimulated for 90 s with KCl (12 mM) with or without nicotine (over a concentration range of 1-100 μM). **(A)** [^{3}H]D-aspartate evoked release from rat striatal synaptosomes using a 6 channel Brandel™ superfusion apparatus. **(B)** [^{3}H]D-aspartate evoked release from rat frontal cortex synaptosomes using a 12 channel Brandel™ superfusion apparatus. Release is expressed as a percentage of KCl (12 mM) alone control taken as 100% of the response. Results represent the mean ± S.E.M of at least three independent experiments.

The percentage fractional release of [^{3}H]D-aspartate by KCl (12 mM) alone showed no significant difference between the two superfusion systems (2.1 ± 0.1% and 1.8 ± 0.2% for rat striatal synaptosomes and rat frontal cortex synaptosomes respectively). This confirmed that similar perfusion and collection rates of the two systems were maintained. Uniformity was also maintained in terms of similar protein concentrations of tissue between the two systems; rat striatal synaptosomes at 0.25 ±0.02 mg per chamber and rat frontal cortex synaptosomes at 0.22 ± 0.01 mg per chamber, also reflected in similar total [^{3}H]D-aspartate counts recorded on the filters at the end of each experiment.

Failure of nicotine to enhance KCl-evoked release of [^{3}H]D-aspartate lead to the use of another depolarising agent, 4-AP, concomitantly applied with nicotine. An initial experiment indicated an enhancement of 1 mM 4-AP-evoked release of [^{3}H]D-aspartate from rat frontal cortex synaptosomes by co-application of nicotine (150 μM). This concentration of nicotine was chosen for further repetition of the experiment on the 6-channel superfusion system. Over a set of experiments, the release evoked by co-application of 4-AP (1 mM) with nicotine (150 μM) showed considerable variability and hence no significant enhancement to control was observed (see Fig. 3.2.2).

In attempt to reduce the variability, the application of nicotine was combined with a lower concentration of 4-AP, but again, no significant enhancement of the 4-AP evoked release was observed (see Fig. 3.2.2). Fractional release of 0.1 mM 4-AP (1.7 ± 0.1%) was approximately 45% lower than that evoked by 1 mM 4-AP (3.0 ± 0.5%), however, the variability at lower concentrations of 4-AP (0.1 mM) evoked release of [^{3}H]D-aspartate was reduced, reflecting only 5% variability of the release between experiments, compared to 4-AP (1 mM) where the variability was 17% between experiments.

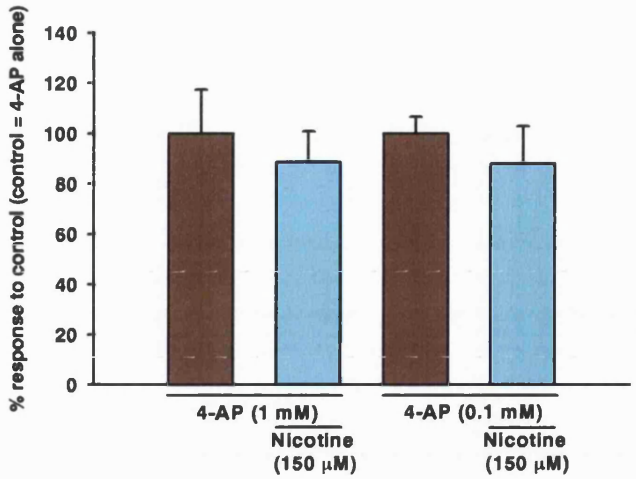

Figure 3.2.2 The effect of 4-AP co-application with nicotine (150 μM) on [^{3}H]D-aspartate release . Rat frontal cortex synaptosomes were superfused with KB buffer and stimulated for 90 s with 4-AP (at 1 and 0.1mM) with or without nicotine (150 μM) using a 6-channel Brandel™ superfusion apparatus. Release is expressed as a percentage of 4-AP alone control taken as 100% of the response. Results represent the mean ± S.E.M of three independent experiments.

Different nAChR agonists were applied concomitantly with KCl (12 mM) as another approach to detect a nAChR enhancement of depolarisation-evoked release. Epibatidine, tested at a concentration range of 0.1-1000 nM concomitantly applied with KCl (12 mM) resulted in a biphasic profile suggesting two phases of increased release (see Fig. 3.2.3).

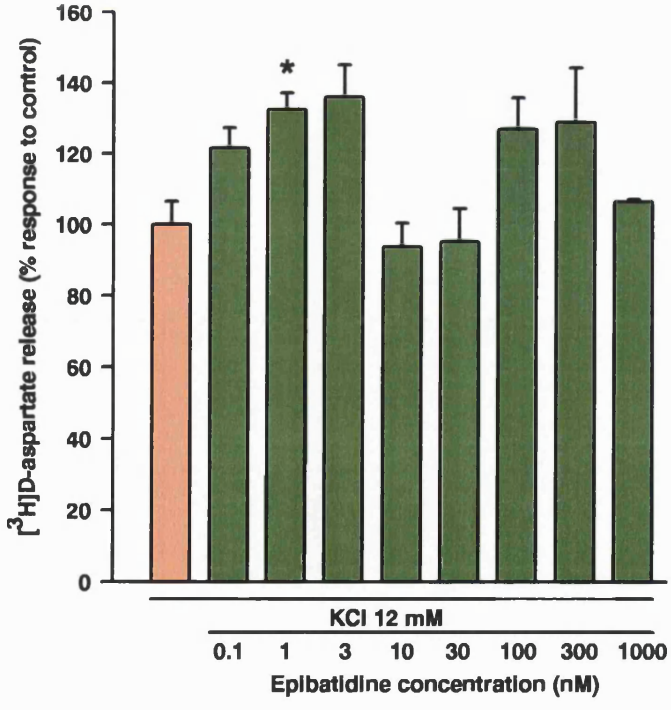

Figure 3.2.3 Epibatidine concentration dependence of enhanced KCl-evoked [^{3}H]D-aspartate release. Rat frontal cortex synaptosomes were superfused with KB buffer and stimulated for 90 s with KCl (12 mM) and epibatidine (over a concentration range of 0.1-100nM) using a 12 channel Brandel™ superfusion apparatus. Release is expressed as a percentage of KCl (12mM) control taken as 100% of the response. Results represent the mean ± S.E.M of at least six independent experiments. * Statistical significance observed $P<0.05$, n=8, one-way ANOVA with post-hoc tukeys analysis.

However, epibatidine only significantly enhanced the KCl-evoked release of [^{3}H]D-aspartate at one concentration: 1 nM (32.0 ± 5.7% above control; KCl 12 mM control = 100 ± 6.4%). Epibatidine at 3 and 100 nM also raised evoked release to 36.2 ± 10.0% and 26.0 ± 8.9% above the effect control, but these values are just outside statistical significance using a one-way ANOVA with post-hoc tukeys analysis. All other concentrations tested failed to evoke a significant enhancement of KCl-evoked [^{3}H]D-aspartate release (Fig. 3.2.3).

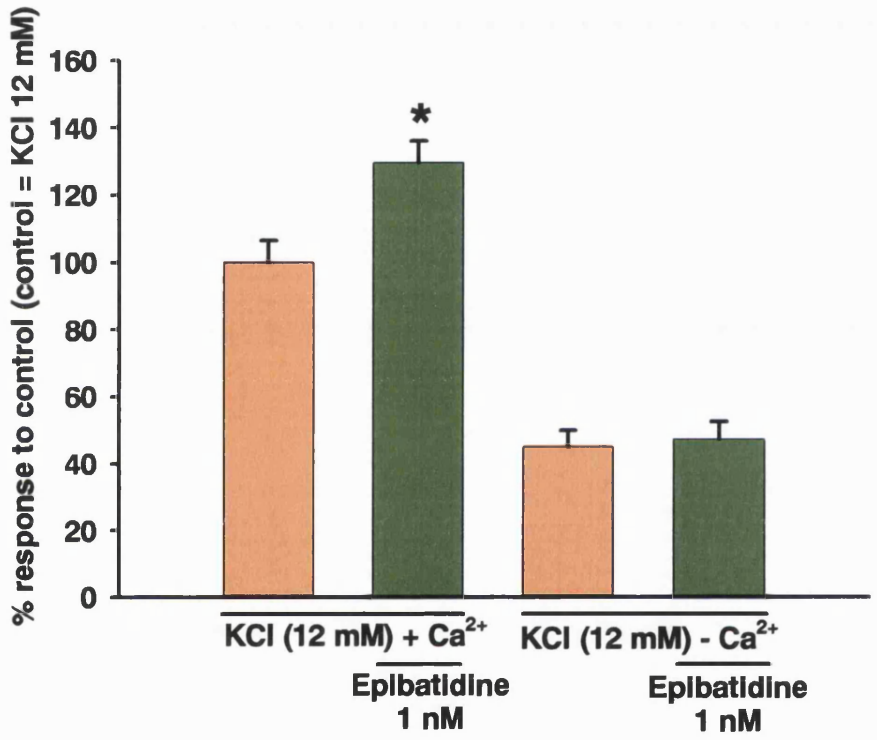

Figure 3.2.4 Calcium dependency of epibatidine (1 nM) enhancement of KCl-evoked release of [^{3}H]D-aspartate. Rat frontal cortex synaptosomes were superfused with KB buffer and stimulated for 90 s with KCl (12 mM) and KCl (12 mM) + epibatidine (1 nM) in the presence and absence of Ca^{2+} (Ca^{2+} was replaced with an equimolar concentration of Mg^{2+}). Release is expressed as a percentage of control (KCl 12mM in the presence of Ca^{2+}), taken as 100% of the response. Results represent the mean ± S.E.M of at three independent experiments. * Statistical significance observed to control, $P<0.05$, n=3, one-way ANOVA with post-hoc tukeys analysis.

Epibatidine (1 nM) enhancement of KCl-evoked [^{3}H]D-aspartate release displayed complete Ca^{2+}-dependency (See Fig. 3.2.4). By removing Ca^{2+} from the perfusing buffer, KCl-evoked release was reduced to 44.97 ± 4.7% of the control response (KCl 12 mM in

the presence of Ca^{2+} = 100 ± 6.4%). This is in agreement with the approximate 50% inhibition of KCl-evoked release of [^{3}H]D-aspartate reported in Chapter 3 Section 3.1.5 (Fig 3.1.10). Concomitant application of epibatidine in the absence of Ca^{2+} produced no enhancement of [^{3}H]D-aspartate release compared to the release evoked by KCl alone. In normal Ca^{2+} containing KB buffer, epibatidine enhanced KCl-evoked release [^{3}H]D-aspartate by 29.5 ± 6.4% above control; the magnitude of this effect is consistent with Fig. 3.2.3.

Anatoxin-a was also examined in the same manner as described for epibatidine, over a concentration range of 10-1000 nM. Similar to the KCl enhancement of [^{3}H]D-aspartate by co-application of epibatidine, only one concentration of anatoxin-a (300 nM) showed a significant enhancement of KCl-evoked release (25.2 ± 10.0% above control; KCl 12mM control = 100 ± 7.3%). At concentrations of anatoxin-a above 600 nM, the variability of the data prevented statistical significance (Fig. 3.2.5).

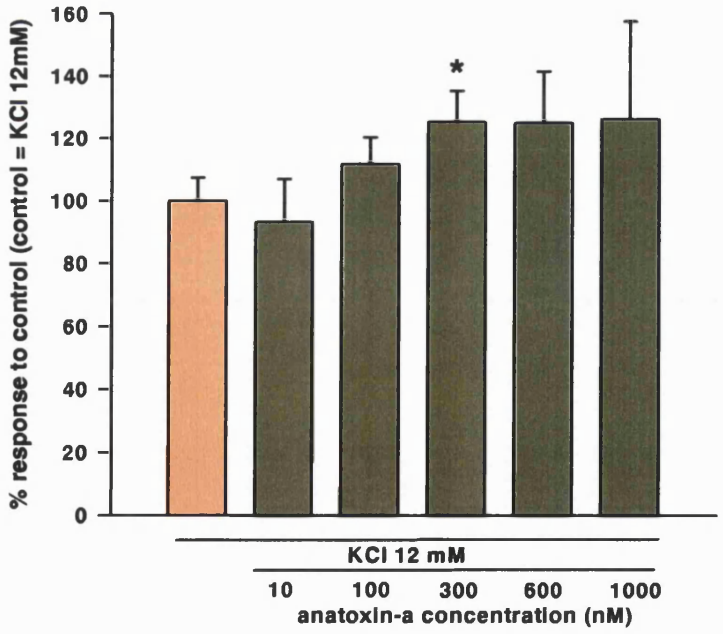

Figure 3.2.5. Anatoxin-a concentration dependence of enhanced KCl-evoked [^{3}H]D-aspartate release. Rat frontal cortex synaptosomes were superfused with KB buffer and stimulated for 90 s with KCl (12 mM) with or without anatoxin-a (over a concentration range of 10-1000 nM) using a 12 channel Brandel™ superfusion apparatus. Release is expressed as a percentage of KCl (12 mM) control taken as 100% of the response. Results represent the mean ± S.E.M of at least five independent experiments. * Statistical significance observed $P<0.05$, n=6, One way ANOVA with post-hoc tukeys analysis.

3.2.4 nAChR specificity of enhanced KCl-evoked [^{3}H]D-aspartate release

In order to confirm nAChR specificity of both epibatidine (1 nM) and anatoxin-a (300 nM) enhancement of KCl–evoked release of [^{3}H]D-aspartate, the nAChR antagonist mecamylamine (20 μM) was perfused for 10 min in the KB buffer, prior to stimulation with agonist and KCl (12 mM) or KCl alone.

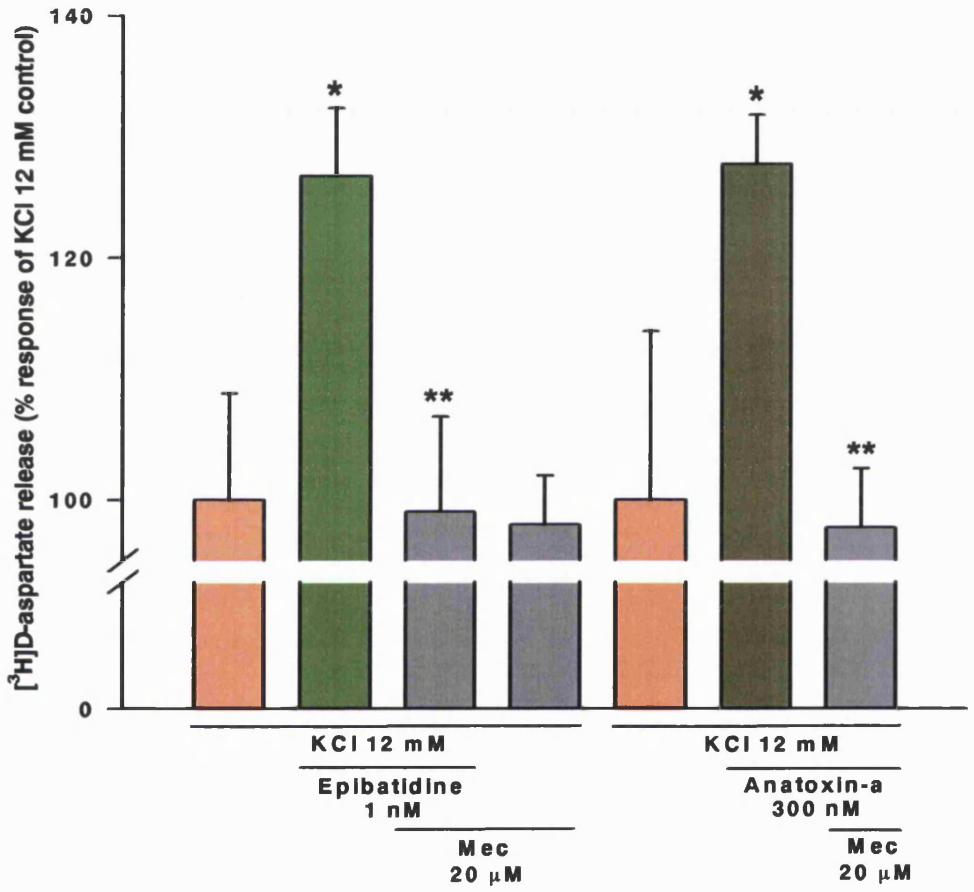

Figure 3.2.6 Mecamylamine antagonism of epibatidine and anatoxin-a enhancement of KCl-evoked [^{3}H]D-aspartate release. Rat frontal cortex synaptosomes were superfused with KB buffer and perfused for 10 min with Mec (20 μM) prior to a 90 s concomitant stimulation with KCl (12 mM) and epibatidine (1 nM) or anatoxin-a (300 nM). Release is expressed as a percentage of KCl (12 mM) control taken as 100% of the response. Results represent the mean ± S.E.M of at least five independent experiments. * Statistical significance observed between KCl + epibatidine/anatoxin-a compared to control $P<0.05$, n=8, One way ANOVA with post-hoc tukeys analysis. ** Statistical significance observed between KCl + epibatidine/anatoxin-a + Mec compared to KCl + epibatidine/anatoxin-a, $P<0.05$, n=8, one way ANOVA with post-hoc tukeys analysis.

Mecamylamine significantly inhibited the epibatidine (1nM) enhancement of KCl-evoked [^{3}H]D-aspartate release by 100 ± 7.9% (Fig. 3.2.6). Release evoked by KCl + epibatidine was 26.7 ± 5.6% above the release evoked by KCl alone (100 ± 8.8%) which is comparable to that obtained from the concentration dependence experiments in Fig. 3.2.3, and reached statistical significance.

For anatoxin-a (300 nM) enhancement of KCl-evoked [^{3}H]D-aspartate release, mecamylamine again significantly inhibited this response by 102.4 ± 4.9% (see Fig 3.2.6). Release evoked by KCl + anatoxin-a was 27.7 ± 4.1% above the release evoked by KCl alone (100 ± 13.9%). Here the KCl (12 mM) evoked release displayed a higher variability than observed in Fig. 3.2.5, however, the enhancement by anatoxin-a is comparable to that obtained from the concentration dependence experiments, and reached statistical significance when compared using one-way ANOVA with post hoc tukeys analysis. Mecamylamine showed no antagonism against the release evoked by KCl alone (See Fig 3.2.6).

To determine the nAChR subtype specificity of the nAChR enhancement of KCl-evoked release of [^{3}H]D-aspartate, nAChR antagonists selective for the α7* nAChR subtype were perfused in the KB buffer for 10 or 20 min prior to the stimulation with the appropriate concentrations of epibatidine or anatoxin-a + KCl (12 mM).

Stimulation with KCl alone and KCl + epibatidine or anatoxin-a (minus antagonist) was carried out as control measures, with each condition examined in triplicate within the same experiment. The effect of MLA (50 nM) was first assessed against epibatidine (1 nM) enhancement of KCl-evoked release of [^{3}H]D-aspartate. However, over a set of four experiments, only one experiment showed enhancement of KCl-evoked release of [^{3}H]D-aspartate by epibatidine necessary for the comparison of effect of MLA (21.5 ± 12.5%

blockade of the enhancement, mean ± S.E.M of 3 replicates). This variability in the response prevented a credible analysis of the effect of MLA. A similar problem was encountered in the assessment of MLA against the enhancement of KCl-evoked release of [^{3}H]D-aspartate by anatoxin-a over three experiments.

The α7 nAChR specific antagonist α-conotoxin ImI (1 μM; Cartier *et al.*, 1996) was assessed against anatoxin-a enhancement of KCl-evoked release of [^{3}H]D-aspartate, in a final attempt to ascertain if the α7 nAChR subtype is associated with this enhancement. Of these experiments, three out of four experiments showed anatoxin-a (300 nM) enhancement of KCl-evoked release of [^{3}H]D-aspartate (27.4 ± 13.3% above control, n=4; KCl 12 mM = 100 ± 9.6%). α-Conotoxin ImI (1 μM) inhibited the anatoxin-a enhancement of KCl-evoked release of [^{3}H]D-aspartate by 54.7 ± 48.9%, hence the variability of the response prevented any conclusion being drawn (see Fig. 3.2.7).

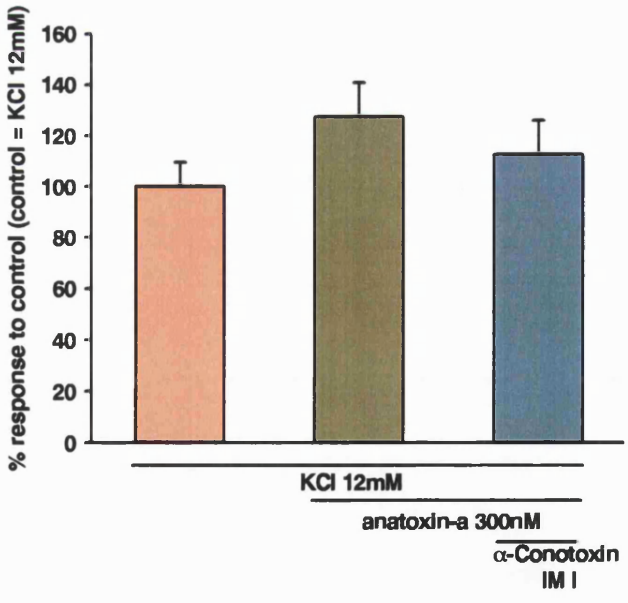

Figure 3.2.7. α-Conotoxin ImI antagonism of anatoxin-a enhancement of KCl-evoked [^{3}H]D-aspartate release. Rat frontal cortex synaptosomes were superfused with KB buffer and stimulated for 90 s with KCl (12 mM) and anatoxin (300 nM) using a 12 channel Brandel™ superfusion apparatus. The α7 antagonist α-Conotoxin ImI (1 μM) was present in the perfusing buffer for 10 min before the application of KCl + anatoxin-a and remained throughout the remainder of the experiment. Release is expressed as a percentage of control (KCl 12 mM alone taken as 100% of the response). Results represent the mean ± S.E.M of four independent experiments.

The increasing variability of KCl-evoked responses and the inability to detect a clear α7 nAChR involvement of the nAChR agonist enhancement of depolarising agent-evoked

release of [^{3}H]D-aspartate halted any further experiments aimed to characterise the nAChR subtype involved in this response. As described in the next section of this chapter (section 3.3), re-assessment of the effects of nAChR agonists applied alone began to reveal a significant effect above basal release. Further experiments then focused on this aspect of nAChR involvement of [^{3}H]D-aspartate release.

3.2.5 Characterisation of electrical-evoked release of [^{3}H]D-aspartate

The release of [^{3}H]D-aspartate from frontal cortex minces was studied using an automated Brandel™ Superfusion system combined with an electrical stimulation generator. To examine the effect of an electrical stimulus, both current intensity and current frequency were tested for their effects on release from frontal cortex minces (see Fig. 3.2.8 A & B). The aim of these particular experiments was to ascertain a suitable level of release that could allow detection of an enhancement of release in the presence of (or pre-treatment with) nAChR agonists. The parameters of these conditions were based on previously established conditions by Savage *et al.* (2001) where electrical-evoked release of [^{3}H]D-aspartate from hippocampal slices was demonstrated.

Maximal [^{3}H]D-aspartate release was observed at a current intensity of 70mA (1.6% of total [^{3}H]D-aspartate released). Increasing the current intensity to 90mA reduced [^{3}H]D-aspartate release. No further experiments were carried on these high current intensities on the basis that the high [^{3}H]D-aspartate evoked release would mask any possibility of being able to detect an enhancement from slices pre-treated with nicotine. At lower current intensities of 30 and 50mA, a more consistent response of [^{3}H]D-aspartate release was observed, releasing 0.29 ± 0.07% and 0.42 ± 0.04% of total [^{3}H]D-aspartate released respectively.

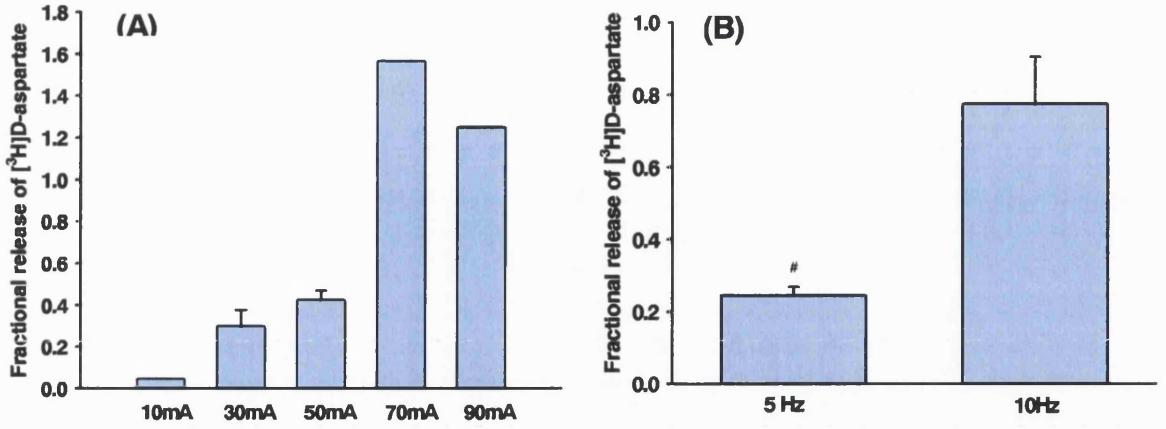

Figure 3.2.8 The effect of current intensity and current frequency effect on [^{3}H]D-aspartate release from rat frontal cortex sections. (A) Rat frontal cortex minces were superfused as described in the methods with KB buffer only. After a 12 min collection of basal perfusates, minces were subjected to a 90 sec, 5Hz electrical stimulus (biphasic square wave pulse at 5Hz for 90 s) with current intensity varying between sets of four chambers across the Brandel superfusion system. (B) As in (A), but subjected to an electrical stimulus (50mA, biphasic square wave pulse for 90 s) with current frequency varying between sets of four chambers across the Brandel superfusion system. [^{3}H]D-aspartate release is expressed as percentage of total radioactivity present in the tissue at the point of electrical stimulation for both conditions. # note that fractional release is half that of the same conditions in (A), reflecting the inherent variability of the assay. Results represent the mean ± S.E.M of at least two independent experiments unless stated otherwise.

At 10mA, the release was considered too small (0.05 ± 0.05%) to provide reliable data for further experiments (see Fig. 3.2.8 A). Two current frequencies were tested for their effect on [^{3}H]D-aspartate (see Fig. 3.2.8 B) (within the ranges used in the literature, see Savage *et al.,* 2001, and Muzzolini *et al.,* 1996), with the current intensity of the electrical pulse set at 50mA. A 10 Hz frequency gave a three fold increase in release (0.77 ± 0.13%) of total [^{3}H]D-aspartate release compared to that evoked by a 5 Hz current intensity (0.25 ± 0.02%). From these experiments, the standard control test stimulus consisted of a 50 mA, biphasic square wave pulses at 5 Hz for 90 s.

3.2.5.1 TTX sensitivity

Application of TTX (1μM), a general Na+ channel blocker, should prevent the depolarisation effect of the electric stimulus and ultimately the release of [^{3}H]D-aspartate

from the frontal cortex minces. To assess if the release of [^{3}H]D-aspartate evoked by the test electrical stimulus depends on the propagation of an action potential through to the presynaptic terminal, TTX was applied to the superfusion medium prior to and during the electric stimulus (see Fig. 3.2.9). Fig. 3.2.9 shows that in the presence of TTX, electrical stimulation-evoked release of [^{3}H]D-aspartate is reduced by 74 ± 8.9%.

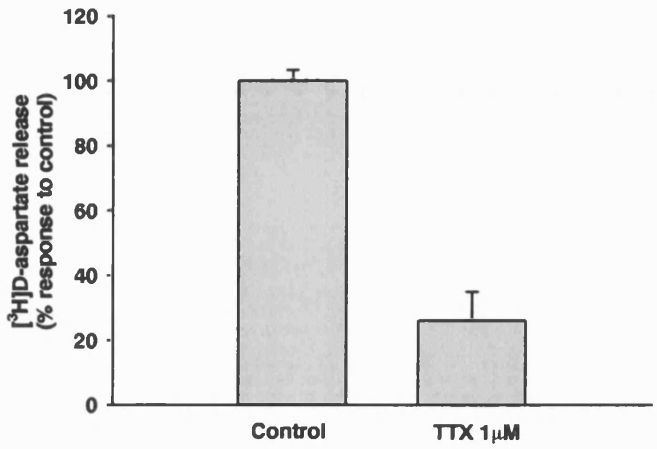

Figure 3.2.9. TTX sensitivity of electrically-evoked release of [^{3}H]D-aspartate from rat frontal cortex minces. Frontal cortex minces were superfused as described in methods and subjected to an electrical stimulus (50mA 2ms biphasic square wave pulse at 5HZ for 90 s) in the absence (control) and presence of TTX 1μM. Results are expressed as a percentage of the control evoked release. Results represent the mean ± S.E.M of two independent experiments.

3.2.5.2 Nicotine enhancement

Having established a suitable level of electrical stimulation to give a relatively consistent response, we then determined the effect of a nicotine stimulus prior to the application of our standard electrical stimulus. In contrast to our previous investigation, where a nAChR agonist stimulus was applied concomitantly with a K^+ depolarising stimulus, the application of both an electrical stimulus and a chemical stimulus at the same time is limited. This is because although flow rates of each chamber are the same, the tubing that provides buffer and drug medium differs slightly in length, enough to warrant that if the drug and electrical stimulus were applied at the same time, some chambers would be with or without drug therefore increasing the possibility of a varied response. Instead we opted to apply the electrical stimulus after an approximate 90 s washout of the agonist. Although some chambers might receive a washout period that may have been longer or shorter than others

it is hypothesised that the downstream effects of 'priming' the presynaptic terminal, via nAChR activation, are sustained long enough to enhance the effects of a subsequent electrical depolarisation. Fig. 3.2.10 A demonstrates the effect of a pre-nicotine stimulus on the enhancement of electrically-evoked release of [^{3}H]D-aspartate.

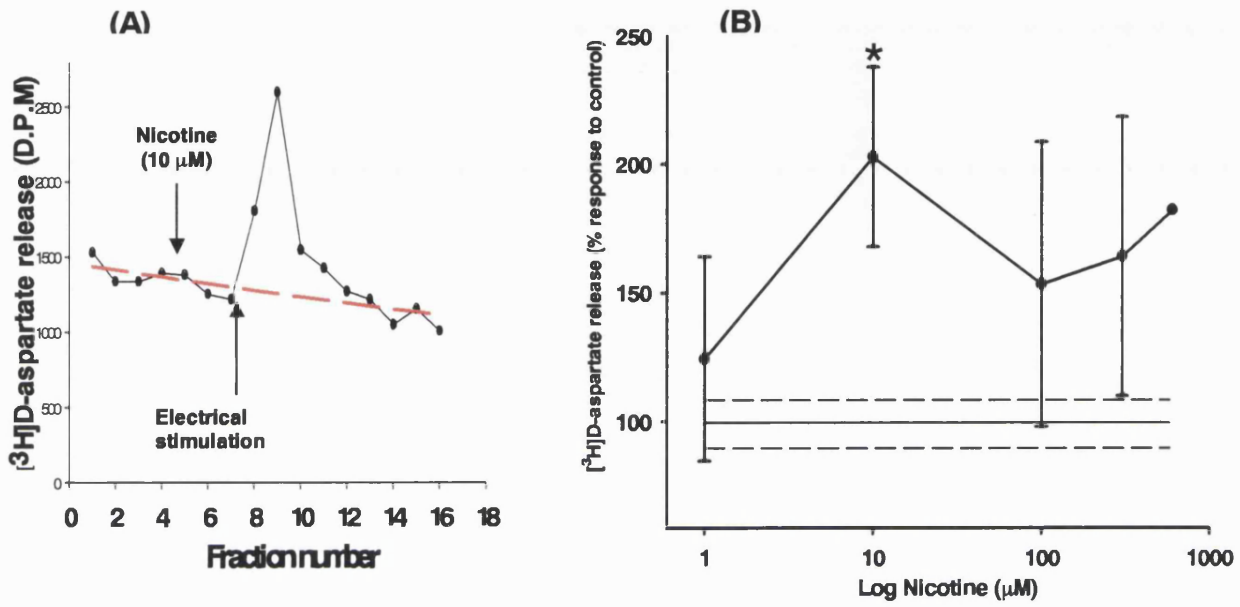

Figure 3.2.10. Enhancement of [^{3}H]D-aspartate release as evoked by a standard electrical stimulus from pre-nicotine treated frontal cortex minces. (A) Raw trace example of [^{3}H]D-aspartate release from rat frontal cortex minces. Frontal cortex minces were superfused as described in methods and subjected to an electrical stimulus. Nicotine (10 μM) was applied to superfusion chambers in parallel 3 min before an electrical stimulus (50mA, 2ms biphasic square wave pulse at 5HZ for 90 s) was applied. This nicotine pulse would reach the chamber at fraction 6, where no increase in release is observed. After a full 90 washout an electrical stimulus (50mA, 2ms biphasic square wave pulse at 5HZ for 90 s) was applied. Baseline (red line) fitted using a double exponential decay equation to the baseline data (see methods) (B) Nicotine (1-600 μM) was applied to superfusion chambers in parallel 3 min before an electrical stimulus (50mA, 2ms biphasic square wave pulse at 5HZ for 90 s) was applied. Release is expressed as a percentage increase compared to control (electrical stimulus with buffer pre-treatment only taken as 100%). Results represent the mean ± S.E.M of three or more experiments. * Statistical significance observed between Nicotine + electrical stimulus compared to control electrical stimulus $P<0.05$, n=3, one way ANOVA with post-hoc tukeys analysis.

A standard 50mA, 2ms biphasic square wave pulse at 5Hz for 90 s was used as a control stimulus and varying nicotine concentrations were applied 3 min before the electrical stimulus (for a 90 s period thus allowing for a 90 s washout period). Concentrations of

nicotine ranged from 1μM through to 600μM, with significant effects (Students unpaired t-test, n=3 P<0.05) seen at 10 μM and a general trend in increase seen at concentrations of 1, 100, 300 and 600μM (see Fig. 3.2.10 B). Release of [^{3}H]D-aspartate from the frontal cortex minces when nicotine was applied alone was not observed.

3.2.5.3 nAChR specificity of electrically evoked release of [^{3}H]D-aspartate

nAChR specificity of the enhanced electrical-evoked release of [^{3}H]D-aspartate was assessed using the nAChR antagonists mecamylamine (20 μM) and α-Bgt (40nM). These antagonists were applied to the minces prior, during and after the nicotine application, and during the electrical stimulation.

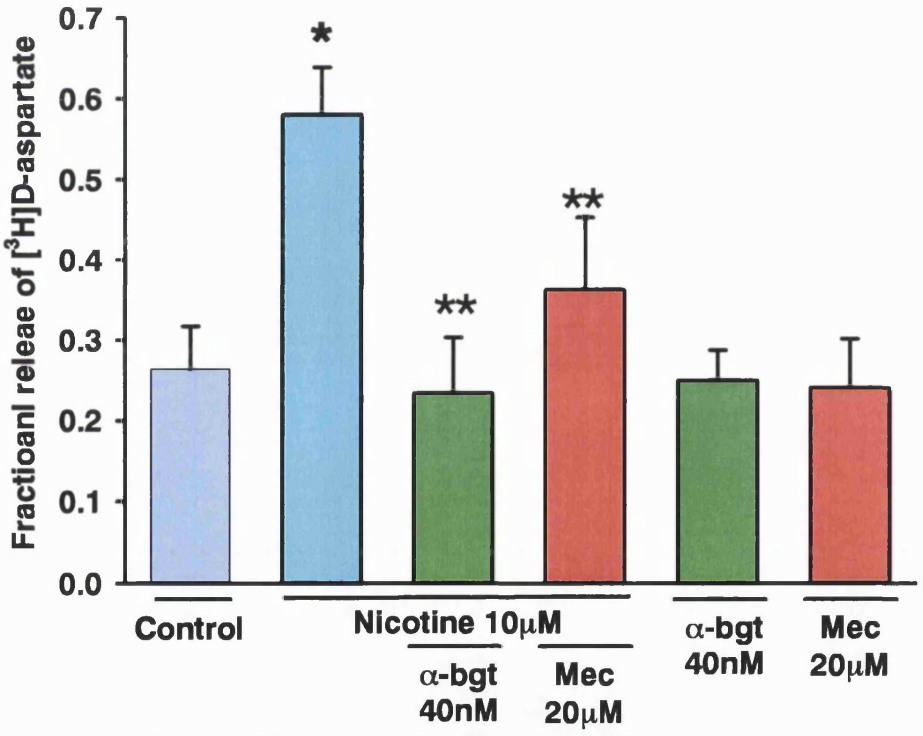

Figure 3.2.11 nAChR specificity of electrically evoked release of [^{3}H]D-aspartate. Frontal cortex slices were superfused (± nAChR antagonists **mec** 20μM and **α-bgt** 40nM) prior (20 min), during and after a 90 s nicotine perfusion. After washout, minces were subjected to a control electrical pulse (2ms biphasic square wave pulse at 5HZ for 90 s). [^{3}H]D-aspartate release is expressed as percentage of total radioactivity present in the tissue at the point of electrical stimulation. Results represent the mean ± S.E.M of at least three experiments. * Statistically different to control conditions, P<0.05 students paired t test n=3. ** Statistically different to nicotine enhancement of electrical-evoked release, P<0.05, Students paired t-test, n=3)

The enhancement shown by the pre-treatment of nicotine (10μM) was substantially blocked by mecamylamine (68.96 ± 28.32% block of nicotine induced enhancement) and completely prevented by α-Bgt (106.3 ± 28.2%) whereas release by electrical stimulation alone was not affected by the presence of nAChR antagonists (See Fig. 3.2.11).

3.2.6 Discussion

In an attempt to emulate two previous studies measuring the direct release of nAChR–evoked EAA release from presynaptic terminals, we examined the effect of nAChR agonists in combination with depolarising stimuli. The first of these two studies (Marchi *et al.,* 2002), showed a nicotinic facilitation of [^{3}H]D-aspartate release from rat and human striatal synaptosomes only when a nicotinic agonist was co-applied with a 12 mM KCl stimulus. We replicated this observation in rat frontal cortex synaptosomes but demonstrate that only certain nAChR agonists enhance KCl-evoked release, which although is Ca^{2+} dependent and mecamylamine sensitive, does not display sensitivity to α7 nAChR antagonists. In the second of these two studies (Beani *et al.*, 2000), the release of [^{3}H]D-aspartate from rat primary cortical cultures is enhanced on concomitant application of nicotine with an electrical stimulus. This release was Ca^{2+} dependent and sensitive to α-Bgt and Mecamylamine. We demonstrate that nicotine enhances the release of [^{3}H]D-aspartate from frontal cortex minces subjected to electrical stimulation, and similar to primary cortical cultures, nicotine enhanced release is sensitive to the nAChR antagonists α-Bgt and mecamylamine (See Fig. 3.2.11), inferring an α7 and non- α7 nAChR mediated enhancement of release, as suggested by Beani *et al.* (2000). However, these assays showed considerable variability and prevented further pharmacological analysis of nAChR subtype specificity of the response.

The exact mechanism by which nAChR enhancement of KCl-evoked release of [^{3}H]D-aspartate occurs has not been investigated. However, the enhancement displayed by epibatidine is Ca^{2+}-dependent (see Fig. 3.2.4.), suggesting that presynaptic nAChR activation causes exocytosis, consistent with a rise in intra-terminal concentration of Ca^{2+} that, in turn, increases the probability, or strength, of depolarisation-induced evoked release as proposed by Dani & colleagues (Gray *et al.*, 1996; Dani *et al.*, 2001; Ji *et al.*, 2001;

Sharma & Vijaraghavan, 2003). The synaptosome population within a superfusion chamber is heterogeneous in size and membrane integrity (Dunkley *et al.*, 1988). A proportion of synaptosomes are likely to display a membrane potential more hyperpolarized than others, making the extent of the KCl depolarisation across the synaptosome population also heterogeneous. By increasing the intra-terminal calcium concentration and/or the membrane potential to a more positive value, caused by nAChR activation, it is then hypothesised that the combined KCl-depolarisation and Ca^{2+} dependent exocytotic release of [^{3}H]D-aspartate may be more uniform across the synaptosome population. A second possibility for the enhancement is that all synaptosomes are depolarised on application of KCl, but concomitant activation of nAChR increases the number of synaptic vesicles 'primed' for exocytotic release of [^{3}H]D-aspartate, thereby increasing the quanta of [^{3}H]D-aspartate release. Observations by McMahon & Nicholls (1991) support this hypothesis, where they revealed a biphasic release of glutamate from cerebrocortical synaptosomes of the guinea pig. These were attributed to a component of synaptic vesicles in close proximity with the plasma membrane that contributed to the fast phase of exocytotic glutamate release, and a second, more slower phase, that was attributed to the Ca^{2+}-dependent 'priming' and dissociation of glutamate containing vesicles from the cytoskeleton and other associated proteins that are away from the active zone of release from the synaptosome plasma membrane.

3.2.6.1 nAChR agonist enhancement of depolarising agent-evoked release

No nAChR enhancement of KCl-evoked release of [^{3}H]D-aspartate was observed using nicotine as the nAChR agonist. Marchi *et al.* (2002) reported that maximal nicotine enhancement of KCl-evoked release of [^{3}H]D-aspartate from rat striatal and human cortical synaptosomes was on concomitant application of 100 μM nicotine. In the present

investigation, this concentration, as well as 1 and 10 μM nicotine, failed to evoke any significant release of [^{3}H]D-aspartate when combined with KCl (12 mM) and compared to a KCl (12 mM) control. This observation was demonstrated in both rat striatal synaptosomes and rat frontal cortex synaptosomes. Initial reasons for this disparity could be due to methodological differences. However, the only methodological differences between the assay used and the assay described by Marchi *et al.* (2002) were the rate of superfusion (0.8 ml/min used in our assay compared to 0.6 ml/min) and a difference in calculation of release. For the former methodological difference, by increasing the superfusion rate, we would expect an enhancement of the detection of [^{3}H]D-aspartate release by overcoming any possible EAA transporter effects of [^{3}H]D-aspartate re-uptake. For the latter methodological difference, release of [^{3}H]D-aspartate was calculated in the same manner as Marchi *et al.* 2002, and compared to our usual method. As described by Marchi *et al.* (2002), KCl + nAChR–evoked release (S1+ S2, counted as C.P.M), was calculated as the overflow after deduction of the basal release (B1 + B2), where B1 is the release in C.P.M. recorded before the stimulus and B2 is the release in C.P.M recorded after the stimulus). This value, and that obtained for KCl alone, is then expressed as a ratio to each other. Using the C.P.M values recorded from our own experiments, the comparison of the two methods of calculation showed no differences on the effect of nicotine-enhancement of KCl-evoked [^{3}H]D-aspartate release. (See Fig. 3.2.13).

Fraction number	KCl 12 mM	KCl 12 mM + Nicotine
4 (B1)	1882	1822
5 (S1)	5455	5172
6 (S2)	1920	1874
7 (B2)	1851	1731

Marchi *et al*., 2002 calculation of release

Evoked release = (S1 +S2) -(B1 + B2)

Enhancement of release = KCl + Nicotine evoke

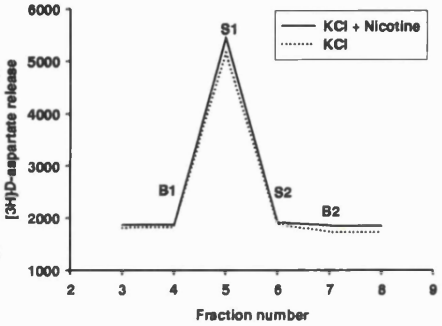

Therefore

KCl 12 mM alone (Control) = (545

KCl 12 mM + nicotine 10 μM = ((517

= 2.0 :2.0

Enhancement of release ratio = 1 (i.e. no enhancement)

Our method of calculation of release (see methods; Soliakov *et al*, 1995)

Evoked release = **Area under peak /Total radioactivity at point of stimulation**

Enhancement of release = ((KCl + Nicotine evoked release /KCl evoked release) x 100) – 100%

Therefore

Area under Peak (see methods for calculation and baseline fit)

Total radioactivity (total release in subsequent fractions + Total left on filters at end of experiment

KCl 12 mM + nicotine 10 μM = 3378/ (17623 + 170720) = 1.79%

KCl 12 mM alone (Control) = 3582/ (18158 + 168897) = 1.914

Enhancement of release % = ((1.8/1.9) x 100) – Control (100%)

= -5%

Fig.3.2.13. Comparison of two calculative methods to examine the nicotine (10 μM) enhancement of KCl–evoked release. Inserted table represents raw C.P.M data of [^{3}H]D-aspartate release expressed as the mean values from each condition examined in triplicate for 4 fractions, taken from an example experiment; B1 and B2 (blue) represent basal release and S1 and S2 (red) represent drug-evoked release. Marchi *et al.* (2002) method expresses enhancement of release as a ratio between control conditions and drug effect. Our method (see methods chapter) expresses enhancement of release as the percentage increase above the effect of control conditions.

In an another attempt to examine nicotine enhancement of depolarisation-evoked release of [^{3}H]D-aspartate, a set of experiments looked at combining nicotine with another depolarising agent, 4-AP. By blocking the K_A channel, the probability of depolarisation is increased, from induction by small changes in membrane potential. This results in spontaneous action potentials rather than 'one cycle' of depolarisation achieved by KCl depolarisation where the membrane potential is 'clamped'. On this basis, 4-AP has been described as a more physiological depolarising agent (Tibbs *et al.*, 1989; Nicholls, 1998) and has been used to reveal PKC modulation of glutamate release (Barrie *et al.*, 1991; Coffrey *et al.*, 1993; Sanchez-Prieto *et al.*, 1996). The release of [^{3}H]D-aspartate evoked by 1 mM 4-AP was similar in magnitude (in terms of fractional release) to KCl-evoked release (12 mM) of [^{3}H]D-aspartate. However, when combined with nicotine, neither 0.1 mM or 1 mM 4-AP-evoked release of [^{3}H]D-aspartate was enhanced. Therefore it appears that nicotine cannot enhance the release of [^{3}H]D-aspartate even when synaptosomes are depolarised in a different manner.

Further differences from the work published by Marchi *et al.* (2002) are revealed from the effect of the nAChR agonists epibatidine and anatoxin-a. Although they significantly enhanced 12 mM KCl-evoked release of [^{3}H]D-aspartate above the effect of 12 mM KCl alone, they only did so at very limited agonist concentrations, although it should be noted that this could simply be a reflection of the variability of the data. As well as this, antagonists could not reliably block the enhancement seen with these agonist concentrations. Specifically, there is a 20-fold higher evoked release of [^{3}H]D-aspartate release when 1nM epibatidine was concomitantly applied with KCl (12 mM) in our experiments compared to the same conditions described by Marchi *et al.* (2002). Lower or higher concentrations of epibatidine had no significant (but high variance) effect on the enhancement of KCl-evoked release, whereas Marchi *et al.* (2002) described an increase

in [^{3}H]D-aspartate release on increasing epibatidine concentration from 1nM to 10 μM. In our experiment, 100 nM epibatidine enhancement of KCl-evoked release only just failed to reach significance and it is plausible that increasing the n number of the experiment at this concentration would have resulted in statistical significance. Interestingly, there seems to be a biphasic nature to the concentration dependence effect of epibatidine combined with KCl, and although the values do not reach significance (bar one) could indicate that there is more than one type of nAChR that governs the enhancement of release; one that is activated by low concentrations of epibatidine and one by high concentrations of epibatidine.

Similar disparities are seen in the results for anatoxin-a. An increase in enhancement of KCl-evoked [^{3}H]D-aspartate release was observed by Marchi *et al.* (2002) on increasing anatoxin-a concentrations from 1 nM to 100 nM. Maximal release of [^{3}H]D-aspartate occurred at 100 nM anatoxin-a + KCl (12mM). Our results displayed no significant enhancement within this concentration range of anatoxin-a, but at 300 nM a significant enhancement was observed. Again, further repetition of each anatoxin-a concentration used may increase the likelihood of obtaining significant results. Unlike the epibatidine enhancement of KCl-evoked release, anatoxin showed no real trend of a biphasic nature to the enhancement, however the concentration that displays the significant enhancement of release is in close agreement with the EC50 value described for anatoxin-a against reconstituted α7 nAChR in Xenopus oocytes (Thomas *et al.*, 1993).

3.2.6.2 nAChR antagonism of the enhancement of KCl-evoked release of [^{3}H]D-aspartate

Mecamylamine inhibition of both epibatidine (1nM) and anatoxin-a (300nM) enhancement of KCl-evoked release of [^{3}H]D-aspartate confirmed that the responses are mediated by

nAChR. However, neither MLA nor α-Conotoxin ImI could convincingly inhibit this enhancement. In comparison, Marchi *et al.* (2002) showed evidence for the participation of α7 nAChR in the anatoxin-a enhancement of KCl-evoked [^{3}H]D-aspartate release, with inhibition by α-Bgt (100 nM) as well as MLA (100 nM). Recently the specificity of MLA, especially at high concentrations of 50 nM above, has come into question; Mogg *et al.* 2003; see also Klink *et al.*, 2001), have demonstrated that this compound interacts with α-Conotoxin MII sensitive presynaptic nAChRs in the rat striatum, suggesting that MLA is also a potent antagonist for non-α7 nAChR. Interestingly, Marchi *et al.* (2002), showed that mecamylamine displayed no significant inhibition of the anatoxin-a enhancement of KCl-evoked [^{3}H]D-aspartate release at 1 and 10 μM, yet at 100 μM, release was completely abolished; this concentration is almost 10 fold higher than that used by a majority of groups who use this antagonist effectively in similar preparations, and could exert non-specific effects. However, low sensitivity to mecamylamine is compatible with the lower sensitivity of α7 nAChR to this antagonist.

3.2.6.3 Calcium dependency

The high Ca^{2+} permeability of the α7* nAChR compared to other nAChR subtypes (Seguela *et al.*, 1993; Delbono *et al.*, 1997) would suitably explain the Ca^{2+} dependence of the nAChR enhancement of KCl-evoked release demonstrated in Fig 3.2.6 and by Marchi *et al.* 2002. However, it is important to highlight that depolarisation-evoked EAA release is dependent on Ca^{2+} entering the presynaptic terminal via the voltage operated calcium channels (VOCC's). VOCC's are more efficiently coupled to EAA exocytosis than Ca^{2+} entering the terminal non-specifically (Nicholls & Attwell, 1990); non-L type calcium channels contribute to the majority of KCl-evoked release of EAA from synaptosomes, where on activation they trigger the release via a highly localised pool of calcium within the

immediate vicinity of the calcium channel (Tibbs *et al.*, 1989; Sanchez-Prieto *et al.*, 1996). The reliance for the detection of nAChR enhancement only in depolarising conditions make it impossible to ascertain whether the nAChRs contributing to the enhancement of release in this study and by Marchi *et al.* (2002), either depolarise the cell membrane and activate VOCC to increase intrasynaptosomal Ca^{2+} concentration or contribute to intrasynaptosomal concentration alone via Ca^{2+} flux through their ion pore or indeed both mechanisms. In a recent report by Dougherty *et al.* (2003) that examines the effect of soluble Aβ peptides on nAChR Ca^{2+} influx into brain synaptosomes, cortical synaptosomes demonstrated both an α7 and non-α7 component to nicotine and Aβ protein activated rise in intra-terminal Ca^{2+}. The α7 component demonstrated a partial activation of VOCC's, where α7 nAChR activation depolarised the synaptosome membrane to activate non-L type VOCC's that contributed to the rise in intra-terminal Ca^{2+}. The non-α7 component of nicotine or Aβ activated rise in intra-terminal Ca^{2+} was independent of VOCC activation. The ambiguous effect of α7 nAChR specific antagonists on the enhanced release of [^{3}H]D-aspartate demonstrated herein does not support the source of intra-terminal Ca^{2+} coming solely from α7 nAChR activation as stated by Marchi *et al.* (2002). An important study by Nayak *et al.* (2001) demonstrated that striatal synaptosomes, loaded with fluo-3 (a fluorescent calcium indicator dye), displayed only non-α7 nAChR mediated increases in intra-terminal Ca^{2+} when activated by nicotine. It was undetermined whether the synaptosomes examined for nAChR-evoked responses in the report by Dougherty *et al.* (2003) were glutamatergic, however, this work is further supported by the contribution of non-L-type Ca^{2+} channels to the anatoxin-a evoked release of [^{3}H]Dopamine from striatal synaptosomes (Soliakov *et al.*, 1996).

Despite these conflicting reports, presynaptic elevation of Ca^{2+} has been shown to demonstrate a predominantly α7 nAChR component in hippocampal presynaptic terminals

(Gray *et al.,* 1996; Sharma & Vijaraghavan, 2003) and in the VTA (Mansvelder & McGehee, 2000) and therefore the nAChR subtype expressed on presynaptic terminals may be specific to certain brain regions. With respect to the frontal cortex, as utilised in this investigation, reports reveal both the presence of α7 and non-α7 nAChRs on presynaptic terminals (Vidal & Changeux., 1989; Vidal & Changeux 1993; Granon *et al.*, 1995; Gioanni *et al.*, 1999; Lambe *et al.*, 2003; and chapter 3 section 3 and chapter 4).

Interestingly, a possible association of nAChR with EAAT reversal can be eliminated due to the lack of enhancement of KCl-evoked release in the absence of Ca^{2+}; an indirect inference made from our results in this section and that from characterising the Ca^{2+} independent component of KCl-evoked release of [^{3}H]D-aspartate (Chapter 3 Section1)

3.2.6.4 Electrical-evoked release of [^{3}H]D-aspartate

This component of study for the nAChR enhancement depolarised-evoked release of [^{3}H]D-aspartate was carried out on placement at Eli Lilly and Company, Erl Wood, Windlesham, Surrey, under the supervision of Dr I.A Pullar. Frontal cortex minces were employed instead of synaptosomes for practical reasons due to the nature of the apparatus employed and on guidance from Clare Roberts (GlaxoSmithKline, Harrow). Therefore the greater degree of synaptic integrity maintained in a slice preparation compared to a synaptosome preparation is an important consideration in the assessment of the data accumulated.

Initial experiments assessed the electrical stimulus parameters of the electrical evoked release of [^{3}H]D-aspartate. These steps were undertaken to determine a suitable level of electrical stimulation that would evoke [^{3}H]D-aspartate release to a degree that was neither too small to evade detection nor too large to mask any future examination of the nAChR enhancement of release. The variability of the release was also taken into consideration as

another determining factor of control condition choice. Both current intensity and current frequency had a positive correlation with the extent of [^{3}H]D-aspartate release. At a set frequency of 5Hz, increasing the current intensity evoked release to a maximum of 1.5% of total radioactivity released, with further increases in current intensity having no greater effect. Only two different frequencies were applied where 10Hz (and a set intensity of 50mA) gave three times the release of [^{3}H]D-aspartate compared to 5Hz stimulation. From Fig. 3.2.8, it was evident that a frequency of 5Hz gave a variability that was less than 10 % of the actual response, whereas at 10Hz the variability was obviously larger. The same was true for the current intensity of 50mA compared to other current intensities, and so control conditions consisted of a 50mA, biphasic square wave pulse at 5HZ for 90 s. In comparison to previously cited electrical stimulation experiments in the superfusion paradigm, this value is in good agreement with test stimuli used in these experiments (Muzzolini *et al.,* 1996; Savage *et al.*, 2000; Sehmisch *et al.,* 2001)

3.2.6.5 Effect of TTX

TTX is an effective antagonist of the spread of an action potential to the terminal regions of an axon, by way of blocking Na^+ channels. If release of [^{3}H]D-aspartate from the presynaptic terminals is solely dependent on this process then we would expect a large degree of inhibition of release on application of TTX. However Fig. 3.2.9 displays a 74.0 ± 8.9% blockade of the electrical evoked release of [^{3}H]D-aspartate in the presence of TTX (1 μM). Although not a complete blockade of release was observed, this value falls within values given previously of an 80% blockade of endogenous glutamate and 65% blockade of [^{3}H]D-aspartate release from hippocampal slices, reported by Muzzolini *et al.* (1996), as well as Sehmisch *et al.* (2001). This remaining 25% release could be attributed to release from the presynaptic terminal that is independent of an action potential terminating in this region. An important note to make is that the perfusing buffer and all other perfusing

solutions contained DL-TBOA (20 μM), a non-transportable blocker of EAAT 1-3, therefore it is assumed that this residual release is not due to reversal of the glutamate transporters under depolarising conditions. Although no literature exists on the use of this compound in rat tissue sections, this concentration was effective at inhibiting the Ca^{2+}-independent component of potassium-evoked release from rat frontal cortex synaptosomes (See Chapter 3 Section 1, Fig 3.1.9 and 3.1.10).

3.2.6.6 nAChR enhancement of electrically evoked release

Technical limitations did not permit the co-application of both agonist and electrical stimulation at the same time (see results section 3.2.5.2) therefore we chose to stimulate the frontal cortex minces with a 90 s perfusion of nicotine and then allow for an approximate 90 s washout prior to the application of an electrical stimulation. Significant enhancement of release was detected at 10 μM nicotine (102.7 ± 34.9% above the effect of control conditions; see Fig 3.2.10 A & B). Other concentrations of nicotine examined did show an enhancement of release but failed to pass significance (one way ANOVA with post hoc Tukeys analysis). No other nAChR agonists were examined in this instance.

These results suggest that the nAChR enhancement of electrical-evoked release of [^{3}H]D-aspartate effect lasts greater than a period of 90 s after exposure to nicotine. With respect to the chemical depolarising agent stimulation, nAChR enhancement is within the 90 s time frame of nAChR agonist + KCl co-application, whereas no enhancement was detected when the depolarising stimulus was applied after the nAChR stimulus. This disparity may be explained by the temporal differences in agonist application of the two systems; synaptosome drug exchange is almost immediate whereas minces are subject to slower drug exchange. Because both drug exchange and removal is a lot slower than that described for synaptosomes, then the effect of the nAChR enhancement may too be

sustained over a longer period. The enhancement described for the shorter nAChR agonist + KCl exposure in synaptosomes could simply be a reflection of a larger calcium conductance, via both activation of voltage operated calcium channels and through the ion channel of the nAChR, whereas the longer exposure of the minces to nicotine could result in the priming of vesicles after nAChR activation via phosphorylation of vesicle docking proteins or changes in the arrangement of cytoskeleton proteins that increases the available pool of synaptic vesicles ready for fusion to the presynaptic membrane and thereby evoking a greater quantum of neurotransmitter release.

3.2.6.7 nAChR antagonism of the enhancement of electrical-evoked release of [^{3}H]D-aspartate

nAChR specificity of the enhancement of release was confirmed in those experiments by blocking the response by the nAChR antagonists α-Bgt and mecamylamine. α-Bgt (40 nM) showed a complete block of the enhancement induced by nicotine (10 μM) supporting the possibility that the enhancement we see is solely due to activation of the α7 nAChR. The lesser effect of mecamylamine (20 μM) compared with α-Bgt may reflect the lower efficacy of this antagonist to the α7 nAChR subtype (Papke *et al.*, 2001). However, the degree of mecamylamine blockade in these experiments does not correspond to the level of blockade seen against nAChR agonist + KCl (where a complete blockade was shown; see Fig. 3.2.6). This could be for a number of reasons: (1) the other nAChR agonists used to enhance KCl-evoked release could be activating a subtype of nAChR that is more sensitive to mecamylamine. (2) More than one nAChR subtype may be activated by nicotine to enhance the electrical-evoked release of [^{3}H]D-aspartate (Beani *et al.*, 2000; see Chapter 3 section 3). (3) Mecamylamine may be more effective as an antagonist when the membrane

is depolarised (in concomitant nAChR agonist + KCl application) compared to a membrane at resting potential (nAChR + a 90 second delay before electrical stimulus application).

.

A further point of consideration is nicotine alone fails to evoke release of [^{3}H]D-aspartate. In synaptosomes this can be readily demonstrated in both the presence and absence of glutamate re-uptake blockers such as DL-TBOA (See Chapter 3 Section 3). In the present study, DL-TBOA (10 μM) was present in all perfusing solutions and therefore theoretically would prevent any re-uptake of nicotine evoked release of [^{3}H]D-aspartate. It is plausible that in slices this concentration is ineffective and that in synaptosomes the marked decrease in glial transporter glutamate uptake helps reveal [^{3}H]D-aspartate release even in the absence of DL-TBOA, compared to the mince preparation where glial cells are in abundance and the effect of DL-TBOA decreased. Secondly, the membrane potential of synaptosomes compared to slices, is thought to be less stable and this may be beneficial to the nAChR in its ability to evoke release, although methodically this would be hard to demonstrate.

3.2.6.9 Summary

In summary, the inherent variability of the KCl-evoked release of [^{3}H]D-aspartate made it difficult to ascertain clear concentration dependent effects of nAChR agonist enhancement of KCl-evoked release of [^{3}H]D-aspartate, in contrast to that described by Marchi *et al.* (2002). This was also the case with nicotine enhancement of electrical-evoked release, although evidence for α7 nAChR mediated enhancement of release was demonstrated in agreement with observations made by Beani *et al.* (2000).

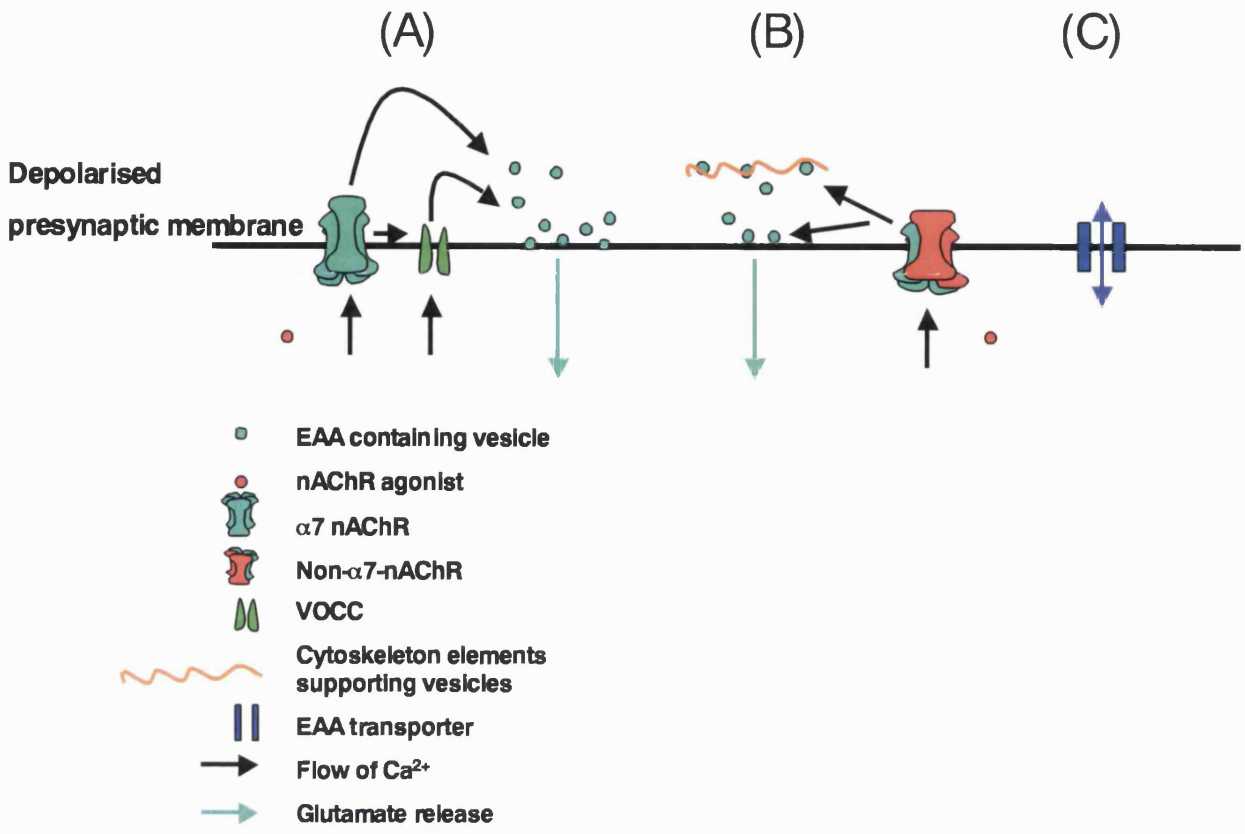

Figure 3.2.14 Summary of the nAChR enhancement of depolarisation-evoked EAA release. **(A)** α7 nAChR mediated facilitation of depolarisation-evoked release of EAA may directly activate EAA vesicles for exocytosis via Ca^{2+} flux through the receptor and/or contribute to the enhanced depolarisation of VOCC's and the concomitant Ca^{2+} influx which couples to a localised pool of EAA vesicles to trigger release by exocytosis. **(B)** Non-α7 nAChR mediated facilitation of depolarisation-evoked release of EAA may directly activate EAA vesicles for exocytosis via Ca^{2+} flux through the receptor and/or increase the available pool of 'primed' vesicles by freeing them from cytoskeletal proteins or mediating CICR in the synaptic terminal (Sharma & Vijaraghavan, 2003). **(C)** Variability of KCl-evoked release may be a consequence of EAA transporter reversal depending on the viability of the synaptosomes.

nAChR agonists that did significantly enhance KCl-evoked release (epibatidine 1nM and anatoxin-a 300 nM) displayed a Ca^{2+} dependent and non-α7 nAChR facilitation of the response, however, the variability of some experiments prevented any clear effects of α7 antagonists being demonstrated and therefore the involvement of α7 nAChR facilitation of KCl-evoked release cannot be ruled out. Figure 3.2.14 represents a schematic of possible relationships between the nAChR and the enhancement of depolarised evoked release.

Chapter 3 Section 3

3.3 nAChR-evoked release of [^{3}H]D-aspartate

3.3.1 Introduction

A substantial body of evidence, mainly from electrophysiological experiments, supports the presynaptic nAChR modulation of glutamate release (see Introduction section 1.7.2). This nAChR mediated facilitation has been recorded in a number of rodent CNS regions such as the hippocampus (Gray *et al.*, 1996; Alkondon *et al.*, 1999; Radcliffe & Dani, 1998; Fischer & Dani, 2000; Sharma & Vijaraghavan, 2003), prefrontal and frontal cortex (Vidal & Changeux, 1989; Vidal & Changeux, 1993; Granon *et al.*, 1995; Gioanni *et al.*, 1999; Lambe *et al.*, 2003), olfactory bulb (Alkondon *et al.*, 1996), midbrain (Schilstrom *et al.*, 2000; Nomikos *et al.*, 2000; Mansvelder & McGehee, 2000; Girod & Role, 2001) and cerebellum (De Filippe *et al.*, 2001). In the majority of these rodent CNS regions, nicotinic agonists provoke an increase in frequency and amplitude of glutamate receptor-mediated post-synaptic excitatory potentials that are sensitive to α-Bgt, Ca^{2+}-dependant and insensitive to tetrodotoxin (TTX) (Alkondon *et al.*, 1996 & 2002; Gray *et al.*, 1996), consistent with stimulation of α7 nAChR located on presynaptic terminals of glutamatergic afferents. However, in the frontal cortex, the region of the rat CNS under examination in this thesis, the majority of nicotine-evoked postsynaptic events are insensitive to α-Bgt. Instead presynaptic non-α7 nAChR have been implicated in the modulation of glutamate release in this region, found on thalamo-cortical glutamatergic afferents (Vidal & Changeux., 1989; Vidal, 1993; Granon *et al.*, 1995; Gioanni *et al.*, 1999; Lambe *et al.*, 2003). Specifically, nicotine-evoked responses in the frontal cortex of mouse brain were reported to be sensitive to dihydro-β-erythroidine (DHβE) and absent in β2 nAChR subunit null mutant mice (Lambe *et al.*, 2003). Together with the loss of [^{3}H]nicotine binding sites in cortical areas after thalamic lesions (Gioanni

et al., 1999), this pharmacology further supports the presence of high affinity, β2* nAChR on these afferents.

3.3.1.1 Direct detection of nAChR-evoked EAA release

As described in Chapter 1 (Introduction), electrophysiological experiments measure the postsynaptic response of glutamate release from the nerve terminal and have used approaches such as the use of TTX, to deduce that the release of glutamate is independent of action potential generation, consistent with presynaptic localisation of nAChR. However, few groups have reported a direct detection of glutamate release evoked by nAChR stimulation from the presynaptic terminal. Microdialysis studies have come the closest to reporting a direct modulation of nAChR-evoked glutamate release in cortical and mid brain areas of the rat (Toth *et al.*, 1992; Gioanni *et al.*, 1999; Reid *et al.*, 2000; Schilstrom *et al.*, 2000). However these reports have drawn different conclusions to the nAChR subtype specificity of the modulation of glutamate release; systemic nicotine elicits glutamate release in the VTA and is blocked by local administration of MLA, (Schilstrom *et al.*, 2000) supporting the presence of α7* containing nAChR on presynaptic terminals, yet in the prelimbic area of the PFC, systemic nicotine elicits glutamate release which was sensitive to DHβE and not α-Bgt or MLA, supporting the presence of non-α7, β2*-containing nAChR on presynaptic terminals (Gioanni *et al.*, 1999). Together these investigations highlight the complexity of those regions of the brain being studied and the different anatomical distribution of the subtypes of nAChR in the CNS (Alkondon *et al.*, 1996a; Role and Berg., 1996; Girod *et al.*, 2000).

A robust model for the determination and pharmacological characterisation of the nAChR modulation of neurotransmitter release is via superfusion of synaptosomes

preloaded with radiolabelled neurotransmitter (Raiteri, 1987; Nicholls, 1998; Raiteri & Raiteri, 2000). This method has been utilised for the demonstration of nAChR modulation of acetylcholine (Wilkie *et al.*, 1996), dopamine (Soliakov *et al.*, 1995; Kaiser & Wonnacott, 2000; Mogg *et al.,* 2003), GABA (Maggi *et al.,* 2001; Zhu & Chiappinelli, 2002; Frazier *et al.*, 2003), noradrenaline (Clarke & Reuben, 1996; Anderson *et al.*, 2000; Lei & Eisenach, 2002; O'Leary & Leslie, 2003) and 5-HT release (Li *et al.*, 1998; Kenny *et al.*, 2000; Cordero-Erausquin & Changeux, 2001). However, superfusion has been less successful for the examination of nAChR-evoked EAA release (see Chapter 1 section 1.7.1). The most common difficulty in measuring EAA release in-vitro is the inability to outweigh re-uptake via the highly efficient nature of glutamate transporters. As well as this, the poor temporal resolution of nAChR agonist delivery to the CNS tissue in this assay may desensitise the receptors before any functional activity can be measured (compared to electrophysiological experiments; see Kaiser & Wonnacott, 2000). A modified superfusion system has achieved sub-second time-scale application of depolarising stimuli to synaptosomes loaded with [^{3}H]L-glutamate (Turner & Dunlap, 1995a and b), but as of yet, there has been no reports of nAChR agonists applied in this same manner. Superfusion *per se*, by continuously removing any extracellular perfusates, should reduce the possibility of neurotransmitter re-uptake (see Raiteri & Raiteri, 2000), thereby increasing the detectable pool of neurotransmitter that is released via activation of the nAChR. It is therefore possible that, in synaptosomes loaded with tritium labelled EAA, the superfusion rate employed in previous attempts to detect nAChR modulation of EAA release was too slow to avoid the possibility of re-uptake. As well as the superfusion rate, the use of a synaptosome preparation itself, particularly with respect to the detection of glutamate, should have a reduced

number of transporter systems (although possible gliosomes contamination of the P2 preparation may provide a source of EAAT) compared to an intact synaptic circuit such as that found in a slice preparation. Sehmisch *et al.* (2001) failed to demonstrate nAChR modulation of electrical-evoked release of [^{3}H]L-glutamate and [^{3}H]D-aspartate, in the presence of EAAT blockers from hippocampal sections. With respect to the dopamine assay (Soliakov *et al.*, 1995; Kaiser & Wonnacott, 2000; Mogg *et al.,* 2002), and the noradrenaline assay (Clarke & Reuben, 1996; Anderson *et al.*, 2000; Lei & Eisenach, 2002; O'Leary & Leslie, 2003) the use of nomifensine and desipramine (DMI) is employed to prevent the re-uptake of these neurotransmitters respectively, thereby increasing the available neurotransmitter pool for detection. Glutamate transporter inhibitors such as PDC and TBOA have yet to be fully examined against either different transporters or species transporter variation (Waagepetersen *et al.*, 2001), but do provide an opportunity to enhance the detection of EAA release as evoked by application of nAChR agonists.

In this chapter we demonstrate that nAChR agonists applied to frontal cortex synaptosomes can evoke the release of [^{3}H]D-aspartate in the absence of a concomitant depolarisation or EAAT inhibitors. This has enabled characterisation with respect to nAChR subtype, using specific agonists and antagonists; an α7 and non-α7 component to the release of [^{3}H]D-aspartate from the rat frontal cortex is demonstrated.

3.3.2 Results

3.3.2.1 nAChR agonist-evoked release of [^{3}H]D-aspartate from rat frontal cortex synaptosomes

The nAChR agonists nicotine or anatoxin-a failed to evoke release of [^{3}H]D-aspartate above the effect of basal conditions during early attempts to detect the release of [^{3}H]D-aspartate from both rat striatal synaptosomes and rat frontal cortex synaptosomes. These initial experiments were carried out using a 6 channel Brandel™ superfusion apparatus which resulted in inconsistent results and large variability, confounded by the small number of chambers available to assess conditions in parallel. However, after obtaining some encouraging results with nicotine applied alone using the 12 chamber Brandel™ superfusion apparatus a thorough investigation into the effect of nAChR agonists on modulating the release of [^{3}H]D-aspartate was carried out using this system.

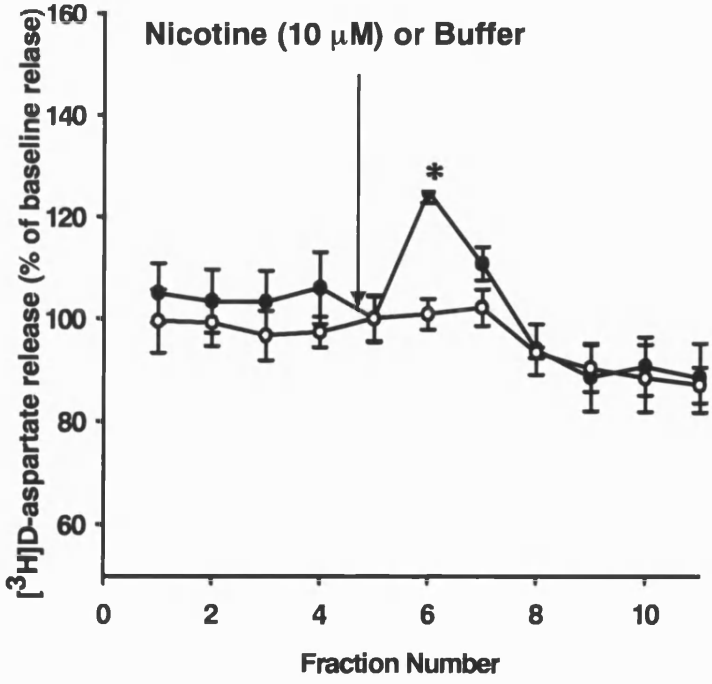

Figure 3.3.1 The effect of nicotine (10 μM) on [^{3}H]D-aspartate release compared to buffer. Rat frontal cortex synaptosomes were superfused with KB buffer and stimulated for 90 s with nicotine (10 μM; closed circles) using a 12 channel Brandel™ superfusion apparatus. A 90 s buffer pulse was also applied to a set of chambers run in parallel (open circles). Release is expressed as a percentage of the average baseline release for both conditions, taken as 100%. Results represent the mean ± S.E.M of three independent experiments. * Statistical significance observed between nicotine 10 μM compared to basal $P<0.05$, n=3, One way ANOVA with post-hoc tukeys analysis.

The first three experiments re-examining the effect of nicotine alone on the release of [^{3}H]D-aspartate from rat frontal cortex synaptosomes, using the 12 channel Brandel superfusion apparatus, showed a significant enhancement of release above the effect of a comparable buffer pulse within each experiment (Fig. 3.3.1). Nicotine (10 μM) evoked [^{3}H]D-aspartate release to 24.87 ± 2.3% above baseline, compared to buffer-evoked release, which showed no significant difference to the baseline release.

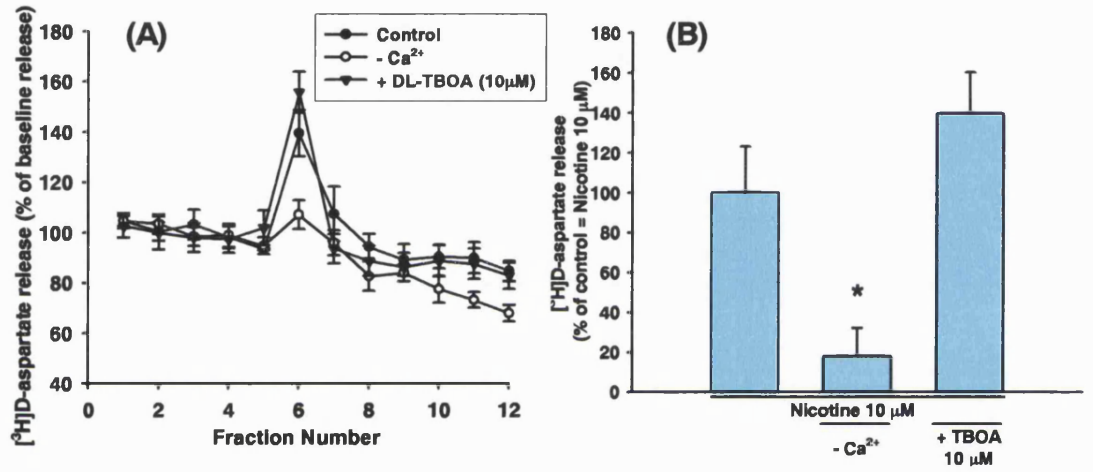

Figure 3.3.2 Calcium dependency and the effect of glutamate transport inhibitors on the release of [^{3}H]D-aspartate evoked by nicotine (10 μM) from rat frontal cortex synaptosomes. Rat frontal cortex synaptosomes were superfused with KB buffer in the presence (control) and absence of Ca^{2+} or in the presence of Dl-TBOA (10 μM) and stimulated for 90 s with nicotine (10 μM) using a 12 channel Brandel™ superfusion apparatus. **(A)** Nicotine-evoked release is expressed as a percentage of the average baseline release for all three conditions (control = normal KB buffer (closed circles), KB buffer – Ca^{2+} (open circles) and KB buffer containing DL-TBOA (10 μM; closed triangles), taken as 100%. Results represent the mean ± S.E.M of three independent experiments. **(B)** Release is expressed as a percentage of control-evoked release (nicotine 10 μM in normal KB buffer) with each condition adjusted for buffer evoked release. Results represent the mean ± S.E.M of three independent experiments. * Statistical significance between nicotine 10 μM in the absence of Ca^{2+} compared to control $P<0.05$, n=4, one way ANOVA with post-hoc tukeys analysis.

In order in assess the specificity of the response in terms of Ca^{2+}-dependency and the possible effect of glutamate transporter reversal; nicotine-evoked release (10 μM) was assessed in the absence of Ca^{2+} or in the presence of the glutamate

transporter inhibitor TBOA (10 μM) (see Fig. 3.3.2 A & B). In the absence of Ca^{2+}, nicotine-evoked release of [^{3}H]D-aspartate from rat frontal cortex synaptosomes was significantly reduced to 12.8 ± 10.4% of the control response (control; Nicotine 10 μM in normal KB buffer = 100 ± 23.0%). In the presence of the glutamate transporter inhibitor (TBOA; 10 μM) neither the baseline release of [^{3}H]D-aspartate nor the release evoked by nicotine was significantly different to control (139.7 ± 20.5% of nicotine control; P>0.05. Fig. 3.3.2 B).

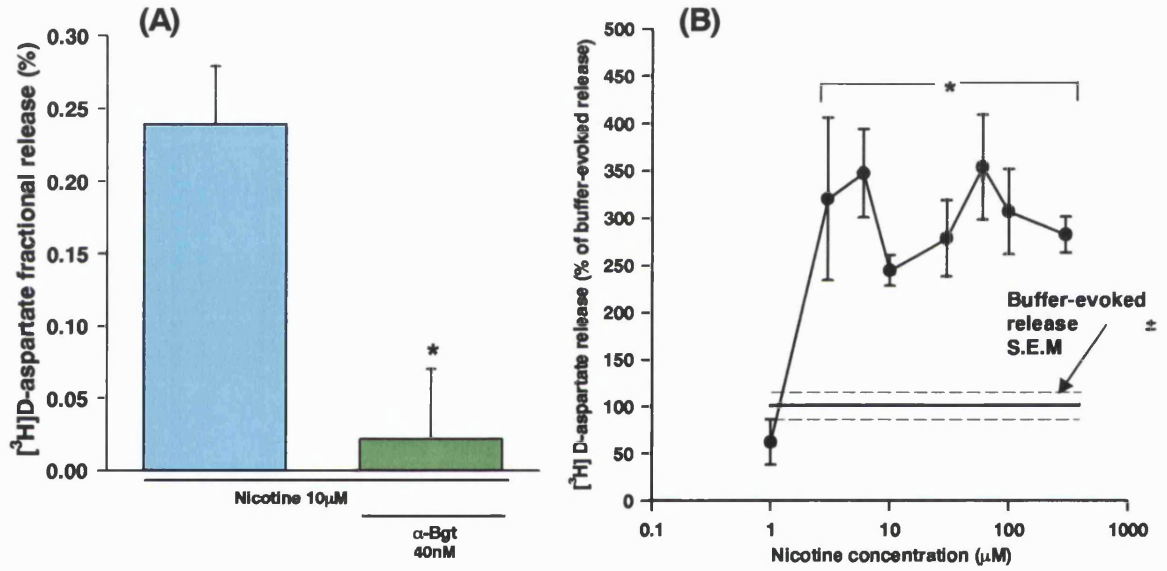

Figure 3.3.3 Nicotine-evoked release of [^{3}H]D-aspartate from rat frontal cortex synaptosomes: α7 nAChR specificity and concentration dependant release. (A) Rat frontal cortex synaptosomes were superfused with KB buffer in the absence (control) and presence of α-Bgt (40 nM). Release is expressed as a percentage of the total radioactivity present at the point of nicotine (10 μM) stimulation (see methods for calculation). Results represent the mean ± S.E.M of three independent experiments. (B) Rat frontal cortex synaptosomes were superfused with KB buffer and stimulated for 90 s with nicotine (over a concentration range of 1-300 μM). Release was calculated as a fraction of the total radioactivity remaining in the preparation at the point of stimulation, and expressed as a percentage of the response to buffer (taken as 100% ± S.E.M). Results represent the mean ± S.E.M of at least three independent experiments for each agonist concentration. (A) * Statistical significance observed between nicotine 10 μM in the presence of α-Bgt (40 nM) compared to control (nicotine 10 μM alone). (B) * Statistical significance between nicotine and buffer evoked release. P<0.05, n=3, one way ANOVA with post-hoc tukeys analysis.

nAChR specificity of the response, in particular, α7* nAChR subtype specificity, was confirmed by examining the effect of α-Bgt (40 nM) on nicotine-evoked release of [^{3}H]D-aspartate. Synaptosomes were incubated for 20 min, with or without α-Bgt, prior to a 90 s pulse of nicotine (10 μM). After adjusting release for buffer-evoked release, nicotine-evoked release was inhibited by 91.4 ± 16.6% in the presence of α-Bgt compared to control (100 ± 16.2%; Fig. 3.3.3 A).

Release of [^{3}H]D-aspartate from rat frontal cortex synaptosomes was significantly different to buffer-evoked release at nicotine concentrations above 1 μM, whereas 1 μM nicotine was without effect. Nicotine increased the release of [^{3}H]D-aspartate to 150-250% above the buffer-evoked release (100 ± 18.9%) between the concentration range 3 and 300 μM (Fig. 3.3.3 B). These results prompted the investigation of a variety of nAChR agonists and antagonists in an attempt to elucidate the nAChR subtype(s) associated with the modulation of EAA release in the frontal cortex.

The general nAChR agonists, anatoxin-a and epibatidine were applied over a broad concentration range; anatoxin-a and epibatidine (0.1-1000 nM; see Fig. 3.3.4 A & B). Significant release of [^{3}H]D-aspartate was observed for anatoxin-a at concentrations above 0.1 nM, whereas 0.1 nM anatoxin-a was without effect (Fig. 3.3.4 A). Anatoxin-a evoked the release of [^{3}H]D-aspartate to 150-175% above the buffer-evoked release (100 ± 16.2%), between the concentration range of 1 and 1000 nM. Maximal anatoxin-a-evoked release of [^{3}H]D-aspartate was observed at 300 nM (270 ± 17.6% above buffer evoked release). This value was statistically different to either release evoked by 1 nM anatoxin-a or buffer-evoked release when compared using one way ANOVA with post hoc tukeys analysis.

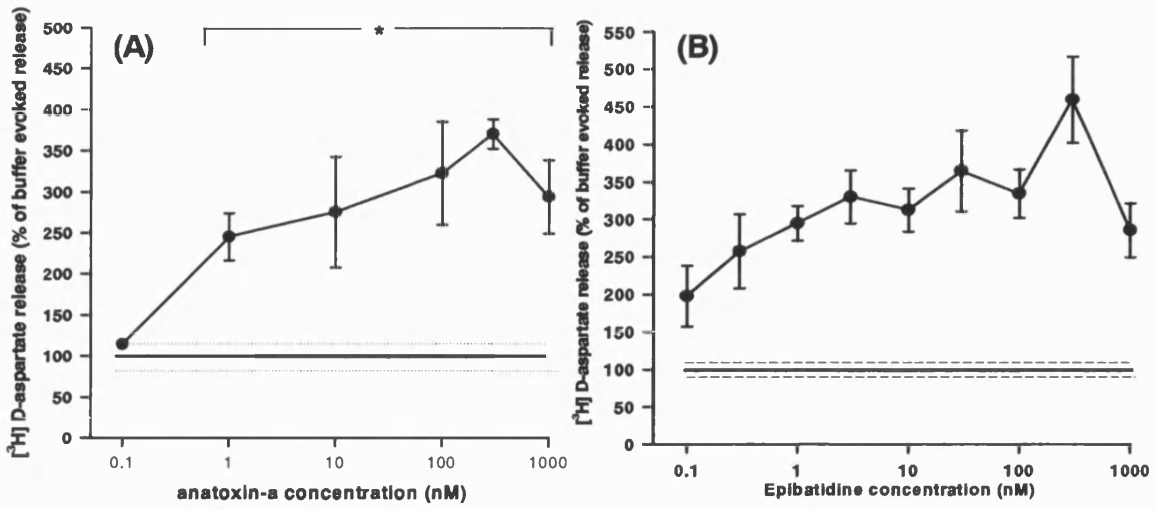

Figure 3.3.4 Concentration dependency anatoxin-a and epibatidine-evoked release of [^{3}H]D-aspartate from rat frontal cortex synaptosomes. Rat frontal cortex synaptosomes were superfused with KB buffer and stimulated for 90 s with (A) anatoxin-a or (B) epibatidine (over a concentration range of 0.1-1000 nM for both agonists) using a 12 channel Brandel™ superfusion apparatus. Release was calculated as a fraction of the total radioactivity remaining in the preparation at the point of stimulation, and expressed as a percentage of the response to buffer. Results represent the mean ± S.E.M of at least three independent experiments for each agonist concentration. * Significantly different from buffer-evoked release. All values shown for epibatidine release are significantly different to buffer-evoked release. $P<0.05$, $n>3$, one-Way ANOVA with post-hoc tukeys analysis.

Epibatidine also elicited the release of [^{3}H]D-aspartate, and this was concentration dependant over the range 0.1 nM to 1 μM (Fig. 3.3.4 B). All concentrations examined in these experiments produced a statistically significant increase in [^{3}H]D-aspartate release compared to buffer-evoked release. The maximum release of [^{3}H]D-aspartate (359.3 ± 57.4% above buffer-evoked release; 100 ± 12.1%) was evoked by 300 nM epibatidine. This value is statistically different to the release evoked by 0.1-1nM epibatidine and buffer-evoked release, but not to other concentrations of epibatidine-evoked release.

The investigation into the nAChR agonist-evoked release of [^{3}H]D-aspartate was extended to the subtype selective agonists choline (α7 selective; Papke *et al.*,1996 & 2002; Alkondon *et al.*, 1997;) and 5-I-A-85380 (β2 selective; Mukhin *et al.,* 2000).

In agreement with reported concentrations of choline that are effective at α7 nAChR (Albuquerque *et al*., 1997), 1 and 10 mM choline increased [^{3}H]D-aspartate release to 240.2 ± 59.2% and 258.6 ± 75.8 above the buffer response (100 ± 24.2%) respectively (Fig. 3.3.5 A). At 1, 10 and 30 mM, choline-evoked release of [^{3}H]D-aspartate was significantly above the effect of buffer-evoked release, whereas 0.3 mM choline was without significant effect. The β2*selective agonist 5-I-A-85380 evoked [^{3}H]D-aspartate release to 107–173% of the buffer response, over the concentration range of 0.1-300 nM (Fig. 3.3.5 B). All concentrations of 5-I-A-85380 significantly increased the release of [^{3}H]D-aspartate above the effect of buffer-evoked release.

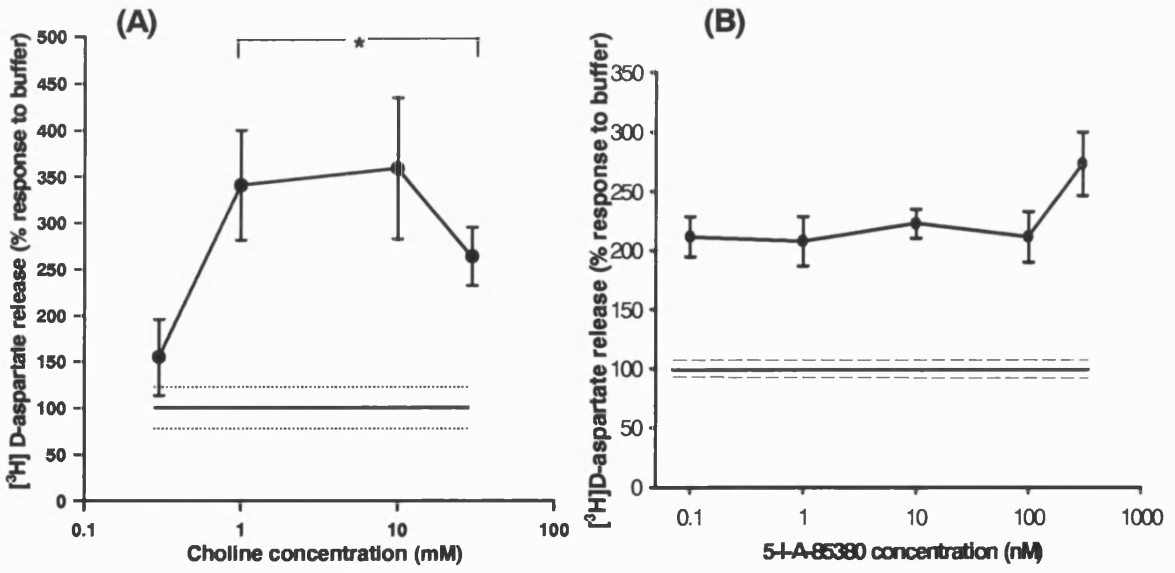

Figure 3.3.5. Concentration dependency of choline and 5-I-A-85380-evoked release of [^{3}H]D-aspartate from rat frontal cortex synaptosomes. Rat frontal cortex synaptosomes were superfused with KB buffer and stimulated for 90 s with choline or 5-I-A-85380 (over a concentration range of 0.3-30 mM and 0.1-300 nM respectively) using a 12 channel Brandel™ superfusion apparatus. Release was calculated as a fraction of the total radioactivity remaining in the preparation at the point of stimulation, and expressed as a percentage of the response to buffer. Results represent the mean ± S.E.M of at least three independent experiments for each agonist concentration. * Statistical significance observed between choline-evoked release (1, 10 and 30 mM) and buffer-evoked release. All values shown for 5-I-A-85380-evoked release are significantly different to buffer-evoked release. $P<0.05$, n=3, One way ANOVA with post-hoc tukeys analysis.

The release profile for 5-I-A-85380 is relatively uniform with no specific 5-I-A-85380 concentration displaying a significantly different amount of release compared to other 5-I-A-85380 concentrations.

3.3.2.2 Determination of subtype specificity of the nAChR modulation of [^{3}H]D-aspartate release

Nicotine, anatoxin-a and epibatidine all display broad concentration dependant release profiles (Fig. 3.3.3 and Fig. 3.3.4 A & B). It is this observation that prompted a pharmacological characterisation of [^{3}H]D-aspartate release to ascertain if more than one nAChR subtype contributes to the facilitation of release over such a broad concentration profile for each agonist.

As described above (Fig. 3.3.3 A & B), nAChR specificity of nicotine–evoked release of [^{3}H]D-aspartate demonstrated that nicotine (10 μM) evoked release was inhibited in the presence of α-Bgt (40 nM). However when [^{3}H]D-aspartate release was evoked by a higher concentration of nicotine (300 μM) the release was not inhibited by α–Bgt (See Fig. 3.3.6).

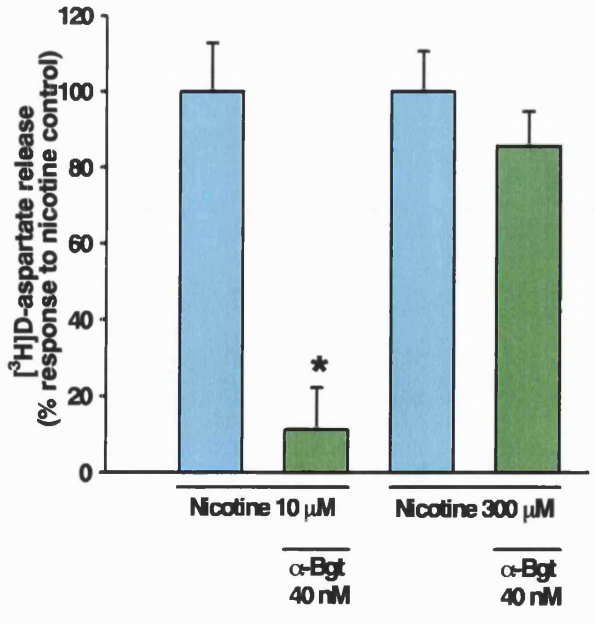

Figure 3.3.6 Concentration dependant sensitivity of nicotine-evoked release of [^{3}H]D-aspartate to α-Bgt. Rat frontal cortex synaptosomes were superfused with KB buffer and then subject to a 90 s pulse of nicotine (either 10 or 300 μM). α-Bgt (40 nM) was introduced 20 min before agonist stimulation and remained throughout the remainder of the experiment. Responses are expressed as a percentage of the corresponding agonist response in the absence of antagonist determined in parallel. Values are the mean ± S.E.M. of at least three independent experiments. * Significantly different from nicotine control in the absence of α-Bgt, $P<0.01$, one way ANOVA with post hoc Tukeys analysis.

Nicotine-evoked release (300 μM control; 100% ± 10.6) was inhibited by 14.5 ± 9.2 % in the presence of α-Bgt (40 nM), which is not statistically different to control. In a repeat measure of α-Bgt inhibition against 10 μM nicotine-evoked release of [^{3}H]D-aspartate, α-Bgt (40 nM) inhibited release by 88.8 ± 11.1%, similar to the initial observation (see Fig. 3.3.3). A second α7* selective nAChR antagonist was also examined (Fig. 3.3.7). At a low concentration of nicotine, MLA inhibited nicotine-evoked release of [^{3}H]D-aspartate by 71.3 ± 8.6 % (nicotine 10 μM control; 100 ± 25.0%). However, at the higher concentration of nicotine, MLA also displayed a high (71.3 ± 9.4%) inhibition of nicotine-evoked [^{3}H]D-aspartate release (nicotine 300 μM control; 100 ± 33.0%).

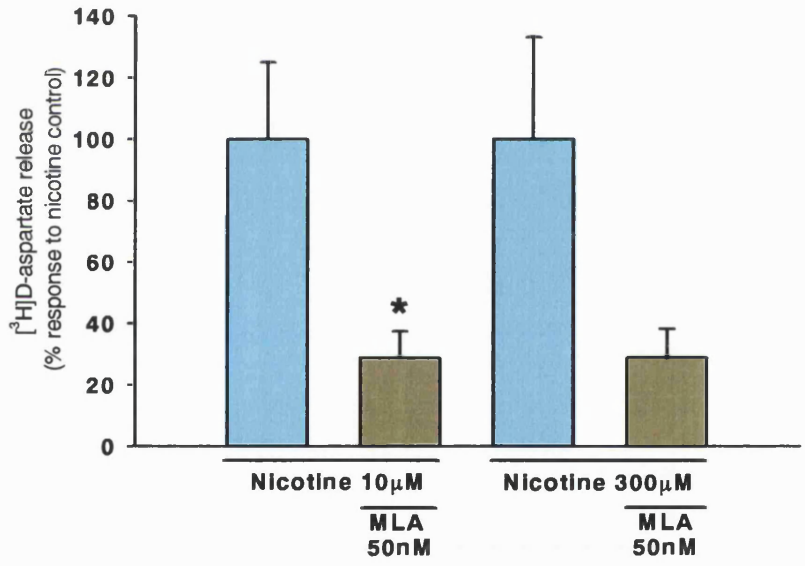

Figure 3.3.7 Concentration dependant sensitivity of nicotine-evoked [^{3}H]D-aspartate release to MLA. Rat frontal cortex synaptosomes were superfused with KB buffer and then subject to a 90 s pulse of nicotine (either 10 or 300 μM). MLA 50 nM was introduced 10 min before agonist stimulation and remained throughout the remainder of the experiment. Responses are expressed as a percentage of the corresponding agonist response in the absence of antagonist determined in parallel. Values are the mean ± S.E.M. of at least three independent experiments. * Significantly different from nicotine control in the absence of MLA, $P<0.05$, one way ANOVA with post hoc Tukeys analysis.

The effect of α-Bgt against low and high concentrations of epibatidine-evoked release of [^{3}H]D-aspartate was also examined.

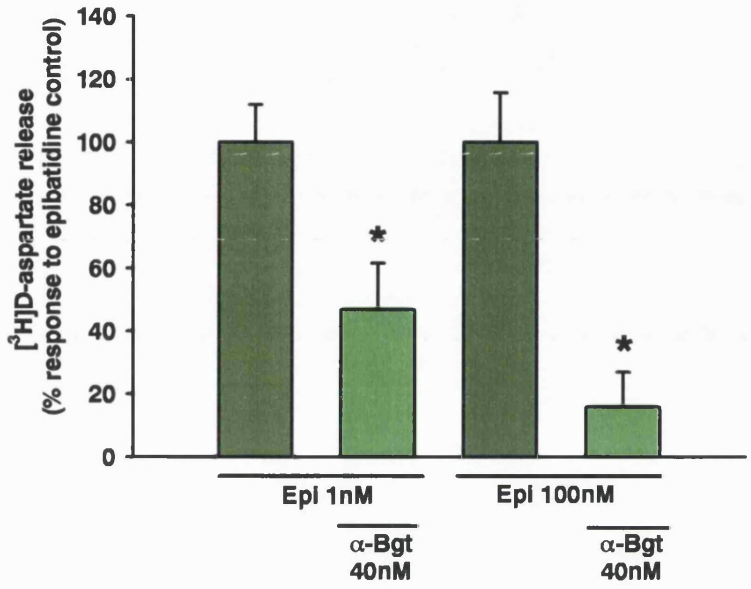

Figure 3.3.8 Concentration dependant sensitivity of epibatidine-evoked [^{3}H]D-aspartate release to α-Bgt. Rat frontal cortex synaptosomes were superfused with KB buffer and then subject to a 90 s pulse of epibatidine (either 1 or 100 nM). α-Bgt (40 nM) was introduced 20 min before agonist stimulation and remained throughout the remainder of the experiment. Responses are expressed as a percentage of the corresponding agonist response in the absence of antagonist determined in parallel. Values are the mean ± S.E.M. of at least three independent experiments. * Significantly different from epibatidine control in the absence of α-Bgt, $P<0.05$, one way ANOVA with post hoc Tukeys analysis.

Against low concentrations of epibatidine (1 nM), α-Bgt (40 nM) inhibited release by 53.3 ± 14.9%, which although was significantly different to the epibatidine 1 nM control response, was approximately 30% less inhibition than that observed against the release evoked by 100 nM epibatidine (84.1 ± 11.1% inhibition of release in the presence of α-Bgt). These results suggest that α7* nAChR account for most of the [^{3}H]D-aspartate release evoked by low concentrations of nicotine and high concentrations of epibatidine, but that another nAChR subtype(s) contributes to the higher and lower ranges, respectively, of the dose response curves of these two agonists. To address this hypothesis, the effect of the β2-preferring antagonist DHβE

was examined (Chavez-Noreiga *et al.*, 1997). In the case of nicotine, 1 μM DHβE produced a similar level of blockade of responses to both 10 μM and 300 μM nicotine, decreasing evoked release by 38.1 ± 17.8% and 39.5 ± 18.3% respectively (see Fig. 3.3.9 A; 100 ± 19.9% for 10 μM nicotine control and 100 ± 13.1% for 300 μM nicotine control).

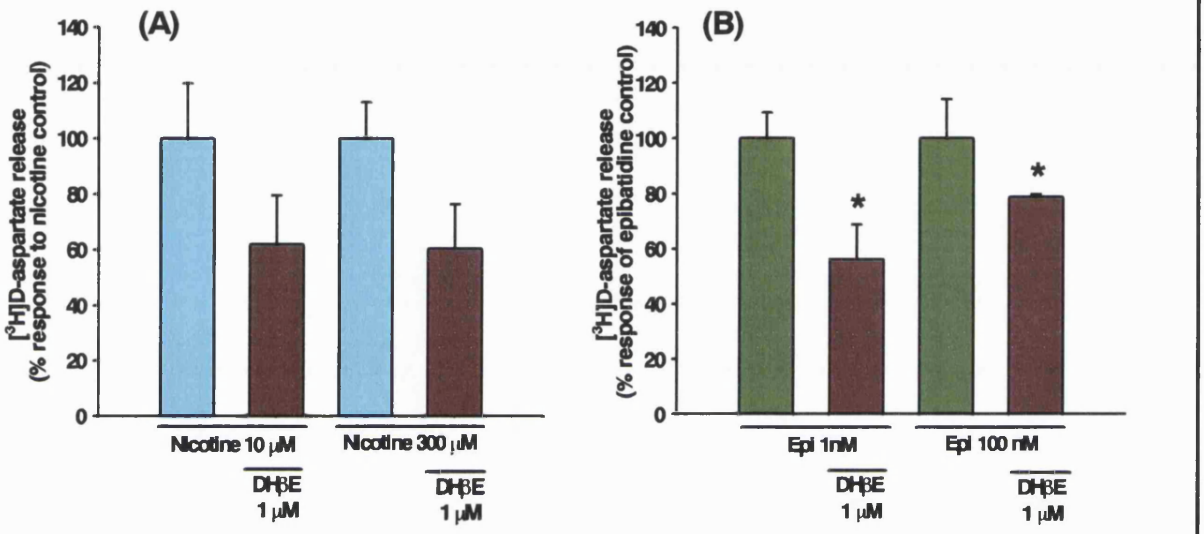

Figure 3.3.9 DHβE antagonism of nicotine and epibatidine-evoked release of [^{3}H]D-aspartate from rat frontal cortex synaptosomes. Rat frontal cortex synaptosomes were superfused with KB buffer and then subject to a 90 s pulse of (A) nicotine (either 10 or 300 mM) or (B) epibatidine (either 1 or 100 nM). DHβE (1 μM) was introduced 10 min before agonist stimulation and remained throughout the remainder of the experiment. Responses are expressed as a percentage of the corresponding agonist response in the absence of antagonist determined in parallel. Values are the mean ± S.E.M. of at least three independent experiments. * Significantly different from epibatidine controls in the absence of DHβE, $P<0.05$, one way ANOVA with post hoc Tukeys analysis.

With respect to epibatidine, DHβE (1 μM) inhibited [^{3}H]D-aspartate release evoked by 1 nM epibatidine by 48.8 ± 13.9% (control = 100 ± 9.8%). When DHβE was applied together with α-Bgt, the evoked release of [^{3}H]D-aspartate was abolished (see Fig. 3.2.13). At the higher concentration of epibatidine (100 nM) DHβE (1 μM) had significantly less effect, inhibiting release by 21.4 ± 1.1% (epibatidine control = 100 ± 16.8 %; see Fig. 3.3.9 B).

The results obtained from the DHβE antagonism experiments, seem to indicate a non-α7 component of the release evoked by low concentrations of epibatidine (the concentration of epibatidine that displayed a low sensitivity to α-Bgt). Unfortunately, the effect of DHβE on high and low concentrations of nicotine-evoked release did not replicate the same observations made with epibatidine; this could be a reflection of the competitive mode of action of DHβE and will be discussed later.

Mecamylamine, a general nAChR antagonist (with a preference for non-α7 nAChR; Papke *et al*., 2001) was also assessed against low and high concentrations of either nicotine or epibatidine. (See Fig 3.3.10 A and B).

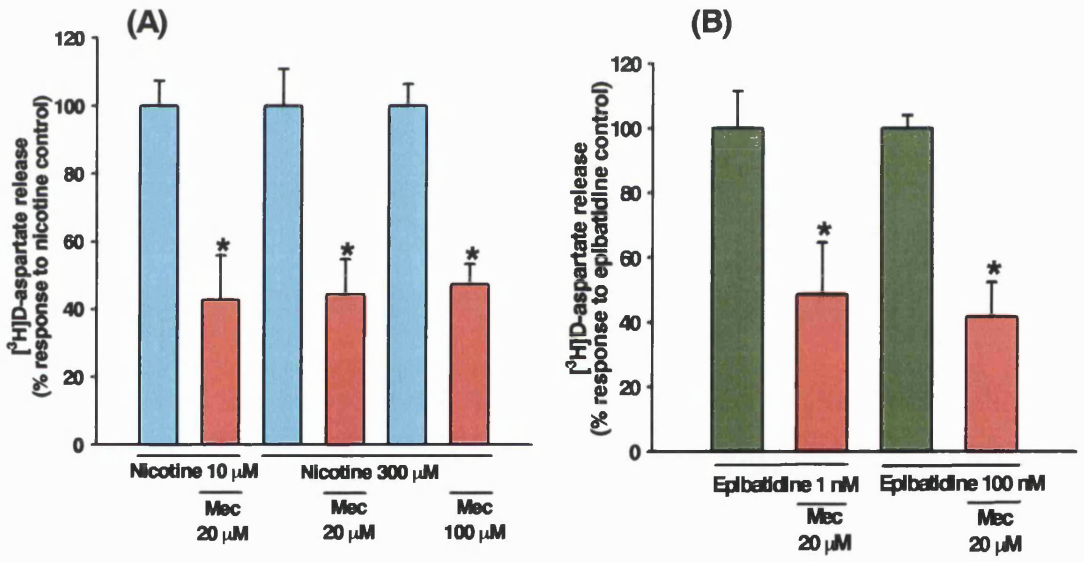

Figure 3.3.10 Mecamylamine antagonism of nicotine and epibatidine-evoked release of [^{3}H]D-aspartate from rat frontal cortex synaptosomes. Rat frontal cortex synaptosomes were superfused with KB buffer and then subject to a 90 s pulse of **(A)** nicotine (either 10 or 300 μM) or **(B)** epibatidine (either 1 or 100 nM). Mecamylamine (20 μM or 100 μM) was introduced 10 min before agonist stimulation and remained throughout the remainder of the experiment. Responses are expressed as a percentage of the corresponding agonist response in the absence of antagonist determined in parallel. Values are the mean ± S.E.M. of at least three independent experiments. * Significantly different from agonist controls in the absence of mecamylamine, $P<0.05$, one way ANOVA with post hoc Tukey*s* analysis.

At a concentration expected to block all nAChR subtypes (20 μM), mecamylamine inhibited responses by 50-60%: responses to 10 μM and 300 μM nicotine were decreased by 57.3±13.1% and 55.6±10.3% respectively, whereas responses to 1 nM and 100 nM epibatidine were decreased by 51.5±16.1% and 58.4±10.8% respectively. Increasing the mecamylamine concentration to 100 μM did not produce a significantly greater block of the 300 μM nicotine-evoked release.

To definitively address the contributions of the α7 and β2* nAChR in modulating [^{3}H]D-aspartate release we re-assessed the effect of subtype-preferring antagonists against the subtype-selective agonists choline (α7 selective; Alkondon *et al.*, 1997) and 5-I-A-85380 (β2 selective; Mukhin *et al.*, 2000).

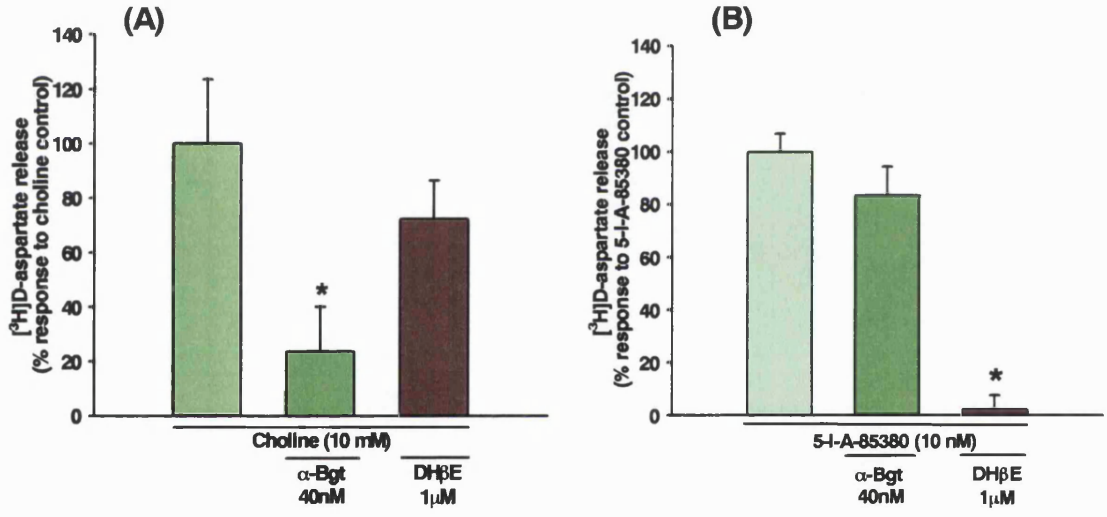

Figure 3.3.11 α-Bgt and DHβE antagonism of nAChR subtype specific agonist-evoked release of [^{3}H]D-aspartate from rat frontal cortex synaptosomes. Rat frontal cortex synaptosomes were superfused with KB buffer and then subject to a 90 s pulse of **(A)** choline (10 mM) or **(B)** 5-I-A-85380 (10 nM). α-Bgt (40 nM) was introduced 20 min before agonist stimulation and remained throughout the remainder of the experiment (DHβE was introduced 10 min before). Responses are expressed as a percentage of the corresponding agonist response in the absence of antagonist determined in parallel. Values are the mean ± S.E.M. of at least three independent experiments. (A)* Significantly different from choline control in the absence of α-Bgt, $P<0.05$, one way ANOVA with post hoc Tukey*s* analysis. (B)* Significantly different from 5-I-A-85380 control in the absence of DHβE, $P<0.05$, one way ANOVA with post hoc Tukey*s* analysis

Incubation of 40 nM α-Bgt significantly inhibited 10 mM choline-evoked [^{3}H]D-aspartate release by 76.4 ± and 16.4%, whereas 1 μM DHβE was without significant effect (Fig. 3.3.11 A). α-Bgt was ineffective at blocking 10 nM 5-I-A-85380-evoked release of [^{3}H]D-aspartate, whereas DHβE (1 μM) completely inhibited the response. (97.8 ± 5.3% inhibition, $P<0.05$, n=4, one way ANOVA with post hoc Tukeys analysis (Fig. 3.3.11 B).

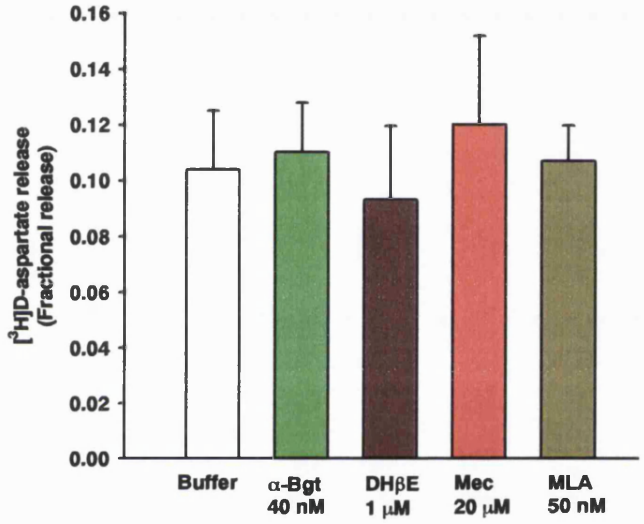

Figure 3.3.12 nAChR antagonist effects on buffer-evoked release of [^{3}H]D-aspartate. Rat frontal cortex synaptosomes were superfused with KB buffer and then subject to a 90 s pulse of KB. Release is expressed as a percentage of the total radioactivity in C.P.M, present at the point of nicotine stimulation (see methods for calculation). Values are the mean ± S.E.M. of at least three independent experiments.

To ensure nAChR antagonists had no inherent effect on [^{3}H]D-aspartate release, the release evoked by KB was examined in the presence of the range of nAChR antagonists used in this study. No nAChR antagonist produced a significant difference to KB-evoked release in the absence of antagonist (See Fig. 3.3.12)

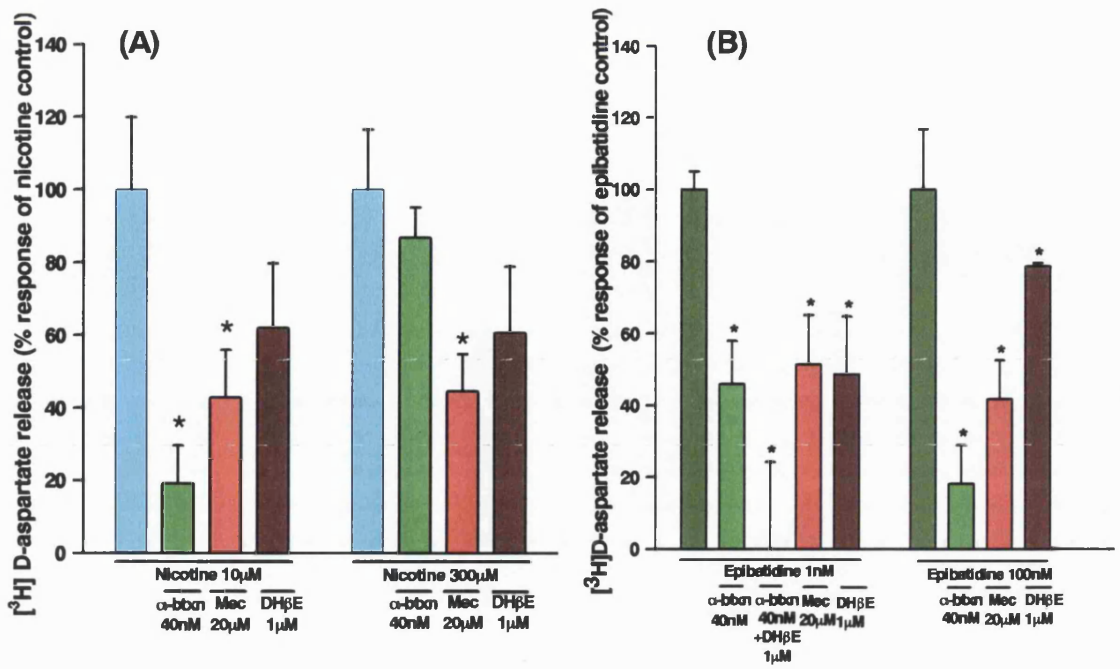

Figure 3.3.13 Summary of the nAChR pharmacology of nicotine and epibatidine evoked release of [^{3}H]D-aspartate from rat frontal cortex synaptosomes: α-Bgt, mecamylamine and DHβE antagonism. Rat frontal cortex synaptosomes were superfused with KB buffer and then subject to a 90 s pulse of (A) nicotine (10 or 300 mM) or (B) epibatidine (1 or 100 nM). α-Bgt (40 nM) was introduced 20 min before agonist stimulation and remained throughout the remainder of the experiment (DHβE and mecamylamine were introduced 10 min before). Responses are expressed as a percentage of the corresponding agonist response in the absence of antagonist determined in parallel. Values are the mean ± S.E.M. of at least three independent experiments. * Significantly different from nicotine or epibatidine control in the absence of antagonist, $P<0.05$, One way ANOVA with post hoc Tukeys analysis.

As possible support for different nAChR subtypes governing the release of [^{3}H]D-aspartate, examination of nAChR desensitisation was assessed using high and low concentrations of nicotine. In parallel experiments, nicotine was applied twice, with each stimulation separated by a 10 min perfusion in KB, for both 10 and 300 μM nicotine. The effect of a nicotine (10 μM) stimulation in the presence of α-Bgt and an initial buffer-evoked release of [^{3}H]D-aspartate followed by a nicotine (10 μM) stimulation were used as controls in each experiment. As displayed in Fig. 3.3.14 A B and C, nicotine (10 μM) initially evoked release to 0.41 ± 0.03% of total [^{3}H]D-

aspartate release, however the second stimulation within the same chamber, reduced the evoked release by approximately 60% to 0.16 ± 0.03%.

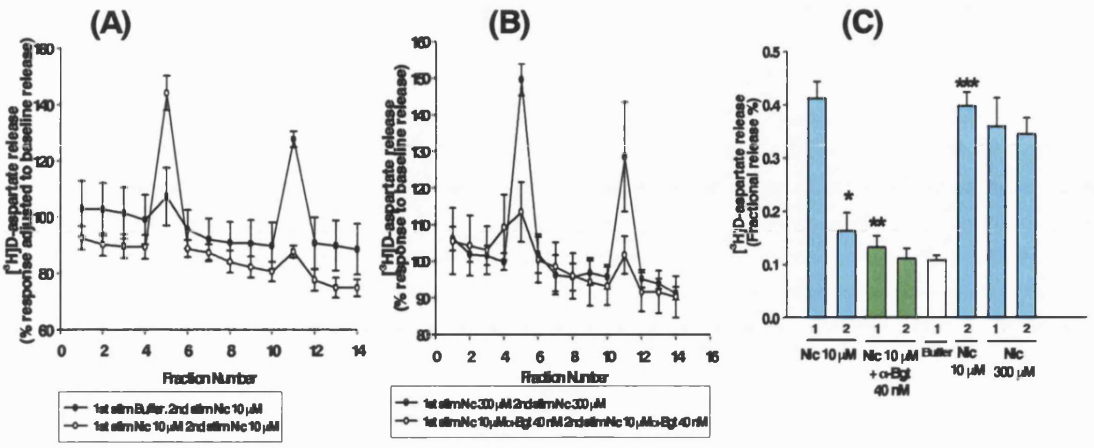

Figure 3.3.14 Desensitisation effect of subsequent nicotine (10 and 300 μM) applications to rat frontal cortex synaptosomes. Rat frontal cortex synaptosomes were superfused with KB buffer and stimulated for 90 s with an initial stimulus of buffer or nicotine (10 or 300 μM) in the presence or absence of α-Bgt 40 nM, using a 12 channel Brandel™ superfusion apparatus. **(A) Nicotine 10 μM**. Evoked release is expressed as a percentage of the average baseline release for both conditions. Closed circles = 1st stimulation with buffer, second stimulation with nicotine 10 μM. Open circles = 1st stimulation with nicotine 10 μM and 2nd stimulation with nicotine 10 μM. **(B) Nicotine 300 μM and α-Bgt sensitivity.** Evoked release is expressed as a percentage of the average baseline release for both conditions. Closed circles = 1st stimulation with nicotine 300 μM, second stimulation with nicotine 300 μM. Open circles = 1st stimulation with nicotine 10 μM + α-Bgt 40 nM and 2nd stimulation with nicotine 10 μM + α-Bgt 40 nM. Results represent the mean ± S.E.M of at least three independent experiments. **(C) Summary.** Release is expressed as a percentage of the total radioactivity in C.P.M, present at the point of nicotine stimulation (see methods for calculation). Results represent the mean ± S.E.M of three independent experiments. * Statistical significance observed between nicotine 10 μM 2nd stimulation and 1st stimulation. ** Statistical significance observed between nicotine 10 μM 1st stimulation and nicotine 10 μM 1st stimulation in the presence of α-Bgt. *** Statistical significance observed between nicotine 10 μM 2nd stimulation and 1st buffer-evoked stimulation. $P<0.05$, n=3, One way ANOVA with post-hoc tukeys analysis.

As a control, buffer evoked release of [^{3}H]D-aspartate was applied as the first stimulation (0.11 ± 0.01%) whereupon the subsequent stimulation with nicotine (10 μM) evoked release similar in magnitude (0.40 ± 0.02%) to that evoked by nicotine in the first instance. To ensure that the nicotinic effect was specific, nicotine-evoked release was also examined in the presence of α-Bgt (40 nM) where on both

applications of nicotine (10 μM), release above the effect of buffer was not demonstrated (0.13 ± 0.02% and 0.11 ± 0.02%).

Interestingly, nicotine at high concentrations displayed no evidence of desensitisation, where the second application of nicotine (300 μM) showed no significant difference to that evoked by the first stimulation within the same set of chambers; First nicotine 300 μM application evoked 0.36 ± 0.03% of total [^{3}H]D-aspartate and second nicotine 300 μM application 0.34 ± 0.03% of total [^{3}H]D-aspartate.

3.3.3 Discussion

The results in this section provide the first direct evidence that activation of presynaptic nAChR by nicotinic agonists alone can facilitate the release of [^{3}H]D-aspartate from rat frontal cortex P2 synaptosomes. Pharmacological characterisation of frontal cortex synaptosomes revealed that both α7* and non-α7 nAChR mediate this response.

The general nAChR agonists anatoxin-a, epibatidine and nicotine, as well as the subtype specific agonists choline and 5-I-A-85380, evoked the release of [^{3}H]D-aspartate from frontal cortex synaptosomes in the absence of KCl. The response to 10 μM nicotine was Ca^{2+}-dependant, consistent with exocytotic release of [^{3}H]D-aspartate from a vesicular store, but in contrast to KCl-evoked release, reversal of the glutamate transporter was not involved (Fig. 3.3.2 A & B). Fig. 3.3.2 B, does however show a trend in the increase of nicotine-evoked release of [^{3}H]D-aspartate compared to control and this may reflect a prevention of re-uptake within the synaptosome chamber, thereby enhancing the evoked release. TBOA was not routinely included because of its expense; nAChR agonist-evoked release of [^{3}H]D-aspartate was clearly detected in the absence of TBOA.

3.3.3.1 nAChR subtype characterisation

The concentration dependence of nicotine and epibatidine-evoked release of [^{3}H]D-aspartate showed a sustained response over a broad concentration range for both agonists (see Fig. 3.3.3 B and 3.3.4 B), prompting the notion that different nAChR could contribute to these profiles. The differential effects of α-Bgt and DHβE at high and low agonist concentrations support this. However, MLA, an α7 nAChR selective antagonist, did not display the same functional effects of inhibition of [^{3}H]D-aspartate

release as described for α-Bgt (see Fig. 3.3.7). This finding could provide support for the current trend of data that this compound has a broader pharmacological specificity for nAChR subtypes than first predicted (Klink *et al.*, 2001; Mogg *et al.*, 2002); these authors report the existence of a putative α3/α6β2β3* or an $\alpha4\alpha6\alpha5\beta2_{(2)}$ nAChR subtype the displays sensitivity to low nM concentrations of MLA in the rat striatum. In this investigation, MLA is able to inhibit the non-α7 component of the nicotine (300 μM) evoked release of [^{3}H]D-aspartate as well as the α7 component of low concentrations of nicotine-evoked release. However, the pharmacologically described non-α7 (β2* containing nAChR) component to nAChR agonist evoked release in the rat frontal cortex is unlikely to incorporate α6 nAChR subunit due to its localised expression in catecholaminergic neurons of the rat brain such as those found in the mesencephalon and locus coeruleus (Le Novere *et al.*, 1996).

The concentrations of nicotine and epibatidine that are more sensitive to α-Bgt (10 μM and 100 nM respectively (Fig. 3.3.6 and 3.3.8), are in the range predicted to activate α7 nAChR (Gerzanich *et al.*, 1994; Alkondon & Albuquerque 1995; Briggs *et al.*, 1995; Delbono *et al.*, 1997). The relative insensitivity to mecamylamine of responses evoked by these agonist concentrations is compatible with its low efficacy at α7 nAChR (see Fig. 3.3.10 A & B; Frazier *et al.*, 1998; Papke *et al.,* 2001), although incomplete blockade of [^{3}H]D-aspartate release by mecamylamine was also observed at agonist concentrations insensitive to α-Bgt.

The choice of selective antagonists for non-α7 nAChR is limited. DHβE (0.1-1 μM) has been reported to inhibit predominantly α4β2 nAChR (Alkondon *et al.*, 1994), although it potently inhibits a variety of β2* and α4* nAChR in heterologous

expression systems. However, within this concentration range, DHβE is two orders of magnitude less potent at α7 nAChR (Harvey *et al.*, 1996; Chavez-Noriega *et al.*, 1997). DHβE, at a concentration of 1 μM, was used to define the non-α7 mediated component of nicotine and epibatidine-evoked [^{3}H]D-aspartate release. Its limited effect against a low concentration of nicotine (10 μM) is consistent with predominantly α7 nAChR-mediated facilitation of [^{3}H]D-aspartate release. But DHβE was also not very effective at the higher nicotine concentration that was insensitive to α-Bgt: its efficacy may be confounded by its competitive mode of antagonism, such that its blocking ability is compromised at increasing agonist concentrations (see Fig. 3.3.9 A). This is consistent with the pharmacological specificity displayed by epibatidine-evoked release of [^{3}H]D-aspartate (Fig. 3.3.9 B): DHβE produced greater inhibition at the lower epibatidine concentration and is additive with α-Bgt, whereas α-Bgt was more effective at the higher epibatidine concentration.

Confirmation of the involvement of at least two nAChR subtypes was provided by the use of subtype-selective agonists (Fig. 3.3.5 A and B, and Fig. 3.3.11 A & B). Choline evoked [^{3}H]D-aspartate release at concentrations reported to activate α7 nAChR (Papke *et al.*, 1996; Alkondon *et al.*, 1997). The magnitude of the response was comparable to that evoked by low and high concentrations of nicotine and epibatidine respectively. Blockade of the choline-evoked response by α-Bgt confirmed the involvement of the α7 nAChR whereas DHβE had no significant effect. The novel agonist 5-I-A-85380 displays over 25000 fold selectivity for α4β2 nAChR, compared to α7 nAChR, in binding studies (Mukhin *et al.,* 2000). In functional assays it displays a somewhat broader specificity, consistent with it being a potent and selective agonist at α4β2 and α6β2* nAChR (A Mogg, F.A.Jones, I.A Pullar,

C.G.V. Sharples, and S. Wonnacott. in preparation). Very low concentrations (0.1 nM) of this agonist evoked [^{3}H]D-aspartate release and this effect was sustained over a broad concentration range. The lack of effect of α-Bgt but complete blockade of evoked release in the presence of DHβE supports the involvement of non-α7, β2* presynaptic nAChR on terminals releasing EAA in the rat frontal cortex.

3.3.3.2 nAChR desensitisation

Homomeric α7 nAChRs and heteromeric non-α7 (β2* containing) nAChRs can also be distinguished based on their desensitisation properties; α7 nAChR imparts the fastest onset of desensitisation (≈ 20 ms described in hippocampal cells) whereas β2* containing nAChR slowly desensitise (≈ 300 ms described in hippocampal cells) (Alkondon & Alburquerque, 1993; Alkondon *et al.*, 1994; Alburquerque *et al.*, 1997; For review see Quick & Lester, 2002). Whole cell currents induced by nAChR activation have been categorised into four different types based on their pharmacological and kinetic characteristics (Table 3.3.1)

Current Type	Desensitisation attribute	Selective antagonists	Affinity to Ach	Possible subunits involved
IA	Fast	MLA, α-Bgt	Low	α7
IB	Fast + slow	MLA + DHβE	Low and High	α7; α4β2
II	Slow	DHβE	High	α4β2
III	Slow	Mecamylamine	High	α3β2

Table 3.1 nAChR pharmacology and kinetic characterisation from currents recorded in rat hippocampal cells. Desensitisation currents time constants assigned fast and slow when they decayed over <30 ms or >500 ms. The antagonists employed are based on their ability to block at specific concentrations that have little effect on other current types. (Table adapted from Alkondon & Alburquerque, 1993)

However, superfusion is unable to differentiate nAChR subtype kinetic characteristics due to the limited temporal resolution of drug application, but instead

may be able to differentiate between nAChR subtype recovery times: the ability to activate on subsequent agonist exposure. Recovery times for α7 nAChR have been reported to be fast, (< 10 s), even after prolonged exposure to nAChR agonist (Dani, 2000; Kawai & Berg, 2001) whereas in non-α7 nAChR recovery times are more diverse dependant upon the subunit combination of nAChR being assessed and the expression system/species being used: α4β4 recovery to ACh ≈ 3 hrs, α3β2α5 recovery to nicotine ≈ 10 min-5hrs, α4β2 recovery to nicotine ≈ 4-60 min (For review see Quick & Lester, 2002). With this information it was hoped that by separating low and high concentrations of nicotine exposure by a selected time period (10 min; Fig 3.3.14) we could also define the nAChR subtypes governing [^{3}H]D-aspartate release based on recovery times. As demonstrated in Fig. 3.3.14, P2 synaptosomes exposed to a second exposure of nicotine (10 μM; α7 nAChR activating, defined pharmacologically) failed to evoke the same extent of [^{3}H]D-aspartate release as that evoked by the first nicotine (10 μM) application 10 minutes earlier during the superfusion. Conversely, a second exposure of nicotine (300 μM; non-α7 nAChR activating, defined pharmacologically), evoked [^{3}H]D-aspartate release to the same extent as the first nicotine (300 μM) application 10 min earlier. This was a surprising result in light of the fact that α7 nAChRs should have recovered from their first nicotine exposure. With respect to the non-α7 nAChR result, it appears that these receptors have recovered from the first high nicotine exposure within 10 min, in agreement with the literature. The α7 component in these studies was confirmed by assessing the effect of α-Bgt (40 nM) in parallel, which displayed complete blockade of the nicotine (10 μM) evoked release, however, the recovery rate is not of that described for α7 nAChR in the literature. This result could be explained on the

premise that the α7 nAChR subtype characterised in the frontal cortex, may be heteromerically assembled, rather than homomeric, as assumed in those investigations studying recovery rates in the hippocampus, cortical cultures and Xenopus ooctyes (Olale *et al.*, 1997; Molinari *et al.*, 1998; Mike *et al.*, 2000; Kawai & Berg, 2001). At present, possible heteromeric nAChR subunit combinations with α7 nAChR subunit have not been defined in terms of recovery rate and therefore provides an interesting opportunity for research in defining α7* heteromeric nAChR.

3.3.3.3 Implications of nAChR heterogeneity for regulation of EAA release

The role of β2* nAChR in [^{3}H]D-aspartate release is consistent with the inference made from microdialysis and electrophysiological experiments that β2* nAChR mediate glutamate release in the rat prefrontal cortex (Vidal and Changeux., 1989; Vidal, 1993; Granon *et al.*, 1995; Gioanni *et al.*, 1999; Lambe *et al.*, 2003). These studies found no evidence for a α7 nAChR-mediated component of glutamate release. Possible reasons for this disparity with the present findings include methodological differences in temporal characteristics or agonist concentrations, or anatomical differences dependant on where recording and stimulating electrodes were placed. However, the involvement of presynaptic α7 nAChR is compatible with the role of this subtype in the facilitation of glutamate release in other areas of the rat brain: hippocampus (Gray *et al.*, 1996; Alkondon *et al.*, 1998; Radcliffe & Dani, 1998; Fischer & Dani, 2000; Sharma & Vijaraghavan, 2003), olfactory bulb (Alkondon *et al.*, 1996), midbrain (Schilstrom *et al.*, 2000; Nomikos *et al.*, 2000; Mansvelder & McGehee, 2000; Girod & Role, 2001;) and cerebellum (De Filippe *et al.*, 2001). It has been suggested that α7 nAChRs increase the probability of glutamate release

by increasing local Ca^{2+} levels in glutamate terminals (Gray *et al.*, 1996). The Ca^{2+}-dependence of [^{3}H]D-aspartate release by 10 μM nicotine, a concentration that elicits a predominantly α-Bgt-sensitive response, is consistent with this model. α7 nAChR can modulate synaptic efficacy at glutamate synapses and promote the induction of LTP in the hippocampus (Ji *et al.*, 2001) and VTA (Mansvelder & McGehee, 2002), and a comparable role in the frontal cortex could be relevant to the positive effects of nicotine on attentional aspects of memory (Levin & Simon, 1998).

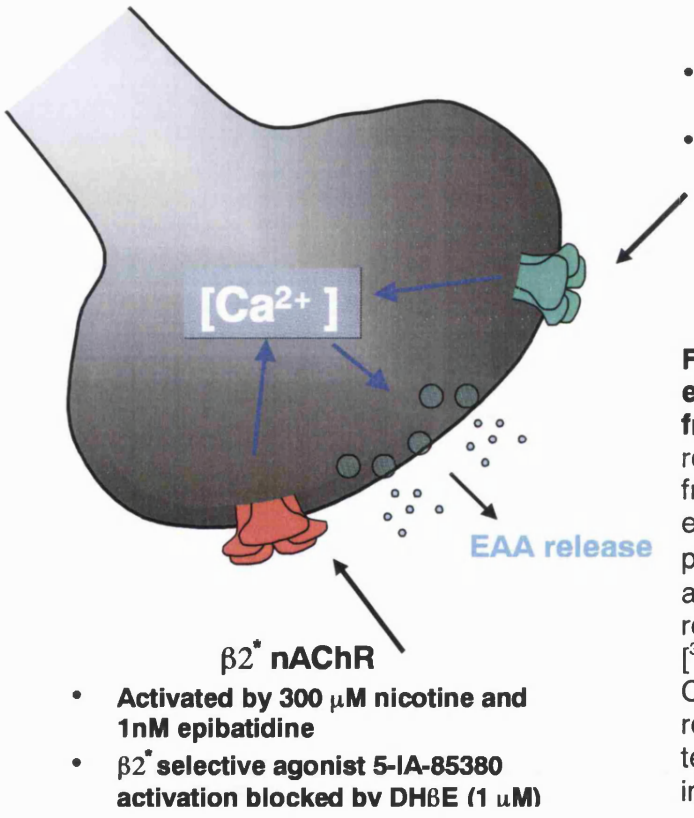

Figure 3.3.15. Summary of nAChR-evoked release of EAA release from frontal cortex terminals. The release of [^{3}H]D-aspartate from rat frontal cortex synaptosomes could be evoked by activating pharmacologically defined α7 nAChR and β2* containing nAChRs. The release of nicotine-evoked release of [^{3}H]D-aspartate was shown to rely on Ca^{2+} and was independent of EAAT reversal. The source of the intra-terminal Ca^{2+} increase remains to be investigated.

This has additional implications in neurological disorders such as schizophrenia and Alzheimer's disease, where reduced glutamatergic and cholinergic transmission in the frontal cortex compromises both attentional processes and memory functions (Sarter & Bruno, 1999). Here we show that at least two nAChR subtypes are involved in the presynaptic regulation of [^{3}H]D-aspartate release in the frontal cortex

(summarised in Fig. 3.3.15), albeit the significance of this heterogeneity is presently unclear. The α7 and β2* nAChRs may serve distinct functions through their localisation on different glutamatergic afferents (which is examined using immunocytochemistry, in the next chapter; Chapter 4), or different domains on the same terminals, or they may couple to complementary regulatory mechanisms to influence different aspects of synaptic function. This study provides an in vitro model that will be useful for exploring this relationship.

Chapter Four

4.1 Localisation of nAChR in the rat frontal cortex: association with VGluT immunoreactivity

4.1.1 Introduction

4.1.2 Techniques utilised for localising nAChR in the vertebrate CNS

The identification and location of nAChR in the vertebrate CNS relies on an array of investigative approaches including autoradiographical analysis, in situ hybridisation, immunocytochemistry and PET scanning.

Autoradiographical analysis, using radiolabelled nAChR agonists and antagonists such as [^{3}H]nicotine, [^{3}H]ACh (in the presence of excess atropine) and [^{125}I]α-Bgt (Yoshida & Imura, 1979; Marks & Collins, 1982; Schwartz *et al.*, 1982: Clarke *et al.*, 1984 & 1985;) incubated with either brain homogenates or brain sections permits the gross identification of nAChR location within the brain. It is generally accepted that [^{3}H]nicotine and [^{125}I]bungarotoxin label $\alpha4\beta2^{*}$ containing nAChR and $\alpha7$ nAChR respectively. Indeed, it was the comparison of different radioligand labelling patterns of [^{3}H]nicotine and [^{125}I]bungarotoxin within the rat brain, that provided the first evidence that more than one nAChR may co-exist, confirmed and summarised by Wonnacott, (1986); coining the term 'high' and 'low' affinity nicotine binding receptors (see Introduction, section 1.2.3). However the majority of nAChR ligands fail to demonstrate specificity against other nAChR subtypes and therefore limits the extent of analysis of nAChR heterogeneity in the brain using autoradiography. Presently, autoradiographical analysis has been extended to human studies and provides a useful gross diagnostic tool for nAChR association with neurodegenerative diseases (Nordberg & Windblad, 1986; Marutle *et al.*, 1998) as well as the characterisation of novel ligands for nAChRs; the compound [^{125}I]5-I-A-85380 is a novel $\beta2$ selective binding ligand that may display similar labelling patterns to other well characterised ligands (Musachio *et al.*, 1998; Muhkin *et al.*, 2000). The suitability of this technique is not favoured in this thesis because

autoradiographical analysis of rat frontal cortex regions, using radiolabel nAChR ligands, would give insufficient detail of the neurochemical identity of the cell bodies or subcellular components associated with the radiolabel as well as possible concerns over the nAChR specificity of the label.

The advent of molecular cloning techniques accelerated the understanding of nAChR in the CNS, namely the revelation of a family of genes encoding for the α and β subunit proteins that could be manipulated to form functional nAChR in a variety of expression systems (Seguela *et al.*, 1993; Leutje *et al.*, 1990; Gopalkrishnan *et al.*, 1995). In terms of nAChR localisation studies, this knowledge has allowed for the progression of either in situ hybridisation or immunocytochemical techniques to identify and localise nAChR subunits by enabling the design of specific nAChR subunit riboprobes or specific nAChR antibodies respectively. These techniques have essentially corroborated the data provided from autoradiographical analysis but have allowed for a greater detail of inspection on the basis of an increased specificity and selectivity for the array of α or β subunits of the nAChR that nAChR ligands cannot discriminate between, as well as provide greater morphological data about the specific cell type and subcellular distribution of the nAChR (For review see Heinemann *et al.*, 1991). However the location of nAChR gene expression from in situ studies are only defined to those regions where the mRNA is expressed, mainly cell bodies and therefore cannot define the location of nAChR subunits located away from the soma. As well as this, disparities also exist between the quantifiable level of in-situ hybridisation labelling and that of autoradiographical or immunocytochemical labelling, demonstrating the point that in situ hybridisation cannot reveal any changes of nAChR protein expression at the level of the membrane (e.g. Marks *et al.,* 1992). For these reasons and for the fact

that the majority of this thesis focuses on the presynaptic function of nAChR, in situ hybridisation techniques do not serve as a suitable means to corroborate the functional data described in Chapter 3 (section 2 and 3), as the α7* or β2* containing nAChR transcript would only be detected in the cell bodies within the frontal cortex. Immunocytochemistry serves as a useful tool in receptor identification and localisation at both the cellular and subcellular level, dependent on the probes being used, e.g. fluorescent-labelled antibodies or ligands. Immunocytochemical identification of nAChR combined with electron microscopy analysis can reveal the micro-architecture of the synapse such as pre and post-synaptic elements, alongside immuno-gold labelled receptors. This has been utilised for anatomical studies of the nAChR in the dorsal striatum e.g. β2 nAChR-immunogold labelling of TH-positive cells (Jones *et al.*, 2001) and α7 nAChR-immunogold labelling of synapses within the dentate gyrus, CA1 and CA3 areas of the rat hippocampus (Fabien-Fine *et al.*, 2001). Confocal imaging of immunolabelled brain tissue permits the differentiation of up to six or seven different components within a sample preparation (mainly due to the limitations of confocal system and its use of wavelength filtration). This technique provides a large amount of information compared to other receptor localisation methods (although not to the resolution of EM), namely: the receptor identification, the identification of other proteins associated with the receptor (i.e. structural or cell membrane associated proteins or other co-localised receptors/transporter/channels) and the neurochemical identity of the cell or presynaptic terminal associated with the receptor (via immunolabelling for neurotransmitter-specific enzymes or transporters). However confocal microscopy is limited with respect to resolution and therefore the interpretation of the pre or postsynaptic location of an immunolabelled receptor has to be exercised with

caution. With respect to our study, this technique is utilised to support the association of nAChR with glutamatergic terminals; nAChR localisation and association with glutamatergic terminals and cell bodies of the rat frontal cortex are examined using fluorescently labelled ligands for the nAChR (Alexa-Fluor488 or 546 α-Bgt), antibodies directed against β2 nAChR, antibodies directed against the vesicular glutamate transporters 1 & 2 (VGluT 1 &2; a marker for glutamatergic terminals; Kaneko *et al.*, 2002) and antibodies directed against presynaptic terminal proteins (synaptophysin) and cell body proteins (Neun) respectively.

Notably we have utilised fluorescent labelled α-Bgt (Alexa-Fluor® 488 or 546 α-Bgt) instead of monoclonal antibodies directed against α7 nAChR such as mAb306 (a mouse monoclonal antibody directed against the predicted cytoplasmic domain of the α7 nAChR (Schoepfer *et al.,* 1990; Mclane *et al.,* 1992)), on the basis that data accumulated in our laboratory has raised grave concerns over antibody specificity for a number of 'supposed' α7 nAChR specific antibodies. α-Bgt on the other hand is a well-characterised selective antagonist for α7 nAChR and the development of a fluorescent-labelled α-Bgt serves as an extremely useful tool in confocal microscopy analysis of α7 nAChR localisation and identification studies (see Fabien-Fine *et al.*, 2001; Kawai *et al.*, 2002; Akaaboune *et al.*, 2002). Added advantages of the confocal microscope software allow for the investigator to selectively obtain serial images through a tissue sample and then generate a 3D image of the tissue as well as the use of 'profiling', where along a selected axis, the relative fluorescence intensities can be assigned for each fluorochrome used. .

4.1.3 Present understanding of α7* and β2* nAChR localisation in the frontal cortex

To date, few studies have specifically examined the rat frontal cortex with respect to the α7 * and β2* nAChR localisation and distribution in the rat CNS (the two nAChRs defined pharmacologically in Chapter 3 section 3). As described in Chapter 1 (see Introduction; see sections 1.3) in situ hybridisation studies have demonstrated a wide anatomical distribution for the β2 subunit of the nAChR (Deneris *et al.*, 1988; Wada *et al.,* 1989, Goldman *et al.*, 1987) in the rat brain; these corresponded with the high affinity nicotine binding sites also described from autoradiographical analysis. With respect to the rat α7 nAChR, in situ hybridisation techniques also displayed a broad distribution of expression of this receptor across the rat brain (Seguela *et al.* 1993; Broide *et al.*, 1995), and these are in agreement with autoradiographical studies using [^{125}I]α-Bgt (Clarke *et al.*, 1985). One specific observation, particularly from autoradiographical analysis of nAChR distribution, is the differences between [^{3}H]nicotine and [^{125}I]α-Bgt labelling found in the cortical layers of the rat brain; [^{125}I]α-Bgt labelling is found predominantly in the superficial (layers I and II) and deep layers (layers V and VI) whereas [^{3}H]nicotine labelling is found in the intermediate layers. This relatively clear difference may reflect the different nAChR subtypes expressed by specific neurons that either innervate these layers of the cortex (i.e found on their presynaptic terminals) or of those neurons found in these layers (i.e found on their dendritic or somatic membranes).

To definitively assign nAChR subcellular location at the presynaptic locus, electron microscopy is required for high-resolution imaging. Again few studies have specifically examined the rat frontal cortex with respect to the α7 and β2* subunit containing nAChR, but nonetheless, these subunits have been identified at the

presynaptic terminal: α7 nAChR have been defined using EM analysis of immuno-gold labelled tissue sections in the guinea pig pre-frontal cortex, rat hippocampus and in the rat sensory cortex (Lubin *et al.*, 1999; Levy & Aoki, 2002; Fabien-Fine *et al.*, 2001). β2* containing nAChRs have been located at presynaptic terminals in axon terminals of the basal ganglia (Hill et al., 1993; Jones *et al.*, 2001).

4.1.4 Physiological significance of nAChR in the frontal cortex

A large number of glutamatergic pathways innervate the frontal cortex regions particularly from the hippocampus (Thierry *et al.*, 2000; Delatour & Witter, 2002) as well as the thalamus (Gigg *et al.*, 1994; Groenewegen, 1988; Pinto *et al.*, 2003). Although not experimentally assessed in this chapter, the relevance of glutamatergic innervation into the frontal cortex is pertinent to the role the frontal cortex plays in cognition, memory and reward (Frith & Dolan, 1996; Mitchell & Laiacon, 1998; Trzcinska & Bielajew, 1998; Buckner *et al.,* 1999). Therefore if nAChR is found at the terminals of these glutamatergic pathways directed towards the frontal cortex, then this may support the notion of how the nAChR may participate in such functions (Granon *et al.*, 1995; For review see Levin & Simon, 1998), notably exampled by the possible involvement of nAChRs with neurological disorders associated with frontal cortex dysfunction such as schizophrenia (Guan *et al.*, 1999; Breese *et al.*, 2000; Marutle *et al.,* 2001) and Alzheimer's disease (Nordberg & Winblad, 1986; Sugaya *et al.*, 1990; Nordberg, 1993; Wevers *et al.*, 2000; Engidawork *et al.*, 2001).

The present chapter describes evidence supporting the presence of α7* and β2* nAChR associated with glutamatergic terminals in the rat frontal cortex, to complement the functional data described in Chapter 3 (sections 2 and 3). The study

also provides a preliminary investigation into the regional localisation of these receptors within the frontal cortex, which could provide an investigative platform for future studies into the functional significance of their location with respect to the physiological roles of the frontal cortex.

4.2. Results

4.2.1 Double Immunolabelling in rat frontal cortex synaptosomes

To address the association of α7 nAChR with presynaptic terminals in the rat frontal cortex, P2 and Percoll™ purified synaptosomes were initially subjected to double-label confocal microscopy analysis. From Fig 4.1 it is clear that the P2 synaptosome preparation incorporates many non-specific membrane elements compared to the Percoll™ purified synaptosomes. Therefore the use of P2 purified synaptosomes for the assessment of nAChR labelling of presynaptic terminals was deemed unsuitable, all subsequent figures utilise and demonstrate results obtained using Percoll™ purified synaptosomes.

Synaptosomes (presynaptic terminals) are identified using an antibody specific to the presynaptic terminal marker protein synaptophysin (identified using a secondary label, anti-mouse 546). α7 nAChRs were visualised using fluorochrome-conjugated α-Bgt (Alexa-Fluor® 488 α-Bgt). The specificity of this toxin conjugate for labelling α7 nAChR has been demonstrated previously (Kawai *et al.*, 2002) and was confirmed in this study by pre-incubating the samples with a 100-fold molar excess of either α-Bgt or MLA, which abolished the toxin labelling.

An average of 180 synaptophysin positive structures were identified per field view. Of these synaptophysin positive structures less than 2% were associated with Alexa-Fluor® 488 α-Bgt binding (See Table 4.1). Of the fifteen field views analysed, approximately 4 individual Alexa-Fluor® 488 α-Bgt labels were not associated with synaptic terminals as indicated by lack of synaptophysin fluorescence when assessed using fluorescence intensity profiles.

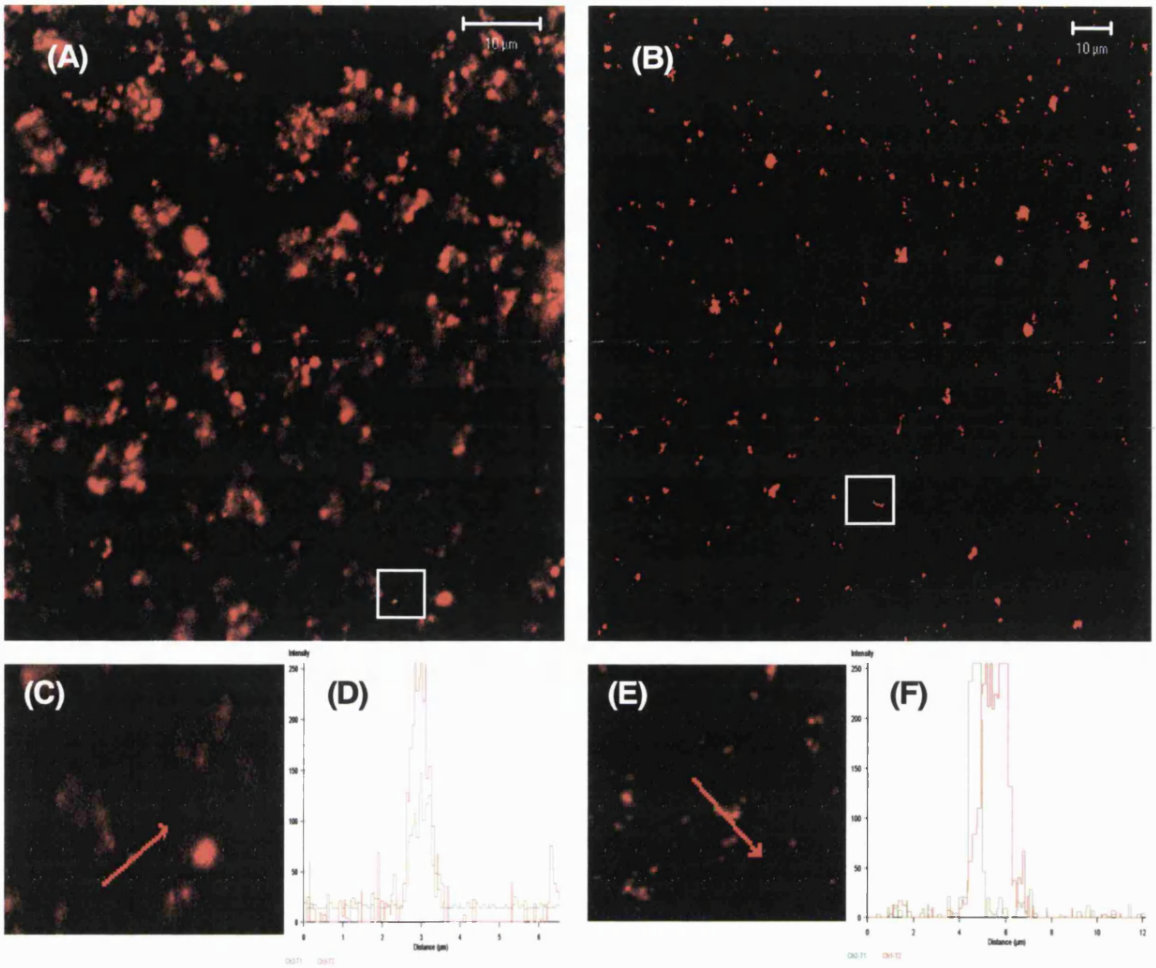

Figure 4.1. Confocal imaging of α-Bgt AlexaFluor 488 labelling in rat frontal cortex P2 purified synaptosomes (A) and Percoll™ purified synaptosomes (B). Example confocal image of both P2 synaptosomes **(A)** and Percoll™ purified synaptosomes **(B)** double labelled with α-Bgt (green) and anti-synaptophysin (red). **(C)** & **(E)** x3 zoom image of area highlighted in **(A)** and **(B)** (square). **(D)** & **(E)**, fluorescence intensity profiling of the α-Bgt labelling in the area delineated in A and B (square) reveals that this labelling is associated with presynaptic terminals in both synaptosome preparations.

	Condition		
	Synaptophysin	α-Bgt	Synaptophysin and α-Bgt
Average number of +ve structures (Per field view)	180.56 ± 25	3.4 ± 0.14	3.1 ± 0.21
% of synaptosome total (Per field view)	100 ± 14 %	1.8 ±0.07%	1.7 ± 0.1 %

Table 4.1. Quantitative analysis of presynaptic terminal immunolabelling with anti-synaptophysin and Alexa-Fluor® 488 α-Bgt in rat frontal cortex Percoll™ purified synaptosomes. Values given are the mean ± S.E.M of positive immunolabelled structures per field view under the confocal microscope from an average of five field views from three independent experiments. (+VE = positive)

4.2.2 Triple Immunolabelling of rat frontal cortex synaptosomes: Identification of α7 nAChR

The association between α-Bgt binding sites and glutamatergic terminals in the frontal cortex was investigated by triple labelling of synaptosomes with antibodies to the vesicular glutamate transporter types 1 & 2 (identified using secondary label anti-rat 633 blue), and synaptophysin (identified using secondary label anti-mouse 546 red). α7 nAChRs were again visualised using fluorochrome-conjugated α-Bgt (Alexa-Fluor® 488 α-Bgt). To avoid any incidence of fluorochrome 'cross-talk', which could result in erroneous examples of co-localisation, samples were analysed using sequential fluorochrome excitation (multi-tracking).

Approximately 80% of all synaptophysin positive synaptosomes were also labelled for VGluT 1 & 2 (See Figure 4.2 and Table 4.2) indicating that the majority of synaptosomes isolated from Percoll™ purified frontal cortex synaptosomes are

glutamatergic. Fluorescence intensity profile examination of α-Bgt fluorescence showed near 85% association with presynaptic terminals (36 out of 44 identified Alexa-Fluor® 488 α-Bgt labels). Of these labelled structures, 75% (32 of the 36 identified Alexa-Fluor® 488 α-Bgt labels that co-associated with anti-synaptophysin labelling) were also co-associated with structures positive for VGluT 1 & 2.

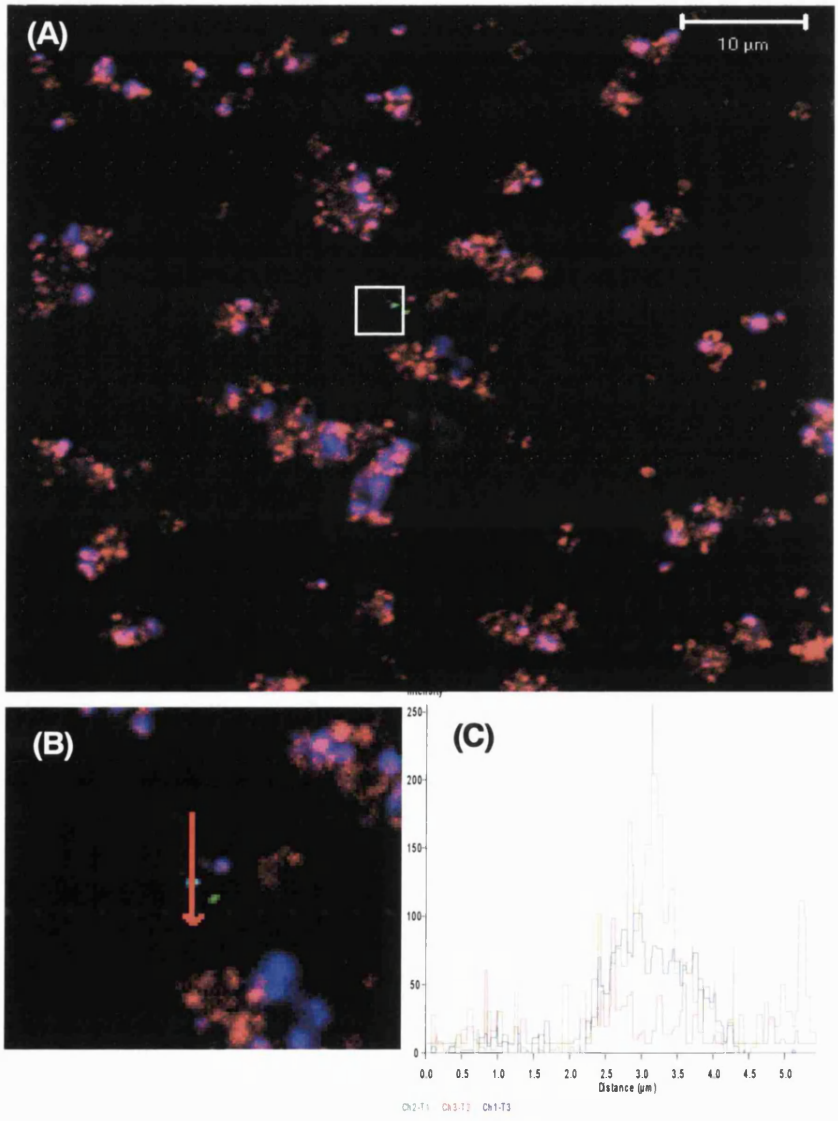

Figure 4.2. Confocal imaging of α-Bgt AlexaFluor 488 labelling in rat frontal cortex Percoll™ purified synaptosomes. (A), Example confocal image Percoll™ purified synaptosomes triple labelled with α-Bgt (green), anti-synaptophysin (red) and anti-VGluT 1 & 2. **(B)** x3 zoom image of area highlighted in **(A)** (white square). **(C)** Fluorescence intensity profiling of the α-Bgt labelling in the area delineated in A and reveals that this labelling is associated with glutamatergic terminals.

This approximates to less than 1.2% of all synaptophysin positive structures co-associated with Alexa-Fluor® 488 α-Bgt labels from an average field view (See Table 4.2). These results are consistent with the presence of presynaptic α7 nAChR on a minority of glutamatergic axon terminals.

Table 4.2. Quantitative analysis of presynaptic terminal immunolabelling with anti-synaptophysin, Alexa-Fluor® 488 α-Bgt and VGluT 1 and 2 in rat frontal cortex Percoll™ purified synaptosomes. Values given are the Mean (± S.E.M where indicated) of positive immunolabelled structures per field view under the confocal microscope. Results are accumulated from an average of five field views from three independent experiments, 15 field views in total. (+VE = positive)

	S'physin +VE	α-Bgt +VE	vGlut1 & 2 +VE	S'physin α-Bgt +VE	S'physin vGlut1 & 2 +VE	S'physin vGlut1 & 2 α-Bgt +VE
Total number of positive structures (from 15 field views)	3208	44	2530	36	2474	32
Average number of positive structures (per field view)	213.8 ± 5.8	2.9 ± 0.3	168.7± 8.6	2.4 ± 0.2	164.9 ± 9.2	2.1 ± 0.2
Range of +VE structures (per field view)	181-261	1-5	144-220	1-4	101-215	1-4
%of total S'physin positive structures (Per field view)	100 ± 2.7			1.1 ± 0.1	77.1 ± 4.3	0.98 ± 0.1
% of total VGluT positive structures (Per field view)			100 ± 5.1		97.7 ± 5.5	1.3 ± 0.1
% of total α-Bgt positive structures (Per field view)		100 ± 0.3		82.7 ± .9		72.4 ± 6.9

From these results it is apparent that a small proportion of Alexa-Fluor® 488 α-Bgt binding is associated with non-glutamatergic structures (12 out of 44 Alexa-Fluor® 488 α-Bgt labels). Of these 12, only 4 Alexa-Fluor® 488 α-Bgt labels are associated

with synaptophysin positive structures indicating that α7 nAChR may also reside on non-glutamatergic terminals. The remainder of Alexa-Fluor® 488 α-Bgt labels displayed could be associated with non-presynaptic structures such as post-synaptic membranes of neurons or glial cells but this was not investigated further.

4.2.3 Triple Immunolabelling of rat frontal cortex synaptosomes: Identification of α7 and β2 nAChR

To corroborate the functional evidence described in Chapter 3 (section 3) for non-α7 nAChR mediated release of [^{3}H]D-aspartate (presumably β2* nAChR containing), Percoll™ purified synaptosomes were triple labelled with antibodies to the vesicular glutamate transporters (VGluT; types 1 & 2; secondary label anti-rat 633 blue) anti-β2 nAChR (mAb 270; anti-rat nAChR- secondary label anti-mouse 546 red) and α7 nAChRs, were again visualised using fluorochrome-conjugated α-Bgt (Alexa-Fluor® 488 α-Bgt). Limitation of the confocal microscope prevented the examination of anti-synaptophysin positive labelling, indicative of presynaptic terminals. However, because the majority of anti-VGluT 1 & 2 labels were identified with the presynaptic terminal marker (97.7%; See Fig 4.2 and Table 4.2), this labelling was taken as also indicative of presynaptic terminals.

Notably, Alexa-Fluor® 488 α-Bgt labelling is more prominent in experiments where anti-synaptophysin is not utilised; there is an increase of Alexa-Fluor® 488 α-Bgt labelling (approximately 8 Alexa-Fluor® 488 α-Bgt labels per field view, compare 3 Alexa-Fluor® 488 α-Bgt labels per field view in table 4.2). Approximately 80% of the Alexa-Fluor® 488 α-Bgt binding was associated with anti-VGluT labelling (95 out of

the 118 Alexa-Fluor® 488 α-Bgt labels from 15 field views) representing less than 4% of all VGluT 1 & 2 labelled synaptic terminals.

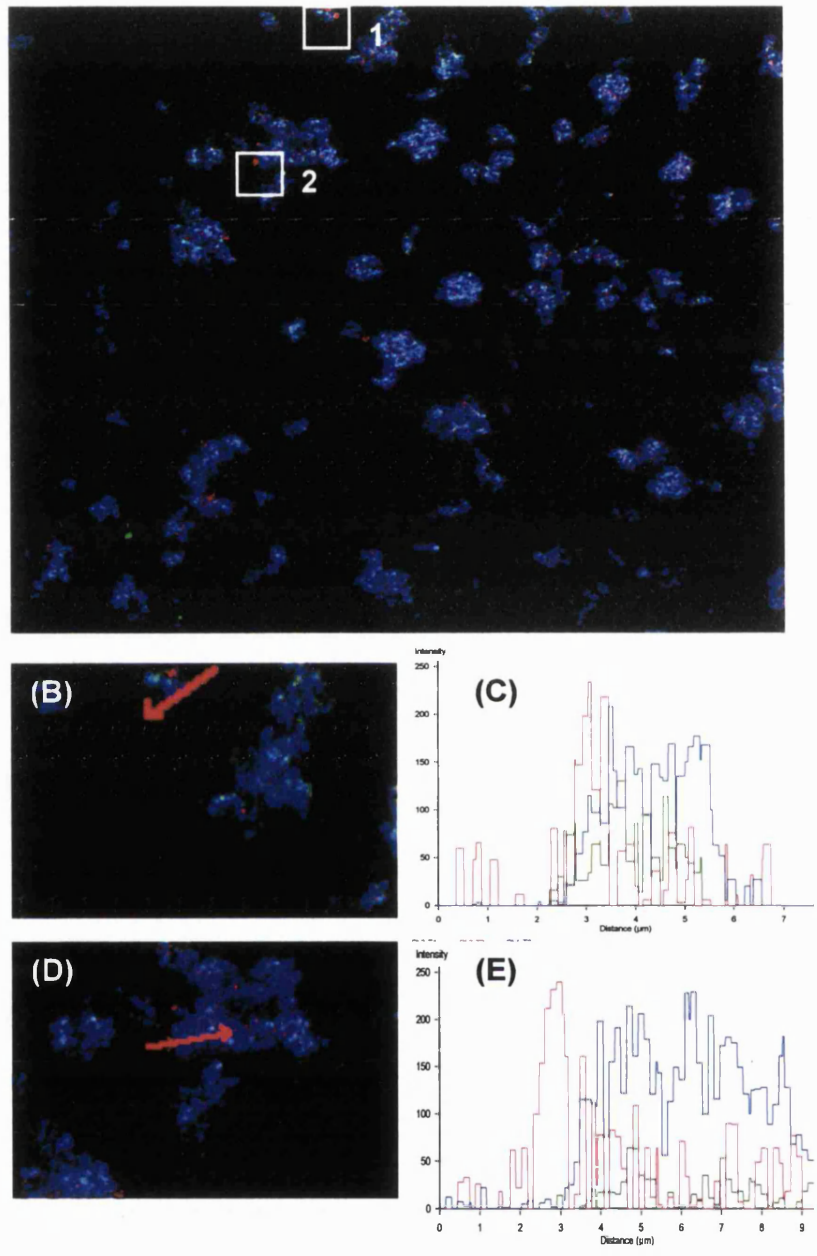

Figure 4.3. Confocal imaging of α-Bgt AlexaFluor 488 and anti-β2 nAChR 546 labelling in rat frontal cortex Percoll™ purified synaptosomes. **(A),** Example confocal image Percoll™ purified synaptosomes triple labelled with α-Bgt (green), anti-β2 nAChR (red) and anti-VGluT 1&2 (Blue). **(B)** x3 zoom image of area highlighted in **(A)** (white square 1) with **(C)** the fluorescence intensity profiling of the β2 nAChR labelling in the area revealing labelling associated with glutamatergic terminals and co-association with Alexa-Fluor® 488 α-Bgt. **(D)** x3 zoom image of area highlighted in **(A)** (white square 2) with **(E)** the fluorescence intensity profiling of the β2 nAChR labelling in the area revealing labelling is associated with glutamatergic terminals.

Table 4.3. Quantitative analysis of presynaptic terminal immunolabelling with anti-β2 nAChR, Alexa-Fluor® 488 α-Bgt and VGluT 1 and 2 in rat frontal cortex Percoll™ purified synaptosomes. Values given are the Mean (± S.E.M where indicated) of positive immunolabelled structures per field view under the confocal microscope. Results are accumulated from an average of five field views from three independent experiments, 15 field views in total. (+VE = positive)

	vGlut1 & 2 +VE	α-Bgt +VE	β2 nAChR +VE	vGlut1 & 2 β2 nAChR +VE	vGlut1 & 2 α-Bgt +VE	vGlut1 & 2 β2 nAChR α-Bgt +VE
Total number of positive structures (from 15 field views)	**2895**	**118**	**65**	**45**	**95**	**10**
Average number of positive structures (Per field view)	**193 ± 6.7**	**7.9± 0.9**	**4.3 ± 0.5**	**3 ± 0.4**	**6.3± 0.7**	**0.7± 0.2**
Range of +VE structures (from 15 field views)	**139-239**	**3-14**	**1-7**	**1-6**	**2-11**	**1-3**
% of total VGluT 1 & 2 positive structures (Per field view)	**100**	-	-	**1.6 ± 0.2**	**3.3 ± 0.1**	**0.3 ± 0.02**
% of total α-Bgt positive structures (Per field view)	-	**100**	-	-	**80.5 ± 2.5**	**8.5 ± 1.4**
% of total β2 nAChR positive structures (Per field view)	-	-	**100**	**69.2 ± 1.9**	-	**15.3 ± 0.8**

Approximately 9% of the Alexa-Fluor® 488 α-Bgt binding was also co-associated with VGluT 1 & 2 and β2 nAChR labelling. The remaining 11% of Alexa-Fluor® 488 α-Bgt was either co-associated with β2 nAChR labelling alone (6%) or found on its own with no co-association (5%).

β2 nAChR labelling was identified with an average of 4 β2 nAChR immunolabels per field view. Almost 70% of this labelling was associated with anti-VGluT 1 & 2 labelling, representing less than 2% of all VGluT 1 & 2-labelled synaptic terminals. A further 15% of this β2 nAChR binding was co-associated with VGluT 1 & 2 and Alexa-Fluor® 488 α-Bgt labelling indicating that two different nAChR receptors may

reside on the same terminal. The remaining 15% of β2 nAChR binding was either associated with Alexa-Fluor® 488 α-Bgt fluorescence (11%) alone with no co-association with anti-VGluT 1 & 2, or found on its own with no co-association with any other label (4%).

4.3 Immunocytochemical labelling of rat frontal cortex sections

4.3.1 Triple Immunolabelling in rat frontal cortex sections: Identification of α7 nAChR

Detergent permeabilised sections of rat frontal cortex were immunolabelled for VGluT 1 & 2 and NeuN. α7 nAChRs were again visualised using fluorochrome-conjugated α-Bgt (Alexa-Fluor® 488 α-Bgt). This allows the assessment of α7 nAChR association with glutamatergic terminals and cell bodies respectively. Both Alexa-Fluor® 488 α-Bgt (green) and Alexa-Fluor® 546 α-Bgt (red) were assessed for their ability to label α7 nAChR in rat frontal sections that were either co-labelled with anti-NeuN (secondary 546 red) and VGlut1 and 2 (Secondary 633 blue) or anti-NeuN (secondary 488 green) and VGlut1 and 2 (Secondary 633 blue) respectively (see Fig 4.4). Both approaches to immunolabelling gave similar results. Sections were initially analysed under the confocal microscope by selection of α-Bgt positive field views. On obtaining α-Bgt positive field views, images were recorded and assessed using the fluorescence intensity software provided with the confocal microscope.

Fluorescence intensity profile lines were used to delineate α-Bgt (either Alexa-Fluor® 488 α-Bgt (green) or Alexa-Fluor® 546 α-Bgt (red)) and its association with any other immunolabels, either anti-NeuN or anti-VGlut1 & 2 or both. Association of α-Bgt fluorescence with either anti-NeuN or anti-VGlut1 & 2 or both (indicative of

α7nAChR association with either cell bodies or glutamatergic terminals respectively) was taken when fluorescence intensity (arbitrary units) of each of the labels was 100% above baseline fluorescence for each of the labels and within 1μm of each other.

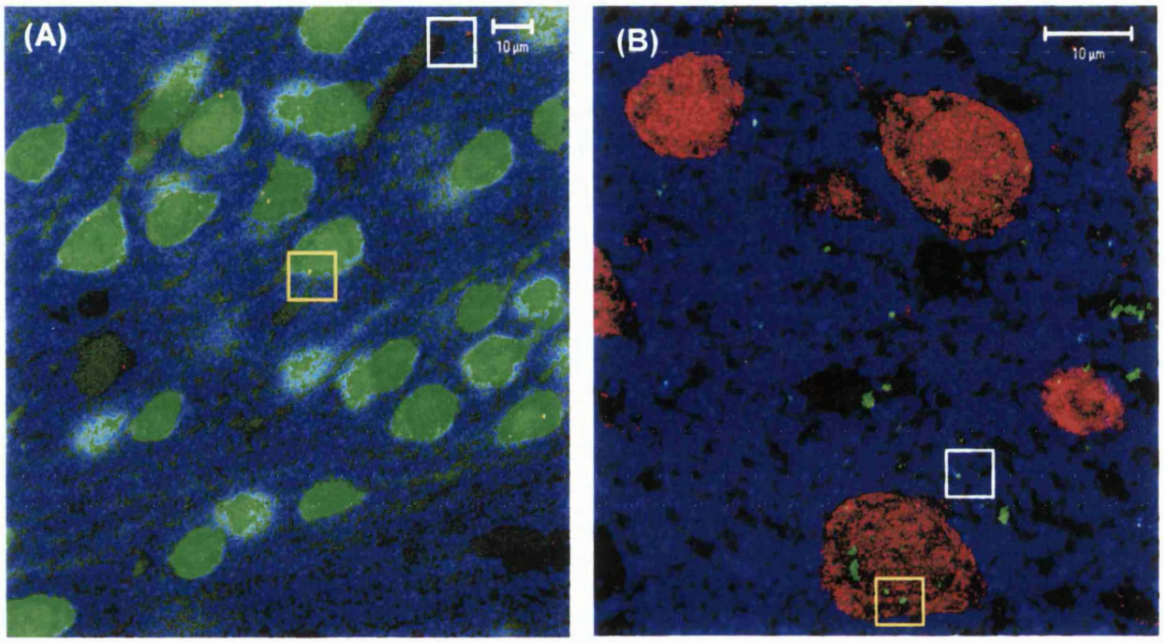

Figure 4.4. Comparison of confocal imaging of α-Bgt AlexaFluor® 488 or 546, anti-Neun and anti-vGluT1 and 2 labelling in rat frontal cortex sections. Example confocal image field view of frontal cortex section triple labelled with α-Bgt AlexaFluor 546 (red) anti-Neun (green) and anti-VGluT 1 and 2 (Blue) **(A)**. Example confocal image field view of frontal cortex section triple labelled with α-Bgt AlexaFluor 488 (green), anti-Neun (red) and anti-VGluT 1 and 2 (Blue) **(B)**. α-Bgt fluorescence can be seen in glutamatergic terminal fields (white square) or cell bodies (yellow square) of rat frontal cortex sections using both immunolabelling methods.

Alexa-Fluor® 488 α-Bgt labelling in frontal cortex sections was observed in the terminal fields as labelled by anti-VGluT 1 & 2 antibodies as well as in association with neuronal cell bodies labelled with anti-NeuN. A small proportion of Alexa-Fluor® 488 α-Bgt binding (less than 11 %; 11 out of a total 103 Alexa-Fluor® 488 α-Bgt binding sites) was observed in the absence of either VGluT 1 & 2 or Neun labelling,

indicating that α7 nAChR associates with non-glutamatergic terminals or non-neuronal cell bodies.

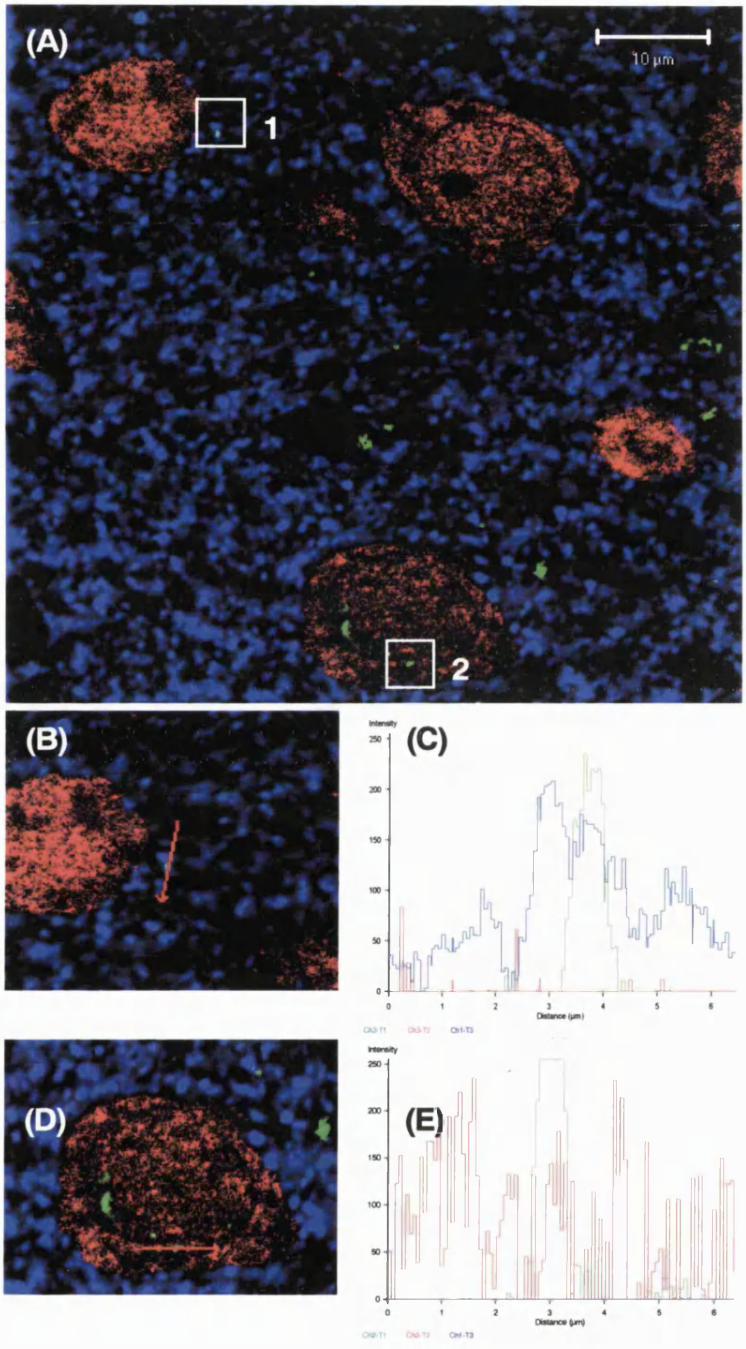

Figure 4.5. Confocal imaging of α-Bgt AlexaFluor 488, anti-Neun and anti-vGluT1 and 2 labelling in rat frontal cortex sections. Example confocal image field view of frontal cortex section triple labelled with α-Bgt AlexaFluor 488 (green), anti-Neun (red) and anti-VGluT 1 and 2 (Blue) **(A).** (**B)** x3 zoom image of area highlighted in **(A)** (white square 1) with **(C)** the fluorescence intensity profiling of the Alexa-Fluor® 488 α-Bgt labelling in the area revealing co-association with VGluT 1 and 2 (glutamatergic terminals). **(D)** x3 zoom image of area highlighted in **(A)** (white square 2) with **(E)** the fluorescence intensity profiling of the Alexa-Fluor® 488 α-Bgt labelling in the area revealing co-association with Neun (cell bodies).

The largest population of Alexa-Fluor® 488 α-Bgt binding was observed in the glutamatergic terminal fields of rat frontal cortex sections (44.6%; 46 out of a total 103 Alexa-Fluor® 488 α-Bgt binding sites) with a further 20% associated with both glutamatergic terminals and neuronal cell bodies (20.4%; 22 out of a total 103 Alexa-Fluor® 488 α-Bgt binding sites). As previously mentioned it is not possible to discriminate at the resolution of the confocal microscope whether these Alexa-Fluor® 488 α-Bgt binding sites are singly associated with glutamatergic terminals or with the neuronal cell body and therefore have been classed as associated with both. Approximately 25% of the total Alexa-Fluor® 488 α-Bgt binding sites were associated with cell bodies alone (25.2%; 28 out of a total 103 Alexa-Fluor® 488 α-Bgt binding sites).

Table 4.4. Field View quantitative analysis of frontal cortex section immunolabelling with anti-Neun, Alexa-Fluor® 488 α-Bgt and VGluT 1 & 2 in rat frontal cortex sections. Values given are the Mean ± S.E.M of positive immunolabelled structures per field view under the confocal microscope. Results are accumulated from an average of five field views from three independent experiments. (+VE = positive)

	Association of α-Bgt binding with other immunolabels				
	Cell body association	**Terminal field association**	**Cell body and terminal field association**	**No association**	**Total**
α-Bgt positive binding (from 15 field views)	28	47	22	11	**103**
Average α-Bgt positive binding (Per field view)	1.8 ± 0.2	3.1 ±0.3	1.4 ± 0.09	0.7 ±0.01	**7 ± 0.9**
Range of α-Bgt +VE structures (from 15 field views)	1-4	1-5	1-4	0-3	**3-12**
% of total α-Bgt (Per field view)	**25.2 ± 2.4**	**44.6 ± 3.9**	**20.4 ± 4.1**	**10.6 ± 1.2**	**100%**

In these instances the Alexa-Fluor® 488 α-Bgt binding sites were either inside the neuronal cell body or within close proximity to the outer perimeter of the neuronal cell body membrane.

4.3.2 Triple Immunolabelling in rat frontal cortex sections: Identification of α7 nAChR and β2 nAChR

In order to assess the presence of α7 nAChR and β2 nAChR in rat frontal cortex, coronal sections were triple labelled for Alexa-Fluor® 488 α-Bgt, anti-β2 nAChR and anti-VGluT 1 & 2. By labelling for two nAChR receptors it became methodologically impossible to also immunolabel for cell bodies due to the limitations of the confocal microscope; it was decided that by omitting neuronal cell body labelling, more information could be obtained with respect to examining the presence of both the α7 and β2 nAChR together in the frontal cortex, since the confocal microscope cannot discriminate between the pre or postsynaptic labelling of the nAChR anyway.

Therefore in this instance the two nAChRs being examined can only be clearly assessed for the co-association with glutamatergic terminals. As shown in Fig 4.6 it is clear from the dark spaces displayed within the field views where neuronal cell bodies or glial cells might be. In many cases the Alexa-Fluor® 488 α-Bgt and anti-β2 nAChR labelling surround the perimeter of these spaces. Those labels that are found in these areas and are not co-associated with the anti-VGluT 1 & 2 labels have been grouped into 'non-glutamatergic structure co-associations' (non-VGluT 1& 2 associated), as described in Table 4.5. However, more importantly, those nAChRs labelled for either Alexa-Fluor® 488 α-Bgt or anti-β2 nAChR that are associated with VGluT 1 and 2 labels could also be associated with neuronal cell bodies or glial cell membranes, as seen with the α7nAChR labelling described in section 4.2.3. Therefore caution must be taken in the interpretation.

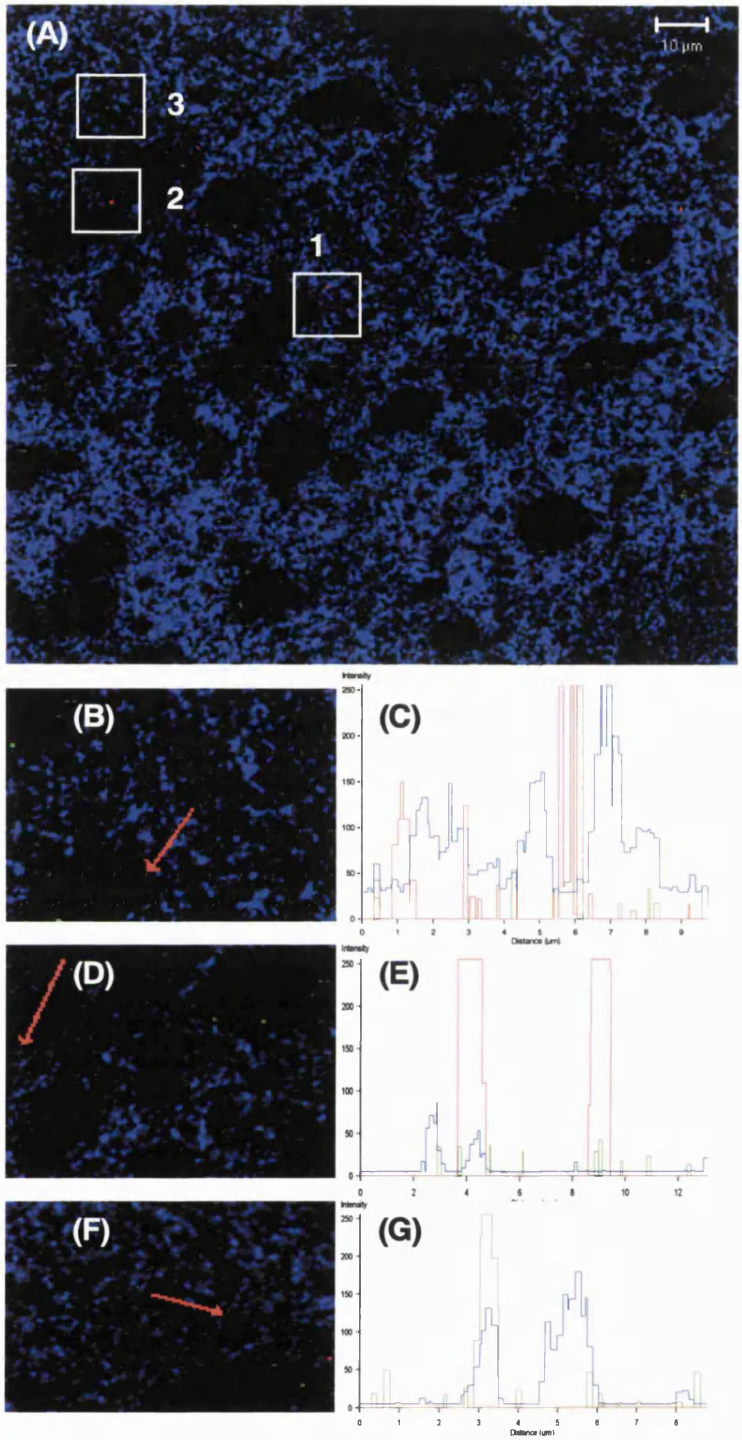

Figure 4.6. Confocal imaging of α-Bgt AlexaFluor 488, anti-β2 nAChR and anti-vGluT1 and 2 labelling in rat frontal cortex section. Example confocal image field view of frontal cortex coronal section triple labelled with α-Bgt AlexaFluor 488 (green), anti-β2 nAChR (red) and anti-VGluT 1 & 2 (Blue) **(A)**. **(B)** x3 zoom image of area highlighted in **(A)** (white square 1) with **(C)** the fluorescence intensity profiling of the anti-β2 nAChR labelling in the area revealing co-association with VGluT 1 and 2 (glutamatergic terminals). **(D)** x3 zoom image of area highlighted in **(A)** (white square 2) with **(E)** the fluorescence intensity profiling of the anti-β2 nAChR labelling in the area revealing no co-association with VGluT 1 & 2. **(F)** x3 zoom image of area highlighted in **(A)** (white square 3) with **(G)** the fluorescence intensity profiling of the α-Bgt AlexaFluor 488 labelling in the area revealing co-association with VGluT 1 and 2

Table 4.5. Field View quantitative analysis of frontal cortex section immunolabelling with Alexa-Fluor® 488 α-Bgt, anti-β2 nAChR and VGluT 1 and 2 in rat frontal cortex sections. Values given are the Mean ± S.E.M of positive immunolabelled structures per field view under the confocal microscope. Results are accumulated from an average of five field views from three independent experiments. (+VE = postiVE)

	Association of α-Bgt and anti β2 nAChR binding with VGluT 1& 2 in rat frontal cortex sections		
	VGluT 1 + 2 associated	**Non-VGluT 1 & 2 associated**	**Totals**
α-Bgt positive binding (from 15 field views)	76	76	**152**
Average α-Bgt positive binding (Per field view)	5.1	5.1	**10.2**
Range of α-Bgt +VE structures (from 15 field views)	3-11	3-8	**5-18**
% of total α-Bgt (Per field view)	**50**	**50**	**100**
Anti-β2 nAChR positive binding (from 15 field views)	53	73	**126**
Average Anti-β2 nAChR positive binding (Per field view)	4.9	3.5	**8.4**
Range of Anti-β2 nAChR +VE structures (from 15 field views)	2-9	0-8	**4-15**
% of total Anti-β2 (Per field view)	**58.3**	**41.7**	**100**

Again, fluorescence intensity profile lines were used to delineate α-Bgt (either Alexa-Fluor® 488 (green) and anti-β2 nAChR (red) and its association with anti-VGluT 1 & 2. This co-association was taken when fluorescence intensity (arbitrary units) of each of the labels was 100% above baseline fluorescence for each of the labels and within 1μm of each other. Equal proportions of Alexa-Fluor® 488 α-Bgt binding was found in co-association with VGluT 1 & 2 structures or on its own (see Table 4.5).

The majority of Alexa-Fluor® 488 α-Bgt observed in co-association with anti-VGluT 1 & 2 antibodies was found in the terminal fields of frontal cortex sections as well as around the perimeter of dark spaces that likely represent either neuronal cell bodies or glial cells. The Alexa-Fluor 488 α-Bgt found with no co-association with anti-VGluT 1 & 2 was found either around the perimeter of dark spaces or in the centre of these dark spaces. With respect to the anti-β2 nAChR binding, approximately 60% was associated with VGluT 1 & 2 structures, similarly found in either the terminal fields or around the perimeter of dark spaces that likely represent neuronal cell bodies or glial cells. The remaining 40% of anti-β2 nAChR binding was found on its own, either around the perimeter of dark spaces that may represent neuronal cell bodies or glial cells, or within the central regions of the dark spaces, perhaps indicating an intracellular localisation of the subunit.

Interestingly, in frontal cortex sections, no co-association was observed for Alexa-Fluor® 488 α-Bgt and anti-β2 nAChR together, in contrast to that described in a small number of observations in the Percoll™ purified synaptosome preparation.

4.3.3 Preliminary investigation into α-Bgt labelling and regional localisation in the rat frontal cortex

The location of α–Bgt labelling within the frontal cortex was assessed in both coronal and sagital rat frontal cortex sections. Rat frontal cortex coronal sections were triple labelled for cell bodies (anti-NeuN), glutamatergic terminals (anti-VGluT1 & 2) and α7 nAChR (either Alexa-Fluor® 488 or 546 α-Bgt). Frontal cortex sections were cut in 30 um sections between

Table 4.6. Number of α-Bgt binding sites in layers I-VI of a rat frontal cortex coronal section. Rat frontal cortex coronal sections were triple labelled for identification of neuronal cell bodies, glutamatergic terminals and α7 nAChR. Along a defined axis (see figure XX), α-Bgt binding sites were counted from three field views per layer of the frontal cortex section (n=3 individual experiments). Results are expressed as the total number of α-Bgt binding sites counted in each of the field views per layer of the frontal cortex and also as Mean ± S.E.M of the average number of α-Bgt binding sites per field view within each layer.

	Frontal cortex layers					
	I	II	III	IV	V	VI
Total number of α-Bgt binding sites (Taken from 9 field views per layer)	37	23	6	1	22	34
Average number of α-Bgt binding sites (per field view of each layer)	4.1 ± 0.4	2.6 ± 0.5	0.7 ± 0.2	0.1 ± 0.1	2.4 ± 0.3	3.8 ± 0.4

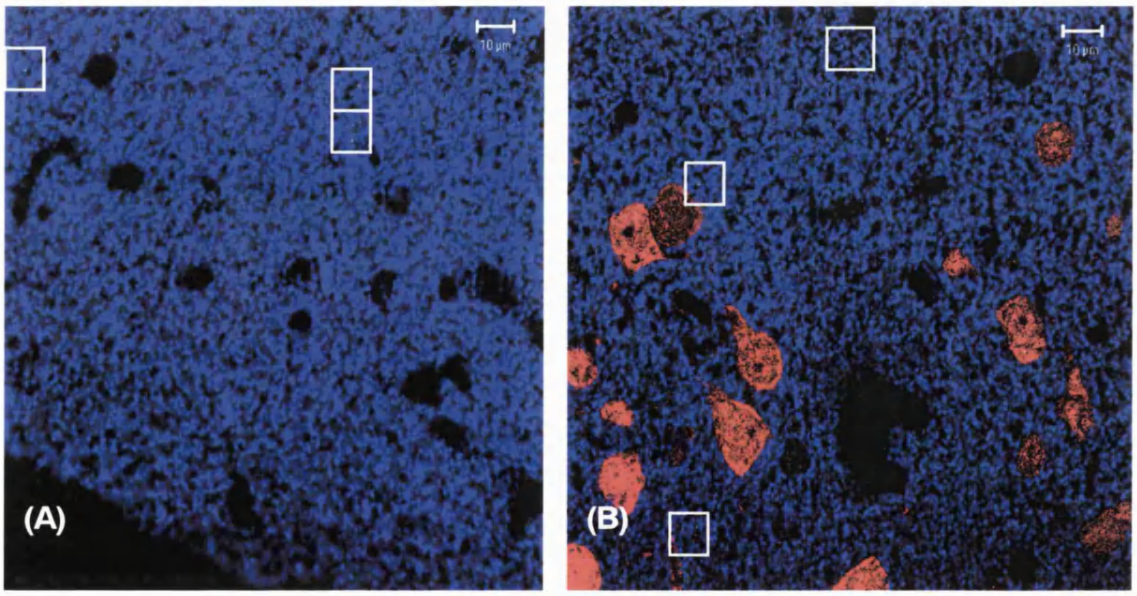

Figure 4.7. Confocal imaging of α-Bgt AlexaFluor 488, anti-NeuN and anti-vGluT1 and 2 labelling in rat frontal cortex coronal sections. Example field view confocal image of layer I from a rat frontal cortex coronal section triple labelled with α-Bgt AlexaFluor 488 (green), anti-NeuN (red) and anti-VGluT 1 and 2 (Blue) **(A).** Example field view confocal image of layer VI (and part of layer V) from a rat frontal cortex coronal section also triple labelled with α-Bgt AlexaFluor 488 (green), anti-NeuN (red) and anti-VGluT 1 and 2 (Blue) **(B).** White squares within field view images (A) and (B) highlight the presence of fluorescent α-Bgt binding.

approximate 2.0 and 3.0 Bregma. Along a defined axis (from the dorsal-lateral region of the coronal section to the midpoint of the medial-ventral axis), these sections were then assessed for Alexa-Fluor® 488 α-Bgt binding by examination of three individual field views for each layer (Layers I through to VI) of the frontal cortex section.

α-Bgt binding sites were consistently found in Layers I and II and layers V and VI (average of 3 or 4 Alexa-Fluor® 488 α-Bgt binding sites per field view in each of these layers; see Fig 4.7) whereas layers III and IV displayed almost negligible α-Bgt binding (average of less than 1 α-Bgt binding site per field view; See Table 4.6).

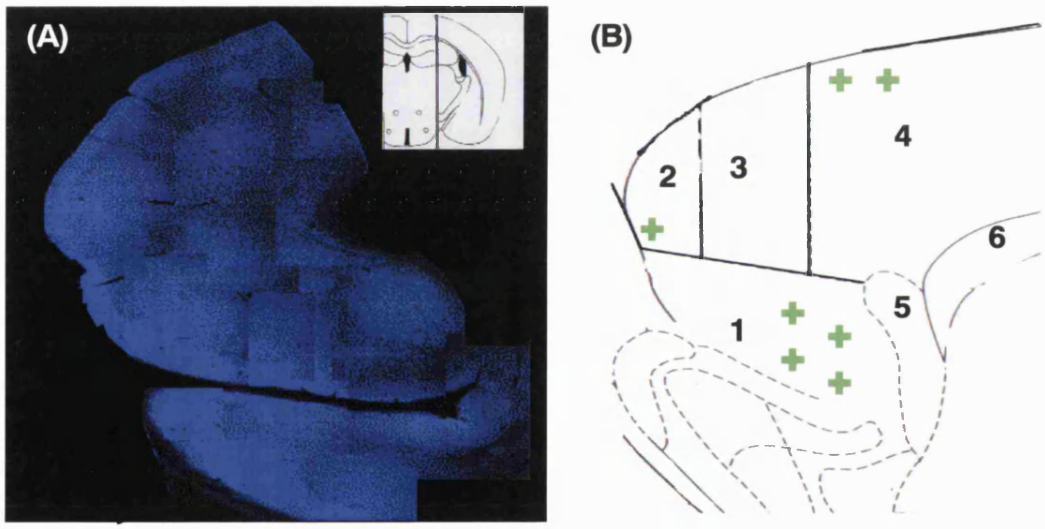

Figure 4.8. Mid-sagital section of rat frontal cortex. Low power magnification (x10) of mid sagital section (approximate Bregma 1-1.5; see insert) triple labelled for α-Bgt AlexaFluor 488 (green), anti-NeuN (red) and anti-VGluT 1 and 2 (Blue) **(A)**. Rat frontal cortex map (Bregma 1.3) illustrating brain regions: 1-Lateral orbital cortex. 2-Frontal association cortex. 3-Secondary motor cortex. 4-Primary motor cortex. 5-forceps minor corpus callosum. 6-Striatum. + denotes approximate areas of the frontal cortex where 5 or more α-Bgt binding sites are found per field view in that area. n=2 independent experiments.

Mid-sagital sections (30nm sections taken between Bregma 1-1.5; see insert Fig 4.8 A) of rat frontal cortex were triple labelled for cell bodies (anti-NeuN), glutamatergic terminals (anti-VGluT1 and 2) and α7 nAChR (either Alexa-Fluor® 488 or 546 α-

Bgt). The sequential analysis of each field view from a whole mid-sagital section revealed that in certain regions of the sagital section, α-Bgt binding was more prominent than others (typically 5 or more Alexa-Fluor® 488 or 546 α-Bgt binding sites per field view) These areas included the rostral-ventral regions of the frontal association cortex, the caudal-ventral regions of the lateral orbital cortex and the rostral-dorsal regions of the primary motor cortex (See Fig 4.8 B).

Regions of the mid-sagital section outside of those areas described above were relatively devoid of α-Bgt binding sites, typically presenting either 0 or a maximum of 2 binding sites per field view. The results represented in Fig 4.8 show only the regions of the mid-sagital section where a large density of α-Bgt binding sites are present.

In those regions of the sagital section where α-Bgt binding was most prominent, α-Bgt binding was increased in the Layers I, II, V and VI, compared to the intermediate layers, as described for coronal sections above.

4.4 Discussion

Immunolabelled rat frontal cortex Percoll™ purified synaptosomes were examined to determine the association of α7 nAChR (identified by labelling with fluorescent labelled α-Bgt; Alexa-Fluor 488 α-Bgt) or β2 nAChR (identified by immunolabelling with anti-β2 nAChR antibody, mAb 270) with glutamatergic terminals, in support of functional the data described in Chapter 3 (sections 2 and 3), where these subunit containing receptors appear to modulate the release of [^{3}H]D-aspartate.

.

4.4.1 α7 nAChR association with glutamatergic terminals

Of the two synaptosome preparations initially used to investigate the association of nAChR with presynaptic terminals, Percoll™ purified synaptosomes, demonstrated a substantially lower degree of non-specific membrane elements labelled with anti-synaptophysin compared to P2 purified synaptosomes. These non-specific membrane elements could represent a number of membrane structures from presynaptic membranes that have failed to re-seal to form a 'closed' synaptic terminal (i.e. a synaptosome) to axonal or postsynaptic membrane elements. Anti-synaptophysin labelling in Percoll™ purified synaptosomes were more homogenous in shape, with the majority of the synaptophysin labelled structures displaying a 'spherical' like shape indicative of a synaptosome, in agreement with the EM observations of Dunkley *et al.* (1988).

When these synaptosomes were double labelled for identification of synaptophysin protein and α-Bgt binding receptors (i.e. α7 nAChR) approximately 2% of the total number of synaptophysin positive structures were labelled for α-Bgt. The same percentage of synaptosomes with α-Bgt bound per field view was observed when synaptosomes were triple labelled with markers for glutamatergic terminals (anti-VGluT1 & 2). The majority of synaptosomes (80%) were labelled for VGlut1 & 2, suggesting that this preparation of synaptosomes from the frontal cortex of rat brain is high in glutamatergic terminals, conversely, almost all VGluT 1 & 2 labelled structures were co-labelled with anti-synaptophysin. Observations made by Dunkley *et al.* (1986) and (1988) using cerebral cortex synaptosomes, and Robinson & Lovenberg. (1986) using striatal synaptosomes, proposed that fractions 3 and 4 of the Percoll™ purified gradient are generally enriched with serotonergic and dopaminergic synaptosomes respectively. These authors did not provide any

evidence for glutamatergic identity in the synaptosomes used, perhaps due to lack of specific tools, and it therefore remains an interesting observation that such a large majority of synaptosomes labelled in this study with anti-synaptophysin also co-label for VGluT1 and 2, raising the question of whether presynaptic terminals contain and release multiple neurotransmitters or that the morphology/density of glutamatergic terminals specifically, is highly favourable for their acquisition from the particular layers of the Percoll™ gradients.

Almost 100% of the α-Bgt fluorescence coincided with VGlut1 & 2 fluorescence in the triple label assessment, indicating that all α7 nAChRs identified in a frontal cortex synaptosome preparation co-localise within the vicinity of glutamatergic terminals. As mentioned in the Introduction (Section 4.1.2), the interpretation that these results are indicative of α7 nAChR residing on glutamatergic terminals has to be exercised with caution. It has been described that synaptosomes (review; Whittaker, 1993), obtained from Percoll™ purification, have elements of the post-synaptic terminal membrane bound to their surface membrane that it made contact with in the intact synapse, prior to homogenisation. It is therefore possible that α-Bgt nAChR could bind to these post-synaptic membranes that are attached to the synaptosome. However as mentioned previously, this cannot be resolved at the level of the confocal microscope and would require EM analysis. In support of a presynaptic association for the nAChR identified herein, synaptosomes prepared in a similar manner as described in this section (Diaz-Hernandez *et al.,* 2002), showed no evidence for labelling with a post synaptic membrane protein PSD-95, demonstrating the absence post synaptic density contamination in the synaptic terminal preparation.

4.4.2 β2 nAChR association with glutamatergic terminals

AlexaFluor 488 α-Bgt was also included with the labelling of frontal cortex synaptosomes during the assessment of anti-β2 nAChR labelling. This was carried out on the basis from previous findings that almost 100% of anti-VGluT 1 & 2 labelling in Percoll purified synaptosomes is in co-association with anti-synaptophysin labelling, therefore anti-synaptophysin could be omitted and replaced with anti-β2 nAChR (mAb 270). This allowed for the examination of both α7 nAChR and β2* nAChR in the same preparation and provides supportive evidence for the functional superfusion experiments described in chapter 3 section 3, where the nAChR pharmacology is consistent with the presence of at least two nAChR subtypes in frontal cortex synaptosomes.

Examination of β2 nAChR labelling of frontal cortex synaptosomes demonstrated analogous findings to that described for α7 nAChR labelling, that is, the majority of β2 nAChR labelling (approximately 70%) was in co-association with VGluT 1 & 2 labelling, indicative of co-association with glutamatergic terminals and therefore in support of the functional data described in chapter 3 section 3, as well as the electrophysiological evidence described by Gioanni *et al,* (1999) and Lambe *et al,* (2003). The same proportions of AlexaFluor-488 α-Bgt labels were identified with anti-VGluT 1 & 2 labelling as previously described (see sections 4.2.2), however the presence of α-Bgt binding per field view was almost twice that of anti-β2 nAChR (see Table 4.3) and twice that described in sections 4.2.2, where α-Bgt was incorporated with the anti-synaptophysin and anti-VGluT 1 & 2 immunolabels. For the former observation it appears that the α7 nAChR is the predominant nAChR associated with glutamatergic terminals over β2* nAChR in the frontal cortex and

also supports the notion that this nAChR is associated with glutamatergic transmission. The reasons for the latter are unknown; the use of 'multi-tracking' (see Chapter 2 section 2.7.3) should prevent the incidence of fluorochrome 'crosstalk' and therefore enable sequential identification of each fluorochrome, it is therefore unlikely that the presence of anti-synaptophysin and its attached secondary label fluorochrome would prevent the identification of AlexaFluor 488 α-Bgt binding. Other plausible reasons are perhaps an increase in the efficiency of the experiment over time and repeat experiments that improve the binding and identification of AlexaFluor 488 α-Bgt.

The most interesting observation from the examination of both α–Bgt and mAb270 immunolabelling within the same synaptosome preparation was that a proportion of the VGluT 1 & 2 labelling (0.3% per field view; see Table 4.3) was found in co-association with both AlexaFluor 488 α-Bgt and anti-β2 nAChR binding. This triple co-association (two receptors and glutamatergic terminal labels) represented 15 and 9 % of the total β2 and α7 nAChR labelling respectively (gathered from the fifteen field views used for analysis; Table 4.2 and 4.3). Two possible explanations for this finding are: (1) More than one nAChR subtype at the glutamatergic terminal or (2) the nAChR at the glutamatergic terminal binds both α-Bgt and anti-β2 nAChR antibody (i.e. is made up of both α7 and β2 nAChR subunits). With respect to the first possibility, the resolution of the confocal microscope limits the assessment of the pre or postsynaptic location of the two different nAChR labels, therefore it is not possible to ascertain at this level whether the triple label described is either representative of two different nAChR attached to the presynaptic membrane of a glutamatergic terminal or attached to postsynaptic elements that remain in contact with the synaptosome membrane from the homogenisation procedures. Another

possibility is that one of each of the labels for α7 and β2 nAChR are on each of the two synaptic membrane components (pre and post). Electron microscopy analysis may provide a clearer definition of the pre or post-synaptic location of the nAChR labelling to discriminate between different types of nAChR using different sized metal particles attached to either ligands or antibodies specific to the nAChR. Secondly, a very interesting possibility is that perhaps the two nAChR labels used actually label one individual nAChR that contains both α7 and β2 nAChR subunits (i.e. α7β2* nAChR). In fact, α7 and β2 nAChR subunits have been heterologously co-expressed in Xenopus oocytes to form a functional nAChR (Khiroug *et al.*, 2002), distinguished from homomeric α7 nAChR on the basis that native nAChRs that contain the α7 subunit in rat hippocampal interneurons express functional properties that differ from observed properties of recombinant homomeric α7 nAChRs (Shao & Yakel, 2000; Sudweeks & Yakel, 2000). This has been a consistent observation even from early electrophysiological studies that first examined the presence of α7 nAChR in the hippocampus (Gray *et al.*, 1996) and to present date an α7β2 heteromeric nAChR has been put forward as a novel subtype of nAChR found in cholinergic cell groups that project to the hippocampus and cortex that are associated with the regulation of cognitive processes (Azam *et al.*, 2003). However, the one underlying report in contrast to these possibilities is that only α7 nAChR subunits compose the α7 nAChR, determined using Western blot analysis of α-Bgt binding proteins from purified rat brains (Chen & Patrick, 1997).

4.4.3 α7* and β2* nAChR in rat frontal cortex sections

Where identified, AlexaFluor 488 (or 546 α-Bgt) and anti-β2 nAChR labels were associated with glutamatergic terminals (as labelled for using anti-VGluT 1 & 2) in

the terminal fields of rat frontal cortex sections as well as around the perimeter of neuronal cell bodies. As mentioned before, the exact location of the latter nAChR labelling cannot be ascribed definitively to a pre or postsynaptic location due to the resolution limitations of the confocal microscope.

With respect to AlexaFluor 488 (or 546) α-Bgt binding, the two types of α-Bgt binding with glutamatergic terminal associations (with or without cell body association) combined make up the majority of α-Bgt binding (60%) in rat frontal cortex sections. This binding supports either the presence of α7 nAChR on glutamatergic terminals, as demonstrated with the α-Bgt binding found in association with frontal cortex synaptosomes labelled for VGluT 1 & 2 or α7 nAChR on either glutamatergic terminals that are located in close proximity to the cell membrane or indeed on the cell membrane itself that is in close proximity to a glutamatergic terminal. The remaining 40% identified was either found in association with cell bodies alone (30%) or found on its own (10%). The first of these two observations could represent the internalisation of α-Bgt binding sites within cell bodies, an observation which has been previously described for immunogold labelled α-Bgt binding inside the pre and postsynaptic membranes of neurons of the stratum radiatum of the CA1 area of the rat hippocampus (Fabien-Fine *et al.*, 2001) and in the rat sensory cortex (Levy & Aoki, 2002). These authors report that this type of 'internalisation' of the receptor may represent α-Bgt binding receptors that are localised to vesicles inside the pre and post synaptic terminals, which allow for the efficient cycling and dynamic regulation of α7 nAChRs to their respective membrane surface, consistent with the role of mediating and/or modulating synaptic transmission. For the latter type of binding, where fluorescent α-Bgt binding was found on its own, is slightly harder to define. Efforts are made to ensure complete

washing of sections to prevent non-specific α-Bgt binding, as well as the fact that α-Bgt is completely absent when sections are pre-incubated with excess α7 antagonists (either α-Bgt or MLA). Most, if not all of this type of fluorescent α-Bgt binding was localised within the vicinity of 'dark spaces' that may represent astyrocytes or blood vessels, but as described in the results this represents the smallest proportion of α-Bgt binding in rat frontal cortex sections (See Sharma & Vijayaraghavan, (2002), for review of nAChR expression and function in non-excitable cells in the CNS). It is also possible that this α-Bgt binding may represent association with non-glutamatergic terminals, such as terminals from GABAergic interneurons, demonstrated in the rat hippocampus (Fabien-Fine *et al.*, 2001) but as of yet not in the rat frontal cortex, which does display immunoreactivity for GABAergic interneurons (Retaux *et al.*, 1993).

Anti-β2 nAChR labelling was found in association with glutamatergic terminals in similar proportions to that described for fluorescent α-Bgt labelling (approximately 60%). Of this 60% it is unknown what proportion are also in association with cell bodies as markers for cell bodies (anti-NeuN) was not utilised in this investigation; fluorescent α-Bgt labelling was also incorporated into the assessment, thereby limiting the number of available fluorochromes available to detect using the confocal microscope system. Nonetheless, anti-β2 nAChR labelling was found either in the terminal fields or in and around the perimeter of dark spaces that presumably represent cell bodies (or astrocytes and blood vessels). The remaining 40% of anti-β2 nAChR labelling was found in areas with no co-association with glutamatergic terminals, nor α-Bgt labelling, the latter only being observed in frontal cortex synaptosomes labelled for both α7 and β2 nAChR. This non-glutamatergic anti-β2

nAChR labelling could again represent the similar findings demonstrated for fluorescent α-Bgt labelling, where anti-β2 nAChR labels 'internalised' nAChR; in many cases anti-β2 nAChR binding was found inside the 'dark spaces' representative of internalisation or in close proximity to the perimeter of these spaces but in sufficient distance away from any anti-VGluT 1 & 2 labelling that appears to terminate on the cell body. The fluorescent α-Bgt labelling carried out within these experiments mirrored the observations displayed in previous experiments in terms of its localisation (i.e. in both the glutamatergic terminal fields and in and around the perimeters of the dark spaces that presumably represent neuronal or glial cells). Its incorporation into these experiments that also co-label for β2 nAChR was hoped to reveal co-expression of the two receptors within the vicinity of each other, as exemplified in a small proportion of labelled synaptosomes (see above) therefore implying that in an intact synaptic circuit, the two different nAChR may have similar or supportive roles in glutamatergic transmission at the same synapse. Unfortunately, this was not demonstrated in frontal cortex sections. This may be a consequence of steric hindrance factors exhibited in labelling fixed sections with the labels used; the large molecular weight of α-Bgt and anti-β2 nAChR antibody may prevent a second immunolabel, (or fluorescent ligand) to bind within close proximity of the other. This may not be a limiting factor in dissociated synaptosomes.

4.4.4 Regional localisation of α7 nAChR in rat frontal cortex sections

Rat frontal cortex sections were assessed for fluorescent α-Bgt binding in specific regions of coronal and mid-sagital sections. In agreement with autoradiographical analysis of the rat frontal cortex using [^{125}I]α-Bgt (Clarke *et al.*, 1985), fluorescent α-

Bgt was found in the majority of the superficial layers I and II and the deeper layers V and VI along a defined axis (see results Fig 4.7), the principal input and output layers respectively to this area of the rat brain (Groenewegen, 1988). The localisation of α7 nAChR in these regions is consistent with the recording of nicotine or ACh-induced glutamate release demonstrated in electrophysiological preparations examining these areas (Vidal & Changeux, 1993; Gioanni *et al.*, 1999*; Lambe *et al.*, 2003), however these authors fail to report clear α7-like physiology and pharmacology which may represent the difficulties in recording α7-like phenomena, due to fast desensitisation properties of the receptor. (* only Gioanni *et al.*, 1999 report inhibition of mEPSC's induced by nicotine in the presence of MLA (100 nM)). Nonetheless, the cells mediating synaptic transmission in this area are predominantly glutamatergic (e.g. pyramidal cells; See Carr & Cesack, (1996), therefore the presence of α7 nAChR may mediate/modulate glutamatergic transmission in these regional layers at both the presynaptic and postsynaptic level, the former also being supported by the inferences made in chapter 3 section 3.

In the mid-sagital section, α-Bgt binding was diffuse across layers I, II and V and VI in the whole plain, however, there existed certain regions within the plane that displayed more prominent α-Bgt binding (defined in Results section 4.4), namely the rostroventral regions of the frontal association cortex, the caudal-ventral regions of the lateral orbital cortex and the rostrodorsal regions of the primary motor cortex. The source of the glutamatergic innervation to these areas was not examined in this study, but all regions receive prominent afferent input from the mediodorsal thalamic nucleus (MD). The immunocytochemical detection of β2 nAChR in rat frontal cortex sections and synaptosomes supports the presynaptic modulation of glutamate release in this area as recorded in the electrophysiological paradigm (Vidal &

Changeux, 1993; Gioanni *et al.*, 1999; Lambe *et al.,* 2003). These authors provide, in the majority, evidence for a β2* nAChR modulation of release, however, the α7 nAChR modulation of release is not completely ruled out (See Gioanni *et al.*, 1999). mRNA transcripts for the α7 subunit are relatively low in the thalamus (Seguela *et al.*, 1993) and therefore it is plausible that the thalamocortical terminals originating from the medial dorsal thalamus do not bind α–Bgt in the frontal cortex (Gioanni *et al.*, 1999). In contrast the hippocampus and parahippocampal regions express high levels of α7 mRNA transcript (Seguela *et al.,* 1993) and these regions have been shown to send afferent projections to the frontal cortex (Theirry et al., 2000; Delatour & Witter, 2002). A detailed study by Delatour & Witter (2002) who employ anterograde-tracing methods demonstrate that projections from parahippocampal regions of the rat brain were found to terminate in regions of the frontal cortex analogous to the regions where α-Bgt labelling is described in our study (in particular the frontal association and lateral orbital cortex areas). Thierry *et al*, (2000), in a review of the hippocampal-frontal cortex pathways, describe prominent innervation of prelimbic/medial orbital areas (corresponding to frontal cortex association areas and lateral orbital areas displayed in Fig 4.8) that originate from the CA1/subiculum fields. By deduction, it is therefore possible that the α7 nAChRs found on the glutamatergic terminals in the frontal cortex may originate from the hippocampal and parahippocampal regions of the brain. It therefore appears from these initial observations that the presence of α7 nAChR at these specific locations is an integral component of those systems that adjoin for efficient execution of attention and memory.

4.4.5 Conclusions

The identification of α7 and β2 immunolabelling found within the vicinity of glutamatergic terminals in both synaptosomes and sections supports the nAChR-enhancement of glutamatergic transmission in the rat frontal cortex.

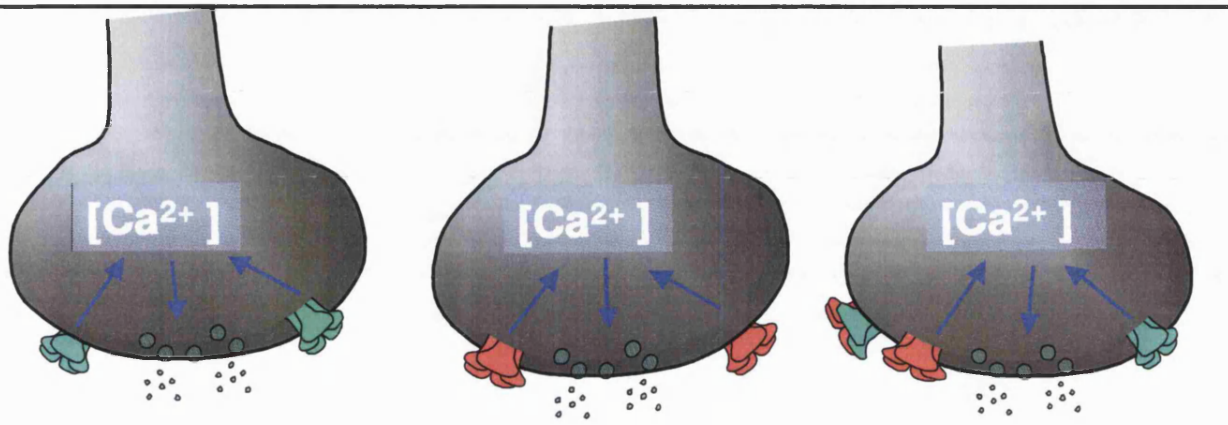

α7 nAChR	β2 nAChR	α7 nAChR & β2 nAChR
Detected by AlexaFluor 488 (or 546) α-Bgt	Detected by mAb270 (anti- β2 nAChR) and secondary labelled with anti-rat 546 IgG	Detected by AlexaFluor 488 (or 546) α-Bgt and mAb270 (anti-β2 nAChR) secondary labelled with anti-rat 546 IgG respectively
Found in approximately 2% of glutamatergic terminals per field of frontal cortex synaptosomes	Found in approximately 2% of glutamatergic terminals per field of frontal cortex synaptosomes	Found co-localised in approximately less than 0.5% of glutamatergic terminals per field of frontal cortex synaptosomes
Hippocampal-cortical afferents?	Thalamocortical afferents?	Unknown

Figure 4.9 Summary diagram and table of the immunocytochemical analysis of frontal cortex synaptosomes. All possible locations of nAChR subtypes co-associated with glutamatergic terminals from immunocytochemical analysis; (A) α7 nAChR detected using fluorescent α-Bgt, (B) β2* nAChR detected using mAb270 and (C) α7 and β2* nAChR using both probes. Diagram (C) also depicts the possible existence of a α7β2* heteromeric nAChR as postulated from the co-localisation of both probes.

The location of α7 and β2 nAChR in the terminal fields of the rat frontal cortex is consistent with a role in facilitating EAA release, as demonstrated from the release of [^{3}H]D-aspartate evoked from frontal cortex P2 synaptosomes using nAChR agonists in this thesis as well as from electrophysiological observations (Vidal & Changeux, 1993; Gioanni *et al*., 1999; Lambe *et al*., 2003).

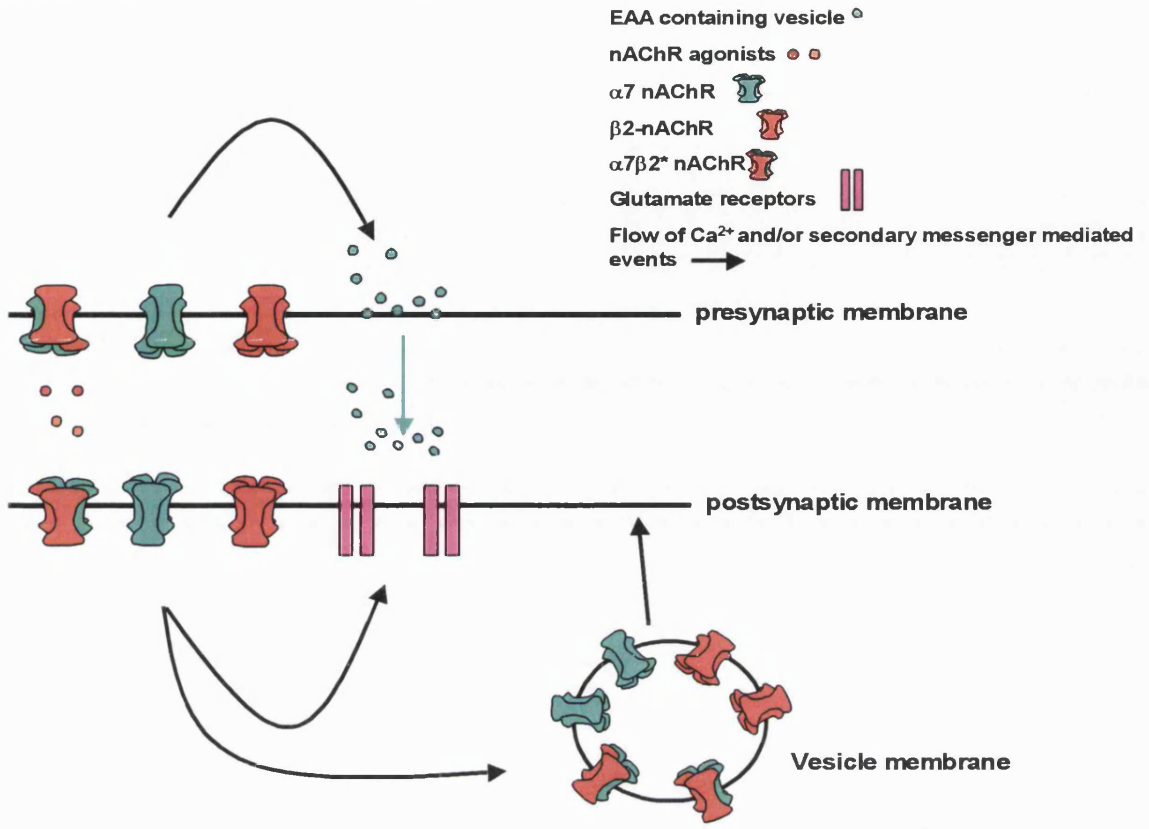

Figure 4.10 Hypothetical diagram of nAChR location and its integration with excitatory neurotransmission. α7 nAChR and β2 nAChR (and possibly α7β2* nAChR) are co-localised with glutamatergic terminals and postsynaptic cell membranes. Evidence also exists for an 'internalised' source of nAChR that may be bound to intracellular vesicles for their insertion into the postsynaptic membrane. nAChR activation is also coupled with AMPA activity and the exact relationship, via investigation of calcium and secondary messenger-mediated events is currently being defined. The presence of both pre and postsynaptic membrane nAChR may be an important criterion for the nAChR modulation of excitatory neurotransmission.

The exact location of nAChRs found in association with glutamatergic terminals and cell bodies is not clear from our immunocytochemical analysis and therefore requires electron microscopy to ascertain their exact location, as deciphered from investigations in the rat hippocampus and sensory cortex (Fabien-fine *et al.*, 2001; Levy & Aoki, 2002). Nonetheless, in accordance with the original hypothesis put forward by Gray *et al.* (1996), both the presence of pre and post-synaptic nAChRs may increase synaptic efficacy of glutamatergic connections as described in the

hippocampus (Gray *et al.*, (1996), Dani *et al.*, 2001; McGehee, 2002; Sharma & Vijayaraghavan, 2003). The exact secondary messenger systems and calcium mediated events that improve synaptic efficacy are still the subject of debate; it is presently understood that the up-regulation of AMPA receptors, via the integration of both calcium and secondary messenger mediated events, to the postsynaptic membrane are crucial for the strengthening of synaptic communication in excitatory synapses (for review see Isaac, 2003). nAChR activation combined with co-activation of AMPA receptors may indeed work together to mediate post-synaptic excitation (Levy & Aoki, 2002; Alkondon *et al.*, 2003). Further to these interactions, nAChR activation, during heightened cholinergic activity, may up-regulate its own expression via insertion of vesicles containing nAChR constructs to the pre or postsynaptic membrane, hinted at from the existence of nAChR labelling defined inside cellular membranes (section 4.3.2 & 4.4.3. see Fabien-Fine *et al.*, 2001).

In summary, this chapter, in particular, has raised a number of undefined issues with respect to nAChR function in the frontal cortex and hence serves as a platform for a number of future studies, namely: (1) determination of the origination of glutamatergic afferents containing nAChR in the frontal cortex (hippocampal afferents and/or thalamocortical afferents), (2) an anatomical assessment of the cholinergic pathways that may serve these projections, (3) precise definition of pre and postsynaptic location of nAChR using electron microscopy, (4) immunocytochemical analysis of cell types (GABAergic etc) that express nAChR in the frontal cortex, (5) exploration of other intracellular events that may regulate nAChR expression in and out of the cell membrane in accordance with heightened

cholinergic and glutamatergic activity and (6) determination of the possible existence of an $\alpha 7\beta 2^*$ heteromer.

Chapter 5

5.1 Summary, Conclusions and Future Perspectives

5.1.1 Summary of the nAChR and modulation of EAA release

Over a number of decades it has emerged that the cholinergic system serves as the major constituent for the execution of cognitive functions such as attention, learning and memory, manifested by the loss of cholinergic-cortical projections common theme to a number of neurological disorders in which cognition is compromised (for review see Sarter et al., 2003).

Because nAChRs mediate cholinergic activity in the form of their activation by ACh and exogenous ligands such as nicotine, nicotinic therapy could serve as a treatment strategy for cognitive disorders in the future. However, the development of future compounds for such a treatment strategy relies on the broad integration of studies that examine nAChR structure, function, and location within the CNS. One of the most interesting facets to nAChR research is the finding that activation of nAChRs can evoke the release of a number of neurotransmitters, including glutamate. Glutamate serves as the major excitatory amino acid in the CNS, and its controlled release and uptake is essential for synaptic efficacy. It is therefore likely that the loss of nAChR function, subsequent to the loss of cholinergic innervation in particular cognitive disorders, is one, of a number of factors, which may affect synaptic efficacy in the form of glutamatergic transmission between synapses. The resultant inefficiency of information flow through the CNS would then culminate in poor execution of tasks that require attention, learning and memory processes.

Indeed the stimulation of nAChR in synaptic circuits of hippocampal slices and cultured neurones, as well as in circuits of midbrain areas, has displayed an increased synaptic efficacy (See Introduction Section 1.7.3), where the modulation of glutamate release from the presynaptic terminal is considered as a contributing factor (For review see McGehee, 2002). These particular inferences have been

made from electrophysiological based experiments and have provided intricate detail of the nAChR modulation of excitatory and inhibitory currents dependant on where the recording and stimulating probes are placed. However, the means of inferring presynaptic modulation of EAA release in electrophysiological investigations are indirect (by recording excitatory currents on postsynaptic neurons) and until now, no direct means of inferring nAChR modulation of EAA release has been described.

Therefore the work presented in this thesis represents the gross response of superfused presynaptic terminals (synaptosomes) from the rat frontal cortex, a region of the brain heavily implicated with cognitive functions such as working memory, but with regard to nAChR function and location has been minimally explored (see Chapter 1). Synaptosomes were pre-loaded with radiolabelled D-aspartate and subjected to stimulation with nAChR agonists. Superfusion per se prevents any possible interference of the nAChR-mediated event by continually removing any other neurotransmitter-receptor auto-regulatory events that may affect EAA release. Second to this, superfusion is particularly advantageous for the examination of EAA release in that, if set at a high flow rate, will prevent the re-uptake of EAA by the highly efficient membrane glutamate transporters, without the need of EAAT blockers.

[^{3}H]D-aspartate was utilised as the preferred choice of EAA analogue in place of glutamate with regard to its limited involvement in other cellular metabolic activities, thereby increasing the available 'neurotransmitter pool' available for release and detection (see Chapter 3 Section 3.1.2). In the first results chapter (Chapter 3 Section 1) we provide evidence in support of the use of [^{3}H]D-aspartate as an analogue for glutamate by revealing both exocytotic and glutamate transporter reversal mechanisms of KCl-evoked release of [^{3}H]D-aspartate from presynaptic

terminals, analogous to that described in previous investigations examining endogenous glutamate release.

Previous attempts to measure the direct detection of nAChR-evoked EAA release have only been recognised when nAChR agonists are combined with a depolarising stimulus (Beani *et al.*, 2000; Marchi *et al.*, 2002). We emulated these findings in Chapter 3 Section 2, by providing evidence of nAChR enhancement of KCl-evoked [^{3}H]D-aspartate release from synaptosomes and nAChR enhancement of electrical-evoked release of [^{3}H]D-aspartate from frontal cortex minces. The results from this chapter demonstrate that the nAChR enhancement of depolarisation-evoked release was Ca^{2+}-dependant and sensitive to mecamylamine. However, only the nAChR enhancement of electrical-evoked release of [^{3}H]D-aspartate displayed sensitivity to α7 nAChR selective antagonists, implying that the pharmacological detection of specific nAChR subtypes may be affected by the type and degree of depolarisation, as well as the effect of synaptic communication i.e. minces versus synaptosomes and the possibility that certain nAChR subtypes may be desensitised. The experimental assessment of nAChR enhancement of depolarisation-evoked release of [^{3}H]D-aspartate was subject to persistent variability and consequently was not explored any further. At the same time, evidence was accumulating in our studies for the release of [^{3}H]D-aspartate evoked by nAChR agonists alone, and subsequently the work in this thesis was directed towards the pharmacological characterisation of this response (Chapter 3 Section 3).

nAChR-evoked release of [^{3}H]D-aspartate from synaptosomes (Chapter 3 Section 3) was Ca^{2+}-dependant, reflecting an exocytotic mechanism of release, but independent of glutamate transporter reversal, in contrast to KCl-evoked release. Pharmacological characterisation of the nAChR-evoked release demonstrated a

broad concentration dependency by a number of nAChR agonists. This inferred that possibly more than one nAChR subtype was associated with EAA release; made evident from differences of α-Bgt blockade (α7 nAChR specific) on low and high concentrations of nAChR agonist-evoked release. This possibility was pharmacologically defined using nAChR specific agonists and antagonists which revealed that both the α7 and β2* containing nAChR mediate the release of EAA from presynaptic terminals of the frontal cortex (See Chapter 3 Section 3.3.2.2).

The second body of direct evidence for presynaptic association with EAA release was inferred from our immunocytochemical investigation of rat frontal cortex synaptosomes. Using fluorescent α-Bgt probes and/or secondary labelled antibodies to the β2 nAChR subunit (mAb270), both α7 nAChR and β2* containing nAChR were found co-localised with glutamatergic terminals (identified by the antibodies directed towards vesicular glutamate transporters). This labelling represented approximately less than 2% of all glutamatergic synaptosomes per field view of the confocal microscope for each nAChR (See Chapter 4 Section 4.2). Although of very small proportion, evidence also existed for the presence of α7 and β2* nAChR co-localised together on glutamatergic terminals; this could infer the existence of more than one nAChR subtype on the same glutamatergic terminal or even the possible existence of a native α7β2* heteromer, however only electron microscopy would confirm this interpretation due to the limitations of the confocal microscope resolution.

Rat frontal cortex sections (both coronal and sagital), displayed labelling for α7 and β2* nAChR using the same probes as for the synaptosome investigation. Both labels were found in association with cell membranes and in glutamatergic terminal fields, but for the former, a precise pre or postsynaptic location could not be defined, again

due to resolution limitations. Interestingly we observed the presence of α7 and β2* labelling inside cells, near to the membrane, corroborative with electron microscopy reports of nAChR found within cells of the hippocampus and rat sensory cortex (Fabien-Fine et al., 2001; Levy & Aoki, 2002). These authors report that this type of 'internalisation' of the receptor may represent nAChRs that are localised to vesicles inside the pre and post synaptic terminals, which may allow for the efficient cycling and dynamic regulation of nAChRs to their respective membrane surface, consistent with the role of mediating and/or modulating synaptic transmission.

With respect to the regional distribution of α7 nAChR in the different layers of the frontal cortex, we demonstrated that both superficial and deeper layers of the frontal cortex (layers I, II and V, VI) are prominently labelled for α7 nAChR compared to intermediate layers, consistent with autoradiographical experiments using radiolabelled α-Bgt (Clarke *et al.*, 1985). In particular, when mid sagital sections of rat frontal cortex were analysed there appeared to be α7 nAChR 'hotspots' which displayed slightly higher levels of α-Bgt fluorescence than in other regions within the same layer of the frontal cortex. Although not experimentally assessed in the chapter, it is inferred from distribution studies of glutamatergic projections to the frontal cortex, that these α7 nAChRs may reside on glutamatergic terminals originating from hippocampal regions of the rat CNS (See Chapter 4 section 4.4.4).

5.1.2 Future perspectives

By direct examination, this thesis has demonstrated certain aspects of nAChR function and subtype specificity in the rat frontal cortex. This work has supported particular elements of previous electrophysiological findings of nAChR modulation of glutamate release in this region, but has also furthered our understanding by

revealing the existence of multiple nAChR subtypes associated with excitatory amino acid release as well as their regional and cellular distribution. However, as a result of the inferences made from this thesis there are a number of specific questions that remain unanswered and would benefit from further experimentation. With respect to understanding the role nAChRs play in cognitive processes of the frontal cortex, those experiments that are relevant are outlined below.

- **Determining specific nAChR subtypes mediating EAA release in the frontal cortex**

Although this thesis ascertained that both α7 and β2* containing nAChR modulate the release of [^{3}H]D-aspartate, the full subunit composition of these nAChRs was not ascertained. Presently, α-Bgt serves as the most specific tool for identifying homomeric α7 nAChRs in expression systems. Yet in native preparations, such as hippocampal slices, there are consistent (yet subtle) indications that although α7 nAChR responses are blocked by α-Bgt, certain aspects of α7 nAChR function (such as desensitisation times and recovery times) do not coorelate with those displayed by homomeric α7 nAChR (Shao & Yakel, 2000; Sudweeks & Yakel, 2000) and therefore indicate the possible existence of a native heteromeric α7* containing nAChR. Heteromeric α7β2* nAChRs have been expressed in Xenopus oocytes and although the effects of α7 specific antagonists were not demonstrated, these receptors did demonstrate altered kinetic responses to choline compared to homomeric α7 nAChRs (Khiroug *et al.*, 2002).

Pharmacological definition of the β2* containing nAChR modulating EAA release was determined in this thesis using the novel β2 selective agonist 5-IA-85380, in

which release evoked by this agonist was completely blocked by DHβE; an α4β2* preferring antagonist, depending on the concentration used (Chavez-Noreiga *et al.*, 1997). Other nAChR ligands, such as Conotoxins from the marine snail of the genus Conus, display specificity for β2* containing nAChR that also contain other nAChR subunits, but have only been implicated in nAChR modulation of other neurotransmitters (see Mogg *et al.*, 2002). It remains to be determined if these toxins inhibit the release of [^{3}H]D-aspartate from rat frontal cortex synaptosomes and therefore provide more detail to the full subunit composition of nAChR mediating EAA release.

Both the expansion of the nicotinic pharmacopoeia and the expression of specific nAChR subunit combinations in expression systems (to ascertain ligand specificity) will help define the nAChR specificity of function in native systems. Over the past 50 years of nicotinic research this effort has been a slow and arduous task, exampled by the development of only a handful of nAChR subtype specific pharmacological tools. However, one particular facet of nAChR drug design is the emergence of nAChR 'potentiator' ligands, nAChR specific tools that appear to potentiate the action of nAChR agonists by altering kinetic properties of the receptor.

An alternative option to drug design is the ability to induce specific nAChR subunit gene mutations or specific nAChR subunit knockouts in experimental animals. By comparison of altered functional responses to nAChR agonists or antagonists in mutant and wild-type animals this approach may provide useful information regarding the subunit composition of native nAChR in the specific regions of the brain examined. Similar to drug design efforts, this would be a difficult and time consuming process, further complicated by possible nAChR subunit compensatory mechanisms that exist to replace lost nAChR subunit expression.

- **nAChR and calcium**

It has been recently made evident that the α7 nAChR-evoked presynaptic release of glutamate from presynaptic terminals innervating the CA3 region of the hippocampus relies heavily on the mobilisation of calcium from internal stores via a calcium-induced-calcium release (CICR) mechanism (Sharma & Vijaraghvan, 2003; see also Dajas-Bailador *et al.*, 2002 for nAChR association with VOCC and CICR in SH-SY5Y cells). As described in Chapter 1 Section 1.5, nAChRs, in particular α7 nAChR, are permeable to calcium and this may serve as the source of calcium mediating CICR. However, at present no evidence exists for the co-operation of nAChR with specific calcium channels in the modulation of EAA release (see Gray *et al.*, 1996), although with respect to nAChR modulation of dopamine release, an association between nAChR and non-L-type calcium channels has been described (Soliakov *et al.*, 1996). It is likely that nAChR activation may increase the presynaptic membrane potential sufficiently to activate VOCC's and therefore further augment the influx of calcium into the presynaptic terminal to evoke the release of EAA. To examine this, the present superfusion system utilised in this thesis should be of sufficient means to explore the effect of nAChR-agonist evoked release of [^{3}H]D-aspartate release from synaptosomes in the presence of calcium channel inhibitors as well as assess the contribution of internal calcium stores using ryanodine and $InsP_3$ receptor blockers.

- **Anatomical studies of nAChR distribution**

Although the results presented in Chapter 4 support the presence of α7 and β2* nAChR on glutamatergic terminals and cell bodies of the rat frontal cortex, a number of questions, outside the scope of this thesis, remain unanswered (See Chapter 4 Section 4.4.5 for overall summary of future perspectives in this area of nAChR research). In particular, the anatomical origination of glutamatergic afferents terminating in the frontal cortex is only inferred from the literature, but strong evidence supports the possibility that the difference in distribution of α7 and β2* nAChRs may be the result of glutamatergic afferents (expressing specific nAChR subtypes) originating from different areas of the rat CNS (See Chapter 4 Section 4.4.4). Retrograde-tracer labelling experiments could provide the means to answer these questions; injection of fluorescent labelled retrograde tracer beads into specific regions of the frontal cortex where either α7 or β2* nAChR have been identified should reveal the cell bodies to which glutamatergic afferents originate from. It may even be possible to ascertain specific differences of nAChR subunit expression between the cells that are identified from retrograde-tracer labelling via single cell PCR experiments.

Other future perspectives for nAChR distribution experiments include electron microscopy studies that can reveal the specific location of nAChR subunits at pre and postsynaptic loci in the frontal cortex. Electron microscopy analysis of α7 nAChR distribution has recently been aided by the development of gold-labelled α-Bgt, intricately detailing the presence of pre and postsynaptic α7 nAChR in the rat VTA and dorsal striatum (see I Jones, J Barik, MJ O'Neill and S Wonnacott. in preparation) and therefore the use of this tool could be extended to future studies of the frontal cortex.

- **Development of high-throughput assays for nAChR modulation of EAA release?**

The superfusion methodology used in this thesis certainly provides a direct and more expedient means of ascertaining presynaptic release of EAA evoked by nAChR than the indirect means employed by electrophysiological experiments. By increasing the number of chambers in standard superfusion systems, the ability to assess more conditions per experiment can be utilised. However, the number of conditions (and replicates of) can be exploited even further with the recent development of a 96 well plate-based superfusion system. 96 well-filtered plates have been utilised to demonstrate the nAChR modulation of noradrenaline release from a number of brain regions that show comparable results to standard superfusion systems (Anderson *et al.*, 2000). It remains to be determined if this assay can be employed for the detection of nAChR modulation of EAA release.

Chapter 6

6.1 References

Adler LE and Waldo MC (1991) Counterpoint: a sensory gating--hippocampal model of schizophrenia. Schizophr Bull 17: 19-24

Adler LE, Olincy A, Waldo M, Harris JG, Griffith J, Stevens K, Flach K, Nagamoto, H, Bickford, P, Leonard S and Freedman R (1998) Schizophrenia, sensory gating, and nicotinic receptors. Schizophr Bull 24: 189-202

Akaaboune M, Grady RM, Turney S, Sanes JR and Lichtman JW (2002) Neurotransmitter receptor dynamics studied in vivo by reversible photo-unbinding of fluorescent ligands. Neuron 34: 865-876

Akabas MH, Kaufmann C, Archdeacon P and Karlin A. (1994). Identification of acetylcholine receptor channel-lining residues in the entire M2 segment of the alpha subunit. Neuron 13: 919-927

Albuquerque EX, Alkondon M, Pereira EF, Castro NG, Schrattenholz A, Barbosa CT, Bonfante-Cabarcas R, Aracava Y, Eisenberg HM and Maelicke, A (1997a) Properties of neuronal nicotinic acetylcholine receptors: pharmacological characterization and modulation of synaptic function. J Pharmacol Exp Ther 280: 1117-1136

Albuquerque EX, Pereira EF, Alkondon M, Schrattenholz A and Maelicke A (1997b) Nicotinic acetylcholine receptors on hippocampal neurons: distribution on the neuronal surface and modulation of receptor activity. J Recept Signal Transduct Res 17: 243-266

Alkondon M and Albuquerque EX (1991) Initial characterization of the nicotinic acetylcholine receptors in rat hippocampal neurons. J Recept Res 11: 1001-1021

Alkondon M and Albuquerque E X (1993) Diversity of nicotinic acetylcholine receptors in rat hippocampal neurons. I. Pharmacological and functional evidence for distinct structural subtypes. J Pharmacol Exp Ther 265: 1455-1473

Alkondon M and Albuquerque EX. (1994) Presence of α-bungarotoxin-sensitive nicotinic acetylcholine receptors in rat olfactory bulb neurons. Neurosci Lett 176: 152-156

Alkondon M and Albuquerque E X (2001) Nicotinic acetylcholine receptor alpha7 and alpha4beta2 subtypes differentially control GABAergic input to CA1 neurons in rat hippocampus. J Neurophysiol 86: 3044-3055

Alkondon M, Reinhardt S, Lobron C, Hermsen B, Maelicke A and Albuquerque EX (1994) Diversity of nicotinic acetylcholine receptors in rat hippocampal neurons. II. The rundown and inward rectification of agonist-elicited whole-cell currents and identification of receptor subunits by in situ hybridization. J Pharmacol Exp Ther 271: 494-506

Alkondon M and Albuquerque EX (1995) Diversity of nicotinic acetylcholine receptors in rat hippocampal neurons. III. Agonist actions of the novel alkaloid epibatidine and analysis of type II current. J Pharmacol Exp Ther 274: 771-782

Alkondon M, Pereira EF and Albuquerque EX (1996a) Mapping the location of functional nicotinic and gamma-aminobutyric acid A receptors on hippocampal neurons. J Pharmacol Exp Ther 279: 1491-1506

Alkondon M, Rocha ES, Maelicke A and Albuquerque EX (1996b). Diversity of nicotinic acetylcholine receptors in rat brain. V. alpha-Bungarotoxin-sensitive nicotinic receptors in olfactory bulb neurons and presynaptic modulation of glutamate release. J Pharmacol Exp Ther 278: 1460-1471

Alkondon M, Pereira EF, Barbosa CT and Albuquerque EX (1997) Neuronal nicotinic acetylcholine receptor activation modulates gamma-aminobutyric acid release from CA1 neurons of rat hippocampal slices. J Pharmacol Exp Ther 283: 1396-1411

Alkondon M, Pereira EF, Eisenberg HM and Albuquerque EX (1999) Choline and selective antagonists identify two subtypes of nicotinic acetylcholine receptors that modulate GABA release from CA1 interneurons in rat hippocampal slices. J Neurosci 19: 2693-2705

Alkondon M, Pereira EF and Albuquerque EX (2003) NMDA and AMPA receptors contribute to the nicotinic cholinergic excitation of CA1 interneurons in the rat hippocampus. J Neurophysiol 90: 1613-1625

Anand R, Bason L, Saedi MS, Gerzanich V, Peng X and Lindstrom J (1993) Reporter epitopes: a novel approach to examine transmembrane topology of integral membrane proteins applied to the α 1 subunit of the nicotinic acetylcholine receptor. Biochemistry 32: 9975-9984

Anand R, Conroy WG, Schoepfer R, Whiting P and Lindstrom J. (1991) Neuronal nicotinic acetylcholine receptors expressed in Xenopus oocytes have a pentameric quaternary structure. J Biol Chem 266: 11192-11198

Anderson CM and Swanson RA (2000) Astrocyte glutamate transport: review of properties, regulation, and physiological functions. Glia 32: 1-14

Anderson DJ, Puttfarcken PS, Jacobs I and Faltynek C (2000) Assessment of nicotinic acetylcholine receptor-mediated release of [^{3}H]-norepinephrine from rat brain slices using a new 96-well format assay. Neuropharmacology 39: 2663-2672

Arqueros L, Abarca J and Bustos G (1985) Release of D-[^{3}H]aspartic acid from the rat striatum. Effect of veratridine-evoked depolarization, fronto-parietal cortex ablation, and striatal lesions with kainic acid. Biochem Pharmacol 34:1217-1224

Azam L, Winzer-Serhan UH, Chen Y and Leslie FM (2002) Expression of neuronal nicotinic acetylcholine receptor subunit mRNAs within midbrain dopamine neurons. J Comp Neurol 444: 260-274

Barrie AP and Nicholls DG (1993) Adenosine A1 receptor inhibition of glutamate exocytosis and protein kinase C-mediated decoupling. J Neurochem 60: 1081-1086

Bartus RT, Dean RL 3rd, Beer B and Lippa AS (1982) The cholinergic hypothesis of geriatric memory dysfunction. Science 217: 408-14.

Beani L, Antonelli T, Tomasini MC, Marani L and Bianchi C (2000) The nicotinic modulation of [^{3}H]D-aspartate outflow in primary cultures of rat neocortical neurons: effect of acute and long term nicotine treatment. Neuropharmacology 39: 2646-2653

Bernarth S (1992) Calcium-independent release of amino acid neurotransmitters: fact or artifact? Prog Neurobiol 38:57-91

Bertrand D, Bertrand S and Ballivet M (1992) Pharmacological properties of the homomeric α7 receptor. Neurosci Lett 146: 87-90

Bertrand D, Glazi JL, Devillers-Thierry, Bertrand S and Changeux JP (1993) Mutations at two distinct sites within the channel domain M2 alter calcium permeability of neuronal α7 nicotinic receptor. Proc Natl Acad Sci U S A 90: 6971-6975

Blanton MP and Cohen JB (1994) Identifying the lipid-protein interface of the Torpedo nicotinic acetylcholine receptor: secondary structure implications. Biochemistry 33: 2859-2872

Bormann J, Flugge G and Fuchs E (1989) Effect of atrial natriuretic factor (ANF) on nicotinic acetylcholine receptor channels in bovine chromaffin cells. Pflugers Arch 414: 11-14

Boulter J, Evans K, Martin G, Mason P, Stengelin S, Goldman D, Heinemann S, and Patrick J (1986) Isolation and sequence of cDNA clones coding for the precursor to the gamma subunit of mouse muscle nicotinic acetylcholine receptor. J Neurosci Res 16: 37-49

Boulter J, O'Shea-Greenfield A, Duvoisin RM, Connolly JG, Wada E, Jensen A, Gardner PD, Ballivet M, Deneris, ES and McKinnon D (1990) α3, alpha 5, and β4: three members of the rat neuronal nicotinic acetylcholine receptor-related gene family form a gene cluster. J Biol Chem 265: 4472-4482

Breese CR, Lee MJ, Adams CE, Sullivan B, Logel J, Gillen KM., Marks MJ, Collins AC and Leonard S (2000) Abnormal regulation of high affinity nicotinic receptors in subjects with schizophrenia. Neuropsychopharmacology 23: 351-364

Brejc K, van Dijk WJ, Klaassen RV, Schuurmans M, van Der Oost, Smit AB and Sixma TK (2001) Crystal structure of an ACh-binding protein reveals the ligand-binding domain of nicotinic receptors. Nature 411: 269-276

Bridges RJ, Stanley MS, Anderson MW, Cotman CW and Chamberlin AR (1991) Conformationally defined neurotransmitter analogues. Selective inhibition of glutamate uptake by one pyrrolidine-2,4-dicarboxylate diastereomer. J.Med.Chem. 34: 717-725

Briggs CA, McKenna DG and Piattoni-Kaplan M (1995) Human α7 nicotinic acetylcholine receptor responses to novel ligands. Neuropharmacology 34: 583-590

Brisson A and Unwin PN (1985) Quaternary structure of the acetylcholine receptor. Nature 315:474-7.

Broide RS, O'Connor LT, Smith MA, Smith JA and Leslie FM (1995) Developmental expression of α7 neuronal nicotinic receptor messenger RNA in rat sensory cortex and thalamus. Neuroscience 67: 83-94

Buckner RL, Kelley WM and Petersen SE (1999) Frontal cortex contributes to human memory formation. Nat Neurosci 2: 311-314

Calabresi P, Picconi B, Saulle E, Centonze D, Hainsworth A and Bernardi G (2000) Is pharmacological neuroprotection dependent on reduced glutamate release? Stroke 31: 766-772

Cartaud J, Benedetti EL, Cohen JB, Meunier JC and Changeux JP (1973) Presence of a lattice structure in membrane fragments rich in nicotinic receptor protein from the electric organ of Torpedo marmorata. FEBS Lett 33: 109-13.

Cartier GE, Yoshikami D, Gray WR, Luo S, Olivera BM and McIntosh JM (1996) A new alpha-conotoxin which targets α3β2 nicotinic acetylcholine receptors. J Biol Chem 271: 7522-7528

Cartmell J. and Schoepp DD (2000) Regulation of neurotransmitter release by metabotropic glutamate receptors. J.Neurochem. 75:889-907

Changeux JP, Kasai M and Lee CY (1970) The use of a snake venom toxin to characterise the cholinergic receptor protein. Proc Natl Acad Sci U S A 67,:1241-1247

Changeux JP and Edelstein SJ (1998) Allosteric receptors after 30 years. Neuron. 21: 959-80

Chavez-Noriega LE, Crona JH, Washburn MS, Urrutia A, Elliott KJ and Johnson EC (1997) Pharmacological characterization of recombinant human neuronal nicotinic acetylcholine receptors h α2 β 2, h α2 β4, h α3 β2, h α3 β4, h α4 β2, h α4 β4 and h α7 expressed in Xenopus oocytes. J Pharmacol Exp Ther 280: 346-356

Chen D and Patrick JW (1997) The α-bungarotoxin-binding nicotinic acetylcholine receptor from rat brain contains only the α7 subunit. J Biol Chem 272: 24024-24029

Chen W, Aoki C, Mahadomrongkul V, Gruber CE, Wang JG, Blitzblau R, Irwin N and Roseberg PA (2002) Expression of a variant form of the glutamate transporter GLT1 in neuronal cultures and in neurons and astrocytes in the rat brain J Neurosci 22:2142-2152

Clarke PB, Pert CB and Pert A (1984) Autoradiographic distribution of nicotine receptors in rat brain. Brain Res 323: 390-395

Clarke PB, Schwartz RD, Paul SM, Pert CB and Pert A (1985) Nicotinic binding in rat brain: autoradiographic comparison of [^{3}H]acetylcholine, [^{3}H]nicotine, and [^{125}I]-α -bungarotoxin. J Neurosci 5: 1307-1315

Clarke PB and Reuben M (1996) Release of [^{3}H]-noradrenaline from rat hippocampal synaptosomes by nicotine: mediation by different nicotinic receptor subtypes from striatal [^{3}H]-dopamine release. Br J Pharmacol 117: 595-606

Cohen BN, Labarca C, Davidson N and Lester HA (1992) Mutations in M2 alter the selectivity of the mouse nicotinic acetylcholine receptor for organic and alkali metal cations. J Gen Physiol 100: 373-400

Collard KJ (1996) On the significance of perfusion rate in the study of glutamate release from superfused synaptosomes. Neurochem.Res. 21: 319-322

Conroy WG and Berg DK (1995) Neurons can maintain multiple classes of nicotinic acetylcholine receptors distinguished by different subunit compositions. J Biol Chem 270: 4424-4431

Corbin J, Methot, N, Wang HH, Baenziger JE and Blanton MP (1998) Secondary structure analysis of individual transmembrane segments of the nicotinic acetylcholine receptor by circular dichroism and Fourier transform infrared spectroscopy. J Biol Chem 273: 771-777

Cordero-Erausquin M and Changeux JP (2001) Tonic nicotinic modulation of serotoninergic transmission in the spinal cord. Proc Natl Acad Sci U S A 98: 2803-2807

Corringer PJ, Le Novere N and Changeux JP (2000) Nicotinic receptors at the amino acid level. Annu Rev Pharmacol Toxicol 40: 431-458

Costa LG and Murphy SD (1983) [^{3}H]-Nicotine binding in rat brain: Alteration after chronic acetylcholinesterase inhibition. J Pharmacol Exp Ther 226: 392-397

Court J and Clementi F (1995) Distribution of nicotinic subtypes in human brain. Alzheimer Dis Assoc Disord 9 Suppl 2, 6-14

Couturier S, Bertrand D, Matter JM, Hernandez MC, Bertrand S, Millar N, Valera S, Barkas T and Ballivet M (1990) A neuronal nicotinic acetylcholine receptor subunit (α7) is developmentally regulated and forms a homo-oligomeric channel blocked by α-BTX. Neuron 5: 847-856

Curro Dossi RPD and Steriade M (1991) Short-lasting nicotinic and long-lasting muscarinic depolarizing responses of thalamocortical neurons to stimulation of mesopontine cholinergic nuclei. J Neurophysiol 65: 393-406

Czajkowski C, Kaufmann C and Karlin A (1993) Negatively charged amino acid residues in the nicotinic receptor delta subunit that contribute to the binding of acetylcholine. Proc Natl Acad Sci U S A 90: 6285-6289

Dajas-Bailador FA, Mogg AJ and Wonnacott S (2002) Intracellular Ca^{2+} signals evoked by stimulation of nicotinic acetylcholine receptors in SH-SY5Y cells: contribution of voltage-operated Ca^{2+} channels and Ca^{2+} stores. J Neurochem 81: 606-614

Dalack GW, Healy DJ and Meador-Woodruff JH (1998) Nicotine dependence in schizophrenia: clinical phenomena and laboratory findings. Am J Psychiatry 155: 1490-1501

Danbolt NC (2001) Glutamate uptake. Prog Neurobiol 65: 1-105

Dani JA (1989) Open channel structure and ion binding sites of the nicotinic acetylcholine receptor channel. J Neurosci 9: 884-892

Dani JA (2000) Properties underlying the influence of nicotinic receptors on neuronal excitability and epilepsy. Epilepsia 41: 1063-1065

Dani JA (2001) Overview of nicotinic receptors and their roles in the central nervous system. Biol Psychiatry 49: 166-174

Dani JA and De Biasi M (2001) Cellular mechanisms of nicotine addiction. Pharmacol Biochem Behav 70: 439-446

Dani JA, Ji D and Zhou FM (2001) Synaptic plasticity and nicotine addiction. Neuron 31: 349-352

Davies AR, Hardick DJ, Blagbrough IS, Potter BV, Wolstenholme AJ and Wonnacott S (1999) Characterisation of the binding of [^{3}H]methyllycaconitine: a new radioligand for labelling α7-type neuronal nicotinic acetylcholine receptors. Neuropharmacology 38: 679-690

Delatour B and Witter MP (2002) Projections from the parahippocampal region to the prefrontal cortex in the rat: evidence of multiple pathways Eur J Neurosci 15: 1400-1207

Delbono O, Gopalakrishnan M, Renganathan M, Monteggia LM, Messi ML and Sullivan JP (1997) Activation of the recombinant human α7 nicotinic acetylcholine receptor significantly raises intracellular free calcium. J Pharmacol Exp Ther 280: 428-438

Deneris ES, Connolly J, Boulter J, Wada E, Wada K, Swanson LW, Patrick, J and Heinemann S (1988) Primary structure and expression of β2: a novel subunit of neuronal nicotinic acetylcholine receptors. Neuron 1: 45-54

Deneris ES, Boulter J, Connolly J, Wada E, Wada K, Goldman D, Swanson, L W, Patrick J, and Heinemann S (1989) Genes encoding neuronal nicotinic acetylcholine receptors. Clin Chem 35: 731-737

Deneris ES, Connolly J., Rogers SW, and Duvoisin R (1991) Pharmacological and functional diversity of neuronal nicotinic acetylcholine receptors. Trends Pharmacol Sci 12: 34-40

Descarries L, Gisiger V and Steriade M (1997) Diffuse transmission by acetylcholine in the CNS. Prog in Neurobiol 53: 603-625.

D'Aniello G, Tolino A, D'Aniello A, Errico F, Fisher GH and Di Fiore MM (2000) The role of D-aspartic acid and N-Methyl-D-aspartic acid in the regulation of prolaction release. Endocrinology 141: 3862-3870

Diaz-Hernandez M, Pintor J, Castro E, and Miras-Portugal MT (2002) Co-localisation of functional nicotinic and ionotropic nucleotide receptors in isolated cholinergic synaptic terminals. Neuropharmacology 42:20-33

Dingledine R, Borges K, Bowie D and Traynelis SF (1999) The glutamate receptor ion channels. Pharmacol Rev 51: 7-61

Dominguez del Toro, Juiz JM, Peng X, Lindstrom J, and Criado, M (1994) Immunocytochemical localization of the α7 subunit of the nicotinic acetylcholine receptor in the rat central nervous system. J Comp Neurol 349: 325-342

Dougherty JJ, Wu J and Nichols RA (2003) β-amyloid regulation of presynaptic nicotinic receptors in rat hippocampus and neocortex. J Neurosci 23: 6740-6747

Drejer J, Larsson OM and Schousboe A (1983) Characterization of uptake and release processes for D- and L-aspartate in primary cultures of astrocytes and cerebellar granule cells. Neurochem Res 8: 231-243

Dunkley PR, Heath JW, Harrison SM, Jarvie PE, Glenfield PJ and Rostas JA (1988) A rapid Percoll gradient procedure for the isolation of synaptosomes directely from an S1 fraction: homogeneity and morphology of subcellular fractions. Brain Res 441: 59-71

Dunlop J, Grieve A and Griffiths R (1993) L-trans-2,4-dicarboxylic acid (L-transPDC) has properties consistent with that of a competitive substrate for the plasma mebrane glutamate transporter. Biochem Soc Trans 21: 111S

Dunlop J (2001) Substrate exchange properties of the high-affinity glutamate transporter EAAT2. J Neurosci Res 66: 482-486

Eiden LE (1998) The cholinergic gene locus. J Neurochem 70: 2227-40.

Elgoyhen AB, Johnson DS, Boulter J, Vetter DE, Heinemann S (1994) α9: an acetylcholine receptor with novel pharmacological properties expressed in rat cochlear hair cells. Cell 79: 705-715

Elgoyhen AB, Vetter DE, Katz E, Rothlin C V, Heinemann SF, and Boulter J (2001) α10: a determinant of nicotinic cholinergic receptor function in mammalian vestibular and cochlear mechanosensory hair cells. Proc Natl Acad Sci U S A 98: 3501-3506

Elliott J, Blanchard SG, Wu W, Miller J, Strader CD, Hartig P, Moore HP, Racs J, and Raftery M A (1980) Purification of Torpedo californica post-synaptic membranes and fractionation of their constituent proteins. Biochem J 185: 667-677

Engidawork E, Gulesserian T, Balic N, Cairn N, and Lubec G (2000) Changes in nicotinic acetylcholine receptor subunits expression in brain of patients with Down syndrome and Alzheimer's disease. J Neural Transm Suppl [61]: 211-222

Erecinska M, Wantorsky D and Wilson DF (1983) Aspartate transport in synaptosomes from rat brain. J Biol Chem 258: 9069-9077

Fabian-Fine R, Skehel P, Errington ML, Davies HA, Sher E, Stewart MG and Fine A (2001) Ultrastructural distribution of the α7 nicotinic acetylcholine receptor subunit in rat hippocampus J Neurosci 21: 7993-8003

Fenster C P, R ains M F, N oerager B , Q uick M W, Lester R AJ (1997) I nfluence of subunit composition on desensitisation of neuronal nicotinic acetycholine receptors at low concentrations of nicotine. J Neurosci 17: 5747-5759

Fenster CP, Hicks J H, Beckman ML, Covernton, PJ, Quick MW, and Lester, RA (1999) Desensitization of nicotinic receptors in the central nervous system. Ann N Y Acad Sci 868: 620-623

Ferguson SM Savchenko V, Apparsundaram S, Zwick M, Wright J, Heilman CJ, Yi H, Levey AI and Blakely RD (2003) Vesicular localisation and activity-dependant trafficking of presynaptic choline transporters 23:9697-9709

Ferkany J and Coyle JT (1986) Heterogeneity of sodium-dependent excitatory amino acid uptake mechanisms in rat brain. J.Neurosci.Res. 16: 491-503

Fischer BO, Ottersen OP, and Storm-Mathisen J (1986) Implantation of D-[^{3}H]aspartate loaded gel particles permits restricted uptake sites for transmitter-selective axonal transport. Exp Brain Res 63: 620-626

Fisher J L and Dani JA. (2000) Nicotinic receptors on hippocampal cultures can increase synaptic glutamate currents while decreasing the NMDA-receptor component. Neuropharmacology 39: 2756-2769

Fleck MW, Barrionuevo G and Palmer AM. (2001) Synaptosomal and vesicular accumulation of L-glutamate, L-aspartate and D-aspartate. Neurochem Int. 39: 217-225

Francis PT, Palmer AM, Snape M and Wilcock GK (1999) The cholinergic hypothesis of Alzheimer's disease: a review of progress. J Neurol Neurosurg Psychiatry 66:137-47

Frazier CJ, Strowbridge BW and Papke RL (2003) Nicotinic receptors on local circuit neurons in dentate gyrus: a potential role in regulation of granule cell excitability. J Neurophysiol 89: 3018-3028

Frith C and Dolan R (1996) The role of the prefrontal cortex in higher cognitive functions. Brain Res Cogn Brain Res 5: 175-81.

Freedman R, Adams CE and Leonard S (2000) The α7-nicotinic acetylcholine receptor and the pathology of hippocampal interneurons in schizophrenia. J Chem Neuroanat 20: 299-306

Freedman R, Coon H, Myles-Worsley M, Orr-Urtreger A, Olincy A, Davis A, Polymeropoulos M, Holik J, Hopkins J, Hoff M, Rosenthal J, Waldo MC, Reimherr F, Wender P, Yaw J, Young DA, Breese CR, Adams C, Patterson D, Adler LE, Kruglyak L, Leonard S and Byerley W (1997) Linkage of a neurophysiological deficit in schizophrenia to a chromosome 15 locus. Proc Natl Acad Sci U S A 94: 587-592

Freedman R, Hall M, Adler LE and Leonard S (1995) Evidence in postmortem brain tissue for decreased numbers of hippocampal nicotinic receptors in schizophrenia. Biol Psychiatry 38: 22-33

Freedman R, Adams CE, Adler LE, Bickford PC, Gault J, Harris JG, Nagamoto HT, Olincy A, Ross RG, Stevens KE, Waldo M and Leonard S (2000) Inhibitory neurophysiological defecit as a phenotype for genetic investigation of schizophrenia. Am J Med Genetics 97: 58-64

Freedman R, Leonard S, Gault JM, Hopkins J, Cloninger CR, Kaufmann CA, Tsuang MT, Farone SV, Malaspina D, Svrakic DM, Sanders A and Gejman, P (2001) Linkage disequilibrium for schizophrenia at the chromosome 15q13-14 locus of the α7-nicotinic acetylcholine receptor subunit gene (CHRNA7). Am J Med Genet 105: 20-22

Fruchart-Gaillard C, Gilquin B, Antil-Delbeke S, Le Novere N, Tamiya T, Corringer P.J, Changeux JP, Menez A and Servent D (2002) Experimentally based model of a complex between a snake toxin and the α7 nicotinic receptor. Proc Natl Acad Sci U S A 99: 3216-3221

Fujii S, Ji Z and Sumikawa K (2000) Inactivation of α7 ACh receptors and activation of non-α7 ACh receptors both contribute to long term potentiation induction in the hippocampal CA1 region. Neurosci Lett 286: 134-138

Fuster JM (2001) The prefrontal cortex--an update: time is of the essence. Neuron. 30: 319-33

Galzi JL and Changeux JP (1995) Neuronal nicotinic receptors: molecular organization and regulations. Neuropharmacology 34: 563-582

Gegelashvili G, Schousboe A (1998) Cellular distribution and kinetic properties of high-affinity glutamate transporters. Brain Res Bull 45: 233-238

Gerzanich V, Anand R and Lindstrom J (1994) Homomers of α8 and α7 subunits of nicotinic receptors exhibit similar channel but contrasting binding site properties. Mol Pharmacol 45: 212-220

Gioanni Y, Rougeot C, Clarke PB, Lepouse C, Thierry AM and Vidal C (1999) Nicotinic receptors in the rat prefrontal cortex: increase in glutamate release and facilitation of mediodorsal thalamo-cortical transmission. Eur J Neurosci 11: 18-30

Gigg J, Tan AM, and Finch DM (1994) Glutamatergic hippocampal formation projections to prefrontal cortex in the rat are regulated by GABAergic inhibition and show convergence with glutamatergic projections from the limbic thalamus. Hippocampus 4: 189-98.

Girod R, Barazangi N, McGehee D and Role LW (2000) Facilitation of glutamatergic neurotransmission by presynaptic nicotinic acetylcholine receptors. Neuropharmacology 39: 2715-2725

Girod R and Role LW (2001) Long-lasting enhancement of glutamatergic synaptic transmission by acetylcholine contrasts with response adaptation after exposure to low-level nicotine. J Neurosci 21: 5182-5190

Goldman D, Deneris E, Luyten W, Kochhar A, Patrick J, and Heinemann S (1987) Members of a nicotinic acetylcholine receptor gene family are expressed in different regions of the mammalian central nervous system. Cell 48: 965-973

Gopalakrishnan M, Buisson B, Touma E, Giordano T, Campbell JE, Hu IC, Donnelly-Roberts D, Arneric SP, Bertrand D, and Sullivan JP (1995) Stable expression and pharmacological properties of the human α7 nicotinic acetylcholine receptor. Eur J Pharmacol 290: 237-246

Gorne-Tschelnokow U, Strecker A, Kaduk C, Naumann D, and Hucho F (1994) The transmembrane domains of the nicotinic acetylcholine receptor contain α-helical and β structures. EMBO J 13: 338-341

Granon S, Poucet B, Thinus-Blanc C, Changeux JP, and Vidal C (1995) Nicotinic and muscarinic receptors in the rat prefrontal cortex: differential roles in working memory, response selection and effortful processing. Psychopharmacology (Berl) 119: 139-144

Gray R, Rajan AS, Radcliffe KA, Yakehiro M, and Dani JA (1996) Hippocampal synaptic transmission enhanced by low concentrations of nicotine. Nature 383: 713-716

Guan ZZ, Zhang X, Blennow K, and Nordberg A (1999) Decreased protein level of nicotinic receptor alpha7 subunit in the frontal cortex from schizophrenic brain. Neuroreport 10: 1779-1782

Gundersen V, Ottersen OP and Storm-Mathisen J (1996) Selective excitatory amino acid uptake in glutamatergic nerve terminals and in glia in the rat striatum: quantitative electron microscopic immunocytochemistry of exogenous (D)-aspartate and endogenous glutamate and GABA. Eur J Neurosci 8: 758-765

Guo JZ and Chiappinelli VA (2002) A novel choline-sensitive nicotinic receptor subtype that mediates enhanced GABA release in the chick ventral lateral geniculate nucleus. Neuroscience 110: 505-513

Haga T and Noda H (1973) Choline uptake systems of rat brain synaptosomes. Biochim Biophys Acta 291: 564-575

Hall M, Zerbe L, Leonard S, and Freedman R (1993) Characterization of [^{3}H]cytisine binding to human brain membrane preparations. Brain Res 600: 127-133

Han ZY, Zoli M, Cardona A, Bourgeois JP, Changeux JP, and Le Novere N (2003) Localization of [^{3}H]nicotine, [^{3}H]cytisine, [^{3}H]epibatidine, and [^{125}I]α-bungarotoxin binding sites in the brain of Macaca mulatta. J Comp Neurol 461: 49-60

Hardwick JC and Parsons R L (1993) Necessity of divalent cations for recovery from carbachol-induced nicotinic acetylcholine receptor inactivation at snake twitch fibre endplates. Br J Pharmacol 110: 889-895

Harrison SM, Jarvie PE and Dunkley PR. (1988) A rapid Percoll gradient procedure for the isolation of synaptosomes directely from an S1 fraction: Viability of subcellular fractions. Brain Res 441: 72-80

Harvey SC, Maddox FN, and Luetje CW (1996) Multiple determinants of dihydro-beta-erythroidine sensitivity on rat neuronal nicotinic receptor α subunits. J Neurochem 67: 1953-1959

Heinemann S, Boulter J, Connolly J, Deneris E, Duvoisin R, Hartley M, Hermans-Borgmeyer I, Hollmann M, O'Shea-Greenfield A, and Papke R (1991) The nicotinic receptor genes. Clin Neuropharmacol 14 Suppl 1, S45-S61

Heron A, Lekieffre D, Le Peillet E, Lasbennes F, Seylaz J, Plotkine M and Boulu RG (1994) Effects of an A1 adenosine receptor agonist on the neurochemical, behavioural and histological consequences of ischemia. Brain Res. 641: 217-224

Hill JA, Zoli M, Bourgeois JP and Changeux JP (1993) Immunocytochemical localization of a neuronal nicotinic receptor: the β2-subunit. J Neurosci 13: 1551-1568

Hsu YN, Amin J, Weiss DS and Wecker L (1996) Sustained nicotine exposure differentially affects α3β2 and α4β2 neuronal nicotinic receptors expressed in Xenopus oocytes. J Neurochem 66: 667-675

Hucho F, Oberthur W and Lottspeich F (1986) The ion channel of the nicotinic acetylcholine receptor is formed by the homologous helices M II of the receptor subunits. FEBS Lett 205: 137-142

Hucho F, Tsetlin VI and Machold J (1996) The emerging three-dimensional structure of a receptor. The nicotinic acetylcholine receptor. Eur J Biochem 239: 539-557

Hunt R (1900) The fall of blood pressure resulting from the stimulation of afferent nerves. J Physiol 18: 384-409

Hyde TM, Nawroz S, Goldberg TE, Bigelow LB, Strong D, Ostrem JL, Weinberger DR, Kleinman JE (1994) Is there cognitive decline in schizophrenia? A cross-sectional study. Br J Psychiatry. 164: 494-500.

Imoto K, Konno T, Nakai J, Wang F, Mishina M and Numa, S (1991) A ring of uncharged polar amino acids as a component of channel constriction in the nicotinic acetylcholine receptor. FEBS Lett 289: 193-200

Isaac JT (2003) Postsynaptic silent synapses: evidence and mechanisms. Neuropharmacology 45: 450-460

Jabaudon D, Shimamoto K, Yasuda-Kamatani Y, Scanziani M, Gahwiler BH and Gerber U (1999) Inhibition of uptake unmasks rapid extracellular turnover of glutamate of nonvesicular origin. Proc Natl Acad Sci U S A 96: 8733-8738

Jarrard (1995) What does the hippocampus really do? Behav Brain Res. 71:1-10

Jay TM, Thierry AM, Wiklund L and Glowinski J (1992) Excitatory amino acid pathway from the hippocampus to the prefrontal cortex. Contribution of AMPA receptors in hippocampal-prefrontal cortex transmission. Eur J Neurosci 4: 1285-1295

Ji D, Lape R and Dani JA (2001) Timing and location of nicotinic activity enhances or depresses hippocampal synaptic plasticity. Neuron 31: 131-141

Jones IW, Bolam JP and Wonnacott S (2001) Presynaptic localisation of the nicotinic acetylcholine receptor β2 subunit immunoreactivity in rat nigrostriatal dopaminergic neurones. J Comp Neurol 439: 235-247

Kaiser SA, Soliakov L, Harvey SC, Luetje CW and Wonnacott S (1998) Differential inhibition by alpha-conotoxin-MII of the nicotinic stimulation of [^{3}H]dopamine release from rat striatal synaptosomes and slices. J Neurochem 70: 1069-76

Kaiser S and Wonnacott S (2000) α–bungarotoxin-sensitive nicotinic receptors indirectly modulate [^{3}H]dopamine release in rat striatal slices via glutamate release. Mol Pharmacol 58: 312-318

Kaneko T and Fujiyama F (2002) Complementary distribution of vesicular glutamate transporters in the central nervous system. Neurosci.Res. 42: 243-250

Karlin A (2003) Emerging structure of the nicotinic acetylcholine receptors. Nat Rev Neurosci 3: 102-114

Karlin A and Akabas MH (1995) Toward a structural basis for the function of nicotinic acetylcholine receptors and their cousins. Neuron 15: 1231-1244

Katz B and Miledi R (1967) A study of synaptic transmission in the absence of nerve impulses. J Physiol 192: 407-436

Kawaguchi Y and Kondo S (2002) Parvalbumin, somatostatin and cholecystokinin as chemical markers for specific GABAergic interneuron types in the rat frontal cortex. J Neurocytol. 31: 277-87.

Kawai H and Berg DK (2001) Nicotinic acetylcholine receptors containing α7 subunits on rat cortical neurons do not undergo long-lasting inactivation even when up-regulated by chronic nicotine exposure. J Neurochem 78: 1367-1378

Kawai H, Zago W and Berg DK (2002) Nicotinic α7 receptor clusters on hippocampal GABAergic neurons: regulation by synaptic activity and neurotrophins. J Neurosci 22: 7903-7912

Kelton MC, Kahn HJ, Conrath CL and Newhouse PA (2000) The effects of nicotine on Parkinson's disease. Brain Cogn 43: 274-282

Kenny PJ, File SE and Neal MJ (2000) Evidence for a complex influence of nicotinic acetylcholine receptors on hippocampal serotonin release. J Neurochem 75: 2409-2414

Keyser KT, Britto LR, Schoepfer R, Whiting P, Cooper J, Conroy W, Brozozowska-Prechtl A, Karten HJ and Lindstrom J (1993) Three type of apha-bungarotoxin-

sensitive nicotinic acetylcholine receptors are expressed in chick retina. J Neurosci 13: 442-454

Khiroug SS, Harkness PC, Lamb, PW, Sudweeks SN, Khiroug L, Millar NS and Yakel JL (2002) Rat nicotinic ACh receptor α7 and β2 subunits co-assemble to form functional heteromeric nicotinic receptor channels. J Physiol 540: 425-434

Klink R, de Kerchove, d'Exaerde, Zoli M and Changeux JP (2001) Molecular and physiological diversity of nicotinic acetylcholine receptors in the midbrain dopaminergic nuclei. J Neurosci 21: 1452-1463

Koelle GB (1961) A proposed dual neurohumoral role of acetylcholine: its functions at the pre- and post-synaptic sites. Nature 190: 208-11.

Kulak JM, McIntosh JM, Yoshikami D and Olivera BM (2001) Nicotine-evoked transmitter release from synaptosomes: functional association of specific presynaptic acetylcholine receptors and voltage-gated calcium channels. J Neurochem 77: 1581-1589

Kuwahara O, Mitsumoto Y, Chiba K and Mohri T (1992) Characterization of D-aspartic acid uptake by rat hippocampal slices and effect of ischemic conditions. J Neurochem. 59: 616-621

Lambe EK, Picciotto MR and Aghajanian GK (2003) Nicotine induces glutamate release from thalamocortical terminals in prefrontal cortex. Neuropsychopharmacology 28: 216-225

Langley JN (1905) On the reaction of cells and nerve-endings to certain poisons, chiefly as regards the reaction of striated muscle tonicotine and to curare. J Physiol 33: 374-413

Lawrence AD and Sahakian BJ (1995) Alzheimer's disease, attention , and the cholinergic system Alzheimer's Dis Assoc Disord Suppl 2; 43-49

Le Novere N and Changeux JP (1995) Molecular evolution of the nicotinic acetylcholine receptor: an example of multigene family in excitable cells. J Mol Evol 40: 155-172

Le Novere N, Zoli M and Changeux JP (1996) Neuronal nicotinic receptor alpha 6 subunit mRNA is selectively concentrated in catecholaminergic nuclei of the rat brain Eur J Neuro 8: 2428-2439

Le Novere N, Corringer, PJ and Changeux JP (1999) Improved secondary structure predictions for a nicotinic receptor subunit: incorporation of solvent accessibility and experimental data into a two-dimensional representation. Biophys J 76: 2329-2345

Leonard RJ, Labarca CG, Charnet P, Davidson N and Lester HA (1988) Evidence that the M2 membrane-spanning region lines the ion channel pore of the nicotinic receptor. Science 242: 1578-1581

Levin ED and Torry D. (1996) Acute and chronic nicotine effects on working memory in aged rats. Psychopharmacology (Berl) 123: 88-97

Levin ED, Torry D, Christopher NC, Yu X, Einstein G, and Schwartz-Bloom, RD (1997) Is binding to nicotinic acetylcholine and dopamine receptors related to working memory in rats? Brain Res Bull 43: 295-304

Levin ED and Simon BB (1998) Nicotinic acetylcholine involvement in cognitive function in animals. Psychopharmacology (Berl) 138: 217-230

Levin ED, Christopher NC, Weaver T, Moore J, and Brucato F (1999) Ventral hippocampal ibotenic acid lesions block chronic nicotine-induced spatial working memory improvement in rats. Brain Res Cogn Brain Res 7: 405-410

Levin ED (2002) Nicotinic receptor subtypes and cognitive function. J Neurobiol 53: 633-640

Levin ED and Rezvani AH (2002) Nicotinic treatment for cognitive dysfunction. Curr Drug Target CNS Neurol Dis 1: 423-431

Levy RB and Aoki C (2002) α7 nicotinic acetylcholine receptors occur at postsynaptic densities of AMPA receptor-positive and negative excitatory synapses in rat sensory cortex. J Neurosci 22: 5001-5015

Li X, Rainnie DG, McCarley RW, and Greene R W (1998) Presynaptic nicotinic receptors facilitate monoaminergic transmission. J Neurosci 18: 1904-1912

Li X and Eisenach JC (2002) Nicotinic acetylcholine receptor regulation of spinal norepinephrine release. Anesthesiology 96: 1450-1456

Lindstrom J, Schoepfer R, Conroy WG, and Whiting, P (1990) Structural and functional heterogeneity of nicotinic receptors. Ciba Found Symp 152, 23-42

Lips KS, Pfeil U and Kummer W. (2002). Coexpression of α9 and α10 nicotinic acetylcholine receptors in rat dorsal root ganglion neurons. Neuroscience 115: 1-5

Lloyd GK and Williams M (2000) Neuronal nicotinic acetylcholine receptors as novel drug targets. J Pharmacol Exp Ther 292: 461-467

Loewi O and Nevratil A (1926) On the humoral propagation of cardiac nerve action. In Cellular Neurophysiology: A source book. I. Cooke and M. Lipkin. Holt, Rinehart and Winston, Orlando, FL. 478-485

Lubin M, Erisir A, and Aoki C (1999) Ultrastructural immunolocalization of the alpha 7 nAChR subunit in guinea pig medial prefrontal cortex. Ann N Y Acad Sci 868: 628-632

Luetje CW, Patrick J and Seguela P (1990) Nicotine receptors in the mammalian brain. FASEB J 4: 2753-60.

Lukas RJ, Changeux JP, Le Novere N, Albuquerque EX, Balfour DJ, Berg DK, Bertrand D, Chiappinelli VA, Clarke P, Collins AC, Dani JA, Grady SR, Kellar KJ, Lindstrom JM, Marks MJ, Quik M, Taylor PW and Wonnacott S (1999) International Union of Pharmacology. XX. Current status of the nomenclature for nicotinic acetylcholine receptors and their subunits. Pharmacol Rev 51: 397-401

Luntz-Leybman V, Bickford PC and Freedman R (1992) Cholinergic gating of response to auditory stimuli in rat hippocampus. Brain Res 587: 130-136

MacDermott AB, Role LW and Siegelbaum SA (1999) Presynaptic ionotropic receptors and the control of transmitter release. Annu.Rev.Neurosci. 22: 443-485

Maggi L, Sher E and Cherubini E (2001) Regulation of GABA release by nicotinic acetylcholine receptors in the neonatal rat hippocampus. J.Physiol 536: 89-100

Maire JC and Wurtman RJ (1985) Effects of electrical stimulation and choline availability on the release and contents of acetylcholine and choline in superfused slices from rat striatum. J Physiol 80: 189-195

Mansvelder HD and McGehee DS (2000) Long-term potentiation of excitatory inputs to brain reward areas by nicotine. Neuron 27: 349-357

Marubio LM, gardier AM, Durier S, David D, Klink R, Arroyo-jimenez MM, McIntosh JM, Rossi F, Champitiaux N, Zoli M and Changeux JP (2003) Effects of nicotine in the dopaminergic system of mice lacking the alpha4 subunit of neuronal nicotinic acetylcholine receptors. Eur J Neurosci 17: 1329-1337

Marchi M, Risso F, Viola C, Cavazzani P and Raiteri M (2002) Direct evidence that release-stimulating α7* nicotinic cholinergic receptors are localized on human and rat brain glutamatergic axon terminals. J Neurochem 80: 1071-1078

Marks MJ and Collins AC (1982) Characterisation of nicotine binding in mouse brain and comparison with the binding of α-bungarotoxin and quinuclidinyl benzilate. Mol Pharmacol 22: 554-564

Marks MJ, Burch JB and Collins AC (1983) Effects of chronic nicotine infusion on tolerance development and nicotinic receptors. J Pharmacol Exp Ther 226: 817-825

Marks MJ, Pauly JR, Gross SD, Deneris ES, Hermans-Borgmeyer I, Heinemann SF and Collins AC (1992) Nicotine binding and nicotinic receptor subunit RNA after chronic nicotine treatment. J Neurosci 12: 2765-2784

Marshall DL, Redfern PH and Wonnacott S (1997) Presynaptic nicotinic modulation of dopamine release in the three ascending pathways studied by in vivo microdialysis: comparison of naive and chronic nicotine-treated rats. J Neurochem 68: 1511-1519

Marutle A, Warpman U, Bogdanovic N and Nordberg A (1998) Regional distribution of subtypes of nicotinic receptors in human brain and effect of aging studied by (+/-)-[^{3}H]epibatidine. Brain Res 801: 143-149

Marutle A, Zhang X, Court J, Piggott M, Johnson M, Perry R, Perry E and Nordberg A (2001) Laminar distribution of nicotinic receptor subtypes in cortical regions in schizophrenia. J Chem Neuroanat 22: 115-126

McEvoy JP (1994) Efficacy of risperidone on positive features of schizophrenia. J Clin Psychiatry. 55: Suppl:18-21.

McGehee DS (2002) Nicotinic receptors and hippocampal synaptic plasticity ... it's all in the timing. Trends Neurosci 25: 171-172

McGehee DS, Heath MJ, Gelber S, Devay P and Role LW. (1995) Nicotine enhancement of fast excitatory synaptic transmission in CNS by presynaptic receptors. Science 269: 1692-1696

McGehee DS and Role LW (1995) Physiological diversity of nicotinic acetylcholine receptors expressed by vertebrate neurons. Annu Rev Physiol 57: 521-546

McLane KE, Wu X, Lindstrom JM and Conti-Tronconi BM (1992) Epitope mapping of polyclonal and monoclonal antibodies against two α-bungarotoxin-binding α subunits from neuronal nicotinic receptors. J Neuroimmunol 38: 115-128

McMahon HT and Nicholls DG (1991) Transmitter glutamate release from isolated nerve terminals: evidence for biphasic release and triggering by localized Ca^{2+} J.Neurochem. 56: 86-94

Mesulam MM, Mufson EJ, Wainer BH and Levey AI (1983) Central cholinergic pathways in the rat: an overview based on an alternative nomenclature (Ch1-Ch6) Neuroscience 10: 1185-1201

Mike A, Castro NG and Albuquerque EX (2000) Choline and acetylcholine have similar kinetic properties of activation and desensitization on the α7 nicotinic receptors in rat hippocampal neurons. Brain Res 882: 155-168

Millar NS (2003) Assembly and subunit diversity of nicotinic acetylcholine receptors. Biochem Soc Trans 31: 869-874

Mitrovic AD and Johnston GA (1995) Regional differences in the inhibition of L-glutamate and L-aspartate sodium-dependent high affinity uptake systems in rat CNS synaptosomes by L-trans-pyrrolidine-2,4-dicarboxylate, threo-3-hydroxy-D-aspartate and D-aspartate. Neurochem Int 24: 583-588

Miyazawa A, Fujiyoshi Y, Stowell M and Unwin N (1999) Nicotinic acetylcholine receptor at 4.6 A resolution: transverse tunnels in the channel wall. J Mol Biol 288: 765-786

Mogg AJ, Whiteaker P, McIntosh JM, Marks M, Collins AC and Wonnacott S (2002) Methyllycaconitine is a potent antagonist of α-conotoxin-MII-sensitive presynaptic nicotinic acetylcholine receptors in rat striatum. J Pharmacol Exp Ther 302: 197-204

Molinari EJ, Delbono O, Messi ML, Renganathan M, Arneric SP, Sullivan JP and Gopalakrishnan M (1998) Up-regulation of human α7 nicotinic receptors by chronic treatment with activator and antagonist ligands. Eur J Pharmacol 347: 131-139

Monod J, Wyman J and Changeux JP (1965) On the nature of allosteric transitions: A plausible model. J Mol Biol 12: 88-118

Moussa Cel, Mitrovic AD, Vandenberg RJ, Provis T, Rae C, Bubb WA and Balcar VJ (2002) Effects of L-glutamate transport inhibition by a conformationally restricted glutamate analogue (2S,1'S,2'R)-2-(carboxycyclopropyl)glycine (L-CCG III) on metabolism in brain tissue in vitro analysed by NMR spectroscopy. Neurochem.Res. 27: 27-35

Mukhin AG, Gundisch D, Horti AG, Koren AO, Tamagnan G, Kimes AS, Chambers J, Vaupel DB, King SL, Picciotto M, Innis RB, and London ED. (2000) 5-Iodo-A-85380, an α4β2 subtype-selective ligand for nicotinic acetylcholine receptors. Mol Pharmacol 57: 642-649

Musachio JL, Scheffel U, Finley PA, Zhan Y, Mochizuki T, Wagner HN and Dannals RF (1998) 5-[I-125/123]Iodo-3(2(S)-azetidinylmethoxy)pyridine, a radioiodinated analog of A-85380 for in vivo studies of central nicotinic acetylcholine receptors. Life Sci 62: L-7

Muzzolini A, Bregola G, Bianchi C, Beani L and Simonato M (1997) Characterization of glutamate and [^{3}H]D-aspartate outflow from various in vitro preparations of the rat hippocampus. Neurochem Int 31: 113-124

Nakamura Y, Iga K, Shibata T, Shudo M and Kataoka K (1993) Glial Plasmalemmal vesicles: a subcellular fraction from rat hippocampal homogenate distinct from synaptosomes. Glia 9: 48-56

Nayak SV, Dougherty JJ, McIntosh JM and Nichols RA (2001) Ca^{2+} changes induced by different presynaptic nicotinic receptors in separate populations of individual striatal nerve terminals. J Neurochem 76: 1860-1870

Newhouse PA, Potter A and Levin ED (1997) Nicotinic system involvement in Alzheimer's and Parkinson's diseases. Implications for therapeutics. Drugs Aging 11: 206-228

Newhouse PA and Kelton M (2000) Nicotinic systems in central nervous system disease: degenerative disorders and beyond. Pharma Acta Helv 74: 91-101

Nicholls DG and Sihra (1986) Synaptosomes possess an exocytotic pool of glutamate. Nature 321: 772-773

Nicholls DG (1989) Release of glutamate, aspartate, and gamma-aminobutyric acid from isolated nerve terminals. J Neurochem 52: 331-341

Nicholls DG and Attwell D (1990) The release and uptake of excitatory amino acids. Trends Pharmacol.Sci. 11: 462-468

Nicholls DG (1993) Ion channels and the regulation of neurotransmitter glutamate release. Biochem Soc Trans 21: 53-58

Nicholls DG (1998) Presynaptic modulation of glutamate release. Prog.Brain Res. 116: 15-22

Nickel E and Potter L T (1973) Ultrastructure of isolated membranes of Torpedo electric tissue. Brain Res 57: 508-17.

Nishihara I, Minami T, Watanabe Y, Ito S and Hayaishi O (1995) Prostaglandin E2 stimulates glutamate release from synaptosomes of rat spinal cord. Neurosci.Lett. 196: 57-60

Nomikos GG, Schilstrom B, Hildebrand BE, Panagis G, Grenhoff J and Svensson TH (2000) Role of α7 nicotinic receptors in nicotine dependence and implications for psychiatric illness. Behav Brain Res 113: 97-103

Nordberg A and Larsson C (1980) Studies of muscuranic and nicotinic binding sites in brain. Acta Physiol Scand Suppl 479: 19-23

Nordberg A and Winblad B (1986) Reduced number of [^{3}H]nicotine and [^{3}H]acetylcholine binding sites in the frontal cortex of Alzheimer brains. Neurosci Lett 72: 115-119

Nordberg A, Adem A, Hardy J and Winblad B (1988) Change in nicotinic receptor subtypes in temporal cortex of Alzheimer brains. Neurosci Lett 86: 317-321

Nordberg A (1993) Clinical studies in Alzheimer patients with positron emission tomography. Behav Brain Res 57: 215-224

Nordberg A (2001) Nicotinic receptor abnormalities of Alzheimer's disease: therapeutic implications. Biol Psychiatry 49: 200-210

O'Leary KT and Leslie FM (2003) Developmental regulation of nicotinic acetylcholine receptor-mediated [^{3}H]norepinephrine release from rat cerebellum. J Neurochem 84: 952-959

Olale F, Gerzanich V, Kuryatov A, Wang F and Lindstrom J (1997) Chronic nicotine exposure differentially affects the function of human α3, α4, and α7 neuronal nicotinic receptor subtypes. J Pharmacol Exp Ther 283: 675-683

Olincy A, Ross RG, Young DA, Roath M and Freedman R (1998) Improvement in smooth pursuit eye movements after cigarette smoking in schizophrenic patients. Neuropsychopharmacology 18:175-85.

Newhouse PA and Kelton M (2000) Clinical Aspects of Nicotinic agents: Therapeutic Applications in Central Nervous System Disorders. Neuronal Nicotinic Receptors. 1: 779-813

Palma E, Bertrand S, Binzoni T and Bertrand D (1996) Neuronal nicotinic α7 receptor expressed in Xenopus oocytes presents five putative binding sites for methyllycaconitine. J Physiol 491: 151-161

Palma E, Maggi L, Barabino B, Eusebi F and Ballivet M (1999) Nicotinic acetylcholine receptors assembled from the α7 and β3 subunits. J Biol Chem 274: 18335-18340

Palmer AM and Reiter CT (1994) Comparison of the superfused efflux of preaccumulated D-[^{3}H]aspartate and endogenous L-aspartate and L-glutamate from rat cerebrocortical minislices. Neurochem Int 25: 441-450

Palmer MJ, Taschenberger H, Hull C, Tremere L and von Gersdorff H (2003) Synaptic activation of presynaptic glutamate transporter currents in nerve terminals. J Neurosci 23: 4831-4841

Papke RL, Bencherif M and Lippiello P (1996) An evaluation of neuronal nicotinic acetylcholine receptor activation by quaternary nitrogen compounds indicates that choline is selective for the α7 subtype. Neurosci Lett 213: 201-204

Papke RL, Porter T and Papke JK (2002) Comparative pharmacology of rat and human alpha7 nAChR conducted with net charge analysis. Br J Pharmacol 137: 49-61

Papke RL, Sanberg PR and Shytle RD (2001) Analysis of mecamylamine stereoisomers on human nicotinic receptor subtypes. J Pharmacol Exp Ther 297: 646-656

Parsons SM, Prior C and Marshall IG (1993) Acetylcholine transport, storage and release. Int Rev Neurobiol 35: 270-390

Pascual JM and Karlin A (1998) State dependent accessibility and electrostatic potential in the channel of the nicotinic acetylcholine receptor. Inferences from rates of reaction with substituted cysteines in the M2 segment of the alpha subunit. J Gen Physiol 111: 717-739

Patel DR and Croucher MJ (1997) Evidence for a role of presynaptic AMPA receptors in the control of neuronal glutamate release in the rat forebrain. Eur J Pharmacol 332: 143-151

Pauly JR, Stitzel JA, Marks MJ and Collins AC (1989) An autoradiographic analysis of cholinergic receptors in mouse brain Brain Res Bull 22: 453-459

Perry DC, Davila-Garcia MI, Stockmeier CA and Kellar KJ (1999) Increased nicotinic receptors in brains from smokers: membrane binding and autoradiography studies. J Pharmacol Exp Ther 289: 1545-1552

Perry DC and Kellar KJ (1995) [^{3}H]epibatidine labels nicotinic receptors in rat brain: an autoradiographic study. J Pharmacol Exp Ther 275: 1030-1034

Perry EK, Martin-Ruiz CM and Court JA (2001) Nicotinic receptor subtypes in human brain related to aging and dementia. Alcohol 24: 63-68

Perry EK, Morris CM, Court JA, Cheng A, Fairbairn AF, McKeith IG, Irving D, Brown A and Perry RH (1995) Alteration in nicotine binding sites in Parkinson's disease, Lewy body dementia and Alzheimer's disease: possible index of early neuropathology. Neuroscience 64: 385-395

Phillis JW, Smith-Barbour M, Perkins LM and O'Regan MH (1994) Characterization of glutamate, aspartate, and GABA release from ischemic rat cerebral cortex. Brain Res Bull 34: 457-466

Picciotto MR (1998) Common aspects of the action of nicotine and other drugs of abuse. Drug Alcohol Depend 51: 165-172

Picciotto MR, Caldarone BJ, King SL and Zachariou, V (2000). Nicotinic receptors in the brain. Links between molecular biology and behavior. Neuropsychopharmacology 22: 451-465

Pinto A, Jankowski M and Sesack SR (2003) projections from the paraventricular nucleus of the thalamus to the rat prefrontal cortex and nucleus accumbens shell: ultrastructural characteristics and spatial relationships with dopamine afferents. J Comp Neurol 459: 142-155

Potter A, Corwin J, Lang J, Piasecki M, Lenox R and Newhouse PA (1999). Acute effects of the selective cholinergic channel activator (nicotinic agonist) ABT-418 in Alzheimer's disease. Psychopharmacology (Berl) 142: 334-342

Puttfarcken PS, Jacobs I and Faltyne CR (2000) Characterization of nicotinic acetylcholine receptor-mediated [^{3}H]-dopamine release from rat cortex and striatum. Neuropharmacology 39: 2673-2680

Quick MW and Lester RA (2002) Desensitization of neuronal nicotinic receptors. J Neurobiol 53: 457-478

Radcliffe KA and Dani JA (1998) Nicotinic stimulation produces multiple forms of increased glutamatergic synaptic transmission. J Neurosci 18: 7075-7083

Raiteri M (1987) Release in vitro as a model to study neurotransmitter receptors. Pharmacol.Res.Commun. 19: 927-941

Raiteri L and Raiteri M (2000) Synaptosomes still viable after 25 years of superfusion. Neurochem Res 25:1265-74.

Reid MS, Herrera-Marschitz M, Kehr J and Ungerstedt U (1990) Striatal dopamine and glutamate release: effects of intranigral injections of substance P. Acta Physiol Scand. 140: 527-537

Reid MS, Hsu K and Berger SP (1997) Cocaine and amphetamine preferentially stimulate glutamate release in the limbic system: studies on the involvement of dopamine. Synapse 27: 95-105

Reid MS, Fox L, Ho LB and Berger SP (2000) Nicotine stimulation of extracellular glutamate levels in the nucleus accumbens: neuropharmacological characterization. Synapse 35: 129-136

Retaux S, Caboche J, Rogard M, Julien JF, Penit-Soria J and Besson MJ (1993) GABA interneurons in the rat medial frontal cortex: characterization by quantitative in situ hybridization of the glutamic acid decarboxylase (GAD67) mRNA. Brain Res 611:187-96.

Revah F, Bertrand D, Galzi JL, Devillers-Thiery A, Mulle C, Hussy N, Bertrand S, Ballivet M and Changeux JP. (1991) Mutations in the channel domain alter desensitisation of a neuronal nicotinic receptor. Nature 353: 846-849

Robinson MB, Djali S and Buchhalter JR (1993) Inhibition of glutamate uptake with L-trans-pyrrolidine-2,4-dicarboxylate potentiates glutamate toxicity in primary hippocampal cultures. J Neurochem 61: 2099-2103

Rogers M and Sargent PB (2003) Rapid activation of presynaptic nicotinic acetylcholine receptors by nerve-released transmitter. Eur J Neuro 18: 2946-2956

Role LW and Berg DK (1996) Nicotinic receptors in the development and modulation of CNS synapses. Neuron 16: 1077-1085

Romano C and Goldstein A (1980) Stereospecific nicotine receptors on rat brain membranes. Science 210: 647-650

Rusted JM, Newhouse PA and Levin ED (2000). Nicotinic treatment for degenerative neuropsychiatric disorders such as Alzheimer's disease and Parkinson's disease. Behav Brain Res 113: 121-129

Saint Marie RL (1996) Glutamatergic connections of the auditory midbrain: selective uptake and axonal transport of D-[^{3}H]aspartate. J Comp Neurol 373: 255-70.

Sanchez-Prieto J, Budd DC, Herrero I, Vazquez E and Nicholls DG (1996) Presynaptic receptors and the control of glutamate exocytosis. Trends Neurosci. 19: 235-239

Sarter M and Bruno JP (1997) Cognitive functions of cortical acetylcholine: toward a unifying hypothesis. Brain Res Rev 104: 243-259

Sarter M and Bruno JP (1999) Abnormal regulation of corticopetal cholinergic neurons and impaired information processing in neuropsychiatric disorders. Trends in Neurosci 22: 67-74

Sarter M, Bruno JP and Givens B (2003) Neurobiology of Learning and Memory. 80: 245-256

Savage DD, Galindo R, Queen SA, Paxton LL and Allan AM (2001) Characterization of electrically evoked [^{3}H]-D-aspartate release from hippocampal slices. Neurochem Int 38: 255-267

Schafer MKH, Eiden LE and Weihe E (1998) Cholinergic neurons and terminal fields revealed by immunohistochemistry for the vesicular acetylcholine transporter. I. Central Nervous System. Neuroscience 84: 331-359

Schell MJ, Cooper OB and Snyder SH (1997) D-aspartate localisations imply neuronal and neuroendocrine roles. Proc Natl Acad Sci U S A 94: 2013-2018

Schilstrom B, Fagerquist MV, Zhang X, Hertel P, Panagis G, Nomikos GG, and Svensson TH (2000) Putative role of presynaptic α7* nicotinic receptors in nicotine stimulated increases of extracellular levels of glutamate and aspartate in the ventral tegmental area. Synapse 38: 375-383

Schilstrom B, Svensson HM, Svensson TH and Nomikos GG (1998) Nicotine and food induced dopamine release in the nucleus accumbens of the rat: putative role of α7 nicotinic receptors in the ventral tegmental area. Neuroscience 85: 1005-1009

Schmidt JT and Freeman JA (1980) Electrophysiological evidence that retinotectal synaptic transmission in the goldfish is nicotinic cholinergic. Brain Res 187: 129-142

Schwartz RD, McGee R and Kellar KJ (1982) Nicotinic cholinergic receptors labeled by [^{3}H]acetylcholine in rat brain. Mol Pharmacol 22: 56-62

Segal M, Dudai Y and Amsterdam A (1978) Distribution of an α-bungarotoxin-binding cholinergic nicotinic receptor in rat brain. Brain Res 148: 105-119

Seguela P, Wadiche J, Dineley-Miller K, Dani JA and Patrick JW (1993) Molecular cloning, functional properties, and distribution of rat brain α7: a nicotinic cation channel highly permeable to calcium. J Neurosci 13: 596-604

Sehmisch,S, Blauth E, Thorn D, Cassel JC, Kelche C, Feuerstein TJ and Jackisch R (2001) Electrically evoked release of glutamate in rat hippocampal slices: effects

of various drugs and fimbria-fornix lesions. Naunyn Schmiedebergs Arch Pharmacol 363: 481-490

Sgard F, Charpantier E, Bertrand S, Walker N, Caput D, Graham D, Bertrand, D, and Besnard F (2002) A novel human nicotinic receptor subunit, α10, that confers functionality to the α9-subunit. Mol Pharmacol 61: 150-159

Shao Z and Yakel JL (2000) Single channel properties of neuronal nicotinic ACh receptors in stratum radiatum interneurons of rat hippocampal slices. J Physiol 527: 507-513

Sharma G and Vijayaraghavan S (2002) Nicotinic receptor signaling in nonexcitable cells. J Neurobiol 53: 524-534

Sharma G and Vijayaraghavan S (2003) Modulation of presynaptic store calcium induces release of glutamate and postsynaptic firing. Neuron 38:929-939

Sharples CG, Kaiser S, Soliakov L, Marks MJ, Collins AC, Washburn M, Wright E, Spencer JA, Gallagher T, Whiteaker P and Wonnacott S (2000) UB-165: a novel nicotinic agonist with subtype selectivity implicates the α4β2* subtype in the modulation of dopamine release from rat striatal synaptosomes. J Neurosci 20: 2783-2791

Shimamoto K, Lebrun B, Yasuda-Kamatani Y, Sakaitani M, Shigeri Y, Yumoto N and Nakajima T (1998) DL-threo-beta-benzyloxyaspartate, a potent blocker of excitatory amino acid transporters. Mol.Pharmacol. 53: 195-201

Simon JR and Kuhar MJ (1976) High Affinity choline uptake: Ionic and energy requirements J Neurochem 27: 93-99

Simonato M, Bregola G, Muzzolini A, Bianchi C and Beani L (1993) Characterization of K(+)-evoked [^{3}H]D-aspartate outflow in the rat hippocampus in vitro. Neurochem Int 23: 555-560

Smit AB, Syed NI, Schaap D, van Minnen J, Klumperman J, Kits KS, Lodder, H, van der Schors RC, van Elk R, Sorgedrager B, Brejc K, Sixma TK and Geraerts WP (2001) A glia-derived acetylcholine-binding protein that modulates synaptic transmission. Nature 411: 261-268

Soliakov L, Gallagher T and Wonnacott S (1995) Anatoxin-a-evoked [3H]dopamine release from rat striatal synaptosomes. Neuropharmacology 34: 1535-41.

Soliakov L and Wonnacott S (1996) Voltage-sensitive Ca^{2+} channels involved in nicotinic receptor-mediated [^{3}H]dopamine release from rat striatal synaptosomes. J Neurochem 67: 163-170

Steriade M, Dossi RC, Pare D and Oakson G (1991) Fast oscillations (20-40 Hz) in thalamocortical systems and their potentiation by mesopontine cholinergic nuclei in the cat. Proc Natl Acad Sci U S A 88: 4396-4400

Storm-Mathisen J and Wold JE (1981) In vivo high-affinity uptake and axonal transport of D-[2,3-^{3}H]aspartate in excitatory neurons. Brain Res 230: 427-433

Suchak SK, Baloyianni NV, Perkinton MS, Williams RJ, Meldrum BS and Rattray M (2003) The 'glial' glutamate transporter, EAAT2 (Glt-1) accounts for high affinity glutamate uptake into adult rodent nerve endings. J.Neurochem. 84: 522-532

Sudweeks SN and Yakel JL (2000) Functional and molecular characterization of neuronal nicotinic ACh receptors in rat CA1 hippocampal neurons. J Physiol 527: 515-528

Sugaya K, Giacobini E and Chiappinelli VA (1990) Nicotinic acetylcholine receptor subtypes in human frontal cortex: changes in Alzheimer's disease. J Neurosci Res 27: 349-359

Swanson LW, Simmons DM, Whiting PJ and Lindstrom J (1987) Immunohistochemical localization of neuronal nicotinic receptors in the rodent central nervous system. J Neurosci 7: 3334-3342

Szatkowski M, Barbour B and Attwell D (1990) Non-vesicular release of glutamate from glial cells by reversed electrogenic glutamate uptake. Nature 348: 443-446

Takahama K and Klee MR (1990) Piperidine discriminates between the transient and the persistent components of the ACH-induced chloride current in Aplysia neurons. Brain Res 508: 161-164

Takahashi M, Billups B, Rossi D, Sarantis M, Hamann M and Attwell D (1997) The role of glutamate transporters in glutamate homeostasis in the brain. J Exp Biol 200: 401-409

Taxt T and Storm-Mathisen J (1984) Uptake of D-aspartate and L-glutamate in excitatory axon terminals in hippocampus: autoradiographic and biochemical comparison with gamma-aminobutyrate and other amino acids in normal rats and in rats with lesions. Neuroscience 11: 79-100

Thierry Am, Gioanni Y, Degenetais E and Glowinski J (2000) Hippocampo-Prefrontal cortex pathway: Anatomical and electrophysiological characteristics. Hippocampus 10: 411-419

Thomas P, Stephens M, Wilkie G, Amar M, Lunt GG, Whiting P, Gallagher T, Pereira E, Alkondon M and Albuquerque EX (1993) (+)-Anatoxin-a is a potent agonist at neuronal nicotinic acetylcholine receptors. J Neurochem 60: 2308-2311

Thomas LS, Jane DE, Harris JR and Croucher MJ (2000) Metabotropic glutamate autoreceptors of the mGlu(5) subtype positively modulate neuronal glutamate release in the rat forebrain in vitro. Neuropharmacology 39:1554-1566

Thorne B, Wonnacott S and Dunkley PR (1991) Isolation of hippocampal synaptosomes on Percoll gradients: cholinergic markers and ligand binding sites. J Neurochem 56:479-484

Tibbs GR, Barrie AP, Van Mieghem FJ, McMahon HT and Nicholls DG (1989) Repetitive action potentials in isolated nerve terminals in the presence of 4-aminopyridine: effects on cytosolic free Ca^{2+} and glutamate release. J.Neurochem. 53: 1693-1699

Toth E, Sershen H, Hashim A, Vizi ES and Lajtha A (1992) Effect of nicotine on extracellular levels of neurotransmitters assessed by microdialysis in various brain regions: role of glutamic acid. Neurochem.Res. 17: 265-271

Trzcinska M and Bielajew C (1998) Functional connections between medial prefrontal cortex and caudate-putamen in brain-stimulation reward of rats. Behav Neurosci 12: 1177-86

Turner TJ and Dunlap K (1995a) Pharmacological characterization of presynaptic calcium channels using subsecond biochemical measurements of synaptosomal neurosecretion. Neuropharmacology 34:1469-1478

Turner TJ and Dunlap K (1995b) Prolonged time course of glutamate release from nerve terminals: relationship between stimulus duration and the secretory event. J.Neurochem. 64: 2022-2033

Umbriaco D, Watkins KC, Descarries L, Cozzari C and Hartman BK (1994) Ultrastructural and morphometric features of the acetylcholine innervation in adult rat parietal cortex. An electron microscopic study in serial sections. J Comp Neurol 348: 351-373

Umbriaco D, Garcia S, Beaulieu C and Descarries L (1995) Relational features of acetylcholine, noradrenaline, serotonin and GABA axon terminals in the stratum radiatum of adult rat hippocampus (CA1). Hippocampus 5: 605-620

Unwin N (1993) Nicotinic acetylcholine receptor at 9 A resolution. J Mol Biol 229: 1101-1124

Unwin, N (1995) Acetylcholine receptor channel imaged in the open state. Nature 373: 37-43

Unwin N (2003) Structure and action of the nicotinic acetycholine receptor explored by electron microscopy FEBS lett 555: 91-95

Vernallis AB, Conroy WG and Berg DK (1993) Neurons assemble acetylcholine receptors with as many as three kinds of subunits while maintaining subunit segregation among receptor subtypes. Neuron 10: 127-134

Vidal C and Changeux, JP (1989) Pharmacological profile of nicotinic acetylcholine receptors in the rat prefrontal cortex: an electrophysiological study in a slice preparation. Neuroscience 29: 261-270

Vidal C and Changeux JP (1993) Nicotinic and muscarinic modulations of excitatory synaptic transmission in the rat prefrontal cortex in vitro. Neuroscience 56: 23-32

Vijayaraghavan S, Pugh PC, Zhang ZW, Rathouz MM and Berg DK (1992) Nicotinic receptors that bind alpha-bungarotoxin on neurons raise intracellular free Ca^{2+}. Neuron 8: 353-362

Waagepetersen HS, Shimamoto K and Schousboe A (2001) Comaprison of the effects of DL-threo-beta-benzoyloxyaspartate (DL-TBOA) and L-trans-2,4-dicarboxylate (t-2,4-PDC) on uptake and release of {3H]D-aspartate in astrocytes and glutamatergic neurons. Neurochem Res 26: 661-666

Wada E, Wada K, Boulter J, Deneris E, Heinemann S, Patrick J and Swanson LW (1989) Distribution of α2, α3, α4, and β2 neuronal nicotinic receptor subunit mRNAs in the central nervous system: a hybridization histochemical study in the rat. J Comp Neurol 284: 314-335

Waldo MC, Carey G, Myles-Worsley M, Cawthra E, Adler LE, Nagamoto HT, Wender P, Byerley W, Plaetka R and Freedman R. (1991) Codistribution of a sensory gating defecit and schizophrenia in multi-affected families. Psychiatry Res 39: 257-268

Wang F, Gerzanich V, Wells GB, Anand R, Peng X, Keyser K and Lindstrom J (1996) Assembly of human neuronal nicotinic receptor α5 subunits with α3, β2, and β4 subunits. J Biol Chem 271:17656-17665

Wang GJ, Chung HJ, Schnuer J, Pratt K, Zable AC, Kavanaugh MP and Rosenberg P A (1998) H igh a ffinity g lutamate t ransport i n r at c ortical n eurons i n culture. Mol.Pharmacol. 53: 88-96

Warpman U and Nordberg A (1995) Epibatidine and ABT 418 reveal selective losses of α4β2 nicotinic receptors in Alzheimer brains. Neuroreport 6: 2419-2423

Wevers A, Burghaus L, Moser N, Witter B, Steinlein OK, Schutz U, Achnitz B, Krempel U, Nowacki S, Pilz K, Stoodt J, Lindstrom J, de Vos RA, Jansen Steur EN and Schroder H (2000) Expression of nicotinic acetylcholine receptors in Alzheimer's disease: postmortem investigations and experimental approaches. Behav Brain Res 113: 207-215

Whiteaker P, Davies AR, Marks MJ, Blagbrough IS, Potter BV, Wolstenholme, AJ, Collins AC and Wonnacott S (1999) An autoradiographic study of the distribution of binding sites for the novel α7-selective nicotinic radioligand [^{3}H]-methyllycaconitine in the mouse brain. Eur J Neurosci 11: 2689-2696

Whiteaker P, Marks MJ, Grady SR, Lu Y, Picciotto MR, Changeux JP and Collins AC (2000) Pharmacological and null mutation approaches reveal nicotinic receptor diversity. Eur J Pharmacol 393: 123-135

Whitehouse PJ, Martino AM, Antuono PG, Lowenstein PR, Coyle JT, Price D L and Kellar KJ. (1986) Nicotinic acetylcholine binding sites in Alzheimer's disease. Brain Res 371: 146-151

Whitehouse PJ, Martino AM, Wagster MV, Price DL, Mayeux R, Atack JR and Kellar KJ (1988) Reductions in [^{3}H]nicotinic acetylcholine binding in Alzheimer's disease and Parkinson's disease: an autoradiographic study. Neurology 38: 720-723

Whiting PJ and Lindstrom JM (1986) Purification and characterization of a nicotinic acetylcholine receptor from chick brain. Biochemistry 25: 2082-2093

Wilkie GI, Hutson P, Sullivan J P, and Wonnacott S (1996) Pharmacological characterization of a nicotinic autoreceptor in rat hippocampal synaptosomes. Neurochem Res 21:1141-1148

Wilson AI, Langley LK, Monley J, Bauer T, Rottunda S, McFalls E, Kovera C and McCarten JR. (1995) Nicotine patches in Alzheimers disease:pilot study on learning, memory and safety. Pharmacol Biochem Behav 51: 509-514

Wilson GG and Karlin A (1998) The location of the gate in the acetylcholine receptor channel. Neuron 20: 1269-1281

Wonnacott S (1986) α-Bungarotoxin binds to low-affinity nicotine binding sites in rat brain. J Neurochem 47: 1706-1712

Wonnacott S (1997) Presynaptic nicotinic ACh receptors. Trends Neurosci 20: 92-98

Woolf NJ (1991) Cholinergic systems in mammalian brain and spinal cord Prog in Neurobiol 37: 475-524

Yamamoto BK and Davy S (1992) Dopaminergic modulation of glutamate release in striatum as measured by microdialysis. J.Neurochem. 58: 1736-1742

Yoshida K and Imura H (1979) Nicotinic cholinergic receptors in brain synaptosomes. Brain Res 172: 453-459

Zatz M and Brownstein MJ (1981) Injection of α-bungarotoxin near the suprachiasmatic nucleus blocks the effects of light on nocturnal pineal enzyme activity. Brain Res. 213: 438-442

Zhang H and Karlin A (1997) Identification of acetylcholine receptor channel-lining residues in the M1 segment of the β-subunit. Biochemistry 36: 15856-15864

Zhang ZW, Vijayaraghavan S, and Berg DK (1994) Neuronal acetylcholine receptors that bind α-bungarotoxin with high affinity function as ligand-gated ion channels. Neuron 12: 167-177

Zhou M, Peterson CL, Lu YB, and Nadler J V (1995) Release of glutamate and aspartate from CA1 synaptosomes: selective modulation of aspartate release by ionotropic glutamate receptor ligands. J.Neurochem. 64: 1556-1566

Zhou Y, Nelson ME, Kuryatov A, Choi C, Cooper J and Lindstrom J (2003) Human alpha4beta2 acetylcholine receptors formed from linked subunits. J Neurosci 23: 9004-9015

Zuo J, Treadaway J, Buckner TW, and Fritzsch B (1999) Visualization of α9 acetylcholine receptor expression in hair cells of transgenic mice containing a

modified bacterial artificial chromosome. Proc Natl Acad Sci U S A 96: 14100-14105

Addendum

Further references

Barrie AP, Nicholls DG, Sanchez-Prieto J and Sihra TS (1991) An ion channel locus for the protein kinase C potentiation of transmitter glutamate release from guinea pig cerebrocortical synaptosomes. J Neurochem. 57:1398-404.

Bradford MM (1976) A rapid and sensitive method for the quantitation of microgram quantities of protein utilizing the principle of protein-dye binding. Anal Biochem 72:248-54.

Coffey ET, Sihra TS and Nicholls DG (1993) Protein kinase C and the regulation of glutamate exocytosis from cerebrocortical synaptosomes. J Biol Chem 268:21060-5.

Nakamura Y, Iga K, Shibata T, Shudo M and Kataoka K (1993) Glial plasmalemmal vesicles: a subcellular fraction from rat hippocampal homogenate distinct from synaptosomes. Glia 9:48-56.